

9. Hydrogen Capacitively and Inductively Coupled RF Plasma and Power Cell and Reactor

A hydrogen capacitively and/or inductively coupled radio frequency (RF) plasma and power cell and reactor of the present invention for the catalysis of atomic hydrogen to form increased-binding-energy-hydrogen species and increased-binding-energy-hydrogen compounds comprises a vessel having a chamber capable of containing a vacuum or pressures greater than atmospheric, a source of atomic hydrogen, a source of RF power to form a plasma, and a catalyst capable of providing a net enthalpy of reaction of $m/2 \cdot 27.2 \pm 0.5 \text{ eV}$ where m is an integer, preferably m is an integer less than 400. The cell may further comprise at least two electrodes and an RF generator wherein the source of RF power may comprise the electrodes driven by the RF generator. Alternatively, the cell may further comprise a source coil which may be external to a cell wall which permits RF power to couple to the plasma formed in the cell, a conducting cell wall which may be grounded and a RF generator which drives the coil which may inductively and/or capacitively couple RF power to the cell plasma.

10. Hydrogen Laser

A laser of the present invention comprises a power and plasma cell and a increased-binding-energy-hydrogen species reactor wherein a water plasma is maintained. In an embodiment, a water plasma is maintained in microwave cavity such as a reentrant cavity such as an Evenson cavity. A stationary inverted H Balmer population was observed from a low pressure water-vapor microwave discharge plasma [R. Mills, P. Ray, R. M. Mayo, "Stationary Inverted Balmer and Lyman Populations for a CW HI Water-Plasma Laser", IEEE Transactions on Plasma Science, submitted]. The ionization and population of excited atomic hydrogen levels was attributed to energy provided by a catalytic resonance energy transfer between hydrogen atoms and molecular oxygen formed in the water plasma. The catalysis by oxygen according to at least Eqs. (39-41) was supported by the observation of O^{2+} and H Balmer line broadening of 55 eV compared to 1 eV for hydrogen alone. The high hydrogen atom temperature with a relatively low electron temperature, $T_e = 2 \text{ eV}$, exhibited characteristics of cold recombining plasmas. These conditions in a water plasma favored an inverted population in the lower levels. Thus, the catalysis of atomic hydrogen may be used to pump a cw H I laser. From our results, laser oscillations are expected i) $n = 3, n = 4, n = 5, n = 6, n = 7$ and $n = 8$ to $n = 2$, ii) $n = 4, n = 5, n = 6$, and $n = 7$ to $n = 3$ and iii) $n = 5$ and $n = 6$ to $n = 4$. High power, highly monochromatic lasers are anticipated at wavelengths, over a broad spectral range from micron to blue which are ideal for many military, industrial,

communications, and microelectronics applications.

An additional laser of the present invention comprises a rt-plasma of hydrogen with an inverted population as described by Mills [R. Mills, P. Ray, R. M. Mayo, "CW HI Laser Based on a Stationary Inverted Lyman Population Formed from Incandescently Heated Hydrogen Gas with Certain Group I Catalysts", IEEE Transactions on Plasma Science, in press] which is
5 herein incorporated by reference in its entirety. Each of the ionization of Rb^+ and cesium and an electron transfer between two K^+ ions (K^+ / K^+) provide a reaction with a net enthalpy of an integer multiple of the potential energy of atomic hydrogen, 27.2 eV. The corresponding Group I nitrates provide these reactants as volatilized ions directly or as atoms by undergoing
10 decomposition or reduction to the corresponding metal. The presence of each of the reactants identified as providing an enthalpy of 27.2 eV formed a low applied temperature, extremely low voltage plasma called a resonance transfer or rt-plasma having strong vacuum ultraviolet (VUV) emission. In contrast, magnesium and aluminum atoms or ions do not ionize at integer multiples of the potential energy of atomic hydrogen. $Mg(NO_3)_2$ or $Al(NO_3)_3$ did not form a
15 plasma and caused no emission.

For further characterization, the width of the 6563 Å Balmer α line was recorded on light emitted from rt-plasmas. Significant line broadening of 18, 12, and 12 eV was observed from a rt-plasma of hydrogen with KNO_3 , $RbNO_3$, and $CsNO_3$, respectively, compared to 3 eV from a hydrogen microwave plasma. These results could not be explained by Stark or
20 thermal broadening or electric field acceleration of charged species since the measured field of the incandescent heater was extremely weak, 1 V/cm, corresponding to a broadening of much less than 1 eV. Rather the source of the excessive line broadening is consistent with that of the observed VUV emission, an energetic reaction caused by a resonance energy transfer between hydrogen atoms and K^+ / K^+ , Rb^+ , and cesium, which serve as catalysts.

25 KNO_3 and $RbNO_3$ formed the most intense plasma. Remarkably, a stationary inverted Lyman population was observed in the case of an rt-plasma formed with potassium and rubidium catalysts. These catalytic reactions may pump a cw HI laser as predicted by a collisional radiative model used to determine that the observed overpopulation was above threshold.

30 11. Photon Power to Electricity Conversion

The present invention of a power and plasma cell and an increased-binding-energy-hydrogen-species reactor further comprises a power converter comprising a hydrogen catalysis cell that produces at least one of a high population of electronically excited state atoms such as

hydrogen atoms and an inverted population such as an atomic hydrogen inverted population. A significant fraction of the power is emitted as photons with spontaneous emission or stimulated emission. In an embodiment, the light is converted to electricity using a photon-to-electric converter of the present invention such as a photoelectric or photovoltaic cell. The power cell
5 comprises a hydrogen laser of the present invention.

In an embodiment of at least one of a hydrogen microwave and a hydrogen RF plasma power cell, a microwave or RF transparent cell such as a quartz tube and a microwave or RF transparent photovoltaic material such as amorphous silicon photovoltaic that is circumferential to the cell are inside of the microwave cavity. The cavity may be a reentrant
10 cavity such as an Evenson cavity. The photovoltaic material may comprise the wall of the cell. The cell may further comprise a cell wall cooler such as an air cooler or a water cooler to maintain the photovoltaic at a desired operating temperature. The cell may also comprise mirrors or lenses to direct the light onto the photovoltaic.

In an embodiment that uses a photovoltaic for power conversion, high energy light may
15 be converted to lower energy light by a phosphor on the transparent walls of the cell so that the photons emitted by the excited phosphor more closely match the peak wavelength efficiency of the photovoltaic.

In an embodiment, a species is added to achieve at least one of atomic hydrogen population inversion or conversion of the power of the catalysis reaction to excited state atomic
20 hydrogen. In an embodiment, the inverting or converting species is a gas comprising at least one molecule from the list of O_2 , H_2O , CO_2 , N_2 , NO_2 , NO , CO , and halogen gas. Percentage inverting or converting species in the catalysis reaction mixture is in the range of 0.1% to 99.9%, preferably in the range of 0.1 to 50%, more preferably in the range 1% to 25%, and most preferably in the range of 1% to 5%.

25

III. BRIEF DESCRIPTION OF THE DRAWINGS

FIGURE 1 is a schematic drawing of a power system comprising a hydrogen power and plasma cell and reactor in accordance with the present invention;

30 FIGURE 2 is a schematic drawing of a hydrogen plasma electrolytic power and plasma cell and reactor in accordance with the present invention;

FIGURE 3 is a schematic drawing of a hydrogen gas power and plasma cell and reactor in accordance with the present invention;

FIGURE 4 is a schematic drawing of a hydrogen gas discharge power and plasma cell and reactor in accordance with the present invention;

FIGURE 5 is a schematic drawing of a hydrogen RF barrier electrode gas discharge power and plasma cell and reactor in accordance with the present invention;

5 FIGURE 6 is a schematic drawing of a hydrogen plasma torch power and plasma cell and reactor in accordance with the present invention;

FIGURE 7 is a schematic drawing of another hydrogen plasma torch power and plasma cell and reactor in accordance with the present invention;

10 FIGURE 8 is a schematic drawing of a hydrogen microwave power and plasma cell and reactor in accordance with the present invention;

FIGURE 9 is a schematic drawing of a hydrogen microwave power and plasma cell, reactor, and laser in accordance with the present invention;

FIGURE 10 is a schematic drawing of a laser in accordance with the present invention;

15 FIGURE 11 is a schematic drawing of a rt-plasma cell laser in accordance with the present invention.

FIGURE 12 is a schematic drawing of a hydrogen power and plasma cell, reactor, and photon-to-electric converter in accordance with the present invention.

FIGURE 13. The experimental set up comprising a filament gas cell to form an rt-plasma light source and an VUV spectrometer which was differentially pumped.

20 FIGURE 14. The 6563 Å Balmer α line width recorded with a high resolution (± 0.06 Å) visible spectrometer on an rt-plasma formed with K and K^+ / K^- catalysts. Significant broadening was observed corresponding to an average hydrogen atom temperature of 18 eV.

FIGURE 15. The 6563 Å Balmer α line width recorded with a high resolution (± 0.06 Å) visible spectrometer on an rt-plasma formed with Rb^+ catalyst. Significant broadening was 25 observed corresponding to an average hydrogen atom temperature of 12 eV.

FIGURE 16. The 6563 Å Balmer α line width recorded with a high resolution (± 0.06 Å) visible spectrometer on an rt-plasma formed with Cs catalyst. Significant broadening was observed corresponding to an average hydrogen atom temperature of 12 eV.

30 FIGURE 17. The 4861 Å Balmer β line width recorded with a high resolution (± 0.06 Å) visible spectrometer on an rt-plasma formed with Rb^+ catalyst. Significant broadening was observed corresponding to an average hydrogen atom temperature of 12 eV.

FIGURE 18. The 4340 Å Balmer γ line width recorded with a high resolution (± 0.06 Å) visible spectrometer on an rt-plasma formed with Rb^+ catalyst. Significant broadening was

observed corresponding to an average hydrogen atom temperature of 14 eV.

FIGURE 19. The 4102 Å Balmer δ line width recorded with a high resolution (± 0.06 Å) visible spectrometer on an rt-plasma formed with Rb^+ catalyst. Significant broadening was observed corresponding to an average hydrogen atom temperature of 11 eV.

5 FIGURE 20. The probe current versus voltage trace of the Langmuir probe of the $RbNO_3$ rt-plasma. The electron density and temperature were measured to be $n_e = 2 \times 10^9 \text{ cm}^{-3}$ and $T_e = 1 - 2 \text{ eV}$. The electron density was over six orders of magnitude less than that required to achieve 1 Å electron Stark broadening.

FIGURE 21. The statistical curve fit of an $RbNO_3$ rt-plasma. The data matched a
10 Gaussian profile having the $X^2 = \sum \frac{(\text{Calculated} - \text{Measured})^2}{\text{Calculated}}$ and R^2 (correlation coefficient squared) values of 0.00023 and 0.99908, respectively. Significant broadening was observed corresponding to an average hydrogen atom temperature of 12 eV.

FIGURE 22. The statistical curve fit of the hydrogen microwave plasma. The data
15 matched a Gaussian profile having the X^2 and R^2 values of 0.00092 and 0.98937, respectively.

FIGURE 23. The VUV spectrum (450 – 800 Å) of the cell emission recorded at about the point of the maximum Lyman α emission from a gas cell at a cell temperature of 700 °C comprising a tungsten filament, a titanium dissociator, 300 mtorr hydrogen, and vaporized K and K^+ from KNO_3 that was recorded with a CEM. Line emission corresponding to K^{3+} was
20 observed at 650 - 670 Å and 740 - 760 Å. K^{2+} was observed at 510 Å and 550 Å, and K^+ was observed at 620 Å.

FIGURE 24. The VUV spectrum (500 – 900 Å) of the emission of the $RbNO_3$ - H_2 gas cell (top curve) and the standard rubidium plasma (bottom curve). The $RbNO_3$ - H_2 gas cell comprised a tungsten filament, a titanium dissociator, 300 mTorr hydrogen, and vaporized Rb^+
25 from $RbNO_3$. The emission was recorded with a CEM at about the point of the maximum Lyman α at a cell temperature of 700 °C. Line emission corresponding to Rb^{2+} was observed at 815.9 Å, 591 Å, 581 Å, 556 Å, and 533 Å. Rb^+ was observed at 741.5 Å, 711 Å, 697 Å, and 643.8 Å.

FIGURE 25. The UV spectrum (3400 – 4150 Å) the cell emission recorded at about the
30 point of the maximum Lyman α emission from a gas cell at a cell temperature of 700 °C comprising a tungsten filament, a titanium dissociator, 300 mtorr hydrogen, and vaporized Cs

from CsNO_3 , that was recorded with a photomultiplier tube (PMT) and a sodium salicylate scintillator. Line emission corresponding to Cs^{2+} was observed at 3477 Å, 3618 Å, and 4001 Å. Cs^+ was observed at 3680 Å, 3806 Å, and 4069 Å. Cs was observed at 3888.6 Å with Cs^{2+} at 3888.4 Å.

- 5 FIGURE 26. The VUV spectrum (400 – 800 Å) of the cell emission from the gas cell at a cell temperature of 700 °C comprising a tungsten filament, vaporized cesium metal, and 300 mtorr hydrogen that was recorded with a PMT and a sodium salicylate scintillator. Emission was observed from a continuum state of Cs^{2+} at 533 Å. The single emission feature with the absence of the other corresponding Rydberg series of lines from Cs^+ confirmed the resonant energy transfer of 27.2 eV from atomic hydrogen to atomic cesium.

10 FIGURE 27. The VUV spectra (900 – 1300 Å) of the cell emission from hydrogen microwave plasma (dotted line) and the KNO_3 - H_2 rt-plasma (solid line) with an inverted Lyman population.

- FIGURE 28. The VUV spectra (900 – 1300 Å) of the cell emission from hydrogen microwave plasma (dotted line) and the RbNO_3 - H_2 rt-plasma (solid line) with an inverted Lyman population.

15 FIGURE 29. The VUV spectra (900 – 1300 Å) of the cell emission from hydrogen microwave plasma (dotted line) and the CsNO_3 - H_2 rt-plasma (solid line) with no inverted Lyman population.

- 20 FIGURE 30. The visible spectrum (4000-6700 Å) recorded on a hydrogen microwave plasma showing the Balmer α , β , γ , and δ line intensities corresponding to $n=3$, $n=4$, $n=5$, and $n=6$ to $n=2$.

FIGURE 31. The visible spectrum (4000-6700 Å) recorded on a KNO_3 rt-plasma showing the Balmer α , β , γ , and δ line intensities corresponding to $n=3$, $n=4$, $n=5$, and $n=6$ to $n=2$.

- 25 FIGURE 32. The visible spectrum (4000-6700 Å) recorded on a RbNO_3 rt-plasma showing the Balmer α , β , γ , and δ line intensities corresponding to $n=3$, $n=4$, $n=5$, and $n=6$ to $n=2$.

FIGURE 33. A plot of the absolute reduced population density $\frac{N_n}{g_n}$ versus quantum number n recorded on a KNO_3 rt-plasma, a RbNO_3 rt-plasma, and a CsNO_3 rt-plasma. In the case of KNO_3 and RbNO_3 rt-plasmas, population inversion was observed for $n=3$. From laser equations and a collisional-radiative model, an overpopulation was achieved for $n=3$.

30

FIGURE 34. The experimental set comprising a quartz tube cell, a source of water vapor, a flow system, and a visible spectrometer.

FIGURE 35. The visible spectrum (4000-6700 Å) of the cell emission from a hydrogen microwave plasma at 90 W input power. No inversion was observed.

5 FIGURE 36. The visible spectrum (4000-6700 Å) of the cell emission from a water microwave plasma with 50 W input power. A stationary inverted H Balmer population was observed. The population of the levels $n = 4, 5$, and 6 of hydrogen were continuously inverted with respect to $n = 3$.

10 FIGURE 37. The visible spectrum (2750-7200 Å) of the cell emission from a water microwave plasma with 90 W input power. A stationary inverted H Balmer population was observed. In addition to the continuous population inversion of the H levels $n = 4, 5$, and 6 with respect to $n = 3$ observed at 50 W, the $n = 5$ and 6 levels were further continuously inverted with respect to $n = 4$ when the input power was increased to 90 W. The levels $n = 7, 8$, and 9 of hydrogen were also continuously inverted with respect to $n = 3$.

15 FIGURE 38. The VUV spectra (900-1300 Å) of the cell emission from hydrogen microwave and water microwave plasmas with 90 W input power. An inverted Lyman population was observed from the water plasma emission with the inversion observed in the visible as shown in FIGURES 36 and 37 extending to the $n = 2$ level.

20 FIGURE 39. The visible spectrum (3000-7200 Å) of the cell emission from an inductively coupled water RF plasma with 90 W input power. No inversion was observed.

FIGURE 40. The visible spectrum (3000-7200 Å) of the cell emission from a capacitively coupled water RF plasma with 90 W input power. No inversion was observed.

25 FIGURE 41. The visible spectrum (2750-7200 Å) of the cell emission from a water high voltage glow discharge plasma with 90 W input power. Strong $OH(A-X)$ emission, but no inversion was observed.

FIGURE 42. The $OH(A-X)$ microwave water plasma emission spectrum in the region of 2750-3300 Å with 90 W input power.

30 42. FIGURE 43. The $OH(A-X)$ (1-0) R-branch and the (1-0) Q-branch were observed in the 2800-2950 Å region of the microwave water plasma emission spectrum shown in FIGURE

FIGURE 44. The $OH(A-X)$ (0-0) R-branch and the (0-0), (1-1), and (2-2) Q-branches were observed in the 3000-3300 Å region of the microwave water plasma emission spectrum shown in FIGURE 42.

FIGURE 45. The 6562.8 Å Balmer α line width recorded with a high resolution (± 0.06 Å) visible spectrometer on a hydrogen microwave discharge plasma. The statistical curve fit of the Balmer α line width profile matched a Gaussian profile having the

$$X^2 = \sum \frac{(\text{Calculated} - \text{Measured})^2}{\text{Calculated}} \text{ and } R^2 \text{ (correlation coefficient squared) values of 4.86 and}$$

5 0.99, respectively. No line excessive broadening was observed corresponding to an average hydrogen atom temperature of 1 eV.

FIGURE 46. The 6562.8 Å Balmer α line width recorded with a high resolution (± 0.06 Å) visible spectrometer on a water vapor microwave discharge plasma. The statistical curve fit of the Balmer α line width profile matched a Gaussian profile having the X^2 and R^2 values of 7.48 and 0.996, respectively. Significant broadening was observed corresponding to an average hydrogen atom temperature of 55 eV.

FIGURE 47. The visible spectrum (3700-3960 Å) of the cell emission from a water microwave plasma with 90 W input power. The catalysis mechanism was supported by the observation of O^{+} at 3715.0 Å, 3754.8 Å, and 3791.28 Å. O^{+} was observed at 3727.2 Å, 15 3749.4 Å, 3771 Å, 3872 Å, and 3946.3 Å. The hydrogen Balmer lines corresponding to the transitions 10-2, 9-2, and 8-2 were also observed.

20 IV. DETAILED DESCRIPTION OF THE INVENTION

The following preferred embodiments of the invention disclose numerous property ranges, including but not limited to, voltage, current, pressure, temperature, microwave power, and the like, which are merely intended as illustrative examples. Based on the detailed written description, one skilled in the art would easily be able to practice this invention within other
25 property ranges to produce the desired result without undue experimentation.

1. Hydrogen Power and Plasma Cell and Reactor

One embodiment of the present invention involves a power system comprising a hydrogen power and plasma cell and reactor shown in FIGURE 1. The hydrogen power and
30 plasma cell and reactor comprises a vessel 52 containing a catalysis mixture 54. The catalysis mixture 54 comprises a source of atomic hydrogen 56 supplied through hydrogen supply passage 42 and a catalyst 58 supplied through catalyst supply passage 41. Catalyst 58 has a net

enthalpy of reaction of about $\frac{m}{2} \cdot 27.21 \pm 0.5 \text{ eV}$, where m is an integer, preferably an integer less than 400. The catalysis involves reacting atomic hydrogen from the source 56 with the catalyst 58 to form lower-energy hydrogen "hydrinos" and produce power. The hydrogen reactor may further include an electron source 70 for contacting hydrinos with electrons, to
5 reduce the hydrinos to hydrino hydride ions.

The source of hydrogen can be hydrogen gas, water, ordinary hydride, or metal-hydrogen solutions. The water may be dissociated to form hydrogen atoms by, for example, thermal dissociation or electrolysis. According to one embodiment of the invention, molecular hydrogen is dissociated into atomic hydrogen by a molecular hydrogen dissociating catalyst.
10 Such dissociating catalysts include, for example, noble metals such as palladium and platinum, refractory metals such as molybdenum and tungsten, transition metals such as nickel and titanium, inner transition metals such as niobium and zirconium, and other such materials listed in the Prior Mills Publications.

According to another embodiment of the invention, a photon source such as a
15 microwave or UV photon source dissociates hydrogen molecules to hydrogen atoms.

In the hydrogen power and plasma cell and reactor embodiments of the present invention, the means to form hydrinos can be one or more of an electrochemical, chemical, photochemical, thermal, free radical, sonic, or nuclear reaction(s), or inelastic photon or particle scattering reaction(s). In the latter two cases, the hydrogen reactor comprises a particle
20 source 75b and/or photon source 75a as shown in FIGURE 1, to supply the reaction as an inelastic scattering reaction. In one embodiment of the hydrogen reactor, the catalyst in the molten, liquid, gaseous, or solid state includes those given in TABLES 1 and 3 and those given in the Tables of the Prior Mills Publications (e.g. TABLE 4 of PCT/US90/01998 and pages 25-46, 80-108 of PCT/US94/02219).

25 When the catalysis occurs in the gas phase, the catalyst may be maintained at a pressure less than atmospheric, preferably in the range about 10 millitorr to about 100 torr. The atomic and/or molecular hydrogen reactant is also maintained at a pressure less than atmospheric, preferably in the range about 10 millitorr to about 100 torr. However, if desired, higher pressures even greater than atmospheric can be used.

30 The hydrogen power and plasma cell and reactor comprises the following: a source of atomic hydrogen; at least one of a solid, molten, liquid, or gaseous catalyst for generating hydrinos; and a vessel for containing the atomic hydrogen and the catalyst. Methods and apparatus for producing hydrinos, including a listing of effective catalysts and sources of

hydrogen atoms, are described in the Prior Mills Publications. Methodologies for identifying hydrinos are also described. The hydrinos so produced may react with the electrons from a reductant to form hydrino hydride ions.

The power system may further comprise a source of electric field 76 which can be used to adjust the rate of hydrogen catalysis. It may further focus ions in the cell. It may further impart a drift velocity to ions in the cell. The cell may comprise a source of microwave power, which is generally known in the art, such as traveling wave tubes, klystrons, magnetrons, cyclotron resonance masers, gyrotrons, and free electron lasers. The present power cell may be an internal source of microwaves wherein the plasma generated from the hydrogen catalysis reaction may be magnetized to produce microwaves.

1.1 Hydrogen Plasma Electrolysis Power and Plasma Cell and Reactor

A hydrogen plasma electrolytic power cell and reactor of the present invention to make lower-energy hydrogen compounds comprises an electrolytic cell forming the reaction vessel 52 of FIGURE 1, including a molten electrolytic cell. The electrolytic cell 100 is shown generally in FIGURE 2. An electric current is passed through the electrolytic solution 102 having a catalyst by the application of a voltage to an anode 104 and cathode 106 by the power controller 108 powered by the power supply 110. Ultrasonic or mechanical energy may also be imparted to the cathode 106 and electrolytic solution 102 by vibrating means 112. Heat can be supplied to the electrolytic solution 102 by heater 114. The pressure of the electrolytic cell 100 can be controlled by pressure regulator means 116 where the cell can be closed. The reactor further comprises a means 101 that removes the (molecular) lower-energy hydrogen such as a selective venting valve to prevent the exothermic shrinkage reaction from coming to equilibrium.

In an embodiment, the plasma electrolytic cell is further supplied with hydrogen from hydrogen source 121 where the over pressure can be controlled by pressure control means 122 and 116. An embodiment of the electrolytic cell energy reactor, comprises a reverse fuel cell geometry which removes the lower-energy hydrogen under vacuum. The reaction vessel may be closed except for a connection to a condensor 140 on the top of the vessel 100. The cell may be operated at a boil such that the steam evolving from the boiling electrolyte 102 can be condensed in the condensor 140, and the condensed water can be returned to the vessel 100. The lower-energy state hydrogen can be vented through the top of the condensor 140. In one embodiment, the condensor contains a hydrogen/oxygen recombiner 145 that contacts the

evolving electrolytic gases. The hydrogen and oxygen are recombined, and the resulting water can be returned to the vessel 100. The heat released from the catalysis of hydrogen and the heat released due to the recombination of the electrolytically generated normal hydrogen and oxygen can be removed by a heat exchanger 60 of FIGURE 1 which can be connected to the
 5 condensor 140.

Hydrino atoms form at the cathode 106 via contact of the catalyst of electrolyte 102 with the hydrogen atoms generated at the cathode 106. The electrolytic cell hydrogen reactor apparatus may further comprises a source of electrons in contact with the hydrinos generated in the cell, to form hydrino hydride ions. The hydrinos are reduced (i.e. gain the electron) in the
 10 electrolytic cell to hydrino hydride ions. Reduction occurs by contacting the hydrinos with other element 160 such as a consumable reductant added to the cell from an outside source. A compound may form in the electrolytic cell between the hydrino hydride ions and cations. The cations may comprise a cation of an added reductant, or a cation of the electrolyte (such as a cation comprising the catalyst).

15 A hydrogen plasma forming electrolytic power cell and reactor of the present invention for the catalysis of atomic hydrogen to form increased-binding-energy-hydrogen species and increased-binding-energy-hydrogen compounds comprises a vessel, a cathode, an anode, an electrolyte, a high voltage electrolysis power supply, and a catalyst capable of providing a net enthalpy of reaction of $m/2 \cdot 27.2 \pm 0.5 \text{ eV}$ where m is an integer. Preferably m is an integer
 20 less than 400. In an embodiment, the voltage is in the range of about 10 V to 50 kV and the current density may be high such as in the range of about 1 to 100 A/cm² or higher. In an embodiment, K^+ is reduced to potassium atom which serves as the catalyst. The cathode of the cell may be tungsten such as a tungsten rod, and the anode of cell of may be platinum. The catalysts of the cell may comprise at least one selected from the group of Li, Be, K, Ca, Ti, V,
 25 Cr, Mn, Fe, Co, Ni, Cu, Zn, As, Se, Kr, Rb, Sr, Nb, Mo, Pd, Sn, Te, Cs, Ce, Pr, Sm, Gd, Dy, Pb, Pt, He^+ , Na^+ , Rb^+ , Sr^+ , Fe^{2+} , Mo^{2+} , Mo^{4+} , and In^{3+} . The catalyst of the cell of may be formed from a source of catalyst. The source of catalyst that forms the catalyst may comprise at least one selected from the group of Li, Be, K, Ca, Ti, V, Cr, Mn, Fe, Co, Ni, Cu, Zn, As, Se, Kr, Rb, Sr, Nb, Mo, Pd, Sn, Te, Cs, Ce, Pr, Sm, Gd, Dy, Pb, Pt, He^+ , Na^+ , Rb^+ , Sr^+ , Fe^{2+} ,
 30 Mo^{2+} , Mo^{4+} , In^{3+} and K^+/K^+ alone or comprising compounds. The source of catalyst may comprise a compound that provides K^+ that is reduced to the catalyst potassium atom during electrolysis.

The compound of formed comprises

(a) at least one neutral, positive, or negative increased binding energy hydrogen species having a binding energy

(i) greater than the binding energy of the corresponding ordinary hydrogen species, or

5 (ii) greater than the binding energy of any hydrogen species for which the corresponding ordinary hydrogen species is unstable or is not observed because the ordinary hydrogen species' binding energy is less than thermal energies at ambient conditions, or is negative; and

(b) at least one other element.

10 The increased binding energy hydrogen species may be selected from the group consisting of H_n , H_n^- , and H_n^+ where n is a positive integer, with the proviso that n is greater than 1 when H has a positive charge. The compound formed may be characterized in that the increased binding energy hydrogen species is selected from the group consisting of (a) hydride ion having a binding energy that is greater than the binding of ordinary hydride ion (about 0.8

15 eV) for $p = 2$ up to 23 in which the binding energy is represented by

$$\text{Binding Energy} = \frac{\hbar^2 \sqrt{s(s+1)}}{8\mu_e a_0^2 \left[\frac{1 + \sqrt{s(s+1)}}{p} \right]^2} - \frac{\pi\mu_e e^2 \hbar^2}{m_e^2} \left\{ \frac{1}{a_H^3} + \frac{2^2}{a_0^3 \left[\frac{1 + \sqrt{s(s+1)}}{p} \right]^3} \right\}$$

where p is an integer greater than one; (b) hydrogen atom having a binding energy greater than about 13.6 eV; (c) hydrogen molecule having a first binding energy greater than about 15.3 eV; and (d) molecular hydrogen ion having a binding energy greater than about 16.3 eV. The

20 compound may be characterized in that the increased binding energy hydrogen species is a hydride ion having a binding energy of about 3, 6.6, 11.2, 16.7, 22.8, 29.3, 36.1, 42.8, 49.4, 55.5, 61.0, 65.6, 69.2, 71.6, 72.4, 71.6, 68.8, 64.0, 56.8, 47.1, 34.7, 19.3, and 0.69 eV. The compound may be characterized in that the increased binding energy hydrogen species is a hydride ion having the binding energy:

25
$$\text{Binding Energy} = \frac{\hbar^2 \sqrt{s(s+1)}}{8\mu_e a_0^2 \left[\frac{1 + \sqrt{s(s+1)}}{p} \right]^2} - \frac{\pi\mu_e e^2 \hbar^2}{m_e^2} \left\{ \frac{1}{a_H^3} + \frac{2^2}{a_0^3 \left[\frac{1 + \sqrt{s(s+1)}}{p} \right]^3} \right\}$$

where p is an integer greater than one. The compound may be characterized in that the increased binding energy hydrogen species is selected from the group consisting of

(a) a hydrogen atom having a binding energy of about $\frac{13.6 \text{ eV}}{\left(\frac{1}{p}\right)^2}$ where p is an integer,

(b) an increased binding energy hydride ion (H^-) having a binding energy of about

$$\frac{\hbar^2 \sqrt{s(s+1)}}{8\mu_e a_0^2 \left[\frac{1 + \sqrt{s(s+1)}}{p} \right]^2} - \frac{\pi\mu_e e^2 \hbar^2}{m_e^2} \left\{ \frac{1}{a_H^3} + \frac{2^2}{a_0^3 \left[\frac{1 + \sqrt{s(s+1)}}{p} \right]^3} \right\};$$

(c) an increased binding energy hydrogen species $H_s^+(1/p)$;

5 (d) an increased binding energy hydrogen species trihydrino molecular ion, $H_3^+(1/p)$,
having a binding energy of about $\frac{22.6}{\left(\frac{1}{p}\right)^2} \text{ eV}$ where p is an integer,

(e) an increased binding energy hydrogen molecule having a binding energy of about

$$\frac{15.3}{\left(\frac{1}{p}\right)^2} \text{ eV}; \text{ and}$$

(f) an increased binding energy hydrogen molecular ion with a binding energy of about

$$10 \frac{16.3}{\left(\frac{1}{p}\right)^2} \text{ eV}.$$

1.2 Hydrogen Gas Power and Plasma Cell and Reactor

According to an embodiment of the invention, a reactor for producing hydrinos, plasma, and power may take the form of a hydrogen gas cell. A gas cell hydrogen reactor of
15 the present invention is shown in FIGURE 3. Reactant hydrinos are provided by a catalytic reaction with a catalyst such as at least one of those given in TABLES 1 and 3 and/or a by a disproportionation reaction. Catalysis may occur in the gas phase.

The reactor of FIGURE 3 comprises a reaction vessel 207 having a chamber 200 capable of containing a vacuum or pressures greater than atmospheric. A source of hydrogen
20 221 communicating with chamber 200 delivers hydrogen to the chamber through hydrogen supply passage 242. A controller 222 is positioned to control the pressure and flow of hydrogen into the vessel through hydrogen supply passage 242. A pressure sensor 223 monitors pressure in the vessel. A vacuum pump 256 is used to evacuate the chamber through

a vacuum line 257. The apparatus may further comprise a source of electrons in contact with the hydrinos to form hydrino hydride ions.

In an embodiment, the source of hydrogen 221 communicating with chamber 200 that delivers hydrogen to the chamber through hydrogen supply passage 242 is a hydrogen
5 permeable hollow cathode of an electrolysis cell. Electrolysis of water produces hydrogen that permeates through the hollow cathode. The cathode may be a transition metal such as nickel, iron, or titanium, or a noble metal such as palladium, or platinum, or tantalum or palladium coated tantalum, or palladium coated niobium. The electrolyte may be basic and the anode may be nickel. The electrolyte may be aqueous K_2CO_3 . The flow of hydrogen into the cell
10 may be controlled by controlling the electrolysis current with an electrolysis power controller.

A catalyst 250 for generating hydrino atoms can be placed in a catalyst reservoir 295. The catalyst in the gas phase may comprise the catalysts given in TABLES 1 and 3 and those in the Mills Prior Publications. The reaction vessel 207 has a catalyst supply passage 241 for the passage of gaseous catalyst from the catalyst reservoir 295 to the reaction chamber 200.
15 Alternatively, the catalyst may be placed in a chemically resistant open container, such as a boat, inside the reaction vessel.

The molecular and atomic hydrogen partial pressures in the reactor vessel 207, as well as the catalyst partial pressure, is preferably maintained in the range of about 10 millitorr to about 100 torr. Most preferably, the hydrogen partial pressure in the reaction vessel 207 is
20 maintained at about 200 millitorr.

Molecular hydrogen may be dissociated in the vessel into atomic hydrogen by a dissociating material. The dissociating material may comprise, for example, a noble metal such as platinum or palladium, a transition metal such as nickel and titanium, an inner transition metal such as niobium and zirconium, or a refractory metal such as tungsten or
25 molybdenum. The dissociating material may be maintained at an elevated temperature by the heat liberated by the hydrogen catalysis (hydrino generation) and hydrino reduction taking place in the reactor. The dissociating material may also be maintained at elevated temperature by temperature control means 230, which may take the form of a heating coil as shown in cross section in FIGURE 3. The heating coil is powered by a power supply 225.

30 Molecular hydrogen may be dissociated into atomic hydrogen by application of electromagnetic radiation, such as UV light provided by a photon source 205, by a hot filament or grid 280 powered by power supply 285, or by the plasma generated in the cell by the catalysis reaction.

The hydrogen dissociation occurs such that the dissociated hydrogen atoms contact a catalyst which is in a molten, liquid, gaseous, or solid form to produce hydrino atoms. The catalyst vapor pressure is maintained at the desired pressure by controlling the temperature of the catalyst reservoir 295 with a catalyst reservoir heater 298 powered by a power supply 272.

5 When the catalyst is contained in a boat inside the reactor, the catalyst vapor pressure is maintained at the desired value by controlling the temperature of the catalyst boat, by adjusting the boat's power supply.

The rate of production of hydrinos and power by the hydrogen gas cell can be controlled by controlling the amount of catalyst in the gas phase and/or by controlling the

10 concentration of atomic hydrogen. The concentration of gaseous catalyst in vessel chamber 200 may be controlled by controlling the initial amount of the volatile catalyst present in the chamber 200. The concentration of gaseous catalyst in chamber 200 may also be controlled by controlling the catalyst temperature, by adjusting the catalyst reservoir heater 298, or by adjusting a catalyst boat heater when the catalyst is contained in a boat inside the reactor. The

15 vapor pressure of the volatile catalyst 250 in the chamber 200 is determined by the temperature of the catalyst reservoir 295, or the temperature of the catalyst boat, because each is colder than the reactor vessel 207. The reactor vessel 207 temperature is maintained at a higher operating temperature than catalyst reservoir 295 with heat liberated by the hydrogen catalysis (hydrino generation) and hydrino reduction. The reactor vessel temperature may also be maintained by

20 a temperature control means, such as heating coil 230 shown in cross section in FIGURE 3. Heating coil 230 is powered by power supply 225. The reactor temperature further controls the reaction rates such as hydrogen dissociation and catalysis.

In an embodiment, the catalyst comprises a mixture of a first catalyst supplied from the catalyst reservoir 295 and a source of a second catalyst supplied from gas supply 221 regulated

25 by flow controller 222. Hydrogen may also be supplied to the cell from gas supply 221 regulated by flow controller 222. The flow controller 222 may achieve a desired mixture of the source of a second catalyst and hydrogen, or the gases may be premixed in a desired ratio. In an embodiment, the first catalyst produces the second catalyst from the source of the second catalyst. In an embodiment, the energy released by the catalysis of hydrogen by the first

30 catalyst produces a plasma in the energy cell. The energy ionizes the source of the second catalyst to produce the second catalyst. The first catalyst may be selected from the group of catalysts given in TABLES 1 and 3 such as potassium and strontium, the source of the second catalyst may be selected from the group of helium and argon and the second catalyst may be

selected from the group of He^+ and Ar^+ wherein the catalyst ion is generated from the corresponding atom by a plasma created by catalysis of hydrogen by the first catalyst. For examples, 1.) the energy cell contains strontium and argon wherein hydrogen catalysis by strontium produces a plasma containing Ar^+ which serves as a second catalyst (Eqs. (15-17))
5 and 2.) the energy cell contains potassium and helium wherein hydrogen catalysis by potassium produces a plasma containing He^+ which serves as a second catalyst (Eqs. (12-14)). In an embodiment, the pressure of the source of the second catalyst is in the range of about 1 millitorr to about one atmosphere. The hydrogen pressure is in the range of about 1 millitorr to about one atmosphere. In a preferred embodiment, the total pressure is in the range of about
10 0.5 torr to about 2 torr. In an embodiment, the ratio of the pressure of the source of the second catalyst to the hydrogen pressure is greater than one. In a preferred embodiment, hydrogen is about 0.1% to about 99%, and the source of the second catalyst comprises the balance of the gas present in the cell. More preferably, the hydrogen is in the range of about 1% to about 5% and the source of the second catalyst is in the range of about 95% to about 99%. Most
15 preferably, the hydrogen is about 5% and the source of the second catalyst is about 95%. These pressure ranges are representative examples and a skilled person will be able to practice this invention using a desired pressure to provide a desired result.

The preferred operating temperature depends, in part, on the nature of the material comprising the reactor vessel 207. The temperature of a stainless steel alloy reactor vessel 207
20 is preferably maintained at about 200-1200°C. The temperature of a molybdenum reactor vessel 207 is preferably maintained at about 200-1800 °C. The temperature of a tungsten reactor vessel 207 is preferably maintained at about 200-3000 °C. The temperature of a quartz or ceramic reactor vessel 207 is preferably maintained at about 200-1800 °C.

The concentration of atomic hydrogen in vessel chamber 200 can be controlled by the
25 amount of atomic hydrogen generated by the hydrogen dissociation material. The rate of molecular hydrogen dissociation can be controlled by controlling the surface area, the temperature, and/or the selection of the dissociation material. The concentration of atomic hydrogen may also be controlled by the amount of atomic hydrogen provided by the atomic hydrogen source 221. The concentration of atomic hydrogen can be further controlled by the
30 amount of molecular hydrogen supplied from the hydrogen source 221 controlled by a flow controller 222 and a pressure sensor 223. The reaction rate may be monitored by windowless ultraviolet (UV) emission spectroscopy to detect the intensity of the UV emission due to the catalysis and the hydrino, dihydrino molecular ion, dihydrino molecule, hydride ion, and

compound emissions.

The gas cell hydrogen reactor further comprises other element as an electron source 260 such a reductant in contact with the generated hydrinos to form hydrino hydride ions.

Compounds comprising a hydrino hydride anion and a cation may be formed in the gas cell.

- 5 The cation which forms the hydrino hydride compound may comprise a cation from an added reductant, or a cation present in the cell (such as the cation of the catalyst). The cell may further comprise a getter or cryotrap 255 to selectively collect the lower-energy-hydrogen species and/or the increased-binding-energy hydrogen compounds.

10 1.3 Hydrogen Gas Discharge Power and Plasma Cell and Reactor

A hydrogen gas discharge power and plasma cell and reactor of the present invention is shown in FIGURE 4. The hydrogen gas discharge power and plasma cell and reactor of FIGURE 4, includes a gas discharge cell 307 comprising a hydrogen isotope gas-filled glow discharge vacuum vessel 313 having a chamber 300. A hydrogen source 322 supplies
15 hydrogen to the chamber 300 through control valve 325 via a hydrogen supply passage 342. A catalyst is contained in catalyst reservoir 395. A voltage and current source 330 causes current to pass between a cathode 305 and an anode 320. The current may be reversible. In another embodiment, the plasma is generated with a microwave source such as a microwave generator.

In one embodiment of the hydrogen gas discharge power and plasma cell and reactor,
20 the wall of vessel 313 is conducting and serves as the anode. In another embodiment, the cathode 305 is hollow such as a hollow, nickel, aluminum, copper, tungsten, molybdenum, or stainless steel hollow cathode. In an embodiment, the cathode material may be a source of catalyst such as iron or samarium.

The cathode 305 may be coated with the catalyst for generating hydrinos and energy.
25 The catalysis to form hydrinos and energy occurs on the cathode surface. To form hydrogen atoms for generation of hydrinos and energy, molecular hydrogen is dissociated on the cathode. To this end, the cathode is formed of a hydrogen dissociative material. Alternatively, the molecular hydrogen is dissociated by the discharge.

According to another embodiment of the invention, the catalyst for generating hydrinos
30 and energy is in gaseous form. For example, the discharge may be utilized to vaporize the catalyst to provide a gaseous catalyst. Alternatively, the gaseous catalyst is produced by the discharge current. For example, the gaseous catalyst may be provided by a discharge in rubidium metal to form Rb^+ , strontium metal to form Sr^+ , or titanium metal to form Ti^{2+} , or

potassium to volatilize the metal. The gaseous hydrogen atoms for reaction with the gaseous catalyst are provided by a discharge of molecular hydrogen gas such that the catalysis occurs in the gas phase.

Another embodiment of the hydrogen gas discharge power and plasma cell and reactor where catalysis occurs in the gas phase utilizes a controllable gaseous catalyst. The gaseous hydrogen atoms for conversion to hydrides are provided by a discharge of molecular hydrogen gas. The gas discharge cell 307 has a catalyst supply passage 341 for the passage of the gaseous catalyst 350 from catalyst reservoir 395 to the reaction chamber 300. The catalyst reservoir 395 is heated by a catalyst reservoir heater 392 having a power supply 372 to provide the gaseous catalyst to the reaction chamber 300. The catalyst vapor pressure is controlled by controlling the temperature of the catalyst reservoir 395, by adjusting the heater 392 by means of its power supply 372. The reactor further comprises a selective venting valve 301.

In another embodiment of the hydrogen gas discharge power and plasma cell and reactor where catalysis occurs in the gas phase utilizes a controllable gaseous catalyst. Gaseous hydrogen atoms provided by a discharge of molecular hydrogen gas. A chemically resistant (does not react or degrade during the operation of the reactor) open container, such as a tungsten or ceramic boat, positioned inside the gas discharge cell contains the catalyst. The catalyst in the catalyst boat is heated with a boat heater using by means of an associated power supply to provide the gaseous catalyst to the reaction chamber. Alternatively, the glow gas discharge cell is operated at an elevated temperature such that the catalyst in the boat is sublimed, boiled, or volatilized into the gas phase. The catalyst vapor pressure is controlled by controlling the temperature of the boat or the discharge cell by adjusting the heater with its power supply.

The gas discharge cell may be operated at room temperature by continuously supplying catalyst. Alternatively, to prevent the catalyst from condensing in the cell, the temperature is maintained above the temperature of the catalyst source, catalyst reservoir 395 or catalyst boat. For example, the temperature of a stainless steel alloy cell is about 0-1200 °C; the temperature of a molybdenum cell is about 0-1800 °C; the temperature of a tungsten cell is about 0-3000 °C; and the temperature of a glass, quartz, or ceramic cell is about 0-1800 °C. The discharge voltage may be in the range of about 1000 to about 50,000 volts. The current may be in the range of about 1 μ A to about 1 A, preferably about 1 mA.

The discharge current may be intermittent or pulsed. Pulsing may be used to reduce the input power, and it may also provide a time period wherein the field is set to a desired strength

by an offset voltage which may be below the discharge voltage. One application of controlling the field during the nondischarge period is to optimize the energy match between the catalyst and the atomic hydrogen. In an embodiment, the offset voltage is between, about 0.5 to about 500 V. In another embodiment, the offset voltage is set to provide a field of about 0.1 V/cm to about 50 V/cm. Preferably, the offset voltage is set to provide a field between about 1 V/cm to about 10 V/cm. The peak voltage may be in the range of about 1 V to 10 MV. More preferably, the peak voltage is in the range of about 10 V to 100 kV. Most preferably, the voltage is in the range of about 100 V to 500 V. The pulse frequency and duty cycle may also be adjusted. An application of controlling the pulse frequency and duty cycle is to optimize the power balance. In an embodiment, this is achieved by optimizing the reaction rate versus the input power. The amount of catalyst and atomic hydrogen generated by the discharge decay during the nondischarge period. The reaction rate may be controlled by controlling the amount of catalyst generated by the discharge such as Ar^{\bullet} and the amount of atomic hydrogen wherein the concentration is dependent on the pulse frequency, duty cycle, and the rate of decay. In an embodiment, the pulse frequency is of about 0.1 Hz to about 100 MHz. In another embodiment, the pulse frequency is faster than the time for substantial atomic hydrogen recombination to molecular hydrogen. Based on anomalous plasma afterglow duration studies [R. Mills, T. Onuma, and Y. Lu, "Formation of a Hydrogen Plasma from an Incandescently Heated Hydrogen-Catalyst Gas Mixture with an Anomalous Afterglow Duration", *Int. J. Hydrogen Energy*, Vol. 26, No. 7, July, (2001), pp. 749-762; R. Mills, "Temporal Behavior of Light-Emission in the Visible Spectral Range from a Ti-K₂CO₃-H-Cell", *Int. J. Hydrogen Energy*, Vol. 26, No. 4, (2001), pp. 327-332], preferably the frequency is within the range of about 1 to about 200 Hz. In an embodiment, the duty cycle is about 0.1% to about 95%. Preferably, the duty cycle is about 1% to about 50%.

In another embodiment, the power may be applied as an alternating current (AC). The frequency may be in the range of about 0.001 Hz to 1 GHz. More preferably the frequency is in the range of about 60 Hz to 100 MHz. Most preferably, the frequency is in the range of about 10 to 100 MHz. The system may comprises two electrodes wherein one or more electrodes are in direct contact with the plasma; otherwise, the electrodes may be separated from the plasma by a dielectric barrier. The peak voltage may be in the range of about 1 V to 10 MV. More preferably, the peak voltage is in the range of about 10 V to 100 kV. Most preferably, the voltage is in the range of about 100 V to 500 V.

The gas discharge cell apparatus further comprises other element as an electron source

360 such a reductant in contact with the generated hydrinos to form hydrino hydride ions. Compounds comprising a hydrino hydride anion and a cation may be formed in the gas cell. The cation which forms the hydrino hydride compound may comprise a cation from an added reductant, or a cation present in the cell (such as the cation of the catalyst).

5 In one embodiment of the gas discharge cell apparatus, alkali and alkaline earth hydrino hydrides and energy are produced in the gas discharge cell 307. In an embodiment, the catalyst reservoir 395 contains potassium, rubidium, or strontium metal which may be ionized to K^+ , Rb^+ or Sr^+ catalyst, respectively. The catalyst vapor pressure in the gas discharge cell is controlled by heater 392. The catalyst reservoir 395 is heated with the heater 392 to maintain
10 the catalyst vapor pressure proximal to the cathode 305 preferably in the pressure range 10 millitorr to 100 torr, more preferably at about 200 mtorr. In another embodiment, the cathode 305 and the anode 320 of the gas discharge cell 307 are coated with potassium, rubidium, or strontium. The catalyst is vaporized during the operation of the cell. The hydrogen supply from source 322 is adjusted with control 325 to supply hydrogen and maintain the hydrogen
15 pressure in the 10 millitorr to 100 torr range.

In an embodiment, the electrode to provide the electric field is a compound electrode comprising multiple electrodes in series or parallel that may occupy a substantial portion of the volume of the reactor. In one embodiment, the electrode comprises multiple hollow cathodes in parallel so that the desired electric field is produced in a large volume to generate a
20 substantial power level. One design of the multiple hollow cathodes comprises an anode and multiple concentric hollow cathodes each electrically isolated from the common anode. Another compound electrode comprises multiple parallel plate electrodes connected in series.

A preferable hollow cathode is comprised of refractory materials such as molybdenum or tungsten. A preferably hollow cathode comprises a compound hollow cathode. A
25 preferable catalyst of a compound hollow cathode discharge cell is neon as described in R. L. Mills, P. Ray, J. Dong, M. Nansteel, B. Dhandapani, J. He, "Vibrational Spectral Emission of Fractional-Principal-Quantum-Energy-Level Atomic and Molecular Hydrogen", Vibrational Spectroscopy, submitted which is herein incorporated by reference in its entirety. In an embodiment of the cell comprising a compound hollow cathode and neon as the source of
30 catalyst with hydrogen, the partial pressure of neon is in the range 99.99%-90% and hydrogen is in the range 0.01-10%. Preferably the partial pressure of neon is in the range 99.9-99% and hydrogen is in the range 0.1-1%.

In an embodiment, metal hydride films such as FeH form with a helium, argon, or

neon-hydrogen mixture plasma such as (99/1%) with a reactor such as a stainless steel reactor and a stainless steel cathode. Preferably the cathode is made of a metal M, and MH is synthesized wherein H is an increased binding energy hydrogen species. In an embodiment, the cathode is iron in the case of the synthesis of FeH. In another embodiment, the cell is operated at an elevated temperature. The cell may be operated in the temperature range of about 25-100°C. Preferably the cell is operated in the range of about 100-3500°C. More preferably the cell is operated in the range of about 200-1500°C. Most preferably the cell is operated in the range of about 400-800°C. The higher operating temperature may also cause hydrido hydride compounds to volatilize from the cathode to increase the power of the hydrogen catalysis reaction.

In an embodiment, the synthesis of the metal hydride films is enhanced by lining the reactor with a dielectric such as quartz and maintaining a plasma with a catalyst gas such as neon, argon, or helium with hydrogen. The hydrido metal hydride can be peeled from the liner such as a quartz liner. The reaction must be run at high temperature in order to achieve a sufficient metal reactant vapor pressure such as in the range of about 300°C to 1000°C and preferably in the range of about 400°C to 600°C in order to achieve a sufficient iron vapor pressure to form iron hydrido hydride.

1.4 Hydrogen Radio Frequency (RF) Barrier Electrode Discharge Power and Plasma

Cell and Reactor

In an embodiment of the hydrogen discharge power and plasma cell and reactor, at least one of the discharge electrodes is shielded by a dielectric barrier such as glass, quartz, Alumina, or ceramic in order to provide an electric field with minimum power dissipation. A radio frequency (RF) barrier electrode discharge cell system 1000 of the present invention is shown in FIGURE 5. The RF power may be capacitively coupled. In an embodiment, the electrodes 1004 may be external to the cell 1001. A dielectric layer 1005 separates the electrodes from the cell wall 1006. The high driving voltage may be AC and may be high frequency. The driving circuit comprises a high voltage power source 1002 which is capable of providing RF and an impedance matching circuit 1003. The frequency is preferably in the range of about 100 Hz to about 10 GHz, more preferably, about 1 kHz to about 1 MHz, most preferably about 5-10 kHz. The voltage is preferably in the range of about 100 V to about 1 MV, more preferably about 1 kV to about 100 kV, and most preferably about 5 to about 10 kV.

1.5 Hydrogen Plasma Torch Power and Plasma Cell and Reactor

A hydrogen plasma torch power and plasma cell and reactor of the present invention is shown in FIGURE 6. A plasma torch 702 provides a hydrogen isotope plasma 704 enclosed by a manifold 706 and contained in plasma chamber 760. Hydrogen from hydrogen supply 738 and plasma gas from plasma gas supply 712, along with a catalyst 714 for forming hydrinos and energy, is supplied to torch 702. The plasma may comprise argon, for example. The catalyst may comprise at least one of those given in TABLES 1 and 3 or a hydrino atom to provide a disproportionation reaction. The catalyst is contained in a catalyst reservoir 716. The reservoir is equipped with a mechanical agitator, such as a magnetic stirring bar 718 driven by magnetic stirring bar motor 720. The catalyst is supplied to plasma torch 702 through passage 728. The catalyst may be generated by a microwave discharge. Preferred catalysts are He^+ or Ar^+ from a source such as helium gas or argon gas.

Hydrogen is supplied to the torch 702 by a hydrogen passage 726. Alternatively, both hydrogen and catalyst may be supplied through passage 728. The plasma gas is supplied to the torch by a plasma gas passage 726. Alternatively, both plasma gas and catalyst may be supplied through passage 728.

Hydrogen flows from hydrogen supply 738 to a catalyst reservoir 716 via passage 742. The flow of hydrogen is controlled by hydrogen flow controller 744 and valve 746. Plasma gas flows from the plasma gas supply 712 via passage 732. The flow of plasma gas is controlled by plasma gas flow controller 734 and valve 736. A mixture of plasma gas and hydrogen is supplied to the torch via passage 726 and to the catalyst reservoir 716 via passage 725. The mixture is controlled by hydrogen-plasma-gas mixer and mixture flow regulator 721. The hydrogen and plasma gas mixture serves as a carrier gas for catalyst particles which are dispersed into the gas stream as fine particles by mechanical agitation. The aerosolized catalyst and hydrogen gas of the mixture flow into the plasma torch 702 and become gaseous hydrogen atoms and vaporized catalyst ions (such as Rb^+ ions from a salt of rubidium) in the plasma 704. The plasma is powered by a microwave generator 724 wherein the microwaves are tuned by a tunable microwave cavity 722. Catalysis may occur in the gas phase.

The amount of gaseous catalyst in the plasma torch can be controlled by controlling the rate at which the catalyst is aerosolized with a mechanical agitator. The amount of gaseous catalyst can also be controlled by controlling the carrier gas flow rate where the carrier gas includes a hydrogen and plasma gas mixture (e.g., hydrogen and argon). The amount of gaseous hydrogen atoms to the plasma torch can be controlled by controlling the hydrogen flow

rate and the ratio of hydrogen to plasma gas in the mixture. The hydrogen flow rate and the plasma gas flow rate to the hydrogen-plasma-gas mixer and mixture flow regulator 721 can be controlled by flow rate controllers 734 and 744, and by valves 736 and 746. Mixer regulator 721 controls the hydrogen-plasma mixture to the torch and the catalyst reservoir. The catalysis
5 rate can also be controlled by controlling the temperature of the plasma with microwave generator 724.

Hydrino atoms, dihydrino molecular ions, dihydrino molecules, and hydrino hydride ions are produced in the plasma 704. Dihydrino molecules and hydrino hydride compounds may be cryopumped onto the manifold 706, or they may flow into a trap 708 such as a cryotrap
10 through passage 748. Trap 708 communicates with vacuum pump 710 through vacuum line 750 and valve 752. A flow to the trap 708 is effected by a pressure gradient controlled by the vacuum pump 710, vacuum line 750, and vacuum valve 752.

In another embodiment of the plasma torch hydrogen reactor shown in FIGURE 7, at least one of plasma torch 802 or manifold 806 has a catalyst supply passage 856 for passage of
15 the gaseous catalyst from a catalyst reservoir 858 to the plasma 804. The catalyst 814 in the catalyst reservoir 858 is heated by a catalyst reservoir heater 866 having a power supply 868 to provide the gaseous catalyst to the plasma 804. The catalyst vapor pressure can be controlled by controlling the temperature of the catalyst reservoir 858 by adjusting the heater 866 with its power supply 868. The remaining elements of FIGURE 7 have the same structure and function
20 of the corresponding elements of FIGURE 6. In other words, element 812 of FIGURE 7 is a plasma gas supply corresponding to the plasma gas supply 712 of FIGURE 6, element 838 of FIGURE 7 is a hydrogen supply corresponding to hydrogen supply 738 of FIGURE 6, and so forth.

In another embodiment of the plasma torch hydrogen reactor, a chemically resistant
25 open container such as a ceramic boat located inside the manifold contains the catalyst. The plasma torch manifold forms a cell which can be operated at an elevated temperature such that the catalyst in the boat is sublimed, boiled, or volatilized into the gas phase. Alternatively, the catalyst in the catalyst boat can be heated with a boat heater having a power supply to provide the gaseous catalyst to the plasma. The catalyst vapor pressure can be controlled by controlling
30 the temperature of the cell with a cell heater, or by controlling the temperature of the boat by adjusting the boat heater with an associated power supply.

The plasma temperature in the plasma torch hydrogen reactor is advantageously maintained in the range of about 5,000-30,000 °C. The cell may be operated at room

temperature by continuously supplying catalyst. Alternatively, to prevent the catalyst from condensing in the cell, the cell temperature can be maintained above that of the catalyst source, catalyst reservoir 858 or catalyst boat. The operating temperature depends, in part, on the nature of the material comprising the cell. The temperature for a stainless steel alloy cell is preferably about 0-1200 °C. The temperature for a molybdenum cell is preferably about 0-1800 °C. The temperature for a tungsten cell is preferably about 0-3000 °C. The temperature for a glass, quartz, or ceramic cell is preferably about 0-1800 °C. Where the manifold 706 is open to the atmosphere, the cell pressure is atmospheric.

An exemplary plasma gas for the plasma torch hydrogen reactor is argon which may also serve as a source of catalyst. Exemplary aerosol flow rates are about 0.8 standard liters per minute (slm) hydrogen and about 0.15 slm argon. An exemplary argon plasma flow rate is about 5 slm. An exemplary forward input power is about 1000 W, and an exemplary reflected power is about 10-20 W.

In other embodiments of the plasma torch hydrogen reactor, the mechanical catalyst agitator (magnetic stirring bar 718 and magnetic stirring bar motor 720) is replaced with an aspirator, atomizer, or nebulizer to form an aerosol of the catalyst 714 dissolved or suspended in a liquid medium such as water. The medium is contained in the catalyst reservoir 716. Or, the aspirator, atomizer, ultrasonic dispersion means, or nebulizer injects the catalyst directly into the plasma 704. The nebulized or atomized catalyst can be carried into the plasma 704 by a carrier gas, such as hydrogen.

The hydrogen plasma torch cell further includes an electron source in contact with the hydrinos, for generating hydrino hydride ions. In the plasma torch cell, the hydrinos can be reduced to hydrino hydride ions by contacting a reductant extraneous to the operation of the cell (e.g. a consumable reductant added to the cell from an outside source). Compounds comprising a hydrino hydride anion and a cation may be formed in the cell. The cation which forms the hydrino hydride compound may comprise a cation of other element, an oxidized species such as a reductant, or a cation present in the plasma (such as a cation of the catalyst).

2. Hydrogen RF and Microwave Power and Plasma Cell and Reactor

According to an embodiment of the invention, a reactor for producing power, plasma, and at least one of hydrinos, hydrino hydride ions, dihydrino molecular ions, and dihydrino molecules may take the form of a hydrogen microwave reactor. A hydrogen microwave gas cell reactor of the present invention is shown in FIGURE 8. Hydrinos are provided by a

reaction with a catalyst capable of providing a net enthalpy of reaction of $m/2 \cdot 27.2 \pm 0.5 \text{ eV}$ where m is an integer, preferably an integer less than 400 such as those given in TABLES 1 and 3 and/or by a disproportionation reaction wherein lower-energy hydrogen, hydrinos, serve to cause transitions of hydrogen atoms and hydrinos to lower-energy levels with the release of power. Catalysis may occur in the gas phase. The catalyst may be generated by a microwave discharge. Preferred catalysts are He^+ or Ar^+ from a source such as helium gas or argon gas. The catalysis reaction may provide power to form and maintain a plasma that comprises energetic ions. Microwaves that may or may not be phase bunched may be generated by ionized electrons in a magnetic field; thus, the magnetized plasma of the cell comprises an internal microwave generator. The generated microwaves may then be the source of microwaves to at least partially maintain the microwave discharge plasma.

The reactor system of FIGURE 8 comprises a reaction vessel 601 having a chamber 660 capable of containing a vacuum or pressures greater than atmospheric. A source of hydrogen 638 delivers hydrogen to supply tube 642, and hydrogen flows to the chamber through hydrogen supply passage 626. The flow of hydrogen can be controlled by hydrogen flow controller 644 and valve 646. In an embodiment, a source of hydrogen communicating with chamber 660 that delivers hydrogen to the chamber through hydrogen supply passage 626 is a hydrogen permeable hollow cathode of an electrolysis cell of the reactor system. Electrolysis of water produces hydrogen that permeates through the hollow cathode. The cathode may be a transition metal such as nickel, iron, or titanium, or a noble metal such as palladium, or platinum, or tantalum or palladium coated tantalum, or palladium coated niobium. The electrolyte may be basic and the anode may be nickel, platinum, or a dimensionally stable anode. The electrolyte may be aqueous K_2CO_3 . The flow of hydrogen into the cell may be controlled by controlling the electrolysis current with an electrolysis power controller.

Plasma gas flows from the plasma gas supply 612 via passage 632. The flow of plasma gas can be controlled by plasma gas flow controller 634 and valve 636. A mixture of plasma gas and hydrogen can be supplied to the cell via passage 626. The mixture is controlled by hydrogen-plasma-gas mixer and mixture flow regulator 621. The plasma gas such as helium may be a source of catalyst such as He^+ or He_2^+ , argon may be a source of catalyst such as Ar^+ , neon may serve as a source of catalyst such as Ne_2^+ or Ne^+ , and neon-hydrogen mixture may serve as a source of catalyst such as Ne^+/H^+ . The source of catalyst and hydrogen of the mixture flow into the plasma and become catalyst and atomic hydrogen in the chamber 660.

The plasma may be powered by a microwave generator 624 wherein the microwaves are tuned by a tunable microwave cavity 622, carried by waveguide 619, and can be delivered to the chamber 660 through an RF transparent window 613 or antenna 615. Sources of microwaves known in the art are traveling wave tubes, klystrons, magnetrons, cyclotron resonance masers, gyrotrons, and free electron lasers. The waveguide or antenna may be inside or outside of the cell. In the latter case, the microwaves may penetrate the cell from the source through a window of the cell 613. The microwave window may comprise Alumina or quartz.

In another embodiment, the cell 601 is a microwave resonator cavity. In an embodiment, the source of microwave supplies sufficient microwave power density to the cell to ionize a source of catalyst such as at least one of helium, neon-hydrogen mixture, and argon gases to form a catalyst such as He^+ , Ne^+ , and Ar^+ , respectively. In such an embodiment, the microwave power source or applicator such as an antenna, waveguide, or cavity forms a nonthermal plasma wherein the species corresponding to the source of catalyst such as helium or argon atoms and ions have a higher temperature than that at thermal equilibrium. Thus, higher energy states such as ionized states of the source of catalyst are predominant over that of hydrogen compared to a corresponding thermal plasma wherein excited states of hydrogen are predominant. In an embodiment, the source of catalyst is in excess compared to the source of hydrogen atoms such that the formation of a nonthermal plasma is favored. The power supplied by the source of microwave power may be delivered to the cell such that it is dissipated in the formation of energetic electrons within about the electron mean free path. In an embodiment, the total pressure is about 0.5 to about 5 Torr and the mean electron free path is about 0.1 cm to 1 cm. In an embodiment, the dimensions of the cell are greater than the electron mean free path. In an embodiment, the cavity is at least one of the group of a reentrant cavity such as an Evenson cavity, Beenakker, McCarrol, and cylindrical cavity. In an embodiment, the cavity provides a strong electromagnetic field which may form a nonthermal plasma. The strong electromagnetic field may be due to a TM_{010} mode of a cavity such as a Beenakker cavity. In a preferred embodiment, the cavity provides an E mode rather than an M mode. In a preferred embodiment, the cavity is a reentrant cavity such as an Evenson cavity that forms a plasma with an E mode. Multiple sources of microwave power may be used simultaneously. For example, the microwave plasma such as a nonthermal plasma may be maintained by multiple Evenson cavities operated in parallel to form the plasma in the microwave cell 601. The cell may be cylindrical and may comprise a quartz cell with Evenson cavities spaced along the longitudinal axis. In another embodiment, a multi slotted antenna

such as a planar antenna serves as the equivalent of multiple sources of microwaves such as dipole-antenna-equivalent sources. One such embodiment is given in Y. Yasaka, D. Nozaki, M. Ando, T. Yamamoto, N. Goto, N. Ishii, T. Morimoto, "Production of large-diameter plasma using multi-slotted planar antenna," *Plasma Sources Sci. Technol.*, Vol. 8, (1999), pp. 530-533
5 which is incorporated herein by reference in its entirety.

In an embodiment, of the hydrogen microwave power and plasma cell and reactor, the output power is optimized by using a cavity such as a reentrant cavity such as an Evenson cavity and tuning the cell to an optimal voltage staging wave. In an embodiment, the reflected versus input power is tuned such that a desired voltage standing wave is obtained which
10 optimizes or controls the output power. Typically, the ratio of the maximum voltage to the minimum voltage on the transmission line determines the voltage standing wave. In another embodiment, the cell comprises a tunable microwave cavity having a desired voltage standing wave to optimize and control the output power.

The cell may further comprise a magnet such as a solenoidal magnet 607 to provide an
15 axial magnetic field. The ions such as electrons formed by the hydrogen catalysis reaction produce microwaves to at least partially maintain the microwave discharge plasma. The microwave frequency may be selected to efficiently form atomic hydrogen from molecular hydrogen. It may also effectively form ions that serve as catalysts from a source of catalyst such as He^+ , Ne^+ , Ne^+ / H^+ , or Ar^+ catalysts from helium, neon, neon-hydrogen mixtures,
20 and argon gases, respectively.

The microwave frequency is preferably in the range of about 1 MHz to about 100 GHz, more preferably in the range about 50 MHz to about 10 GHz, most preferably in the range of about 75 MHz \pm 50 MHz or about 2.4 GHz \pm 1 GHz.

A hydrogen dissociator may be located at the wall of the reactor to increase the atomic
25 hydrogen concentrate in the cell. The reactor may further comprise a magnetic field wherein the magnetic field may be used to provide magnetic confinement to increase the electron and ion energy to be converted into power by means such as a magnetohydrodynamic or plasmadynamic power converter.

A vacuum pump 610 may be used to evacuate the chamber 660 through vacuum lines
30 648 and 650. The cell may be operated under flow conditions with the hydrogen and the catalyst supplied continuously from catalyst source 612 and hydrogen source 638. The amount of gaseous catalyst may be controlled by controlling the plasma gas flow rate where the plasma gas includes a hydrogen and a source of catalyst (e.g., hydrogen and argon or helium). The

amount of gaseous hydrogen atoms to the plasma may be controlled by controlling the hydrogen flow rate and the ratio of hydrogen to plasma gas in the mixture. The hydrogen flow rate and the plasma gas flow rate to the hydrogen-plasma-gas mixer and mixture flow regulator 621 are controlled by flow rate controllers 634 and 644, and by valves 636 and 646. Mixer 5 regulator 621 controls the hydrogen-plasma mixture to the chamber 660. The catalysis rate is also controlled by controlling the temperature of the plasma with microwave generator 624.

Catalysis may occur in the gas phase. Hydrino atoms, dihydrino molecular ions, dihydrino molecules, and hydrino hydride ions are produced in the plasma 604. Dihydrino molecules and hydrino hydride compounds may be cryopumped onto the wall 606, or they may 10 flow into a 608 such as a cryotrap through passage 648. Trap 608 communicates with vacuum pump 610 through vacuum line 650 and valve 652. A flow to the trap 608 can be effected by a pressure gradient controlled by the vacuum pump 610, vacuum line 650, and vacuum valve 652.

In another embodiment of the hydrogen microwave reactor shown in FIGURE 8, the 15 wall 606 has a catalyst supply passage 656 for passage of the gaseous catalyst from a catalyst reservoir 658 to the plasma 604. The catalyst in the catalyst reservoir 658 can be heated by a catalyst reservoir heater 666 having a power supply 668 to provide the gaseous catalyst to the plasma 604. The catalyst vapor pressure can be controlled by controlling the temperature of the catalyst reservoir 658 by adjusting the heater 666 with its power supply 668. The catalyst 20 in the gas phase may comprise those given in TABLES 1 and 3, hydrinos, and those described in the Mills Prior Publication.

In another embodiment of the hydrogen microwave reactor, a chemically resistant open container such as a ceramic boat located inside the chamber 660 contains the catalyst. The reactor further comprises a heater that may maintain an elevated temperature. The cell can be 25 operated at an elevated temperature such that the catalyst in the boat is sublimed, boiled, or volatilized into the gas phase. Alternatively, the catalyst in the catalyst boat can be heated with a boat heater having a power supply to provide the gaseous catalyst to the plasma. The catalyst vapor pressure can be controlled by controlling the temperature of the cell with a cell heater, or by controlling the temperature of the boat by adjusting the boat heater with an associated power 30 supply.

In an embodiment, the hydrogen microwave reactor further comprises a structure interact with the microwaves to cause localized regions of high electric and/or magnetic field strength. A high magnetic field may cause electrical breakdown of the gases in the plasma

chamber 660. The electric field may form a nonthermal plasma that increases the rate of catalysis by methods such as the formation of the catalyst from a source of catalyst. The source of catalyst may be argon, neon-hydrogen mixture, helium to form He^+ , Ne^+ , and Ar^+ , respectively. The structures and methods are similar to those given in the Plasma Torch Cell
5 Hydride Reactor section of my previous published PCT/US02/06945.

The nonthermal plasma temperature corresponding to the energetic ion and/or electron temperature as opposed to the relatively low energy thermal neutral gas temperature in the microwave cell reactor is advantageously maintained in the range of about 5,000-5,000,000 °C. The cell may be operated without heating or insulation. Alternatively, in the case that the
10 catalyst has a low volatility, the cell temperature is maintained above that of the catalyst source, catalyst reservoir 658 or catalyst boat to prevent the catalyst from condensing in the cell. The operating temperature depends, in part, on the nature of the material comprising the cell. The temperature for a stainless steel alloy cell is preferably about 0-1200°C. The temperature for a molybdenum cell is preferably about 0-1800 °C. The temperature for a
15 tungsten cell is preferably about 0-3000 °C. The temperature for a glass, quartz, or ceramic cell is preferably about 0-1800 °C.

The molecular and atomic hydrogen partial pressures in the chamber 660, as well as the catalyst partial pressure, is preferably maintained in the range of about 1 mtorr to about 100 atm. Preferably the pressure is in the range of about 100 mtorr to about 1 atm, more preferably
20 the pressure is about 100 mtorr to about 20 torr.

An exemplary plasma gas for the hydrogen microwave reactor is argon. Exemplary flow rates are about 0.1 standard liters per minute (slm) hydrogen and about 1 slm argon. An exemplary forward microwave input power is about 1000 W. The flow rate of the plasma gas or hydrogen-plasma gas mixture such as at least one gas selected for the group of hydrogen,
25 argon, helium, argon-hydrogen mixture, helium-hydrogen mixture, water vapor, ammonia is preferably about 0-1 standard liters per minute per cm^3 of vessel volume and more preferably about 0.001-10 sccm per cm^3 of vessel volume. In the case of an helium-hydrogen, neon-hydrogen, or argon-hydrogen mixture, preferably helium, neon, or argon is in the range of about 99 to about 1 %, more preferably about 99 to about 95%. The power density of the
30 source of plasma power is preferably in the range of about 0.01 W to about 100 W/ cm^3 vessel volume.

In other embodiments of the microwave reactor, the catalyst may be agitated and supplied through a flowing gas stream such as the hydrogen gas or plasma gas which may be

an additional source of catalyst such as helium or argon gas. The source of catalyst may also be provided by an aspirator, atomizer, or nebulizer to form an aerosol of the source of catalyst. The catalyst which may become an aerosol may be dissolved or suspended in a liquid medium such as water. The medium may be contained in the catalyst reservoir 614. Alternatively, the aspirator, atomizer, or nebulizer may inject the source of catalyst or catalyst directly into the plasma 604. In another embodiment, the nebulized or atomized catalyst may be carried into the plasma 604 by a carrier gas, such as hydrogen, helium, neon, or argon where the helium, neon-hydrogen, or argon may be ionized to He^+ , Ne^+ , or Ar^+ , respectively, and serve as hydrogen catalysts.

Hydrogen may serve as the catalyst according to Eqs. (30-32). In an embodiment the catalysis of atomic hydrogen to form increased-binding-energy-hydrogen species is achieved with a hydrogen plasma. The cavity may be reentrant cavity such as an Evenson cavity. The hydrogen pressure may be in the range of about 1 mtorr to about 100 atm. Preferably the pressure is in the range of about 100 mtorr to about 1 atm, more preferably the pressure is about 100 mtorr to about 10 torr. The microwave power density may be in the range of about 0.01 W to about 100 W/cm³ vessel volume. The hydrogen flow rate may be in the range of about 0-1 standard liters per minute per cm³ of vessel volume and more preferably about 0.001-10 sccm per cm³ of vessel volume.

The microwave cell may be interfaced with any of the converters of plasma or thermal energy to mechanical or electrical power described herein such as the magnetic mirror magnetohydrodynamic power converter, plasmadynamic power converter, or heat engine, such as a steam or gas turbine system, sterling engine, or thermionic or thermoelectric converter given in Mills Prior Publications. In addition it may be interfaced with the gyrotron, photon bunching microwave power converter, charge drift power, or photoelectric converter as disclosed in Mills Prior Publications.

The hydrogen microwave reactor further includes an electron source in contact with the hydrinos, for generating hydrino hydride ions. In the cell, the hydrinos may be reduced to hydrino hydride ions by contacting a reductant extraneous to the operation of the cell (e.g. a consumable reductant added to the cell from an outside source). In an embodiment, the microwave cell reactor further comprise a selective valve 618 for removal of lower-energy hydrogen products such as dihydrino molecules. Compounds comprising a hydrino hydride anion and a cation may be formed in the gas cell. The cation which forms the hydrino hydride compound may comprise a cation of other element, a cation of an oxidized added reductant, or

a cation present in the plasma (such as a cation of the catalyst).

Metal hydrido hydrides may be formed in the microwave plasma reactor having a hydrogen plasma and a source of metal such as a source of the metals given in TABLE 3 that serve as both the catalyst and the reactant. The metal atoms may be provided by vaporization through heating. In one embodiment, the metal is vaporized from a hot filament containing the metal. The vapor pressure of the metal is maintained in the range 0.001 Torr to 100 Torr and the hydrogen plasma is maintained in the range 0.001 Torr to 100 Torr. Preferably the range for both metal and hydrogen is 0.1 Torr to 10 Torr.

3. Hydrogen Capacitively and Inductively Coupled RF Plasma and Power Cell and Reactor

According to an embodiment of the invention, a reactor for producing power and at least one of hydridos, hydrido hydride ions, dihydrido molecular ions, and dihydrido molecules may take the form of a hydrogen capacitively or inductively coupled RF power and plasma cell and reactor. A hydrogen RF plasma reactor of the present invention is also shown in FIGURE 8. The cell structures, systems, catalysts, and methods may be the same as those given for the microwave plasma cell reactor except that the microwave source may be replaced by a RF source 624 with an impedance matching network 622 that may drive at least one electrode and/or a coil. The RF plasma cell may further comprise two electrodes 669 and 670. The coaxial cable 619 may connect to the electrode 669 by coaxial center conductor 615. Alternatively, the coaxial center conductor 615 may connect to an external source coil which is wrapped around the cell 601 which may terminate without a connection to ground or it may connect to ground. The electrode 670 may be connected to ground in the case of the parallel plate or external coil embodiments. The parallel electrode cell may be according to the industry standard, the Gaseous Electronics Conference (GEC) Reference Cell or modification thereof by those skilled in the art as described in G. A. Hebner, K. E. Greenberg, "Optical diagnostics in the Gaseous electronics Conference Reference Cell, J. Res. Natl. Inst. Stand. Technol., Vol. 100, (1995), pp. 373-383; V. S. Gathen, J. Ropcke, T. Gans, M. Kaning, C. Lukas, H. F. Dobeles, "Diagnostic studies of species concentrations in a capacitively coupled RF plasma containing $CH_4 - H_2 - Ar$," Plasma Sources Sci. Technol., Vol. 10, (2001), pp. 530-539; P. J. Hargis, et al., Rev. Sci. Instrum., Vol. 65, (1994), p. 140; Ph. Belenguer, L. C. Pitchford, J. C. Hubinois, "Electrical characteristics of a RF-GD-OES cell," J. Anal. At. Spectrom., Vol. 16, (2001), pp. 1-3 which are herein incorporated by reference in their entirety.

The cell which comprises an external source coil such as a 13.56 MHz external source coil microwave plasma source is as given in D. Barton, J. W. Bradley, D. A. Steele, and R. D. Short, "investigating radio frequency plasmas used for the modification of polymer surfaces," *J. Phys. Chem. B*, Vol. 103, (1999), pp. 4423-4430; D. T. Clark, A. J. Dilks, *J. Polym. Sci. Polym. Chem. Ed.*, Vol. 15, (1977), p. 2321; B. D. Beake, J. S. G. Ling, G. J. Leggett, *J. Mater. Chem.*, Vol. 8, (1998), p. 1735; R. M. France, R. D. Short, *Faraday Trans. Vol. 93*, No. 3, (1997), p. 3173, and R. M. France, R. D. Short, *Langmuir*, Vol. 14, No. 17, (1998), p. 4827 which are herein incorporated by reference in their entirety. At least one wall of the cell 601 wrapped with the external coil is at least partially transparent to the RF excitation. The RF frequency is preferably in the range of about 100 Hz to about 100 GHz, more preferably in the range about 1 kHz to about 100 MHz, most preferably in the range of about 13.56 MHz \pm 50 MHz or about 2.4 GHz \pm 1 GHz.

In another embodiment, an inductively coupled plasma source is a toroidal plasma system such as the Astron system of Astex Corporation described in US Patent No. 6,150,628 which is herein incorporated by reference in its entirety. In an embodiment, the field strength is high to cause a nonthermal plasma. The toroidal plasma system may comprise a primary of a transformer circuit. The primary may be driven by a radio frequency power supply. The plasma may be a closed loop which acts as a secondary of the transformer circuit. The RF frequency is preferably in the range of about 100 Hz to about 100 GHz, more preferably in the range about 1 kHz to about 100 MHz, most preferably in the range of about 13.56 MHz \pm 50 MHz or about 2.4 GHz \pm 1 GHz.

In an embodiment, the plasma cell is driven by at least one of a traveling and a standing wave plasma generators such as given in Fossa [A. C. Fossa, M. Moisan, M. R. Wertheimer, "vacuum ultraviolet to visible emission from hydrogen plasma: effect of excitation frequency", *Journal of Applied Physics*, Vol. 88, No. 1, (2000), pp. 20-33 which is herein incorporated by reference in its entirety].

In another embodiment, the frequency of the cell is 50 kHz and is driven by a radio frequency generator such as that given by Bzenic et. al. [S. A. Bzenic, S. B. Radovanov, S. B. Vrhovac, Z. B. Velikic, and B. M. Jelenkovic, "On the mechanism of Doppler broadening of H_β after dissociative excitation in hydrogen glow discharges", *Chem. Phys. Lett.*, Vol. 184, (1991), pp. 103-112 which is herein incorporated by reference in its entirety].

In another embodiment of the plasma cell for the production of power and lower-energy-hydrogen compounds, the cell comprises a helicon as described in Asian Particle

Accelerator Conference (APAC98), March 26th – Poster Presentation 6D-061, Development of DC Accelerator Ion Sources using Helicon Plasmas p.825, G.S. Eom, I.S. Hong, Y.S. Hwang, KAIST, Taejeon,

<<http://accelconf.web.cern.ch/AccelConf/a98/APAC98/6D061.PDF>><http://accelconf.web.cern.ch/AccelConf/a98/APAC98/6D061.PDF>

5 ch/AccelConf/a98/APAC98/6D061.PDF which is herein incorporated by reference in its entirety.

4. Plasma Confinement by Spatially Controlling Catalysis

The plasma formed by the catalysis of hydrogen may be confined to a desired region of
10 the reactor by structures and methods such as those that control the source of catalyst, the source of atomic hydrogen, or the source of an electric or magnetic field which alters the catalysis rate as given in the Adjustment of Catalysis Rate section. In an embodiment, the reactor comprises two electrodes, which provide an electric field to control the catalysis rate of atomic hydrogen. The electrodes may produce an electric field parallel to the z-axis. The
15 electrodes may be grids oriented in a plane perpendicular to the z-axis such as grid electrodes 305 and 320 shown in FIGURE 4. The space between the electrodes may define the desired region of the reactor. The electrodes may be used in any or the other reactor of the present invention to catalyze atomic hydrogen to lower-energy states such as a plasma electrolysis reactor, barrier electrode reactor, RF plasma reactor, pressurized gas energy reactor, gas
20 discharge energy reactor, microwave cell energy reactor, and a combination of a glow discharge cell and a microwave and or RF plasma reactor.

In another embodiment, a magnetic field may confine a charged catalyst such as Ar^+ to a desired region to selectively form a plasma as described in the Noble Gas Catalysts and Products section. In an embodiment of the cell, the reaction is maintained in a magnetic field
25 such as a solenoidal or minimum magnetic (minimum B) field such that a second catalyst such as Ar^+ is trapped and acquires a longer half-life. The second catalyst may be generated by a plasma formed by hydrogen catalysis using a first catalyst. By confining the plasma, the ions such as the electrons become more energetic, which increases the amount of second catalyst such as Ar^+ . The confinement also increases the energy of the plasma to create more atomic
30 hydrogen.

In another embodiment, a hot filament which dissociates molecular hydrogen to atomic hydrogen and which may also provide an electric field that controls the rate of catalysis may be used to define the desired region in the cell. The plasma may form substantially in the region

surrounding the filament wherein at least one of the atomic hydrogen concentration, the catalyst concentration, and the electric field provides a much faster rate of catalysis there than in any undesired region of the reactor.

In another embodiment, the source of atomic hydrogen such as the source of molecular hydrogen or a hydrogen dissociator may be used to determine the desired region of the reactor by providing atomic hydrogen selectively in the desired region.

In an another embodiment, the source of catalyst may determine the desired region of the reactor by providing catalyst selectively in the desired region.

In an embodiment of a microwave power cell, the plasma may be maintained in a desired region by selectively providing microwave energy to that region with at least one antenna 615 or waveguide 619 and RF window 613 shown in FIGURE 8. The cell may comprise a microwave cavity which causes the plasma to be localized to the desired region.

5. Hydrogen Multicusp Power and Plasma Cell and Reactor

In an embodiment, the power and plasma cell and reactor comprises a filament, a vacuum vessel capable of pressures above and below atmospheric, a source of atomic hydrogen, a source of catalyst to catalyze atomic hydrogen to a lower-energy state given by Eq. (1), a means to negatively bias the walls of the cell relative to the filament, and magnets to confine a plasma generated in the cell which is formed or enhanced by the catalysis reaction (rt-plasma). In an embodiment, the reactor is described in M. Pealat, J. P. E. Taran, M. Bacal, F. Hillion, J. Chem. Phys., Vol. 82, (1985), p. 45943-4953 and J. Perrin, J. P. M. Schmitt, Chem. Phys. Letts., Vol. 112, (1984), pp. 69-74 which are herein incorporated by reference in their entirety. In this case, in addition, the cell further comprises a source of catalyst to catalyze atomic hydrogen to a lower-energy state given by Eq. (1). An embodiment of the multicusp cell is shown in FIGURE 3 wherein the walls are negative biased by a power supply, and magnets such as permanent magnets that enclose the cell to confine the plasma generated inside the cell 200.

6. Hydrogen Laser

Another objective of the present invention is to create an inverted population of an energy level of a species such as an atom, molecule, or ion capable of lasing. The inverted population forms due to catalysis of atomic hydrogen to lower-energy states. The present invention further comprises a laser wherein the catalysis cell serves as the laser cavity, and an

inverted population is formed due to hydrogen catalysis to lower energy states given by Eq. (1).

An embodiment of the hydrogen laser of the present invention comprises a reactor of the present invention to catalyze atomic hydrogen to lower-energy states such as an rt-plasma cell and a plasma electrolysis reactor, a barrier electrode reactor, an RF plasma reactor, a
5 pressurized gas energy reactor, a gas discharge energy reactor, a microwave cell energy reactor, and a combination of a glow discharge cell and a microwave and or RF plasma reactor. An embodiment of a water plasma laser shown in FIGURE 9 comprises a cavity that is a reactor such as a quartz tube 501 and means to maintain a water vapor plasma in the cavity such a microwave generator 502, and a microwave cavity 503. The microwave cavity preferably
10 maintains an E mode such as an Evenson cavity which is a reentrant cavity. The source of water vapor may be water from a supply of deionized water such as a water reservoir 511 with a valved connection 517 to a water vapor generator 505 which may comprise a vessel with thermal insulation and a heater 515 and a temperature measurement device such as a thermocouple 516 with a supply line 506 to the cell 501. The flow may be controlled by a
15 valve 507 and a mass flow controller 508. The pressure may be read with a pressure gauge 509. The water vapor may be flowed through the cell to a vacuum pump 510 through vacuum line 504 which also maintains the pressure in the cell with the valve 507 and mass flow controller 508.

In an embodiment, the water vapor pressure is maintained in the range of about 0.1
20 mTorr to 10,000 Torr, preferably the water vapor pressure of the water vapor plasma is in the range of 10 mTorr to 100 Torr; more preferably, the water vapor pressure of the water vapor plasma is in the range of 10 mTorr to 10 Torr, and most preferably, the water vapor pressure of the water vapor plasma is in the range of 10 mTorr to 1 Torr. The water vapor flow rate is preferably about 0-1 standard liters per minute per cm^3 of vessel volume and more preferably
25 about 0.001-10 sccm per cm^3 of vessel volume. The power density of the source of plasma power is preferably in the range of about 0.01 W to about 100 W/ cm^3 vessel volume; more preferably it is in the range of about 1 to 10 W/ cm^3 vessel volume.

In an embodiment, the water vapor may also be supplied by flowing hydrogen and oxygen into the cell which forms water vapor. The mole fraction of hydrogen and oxygen may
30 be stoichiometric for water. Alternatively, an excess of hydrogen or oxygen may be maintained. Preferably the mole fraction of H_2 or O_2 does not vary from that which is stoichiometric for water by more than about $\pm 99\%$, preferably it differs by less than $\pm 50\%$, more preferably it differs by less than $\pm 10\%$, most preferably it differs by less than $\pm 2\%$.

An further embodiment of the hydrogen laser of the present invention comprises a reactor of the present invention to catalyze atomic hydrogen to lower-energy states such as an rf-plasma cell and a plasma electrolysis reactor, a barrier electrode reactor, an RF plasma reactor, a pressurized gas energy reactor, a gas discharge energy reactor, a microwave cell energy reactor, and a combination of a glow discharge cell and a microwave and or RF plasma reactor. Nitrogen may serve as a catalysis, and the energy of the catalysis reaction may form an inverted hydrogen population. An embodiment of an ammonia plasma laser shown in FIGURE 9 comprises a cavity that is a reactor such as a quartz tube 501 and means to maintain an ammonia plasma in the cavity such a microwave generator 502, and a microwave cavity 503. The microwave cavity preferably maintains a reentrant cavity such as one with an E mode such as an Evenson cavity. The source of ammonia may be ammonia from a supply such as gaseous source 515 with a supply line 506 to the cell 501. The flow may be controlled by a valve 507 and a mass flow controller 508. The pressure may be read with a pressure gauge 509. The ammonia may be flowed through the cell to a vacuum pump 510 through vacuum line 504 which also maintains the pressure in the cell with the valve 507 and mass flow controller 508.

In an embodiment, the ammonia pressure is maintained in the range of about of 0.1 mTorr to 10,000 Torr, preferably the ammonia pressure of the ammonia plasma is in the range of 10 mTorr to 100 Torr; more preferably, the ammonia pressure of the ammonia plasma is in the range of 10 mTorr to 10 Torr, and mostpreferably, the ammonia pressure of the ammonia plasma is in the range of 10 mTorr to 1 Torr. The ammonia flow rate is preferably about 0-1 standard liters per minute per cm^3 of vessel volume and more preferably about 0.001-10 secm per cm^3 of vessel volume. The power density of the source of plasma power is preferably in the range of about 0.01 W to about 100 W/ cm^3 vessel volume; more preferably it is in the range of about 1 to 10 W/ cm^3 vessel volume.

In an embodiment, the ammonia may also be supplied by flowing hydrogen and nitrogen into the cell which forms ammonia. The mole fraction of hydrogen and nitrogen may be stoichiometric for ammonia. Alternatively, an excess of hydrogen or nitrogen may be maintained. Preferably the mole fraction of H_2 or N_2 does not vary from that which is stoichiometric for ammonia by more than about $\pm 99\%$, preferably it differs by less than $\pm 50\%$, more preferably it differs by less than $\pm 10\%$, most preferably it differs by less than $\pm 2\%$.

An inverted population is formed by the catalysis of atomic hydrogen. In one

embodiment, the hydrogen nonradiatively transfers energy to the catalyst, and the remaining energy may be emitted until the next stable electronic state is achieved with energy given by Eq. (1). The energy transfer may yield $H(n > 2)$ atoms directly by multipole coupling [R. L. Mills, P. Ray, B. Dhandapani, J. He, "Spectroscopic Identification of Fractional Rydberg States of Atomic Hydrogen Formed by a Catalytic Helium-Hydrogen Plasma Reaction", Applied Spectroscopy: General, submitted which is herein incorporated by reference in its entirety] and fast $H(n = 1)$ atoms. The energy transfer may occur to a third body such as atomic hydrogen or molecular hydrogen to form fast H as reported previously [R. L. Mills, P. Ray, B. Dhandapani, J. He, "Comparison of Excessive Balmer α Line Broadening of Glow Discharge and Microwave Hydrogen Plasmas with Certain Catalysts", J. of Applied Physics, January, 1, (2003) which is herein incorporated by reference in its entirety]. Then, excited state H may be formed from fast $H(n = 1)$ atoms by collisions with the background gas such as H_2 . Inversion may be achieved by collisions with heavier gases or gases which provide a resonant excitation by the collision with fast H such as at least one molecule from the list of O_2 , H_2O , CO_2 , N_2 , NO_2 , NO , CO , and a halogen gas.

Laser oscillators occur in the cavity 501 which has the appropriate dimensions and mirrors for lasing that is known to those skilled in the art as described in J. J. Ewing, "Excimer Lasers", *Laser Handbook*, Edited by M. L. Stitch, North-Holland Publishing Company, Vol. A4, (1979); *Laser Handbook*, Edited by F. T. Arecchi and E. O. Schulz-Dubois, North-Holland Publishing Company, Amsterdam, 1972-, Vol. 1-6 which are herein incorporated by reference in their entirety. The laser light is contained in the cavity 501 between the mirrors 512 and 513. The mirror 513 may be semitransparent, and the light may exit the cavity through this mirror.

In an embodiment, the laser medium comprises an excimer comprising at least one hydrino atom that is undergoing a transition to a lower-energy state. Hydrogen transitions from continuum excited states may couple to fractional Rydberg transitions of the same multipolarity as broad excimer emission. In an embodiment, the excimer is formed by a helium-hydrogen microwave discharge. For example, the novel emission lines observed at 44.2 nm and 40.5 nm described in R. L. Mills, P. Ray, B. Dhandapani, J. He, "Spectroscopic Identification of Fractional Rydberg States of Atomic Hydrogen Formed by a Catalytic Helium-Hydrogen Plasma Reaction", Applied Spectroscopy: General, submitted which incorporated by reference in its entirety correspond to energies of

$$q \cdot 13.6 + \left(\frac{1}{n_f^2} - \frac{1}{n_i^2} \right) \times 13.6 \text{ eV where } q = 2 \text{ and } n_f = 2, 4 \text{ } n_i = \infty \text{ and can be explained by}$$

multipole coupling of the transitions to $n = 1/4$ and $n = 1/2$ with the transition from continuum states to $n = 4$ and $n = 2$, respectively, to give two photon emission. This excimer emission is the basis of a laser of the present invention using techniques well known to those skilled in the art as given in J. J. Bwing. "Excimer Lasers", *Laser Handbook*, Edited by M. L. Stich, North-Holland Publishing Company, Vol. A4, (1979); *Laser Handbook*, Edited by F. T. Arecchi and E. O. Schulz-Dubois, North-Holland Publishing Company, Amsterdam, 1972-, Vol. 1-6 which are herein incorporated by reference in their entirety.

A laser according to the preset invention is shown in FIGURE 10. It comprises a plasma of a catalyst and hydrogen and laser optics. The plasma may be maintained in an rt-plasma reactor, a plasma electrolysis reactor, a barrier electrode reactor, an RF plasma reactor, a pressurized gas energy reactor, a gas discharge energy reactor, a-microwave cell energy reactor, and a combination of a glow discharge cell and a microwave and or RF plasma reactor. The plasma 400 may be a microwave water vapor plasma (microwave generator and cavity are shown in FIGURE 9). The plasma gas containing hydrogen and catalyst such as water vapor may flow through the plasma cell via inlet 401 and outlet 402. The laser beam 412 and 413 is directed to a high reflectivity mirror 405 such as a 95 to 99.9999% reflective spherical cavity mirror and to the output coupler 406 by windows 403 and 404 such as Brewster angle windows. The output coupler may have a transmission in the range 0.1 to 50%, and preferably in the range 1 to 10%. The beam power may be measured by a power meter 407. The laser may mounted on an optical rail 408 on an optical table 411 which allows for adjustments of the cavity length to achieve lasing at a desired wavelength. Vibrations may ameliorated by vibration isolation feet 409. The plasma tube may be supported by a plasma tube support structure 410.

An embodiment of a hydrogen rt-plasma laser shown in FIGURE 11 comprises a cavity that is a reactor such as a quartz tube 551 and a source of catalyst such as those given in Tables 1 and 3 that produce a plasma when heated with atomic hydrogen as described in R. Mills, J. Dong, Y. Lu, "Observation of Extreme Ultraviolet Hydrogen Emission from Incandescently Heated Hydrogen Gas with Certain Catalysts", *Int. J. Hydrogen Energy*, Vol. 25, (2000), pp. 919-943 which is herein incorporated by reference in its entirety. A source of catalyst such as at least one of KNO_3 and $RbNO_3$ may be coated on to a hydrogen dissociator 552 such as a titanium screen. The hydrogen may be dissociated by a hot filament such as a tungsten

filament 553 which may heat the hydrogen dissociator 552 as well as heat the catalyst. In an embodiment, the catalyst is vaporized by the heating and reacts with atomic hydrogen to form the resonance transfer or rt-plasma due to hydrogen catalysis. The hydrogen may be flowed through the cell from a source 560 through the inlet 554 controlled by valve 561 and mass flow controller 555. In addition, the gas flow and pressure may be maintained and controlled with pump 557 through cell outlet 556 together with valve 561 and flow controller 555. The pressure may be read with pressure gauge 563. Embodiments of conditions for operation of the rt-plasma laser cell are given in the Gas Power, Plasma, and Hydride Reactor section.

The catalysis of atomic hydrogen forms an rt-plasma with an inverted hydrogen population. Laser oscillators occur in the cavity 551 which has the appropriate dimensions and mirrors for lasing that is known to those skilled in the art as described in *Laser Handbook*, Edited by F. T. Arecchi and E. O. Schulz-Dubois, North-Holland Publishing Company, Amsterdam, 1972-, Vol. 1-6 which is herein incorporated by reference in its entirety. The laser light is contained in the cavity 551 between the mirrors 558 and 559. The mirror 558 may be semitransparent, and the light may exit the cavity through this mirror.

6.1 Exemplary Water-Plasma Laser

The laser set up shown in FIGURE 9 comprised a quartz tube cell, a source of water vapor or ultrapure hydrogen, a flow system, and a pump. Water vapor was formed in a heated insulated reservoir and flowed through the half inch diameter quartz tube at a flow rate of 10 standard $\text{cm}^3 \cdot \text{s}^{-1}$ (sccm) at a corresponding pressure of 50-100 milli Torr. At this pressure, room temperature was sufficient for maintaining the water vapor. The tube was fitted with an Evenson coaxial microwave cavity (Ophos) having an E-mode [F. C. Fehsenfeld, K. M. Evenson, H. P. Broida, "Microwave discharges operating at 2450 MHz", Review of scientific Instruments, Vol. 35, No. 3, (1965), pp. 294-298; B. McCarroll, "An improved microwave discharge cavity for 2450 MHz", Review of Scientific Instruments, Vol. 41, (1970), p. 279 which are herein incorporated by reference in their entirety]. The input power to the plasma at 2.45 GHz by an Ophos model MPG-4M generator was set at 50 W and 90 W as described previously [R. Mills, P. Ray, "Spectral Emission of Fractional Quantum Energy Levels of Atomic Hydrogen from a Helium-Hydrogen Plasma and the Implications for Dark Matter", Int. J. Hydrogen Energy, Vol. 27, No. 3, pp. 301-322 which is herein incorporated by reference in its entirety]. The water vapor gas flow was controlled by a 0-20 sccm range mass flow controller (MKS 1179A21CS1BB) with a readout (MKS type 246). The cell pressure was

monitored by a 0-10 Torr MKS Baratron absolute pressure gauge.

Inverted Balmer and Lyman populations were achieved as shown in R. Mills, P. Ray, R. M. Mayo, "Stationary Inverted Balmer and Lyman Populations for a CW III Water-Plasma Laser", IEEE Transactions on Plasma Science, submitted and R. Mills, P. Ray, R. M. Mayo, "Spectroscopic Evidence for CW H I Lasing in a Water-Plasma", J. of Applied Physics, submitted which are herein incorporated by reference in their entirety. Laser oscillations occur between mirrors at opposite ends of the cavity shown in FIGURE 9. One of the mirrors is semi transparent to allow the laser light to exit. Appropriate mirrors and cavity dimensions are used as known by those skilled in the art.

10

6.2 Exemplary rt-plasma Laser

The laser set up shown in FIGURE 11 and described previously [R. Mills and M. Nansteel, P. Ray, "Argon-Hydrogen-Strontium Discharge Light Source", IEEE Transactions on Plasma Science, Vol. 30, No. 2, (2002), pp. 639-653] was used to maintain rt-plasmas of hydrogen with KNO_3 and $RbNO_3$. It comprised a thermally insulated quartz cell with a cap that incorporated ports for gas inlet, outlet, and photon detection. A tungsten filament heater and hydrogen dissociator were in the quartz tube as well as a cylindrical titanium screen that served as a second hydrogen dissociator that was coated with catalysts KNO_3 , $RbNO_3$. The cell was maintained at 50 °C for four hours with helium flowing at 30 sccm at a pressure of 0.1 Torr. The cell was then operated with and without an ultrapure hydrogen flow rate of 5.5 sccm maintained at 300 mTorr. The titanium screen was electrically floated with 250 W of power applied to the filament. The temperature of the tungsten filament was estimated to be in the range 1100 to 1500 °C. The external cell wall temperature was about 700 °C.

Inverted Balmer and Lyman populations were achieved as shown in R. Mills, P. Ray, R. Mayo, "Chemically-Generated Stationary Inverted Lyman Population for a CW HI Laser", J Vac. Sci. and Tech. A, submitted and R. Mills, P. Ray, R. M. Mayo, "CW HI Laser Based on a Stationary Inverted Lyman Population Formed from Incandescently Heated Hydrogen Gas with Certain Group I Catalysts", IEEE Transactions on Plasma Science, in press which are herein incorporated by reference in their entirety. Laser oscillations occur between mirrors at opposite ends of the cavity shown in FIGURE 11. One of the mirrors is semi transparent to allow the laser light to exit. Appropriate mirrors and cavity dimensions are used as known by those skilled in the art.

6.3 Photon Power to Electricity Conversion

The present invention of a hydrogen power and plasma cell and reactor further comprises a power converter comprising a hydrogen catalysis cell that produces atoms having binding energies given by Eq. (1) and at least one of a high population of electronically excited state atoms such as hydrogen atoms and an inverted population such as an atomic hydrogen inverted population. The power is emitted as photons with spontaneous emission or stimulated emission. The light is converted to electricity using a photon-to-electric converter of the present invention such as a photoelectric or photovoltaic cell. In an embodiment, the power cell further comprises a hydrogen laser of the present invention.

10 In an embodiment, the photons exit the semitransparent mirror of the laser cavity and irradiate a photovoltaic cell. The laser power may be converted to electricity using photovoltaic cells as described in the following references of photovoltaic cells to convert laser power to electric power which are incorporated by reference in their entirety: L. C. Olsen, D. A. Huber, G. Dunham, F. W. Addis, "High efficiency monochromatic GaAs solar cells", in
15 *Conf. Rec. 22nd IEEE Photovoltaic Specialists Conf.*, Las Vegas, NV, Vol. I, Oct. (1991), pp. 419-424; R. A. Lowe, G. A. Landis, P. Jenkins, "Response of photovoltaic cells to pulsed laser illumination", *IEEE Transactions on Electron Devices*, Vol. 42, No. 4, (1995), pp. 744-751; R. K. Jain, G. A. Landis, "Transient response of gallium arsenide and silicon solar cells under laser pulse", *Solid-State Electronics*, Vol. 4, No. 11, (1998), pp. 1981-1983; P. A. Iles, "Non-
20 solar photovoltaic cells", in *Conf. Rec. 21st IEEE Photovoltaic Specialists Conf.*, Kissimmee, FL, Vol. I, May, (1990), pp. 420-423.

In an embodiment of the laser power converter, using beam forming optics, the laser beam is reduced spread over a larger area as described in L. C. Olsen, D. A. Huber, G. Dunham, F. W. Addis, "High efficiency monochromatic GaAs solar cells", in *Conf. Rec. 22nd*
25 *IEEE Photovoltaic Specialists Conf.*, Las Vegas, NV, Vol. I, Oct. (1991), pp. 419-424 which is herein incorporated by reference in its entirety. The beam forming optics may be a lens or a diffuser.

In another embodiment, the spontaneous or stimulated emission is converted to electrical power using a photovoltaic. Conversion of monochromatic spontaneous and/or
30 stimulated emission from the water plasma cell [R. Mills, P. Ray, R. M. Mayo, "Stationary Inverted Balmer and Lyman Populations for a CW HI Water-Plasma Laser", *IEEE Transactions on Plasma Science*, submitted which is herein incorporated by reference in its entirety] to electricity using a photovoltaic with a band gap that is matched to the wavelength

can be achieved at significant power densities and efficiencies using existing photovoltaic (PV) cells. Photocells of the power converter of the present invention that respond to ultraviolet and extreme ultraviolet light comprise radiation hardened conventional cells. Due to the higher energy of the photons potentially higher efficiency is achievable compared to those that convert lower energy photons. The hardening may be achieved by a protective coating such as a
5 atomic layer of platinum or other noble metal.

An embodiment of the power cell and photon-to-electric converter is shown in FIGURE 12. It comprises a vacuum vessel 451, a source of catalyst and hydrogen such as a water vapor generator 452 containing water 453. The catalyst and hydrogen flow to the
10 reaction vessel 451 by a line 454 controlled by a valve 455. The flow through the cell may be maintained by a pump 456, a vacuum line 457, and a vacuum valve 458. A hydrogen and catalyst plasma 459 is maintained in the reaction cell 451 by a plasma generator such as an open mesh microwave cavity 460 powered by a microwave power supply 461. The photons
15 462 generated by the catalysis and microwave input power are received by a photon-to-electric converter 463 such as photovoltaic tiling of the inside of the vacuum vessel 451. The electrical power is delivered to an electrical load 464 by electrical lines 465.

In an embodiment of at least one of a hydrogen microwave and a hydrogen RF plasma cell, a microwave or RF transparent cell such as a quartz tube and a microwave or RF transparent photovoltaic material such as amorphous silicon photovoltaic that is
20 circumferential to the cell are inside of the microwave cavity. The cavity may be a reentrant cavity such as an Evenson cavity. The photovoltaic material may comprise the wall of the cell. The cell may further comprise a cell wall cooler such as an air cooler or a water cooler to maintain the photovoltaic at a desired operating temperature. In an embodiment, the photocell is cooled with a heat pipe. The cell may also comprise mirrors or lenses to direct the light onto
25 the photovoltaic. Mirrors may also be present at the cell wall to increase the path length of light such as hydrogen Lyman series emission to maintain excited states which may be further excited by collisions or photons.

In an embodiment that uses a photovoltaic for power conversion, high energy light may be converted to lower energy light by a phosphor on the transparent walls of the cell so that the
30 photons emitted by the excited phosphor more closely match the peak wavelength efficiency of the photovoltaic. In an embodiment, the phosphor is a gas which efficiently converts short wavelength light of the cell to long wavelength light to which the photovoltaic cell is more responsive.

In an embodiment of the power converter, photons are incident on a photoelectric material that is responsive to the wavelength of the spontaneous emission or laser light such that electrons are ejected and collected at a grid or electrode. The photoelectric material such as barium, tungsten, pure metals (e.g. Cu, Sm), Ba , Cs_2Te , K_2CsSb , LaB_6 , Sb - alkali, $GaAs$ serves as a photocathode (positive electrode) as given in the following references which are incorporated by reference in their entirety: M. D. Van Loy, "Measurements of barium photocathode quantum yields at four excimer wavelengths", *Appl. Phys. Letts.*, Vol. 63, No. 4, (1993), pp. 476-478; S. D. Moustazis, C. Fotakis, J. P. Girardeau-Montaut, "Laser photocathode development for high-current electron source", *Proc. SPIE*, Vol. 1552, pp. 50-56, Short-wavelength radiation sources, Phillip Sprangle, Ed.; D. H. Dowell, S. Z. Bethel, K. D. Friddell, "Results from the average power laser experiment photocathode injector test", *Nuclear Instruments and Methods in Physics Research A*, Vol. 356, (1995), pp. 167-176; A. T. Young, B. D'Etat, G. C. Stutzin, K. N. Leung, W. B. Kunkel, "Nanosecond-length electron pulses from a laser-excited photocathode", *Rev. Sci. Instrum.*, Vol. 61, No. 1, (1990), pp. 650-652; Q. Minquan, et al., "Investigation of photocathode driven by a laser", *Qiangguang Yu Lizishu/High Power Laser and Particle Beams*, *Nucl. Soc. China*, Vol. 9, No. 2, May (1997), pp. 185-191. And, the electron collector serves as an anode (negative electrode). The electrical circuit completed between these electrodes through a load such that the voltage developed between the electrodes drives a current. Thus, electrical power is delivered to and dissipated in the load.

In an embodiment of the hydrogen laser, the inverted population is due to the catalysis of atomic hydrogen to lower energy states wherein $m \cdot 27.2 \text{ eV}$ of energy is nonradiatively transferred from the hydrogen to the catalyst. The remaining energy due to the transition to the corresponding stable state corresponding to a fractional Rydberg state may be transferred to atomic hydrogen which serves as a third body. The resulting fast H may undergo collisions to form excited state hydrogen which comprises an inverted population capable of lasing. In an embodiment, the catalysis mixture contains oxygen in addition to the catalyst and hydrogen. The oxygen may be from a source such as gaseous oxygen or it may be from a source such as a carbonate or a nitrate as given in Mills publication [R. Mills, P. Ray, R. M. Mayo, "CW HI Laser Based on a Stationary Inverted Lyman Population Formed from Incandescently Heated Hydrogen Gas with Certain Group I Catalysts", *IEEE Transactions on Plasma Science*, in press] which is herein incorporated by reference in its entirety. The fast atomic hydrogen formed by catalysis may collide with the oxygen to form the excited state hydrogen which

comprises an inverted population. The laser power may be converted to electricity using a photovoltaic cell.

In an embodiment, a species is added to achieve at least one of atomic hydrogen population inversion or conversion of the power of the catalysis reaction to excited state atomic hydrogen. In an embodiment, the inverting or converting species is a gas comprising at least

one molecule from the list of O_2 , H_2O , CO_2 , N_2 , NO_2 , NO , CO , and a halogen gas. Percentage inverting or converting species in the catalysis reaction mixture is in the range of 0.1% to 99.9%, preferably in the range of 0.1 to 50%, more preferably in the range 1% to 25%, and most preferably in the range of 1% to 5%.

In an embodiment of the power cell, the walls cool the plasma electrons to maintain a low electron temperature while the hydrogen atom temperature is very high so that the condition to achieve an inverted hydrogen atom population are maintained.

In an embodiment of the laser power converter, species which form an excimer are added to the catalytic plasma to absorb the power of the pumping mechanism which forms at least one of a large population of excited states and an inverted population. In an embodiment, the lasing species is at least one of OH^* , CO_2 , and H_2O . In an embodiment, at least one halogen gas is added to the plasma of hydrogen mixed with at least one noble gas such as helium, neon, and argon such that excimers form. The power is extracted by the excimer laser emission. In another embodiment, a species is added which is excited by at least one of the pumping mechanism and an energy transfer from the excited state species such as excited atomic hydrogen. The power is extracted by at least one of spontaneous and stimulated emission of the excited species. The light from the cell may be converted to a different frequency by a phosphor so that the photovoltaic conversion is more efficient.

In an embodiment, the hydrogen reactor and power converter comprises a microwave cavity such as a reentrant cavity such as an Evenson cavity wherein the cavity is comprised of a conductor with open spaces for the propagation of the light generated in the cavity. In an embodiment, the cavity comprises walls of a conducting wire mesh or a grid of wires. In an embodiment, the conductor with open spaces is coated with a dielectric material that is nonconducting to the plasma, but is transparent to microwaves such as quartz or Alumina. The light generated in the cavity may travel through the open areas in the wall with the microwave generated plasma contained substantially in the microwave cavity. The power converter may further comprises a vacuum chamber which is larger than the microwave cavity and contains the cavity and at least one photon-to-electric converter such as at least one of a photovoltaic

cell and a photocathode. The photon-to-electric converter may be at the walls of the vacuum chamber and receive the photons and convert them to electricity. An advantage of the present embodiment, is the conversion of extreme ultraviolet and ultraviolet photons to electricity without the need of a window from the cell to the photon-to-electric converter. An additional
5 advantage is to separate the plasma from the photon-to-electric converter in order to minimize plasma damage to the converter. In another embodiment, the plasma is confined by magnetic or electric field confinement to minimize the contact of the plasma with the photon-to-electric converter. In a further embodiment, the converter converts kinetic energy from charged or neutral species in the plasma such as energetic electrons, ions, and hydrogen atoms into
10 electricity. This converter may be in contact with the plasma to receive the energetic species.

In an embodiment, the photovoltaic has a high band-gap such as a photovoltaic comprised of gallium nitride.

7. EXPERIMENTAL

7.1 Chemically-Generated Stationary Inverted Lyman Population for a CW HI Laser

15

ABSTRACT

Each of the ionization of Rb^+ and cesium and an electron transfer between two K^+ ions (K^+ / K^+) provide a reaction with a net enthalpy of an integer multiple of the potential
20 energy of atomic hydrogen, 27.2 eV. The corresponding Group I nitrates provide these reactants as volatilized ions directly or as atoms by undergoing decomposition or reduction to the corresponding metal. The presence of each of the reactants identified as providing an enthalpy of 27.2 eV formed a low applied temperature, extremely low voltage plasma in atomic hydrogen called a resonant transfer or rt-plasma having strong vacuum ultraviolet
25 (VUV) emission. In contrast, magnesium and aluminum atoms or ions do not ionize at integer multiples of the potential energy of atomic hydrogen. $Mg(NO_3)_2$ or $Al(NO_3)_3$ did not form a plasma and caused no emission.

For further characterization, we recorded the width of the 6563 Å Balmer α line on light emitted from rt-plasmas. Significant line broadening of 18, 12, and 12 eV was observed
30 from a rt-plasma of hydrogen with KNO_3 , $RbNO_3$, and $CsNO_3$, respectively, compared to 3 eV from a hydrogen microwave plasma. These results could not be explained by Stark or thermal broadening or electric field acceleration of charged species since the measured field of the incandescent heater was extremely weak, 1 V/cm, corresponding to a broadening of much

less than 1 eV. Rather the source of the excessive line broadening is consistent with that of the observed VUV emission, an energetic reaction caused by a resonant energy transfer between hydrogen atoms and K^+ / K^* , Rb^+ , and cesium, which serve as catalysts.

KNO_3 and $RbNO_3$ formed the most intense plasma. Remarkably, a stationary inverted

- 5 Lyman population was observed in the case of an rt-plasma formed with potassium and rubidium catalysts. These catalytic reactions may pump a cw HI laser as predicted by a collisional radiative model used to determined that the observed overpopulation was above threshold.

10 1. Introduction

- The Lyman α , β , and γ lines of atomic hydrogen at 121.6 nm, 102.6 nm, and 97.3 nm in the vacuum ultraviolet (VUV) region are due to the transitions from $n = 2$, $n = 3$, and $n = 4$ to $n = 1$, respectively. These lines are of great importance in many applications ranging from photochemistry, to laboratory simulations of planetary atmospheres, to astrophysics and plasma physics. In plasma physics, the Lyman series line intensities and their ratios are frequently used in the determination of plasma parameters such as hydrogen number densities and other quantities such as particle fluxes or ion recombination processes [1-2, Numbers in brackets represent a specific reference listed by number following section 4 Conclusion] For the last four decades, scientists from academia and industry have been searching for lasers using a hydrogen plasma [3-6]. Developed sources that provide a usefully intense hydrogen plasma are high powered lasers, arcs and high voltage DC and RF discharges, synchrotron devices, inductively coupled plasma generators, and magnetically confined plasmas. However, the generation of population inversion in these sources is very difficult.
- 25 Recombining expanding plasmas jets formed by methods such as arcs or pulsed discharges is considered one of the most promising methods of realizing an HI laser.

- It was reported previously that a new plasma source has been developed that operates by incandescently heating a hydrogen dissociator to provide atomic hydrogen. Simultaneously a catalyst is heated such that it becomes gaseous and reacts with the atomic hydrogen to produce a plasma by a resonant transfer process. Such a plasma is referred to as an rt-plasma.
- 30 It was extraordinary, that intense VUV emission was observed at low temperatures (e.g. $\approx 10^3$ K) and the extraordinary low field strength of about 1-2 V/cm from atomic hydrogen and certain atomized elements or selected gaseous ions which singly or multiply ionize at

integer multiples of the potential energy of atomic hydrogen, 27.2 eV [7-8]. A proposed theory of this unique process was given previously [9-11].

The Group I and Group VIII elements are unique in that atoms and or ions from these groups, with the exception of xenon, provide a reaction with a net enthalpy that is a close match to an integer multiple of the potential energy of atomic hydrogen, $m \cdot 27.2$ eV where m is an integer. The corresponding reactions of Group I elements with a net enthalpy of $m \cdot 27.2$ eV which are proposed to form an rt-plasma follow:

The first and second ionization energies of lithium are 5.39172 eV and 75.6402 eV, respectively [12]. The double ionization reaction of Li to Li^{2+} , then, has a net enthalpy of reaction of 81.032 eV, which is equivalent to $m = 3$.

The second, third, and fourth ionization energies of sodium are 47.2864 eV, 71.6200 eV, and 98.91 eV, respectively [12]. The triple ionization reaction of Na^+ to Na^{4+} , then, has a net enthalpy of reaction of 217.8164 eV, which is equivalent to $m = 8$.

The second ionization energy of potassium is 31.63 eV, and K^+ releases 4.34 eV when it is reduced to K [12]. The combination of reactions K^+ to K^{2+} and K^+ to K , then, has a net enthalpy of reaction of 27.28 eV, which is equivalent to $m = 1$. Also, the first, second, and third ionization energies of potassium are 4.34066 eV, 31.63 eV, and 45.806 eV, respectively [12]. The triple ionization reaction of K to K^{3+} , then, has a net enthalpy of reaction of 81.7766 eV, which is equivalent to $m = 3$.

The second ionization energy of rubidium is 27.28 eV [12]; thus, the reaction Rb^+ to Rb^{2+} has a net enthalpy of reaction of 27.28 eV, which is equivalent to $m = 1$.

The first and second ionization energies of cesium are 3.89390 eV and 23.15745 eV, respectively [12]. The double ionization reaction of Cs to Cs^{2+} , then, has a net enthalpy of reaction of 27.05135 eV, which is equivalent to $m = 1$.

Rt-plasmas with Group I catalysts were reported previously [7]. In this paper, we report on further characterization of rt-plasmas with Group I catalysts wherein $m = 1$. Group I nitrates were used since they are volatile at relatively low temperatures and also undergo hydrogen reduction and gradual thermal decomposition. Thus, they provide gaseous Group I ions M^+ or atoms M .

The energetic atomic hydrogen densities and energies were calculated from the width of the 6563 Å Balmer α line emitted from a control hydrogen microwave plasma and rt-plasmas. The characteristic emission from the catalyst was also measured. KNO_3 and $RbNO_3$ formed the most intense plasmas. Remarkably, the population of the levels $n = 3$ and $n = 4$ of

hydrogen were continuously inverted with respect to the $n = 2$ levels in an rt-plasma formed with the K^+ and Rb^+ catalysts. To our knowledge, this is the first report of population inversion in a chemically generated plasma. This plasma was further characterized by measuring the electron temperature T_e from the intensity ratios of alkali lines.

5

2. Experimental

The VUV spectrum (900–1300 Å), the width of the 6563 Å Balmer α line, and the high resolution visible spectrum were recorded on light emitted from a hydrogen microwave discharge performed according to methods reported previously [13-14] that served as a control for measurements recorded on light emitted from rt-plasmas of hydrogen with KNO_3 , $RbNO_3$, or $CsNO_3$. The experimental set up described previously [7-8] and shown in FIGURE 13 comprised a thermally insulated quartz cell with a cap that incorporated ports for gas inlet, outlet, and photon detection. A tungsten filament heater and hydrogen dissociator were in the quartz tube as well as a cylindrical titanium screen that served as a second hydrogen dissociator that was coated with catalysts KNO_3 , $RbNO_3$, or $CsNO_3$ and control materials $Mg(NO_3)_2$ or $Al(NO_3)_3$. The cell was maintained at 50 °C for four hours with helium flowing at 30 sccm at a pressure of 0.1 Torr. The cell was then operated with and without an ultrapure hydrogen flow rate of 5.5 sccm maintained at 300 mTorr. The titanium screen was electrically floated with 250 W of power applied to the filament. The temperature of the tungsten filament was estimated to be in the range 1100 to 1500 °C. The external cell wall temperature was about 700 °C.

The rt-plasma phenomena was also studied for cesium metal with hydrogen compared to additional controls. The quartz cell was operated under the same conditions as for the Group I nitrates with 1.) hydrogen, argon, neon, and helium alone; 2.) sodium, magnesium, barium, and cesium metals alone, and 3.) sodium, magnesium, barium, and cesium with hydrogen. The pure elements of sodium, magnesium, barium, and cesium were placed in the bottom of the cell and vaporized by filament heating.

The VUV spectrometer was a normal incidence McPherson 0.2 meter monochromator (Model 302, Seya-Namioka type) equipped with a 1200 lines/mm holographic grating with a platinum coating that covered the region 20–5600 Å. The VUV spectrum was recorded with a CEM at 2500–3000 V. The wavelength resolution was about 0.2 Å (FWHM) with slit widths of 50 μm . The increment was 2 Å and the dwell time was 500 ms. The VUV

30

spectrum (900 – 1300 Å) of the rt-plasma cell emission was recorded at about the point of the maximum Lyman α emission to confirm the rt-plasma before the line broadening and high resolution visible spectra were recorded.

In addition, regions of the VUV, ultraviolet (UV) and visible (VIS) spectra
5 (400 – 5600 Å) were recorded with the normal incidence VUV spectrometer using a PMT and a sodium salicylate scintillator to record emission from the atoms and ions of rt-plasma catalysts. The emission was compared with a standard VUV emission spectrum that was obtained with a gas discharge cell comprised a five-way stainless steel cross that served as the anode with a hollow stainless steel cathode that was coated with KNO_3 , $RbNO_3$, or $CsNO_3$ by
10 the same procedure used to coat the titanium dissociator. The five-way cross was pressurized with 1 torr of hydrogen to initiate the discharge. The hydrogen was then evacuated so that only catalyst lines were observed. The DC voltage at the time the spectra were recorded was 300 V.

The electron temperatures T_e of the $RbNO_3$ and KNO_3 cells were measured from the ratio of the intensity of the Rb^+ 741.4 Å line to that of the Rb^{2+} 815.3 Å line and the ratio of
15 the K^+ 612.6 Å line to that of the K^{2+} 546.1 Å line, respectively, as described by Griem [15].

The spectrometer was calibrated between 400-2000 Å with a standard discharge light source using He, Ne, Ar, Kr, and Xe lines: He I (584 Å), He II (304 Å), Ne I (735 Å), Ne II (460.7 Å), Ar I (1048 Å), Ar II (932 Å), Kr II (964 Å), Xe I (1295.6 Å), Xe II (1041.3 Å), Xe II (1100.43 Å). The wavelength and intensity ratios matched those given by NIST [16]. The
20 spectrometer response was determined to be approximately flat in the 1000-1300 Å region. The calculation of the number density of the $n=2$, 3, and 4 states was corrected for the minor variation of the sensitivity with wavelength in this region. To improve background identification, 10-15 spectra were recorded at each condition before data reduction. Variations in peak line intensities between spectra run under identical conditions were less than 5%.

25 The plasma emission from a hydrogen microwave discharge [14] control and each rt-plasma maintained in the filament heated cell was fiber-optically coupled through a 220F matching fiber adapter positioned 2 cm from the cell wall to a high resolution visible spectrometer with a resolution of ± 0.06 Å over the spectral range 1900 - 8600 Å. The spectrometer was a Jobin Yvon Horiba 1250 M with 2400 grooves/mm ion-etched holographic
30 diffraction grating. The entrance and exit slits were set to 20 μm . The spectrometer was scanned between 4100.5 – 4103.5 Å, 4338.5 – 4343.5 Å, 4859.0 – 4864.0 Å, and 6560 – 6570 Å using a 0.1 Å step size. The signal was recorded by a PMT with a stand alone high voltage power supply (950 V) and an acquisition controller. The data was obtained in a

single accumulation with a 1 second integration time.

To measure the absolute intensity, the high resolution visible spectrometer and detection system were calibrated [17] with 5460.8 Å, 5799.6 Å, and 6965.4 Å light from a Hg-Ar lamp (Ocean Optics, model HG-1) that was calibrated with a NIST certified silicon photodiode. The population density of the $n=3$ hydrogen excited state N_3 was determined from the absolute intensity of the Balmer α (6562.8 Å) line measured using the calibrated spectrometer. The absolute intensities of Balmer β , γ , and δ were determined from the absolute intensity of Balmer α and the relative intensity ratios.

10 3. Results and Discussion

A. Measurement of Hydrogen Atom Temperature and Number Density from Balmer line Broadening

15 The method of Videnovic et al. [18] was used to calculate the energetic hydrogen atom densities and energies from the width of the 6563 Å Balmer α line emitted from microwave and rt-plasmas. The full half-width $\Delta\lambda_G$ of each Gaussian results from the Doppler ($\Delta\lambda_D$) and instrumental ($\Delta\lambda_I$) half-widths:

$$\Delta\lambda_G = \sqrt{\Delta\lambda_D^2 + \Delta\lambda_I^2} \quad (69)$$

20 $\Delta\lambda_I$ in our experiments was 0.06 Å. The temperature was calculated from the Doppler half-width using the formula:

$$\Delta\lambda_D = 7.16 \times 10^{-6} \lambda_0 \left(\frac{T}{\mu} \right)^{1/2} (\text{Å}) \quad (70)$$

where λ_0 is the line wavelength in Å, T is the temperature in K (1 eV = 11,605 K), and μ is the molecular weight (=1 for hydrogen). In each case, the average Doppler half-width that was not appreciably changed with pressure varied by $\pm 5\%$ corresponding to an error in the energy of $\pm 5\%$. The corresponding number densities varied by $\pm 20\%$ depending on the pressure..

The results of the 6563 Å Balmer α line width measured with the high resolution (± 0.06 Å) visible spectrometer on light emitted from rt-plasmas of hydrogen with KNO_3 , $RbNO_3$, and $CsNO_3$ are shown in FIGURES 14-16, respectively. Significant line broadening of 18, 12, and 12 eV and atom densities of 4×10^{11} , 6×10^{11} , and 4×10^{11} atoms/cm³ were observed from a rt-plasma of hydrogen with KNO_3 , $RbNO_3$, and $CsNO_3$, respectively, as

shown in TABLE 4. A hydrogen microwave plasma maintained at the same total pressure showed no excessive broadening corresponding to an average hydrogen atom temperature of ≈ 3 eV and a density of 2×10^{11} atoms/cm³.

5 TABLE 4. Energetic hydrogen atom densities and energies for rt-plasmas determined from the 6563 Å Balmer α line width.

Plasma Gas	Hydrogen Atom Density ^a (10^{11} atoms/cm ³)	Hydrogen Atom Energy ^b (eV)
H_2	2	2-3 ^c
$K, K^+ / K^+ / H_2$	4	15-18
Rb^+ / H_2	6	9-12
Cs / H_2	4	10-12

^a Approximate Calculated after [18].

^b Calculated after [18].

^c Measured on a microwave discharge after [14].

10

In addition to the Balmer α line, the Balmer β , γ , and δ lines corresponding to $n=3$, $n=4$, and $n=5$ were also broadened as shown for the case of the $RbNO_3$ rt-plasma emission in FIGURES 17-19, respectively. The line broadening results could not be explained by Stark or thermal broadening or electric field acceleration of charged species since the measured field of the incandescent heater was extremely weak, 1 V/cm, corresponding to a broadening of much less than 1 eV. We propose that the Doppler broadening was caused by the novel energetic reaction of atomic hydrogen with Group I catalysts which forms the rt-plasma.

Prior studies that reported fast H attributed the observation to acceleration of ions in a high electric fields at the cathode fall region and an external field Stark effect [18-21]. The authors have reported observations with a microwave plasma having no high field present [14, 22]. Microwave helium-hydrogen and argon-hydrogen plasmas showed extraordinary broadening corresponding to an average hydrogen atom temperature of 180-210 eV and 110-130 eV, respectively. Whereas, pure hydrogen and xenon-hydrogen microwave plasmas showed no excessive broadening corresponding to an average hydrogen atom temperature of < 4 eV [14].

25

None of the hydrogen species, H^+ , H_2^+ , H_3^+ , H^- , H , or H_2 , responds to the microwave field; rather, only the electrons respond. But, the measured electron temperature in the argon-hydrogen microwave plasmas was about 1 eV; whereas, the measured neutral hydrogen temperature was 110-130 eV [14, 22]. This requires that $T_e \gg T_g$. This result can not be explained by electric field acceleration of charged species. In microwave driven plasmas, there is no high electric field in a cathode fall region ($> 1kV/cm$) to accelerate positive ions as proposed previously [18-21] to explain significant broadening in hydrogen containing plasmas driven at a high voltage electrodes. It is impossible for H or any H -containing ion which may give rise to H to have a higher temperature than the electrons in a microwave plasma. The microwave field couples to electrons, not ions. And, the H atom temperature can not be attributed to the mechanisms proposed previously [18-21]. In fact, in the argon microwave case, the argon atoms and ions would have the highest energies since they have the largest cross section for electron collisions. No broadening of argon lines is observed. Only the hydrogen lines are broadened. The observation of excessive Balmer line broadening in a microwave driven plasma requires a source of free energy. Sources other than that provided by the electric field or known chemical reactions must be considered. We propose that the source is the energy released by the reaction which formed the rt-plasma.

We have assumed that Doppler broadening due to thermal motion was the dominant source in rt-plasmas to the extent that other sources may be neglected. To confirm this assumption, each source is now considered. In general, the experimental profile is a convolution of two Doppler profiles, an instrumental profile, the natural (lifetime) profile, Stark profiles, van der Waals profiles, a resonance profile, and fine structure. The instrumental half-width is measured to be $\pm 0.06 \text{ \AA}$. The natural half-width of the Balmer α line given by Djurovic and Roberts [21] is $1.4 \times 10^{-3} \text{ \AA}$ which is negligible. The fine structure splitting is also negligible.

Stark broadening of hydrogen lines in plasmas can not be measured at low electron densities using conventional emission or absorption spectroscopy because it is hidden by Doppler broadening. In the case of the Lyman α line, the Stark width exceeds the Doppler width only at $n_e > 10^{17} \text{ cm}^{-3}$ for temperatures of about 10^4 K [23].

The relationship between the Stark broadening $\Delta\lambda_s$ of the Balmer β line in nm, the electron density n_e in m^{-3} , and the electron temperature T_e in K is

$$\log n_e = C_0 + C_1 \log(\Delta\lambda_s) + C_2 [\log(\Delta\lambda_s)]^2 + C_3 \log(T_e) \quad (71)$$

where $C_0 = 22.578$, $C_1 = 1.478$, $C_2 = -0.144$, and $C_3 = 0.1265$ [24]. From Eq. (71), to get a Stark broadening of only 1 Å with $T_e = 9000$ K, an electron density of about $n_e \sim 3 \times 10^{15} \text{ cm}^{-3}$ is required compared to that of the rt-plasma of $n_e = 2 \times 10^9 \text{ cm}^{-3}$ determined using a Langmuir probe as shown in FIGURE 20, over six orders of magnitude less. Gigoso and Cardenoso [25] give the observed Balmer α Stark broadening for plasmas of hydrogen with helium or argon as a function of the electron temperature and density. For example, the Stark broadening of the Balmer α line recorded on a $H + He^+$ plasma is only 0.33 Å with $T_e = 20,000$ K and $n_e = 1.4 \times 10^{14} \text{ cm}^{-3}$. Thus, the Stark broadening was also insignificant.

The statistical curve fit of the $RbNO_3$ rt-plasma and hydrogen microwave plasma emission are shown in FIGURES 21 and 22, respectively. In each case, the data matched a Gaussian profile having the χ^2 and R^2 values given in FIGURES 21 and 22. The absence of Stark broadening in the $RbNO_3$ rt-plasma is also evident by the good fit to a Gaussian profile rather than a Voigt profile as shown in FIGURE 21.

A linear Stark effect arises from an applied electric field that splits the energy level with principal quantum number n into $(2n - 1)$ equidistant sublevels. The magnitude of this effect given by Videnovic et al. [18] is about $2 \times 10^{-1} \text{ Å/kV} \cdot \text{cm}^{-1}$. The applied electric field was present in our study was extremely weak, 1 V/cm; thus, the linear Stark effect should be negligible.

To investigate whether the rt-plasmas of this study were optically thin or thick at a given frequency ω , the effective path length $\tau_\omega(L)$ was calculated from

$$\tau_\omega(L) = \kappa_\omega L \quad (72)$$

where L is the path length and κ_ω is the absorption coefficient given by

$$\kappa_\omega = \sigma_\omega N_H \quad (73)$$

where σ_ω is the absorption cross section and N_H is the number density of the absorber. For optically thin plasmas $\tau_\omega(L) < 1$, and for optically thick plasmas $\tau_\omega(L) > 1$. The absorption cross section for Balmer α emission is $\sigma = 1 \times 10^{-16} \text{ cm}^2$ [26]. As discussed *infra.*, an estimate of the $n=2$ H atom density based on Lyman line intensity is $\sim 1 \times 10^8 \text{ cm}^{-3}$. Thus, for a plasma length of 50 cm, $\tau_\omega(50 \text{ cm})$ for Balmer α is

$$\tau_\omega(50 \text{ cm}) = \kappa_\omega L = (1 \times 10^{-16} \text{ cm}^2)(1 \times 10^8 \text{ cm}^{-3})(50 \text{ cm}) = 5 \times 10^{-7} \quad (74)$$

Since $\tau_\omega(50) \ll 1$, the rt-plasmas were optically thin; so, the self absorption of 6563 Å emission by $n=2$ state atomic hydrogen may be neglected as a source of the observed

broadening.

As discussed above, an estimate based on emission line profiles places the total H atom density of the rt-hydrogen plasma at $\sim 5 \times 10^{11} \text{ cm}^{-3}$. Since this is overwhelmingly dominated by the ground state, $N_H = 5 \times 10^{11} \text{ cm}^{-3}$ will be used. Usually, the atomic hydrogen collisional cross section in plasmas is on the order of 10^{-18} cm^2 [27]. Thus, for $N_H = 5 \times 10^{11} \text{ cm}^{-3}$, collisional or pressure broadening is negligible.

Since the line broadening was measured with sufficient resolution ($\pm 0.06 \text{ \AA}$) to clearly separate the RbII and KII peaks at 6555 \AA and 6595 \AA , respectively, from the 6563 \AA Balmer α line, the possibility of a contribution of the alkali ion lines to the hydrogen line broadening was eliminated.

B. rt-plasma catalyst emission

The VUV spectrum (450 – 800 \AA) of the emission of the $\text{KNO}_3 - \text{H}_2$ gas cell is shown in FIGURE 23. The lines of K^* , K^{2*} , and K^{3*} corresponding to the two possible catalytic reactions were observed as reported previously [28] with the assignments confirmed by a standard potassium plasma spectrum and NIST tables [16, 29]. Line emission corresponding to K^{3*} was observed at 650 - 670 \AA and 740 - 760 \AA . K^{2*} was observed at 510 \AA and 550 \AA , and K^* was observed at 620 \AA . A large K^{3*} peak was also observed at 892 \AA . K^* was observed at 3447 \AA , 4965 \AA , and 5084 \AA .

The VUV spectrum (500 – 900 \AA) of the emission of the $\text{RbNO}_3 - \text{H}_2$ gas cell (top curve) and the standard rubidium discharge plasma (bottom curve) are shown in FIGURE 24. The standard rubidium discharge spectrum according to Sec. 2 is exemplary of the light source used to confirm the line assignments of each of the Group I nitrates studied. Line emission corresponding to Rb^{2*} was observed at 815.9 \AA , 591 \AA , 581 \AA , 556 \AA , and 533 \AA . Rb^* was observed at 741.5 \AA , 711 \AA , 697 \AA , and 643.8 \AA . The assignments of the Rb^{2*} and Rb^* lines were confirmed by the NIST tables [16].

The UV spectrum (3400 – 4150 \AA) of the emission of the $\text{CsNO}_3 - \text{H}_2$ gas cell is shown in FIGURE 25. Line emission corresponding to Cs^{2*} was observed at 3477 \AA , 3618 \AA , and 4001 \AA . Cs^* was observed at 3680 \AA , 3806 \AA , and 4069 \AA . Cs was observed at 3888.6 \AA with Cs^{2*} at 3888.4 \AA . The assignments of the Cs^{2*} , Cs^* , and Cs lines were confirmed by a standard cesium plasma spectrum and the NIST tables [16].

No plasma and no emission except blackbody radiation at long wavelengths was

observed for 1.) hydrogen, argon, neon, and helium alone; 2.) sodium, magnesium, barium, and cesium metals alone, and 3.) sodium, magnesium, and barium, with hydrogen; whereas, a bright plasma with strong VUV emission was observed in the case of cesium metal with flowing hydrogen. The VUV spectrum (400 – 800 Å) of the emission of the $CsNO_3-H_2$ gas cell is shown in FIGURE 26. Line emission corresponding to the second ionization energy of cesium, 23.15745 eV [12], for the decay transition Cs^{2+} to Cs^+ was observed at 533 Å. (The 533 Å emission shown in FIGURE 26 is actually significantly larger than shown due to the low grating efficiency at the short wavelengths.) The only cesium lines observed for the standard cesium microwave plasma were in the visible region, and no lines were observed at wavelengths shorter than 800 Å in the case of the standard hydrogen microwave plasma.

The resonance lines of Cs II were observed with a sliding spark on the 10.7 m normal incidence vacuum spectrometer at the National Bureau of Standards (NBS) [30] as given in TABLE 5. The 533 Å emission of the hydrogen catalysis reaction with cesium shown in FIGURE 26 is dramatically different from the NBS standard cesium spectrum wherein a series of lines of Cs^+ was observed that vanished at the limit of the ionization energy of Cs^+ to Cs^{2+} . In fact, the ionization limit was not observed; rather, it was derived by NBS to be 23.17(4) eV [30]. Furthermore, I. S. Aleksakhin et al. recorded the emission of cesium in the 450-750 Å region during electron-atom collisions [31]. The ionization energy limit at 533 Å was not observed by I. S. Aleksakhin et al. either.

TABLE 5. Resonance lines of Cs II observed with a sliding spark on the 10.7 m normal incidence vacuum spectrometer at NBS [30]. The uncertainty of the wavelengths is ± 0.005 Å.

λ (Å)	Intensity	σ (cm ⁻¹)	Upper Level
926.657	40000	107914.8	$6p^6 5d^3 P_1$
901.270	35000	110954.5	$6s3/2[3/2]_1$
813.837	15000	122874.7	$6s1/2[1/2]_1$
808.761	15000	123645.9	$5d^3 D_1$
718.138	15000	139249.0	$5d^3 P_1$
668.386	500	149614	$7s3/2[3/2]_1$
657.112	100	152181	$6d^3 P_1$
639.356	2000	156407	$6d^3 D_1$
612.756	35	163189	$7s1/2[1/2]_1$

104			
591.044	250	169192	$6d\ ^1P_1$
607.291	50	164666	$8s3/2[3/2]_1$
575.320	10	173816	$6d\ ^3D_1$
564.158	1	177256	$7d\ ^1P_1$

Atomic hydrogen may resonantly transfer energy to cesium to cause its double ionization to Cs^{2+} . Considering broadening by the thermal energies, the net enthalpy may be 27.2 eV, a match with the potential energy of atomic hydrogen; thus, it meets the conditions for producing an rt-plasma. Cs^{2+} may then decay and emit the radiation. The vacuum reaction is



Following the resonant transfer, the decay energy for the transition Cs^{2+} to Cs^+ is predicted to give 23.2 eV (533 Å) line emission corresponding to the second ionization energy of cesium, 23.15745 eV. This line emission was observed as shown in FIGURE 26 without the Rydberg series of lines of Cs^+ as observed by NBS with a sliding spark method [30] as shown in TABLE 5. The observed Cs^{2+} single line emission at 533 Å supports the resonant energy transfer of 27.2 eV from atomic hydrogen to atomic cesium to form an rt-plasma.

15 C. Hydrogen Lyman and Balmer series emission

The VUV spectra (900 ~ 1300 Å) of the cell emission recorded at about the point of the maximum Lyman α emission from the KNO_3 , $RbNO_3$, and $CsNO_3$ gas cells are shown in FIGURES 27-29, respectively, with the superimposed spectrum from the hydrogen microwave plasma. Strong Lyman series VUV emission was observed only with KNO_3 , $RbNO_3$, or $CsNO_3$ (or cesium metal) and hydrogen. The $CsNO_3$ emission was similar to that of the hydrogen microwave plasma; whereas, the Lyman series lines of the KNO_3 and $RbNO_3$ rt-plasmas showed population inversion with much greater intensity of atomic hydrogen versus molecular hydrogen compared to the microwave plasma emission.

25 The Balmer spectra corresponding to the emission from the $n=3$, $n=4$, $n=5$, and $n=6$ states to the $n=2$ state recorded on a hydrogen microwave plasma, a KNO_3 rt-plasma, and a $RbNO_3$ rt-plasma are shown in FIGURES 30, 31, and 32, respectively. No population inversion was observed in the Balmer lines, but the Balmer α to Balmer β ratios of the KNO_3

rt-plasma and the $RbNO_3$ rt-plasma were higher relative to that of the control microwave plasma. This result indicates that the $n=3$ level was the most populated state and was consistent with the observed population inversion of the Lyman emission.

The Lyman population density of the excited hydrogen atoms N_α , N_β , and N_γ with principal quantum numbers $n = 2, 3$, and 4 , respectively, were obtained from their intensity integrated over the spectral peaks corrected by their Einstein coefficients. The population ratios, $\frac{N_\beta}{N_\alpha}$ and $\frac{N_\gamma}{N_\alpha}$, for pure H_2 and H_2 with KNO_3 , $RbNO_3$, or $CsNO_3$ are given in TABLE 6.

TABLE 6. The population density ratios $\frac{N_\beta}{N_\alpha}$ and $\frac{N_\gamma}{N_\alpha}$ for pure H_2 , KNO_3 , and $RbNO_3$.

Plasma Gas	$\frac{N_\beta}{N_\alpha}$	$\frac{N_\gamma}{N_\alpha}$
Pure H_2 ^a	0.664	0.521
KNO_3	4.72	3.48
$RbNO_3$	4.30	1.26
$CsNO_3$	1.194	0.33

^a Measured on microwave discharge maintained after [13-14].

The important parameter for a lasing medium is the reduced population density $\frac{N}{g}$ given by the population density N divided by the statistical weight g as discussed by Akatsuka et al. [6]. The ratio of $\frac{N}{g}$ for L_β to L_α and L_γ to L_α given in TABLE 7 demonstrate that with appropriate cavity length and mirror reflection coefficient cw laser oscillations may be obtained between $n = 3$ and $n = 2$ since the corresponding $\frac{N_\beta g_\alpha}{N_\alpha g_\beta} > 1$ [6]. Lasing further requires an overpopulation which may be determined from the absolute intensity of the Balmer α line.

TABLE 7. The reduced population density ratios $\frac{N}{g}$ for pure H_2 , KNO_3 , and $RbNO_3$.

106

Plasma Gas	$\frac{N_p}{N_a} \frac{g_a}{g_p}$ ^a	$\frac{N_r}{N_a} \frac{g_a}{g_r}$ ^b
Pure H_2 ^c	0.292	0.130 ^c
KNO_3	2.07	0.870
$RbNO_3$	1.89	0.314
$CsNO_3$	0.531	0.080

^a $\frac{g_a}{g_p} = 0.444$ where $g = 2n^2$ and n is the principal quantum number

^b $\frac{g_a}{g_r} = 0.250$

^c Measured on microwave discharge after [14].

- 5 From the population ratios, $\frac{N_p}{N_a} \left(\frac{N_1}{N_2} \right)$ and $\frac{N_r}{N_a} \left(\frac{N_4}{N_2} \right)$, shown in TABLE 6, the corresponding $\frac{N_4}{N_3}$ was determined to be 0.78, 0.74, and 0.29 for the hydrogen microwave plasma, KNO_3 rt-plasma, and $RbNO_3$ rt-plasma, respectively. Whereas, from the Balmer line intensities, $\frac{N_4}{N_3}$ was determined to be 0.78, 0.76, and 0.29 for the hydrogen microwave plasma, KNO_3 rt-plasma, and $RbNO_3$ rt-plasma, respectively (cf. FIGURES 31 and 32). Since $\frac{N_4}{N_3}$
- 10 determined from the Lyman series and the Balmer series was the same, and the Balmer α line was absolutely measured, the absolute reduced number densities for $n=2$ to $n=6$ were determined from the absolute Balmer α line intensity (i. e. using the experimental $N_3 \sim 1.25 \times 10^8 \text{ cm}^{-3}$) and the relative ratio of the Lyman and Balmer series lines). A plot of the absolute reduced population density $\frac{N_a}{g_a}$ versus quantum number n recorded on recorded
- 15 on a $RbNO_3$ rt-plasma, a KNO_3 rt-plasma, and a $CsNO_3$ rt-plasma is shown in FIGURE 33. An inverted population was only observed for $n=3$ in the case of KNO_3 and $RbNO_3$ rt-plasmas.
- For the plasma conditions of this experiment ($T_e \approx 0.7 - 0.8 \text{ eV}$, $n_e \approx 10^9 \text{ cm}^{-3}$), a threshold reduced overpopulation of $4.4 \times 10^6 \text{ cm}^{-3}$ is required for lasing assuming a cavity length of 100 cm and a combined mirror reflection coefficient of 0.99. Modeling results based
- 20 on the collisional-radiative model [6] given in Sec. 3D show that the threshold condition is

achievable for these plasmas.

Other explanations of the over population were ruled out. The spectrometer response was determined to be approximately flat in the 1000-1300 Å region. To investigate whether the rt-plasmas of this study were optically thin or thick at 1216 Å, the effective path length $\tau_{\alpha}(50 \text{ cm})$ was calculated from Eq. (74) using the absorption cross section for Lyman α emission, $\sigma = 4 \times 10^{-16} \text{ cm}^2$ [26], and $N_H = 5 \times 10^{11} \text{ cm}^{-3}$.

$$\tau_{\alpha}(50 \text{ cm}) = \kappa_{\alpha} L = (4 \times 10^{-16} \text{ cm}^2) (5 \times 10^{11} \text{ cm}^{-3}) (50 \text{ cm}) = 1 \times 10^{-2} \quad (76)$$

Since $\tau_{\alpha}(50) \ll 1$, the rt-plasmas were optically thin; so, the self absorption of 1216 Å emission by $n=1$ state atomic hydrogen may be neglected as the cause of the inverted ratio.

Furthermore, the L_{α}/L_p intensity ratios of the control hydrogen plasmas closely matched the NIST intensity ratio using the NIST Einstein A coefficients [16]. Since the hydrogen pressure was the same in the rt-plasmas and the control hydrogen plasma, the same Einstein A coefficients were used to calculate the number density ratio in both cases.

In a non-recombining plasma [6], thermal electron collisional mechanisms can not produce the conditions necessary for population inversion. The highly ionized alkali ions observed in the plasma may ionize atomic hydrogen which may recombine in an excited state; yet, no such reaction has ever been observed which gives rise to an inverted Lyman population. Neither electrical ionization nor chemical ionization is known to form an inverted Lyman population. All known sources of excitation were exhausted [32].

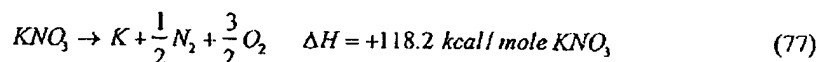
Not only the observation of a stationary inverted Lyman population, but also the observed emission of VUV radiation, and in particular, Lyman series and Werner band emission from a low density plasma of quite moderate temperature was extraordinary. The incandescently heated cell should not emit VUV radiation. The spectra showed that the plasma was far from thermal equilibrium. It was unlikely that the cell components, such as the heater and titanium mesh contributed to a non Maxwellian free-electron velocity distribution. And, if the velocity distribution of free electrons determined the population of the electronic levels, it must have been an unusual one because of the preference for emission from a few specific electronic states of low quantum number. A corona equilibrium was also an inappropriate model for the plasma. Given the observations, free electrons could not excite these states. In the case that the free electrons should have been thermalized, their temperature was too low to contribute to excitation or ionization even from the tail of the velocity distribution. Longer range fields (of the order of mm) were only about a 1 V/cm. In addition to electron collisional excitation, known chemical reactions, resonant photon transfer, and multiphoton absorption,

and the lowering of the ionization and excitation energies by the state of "non ideality" in dense plasmas were also rejected as the source of ionization or excitation to form the hydrogen plasma. The observation lead to the conclusion that a novel chemical power source was present.

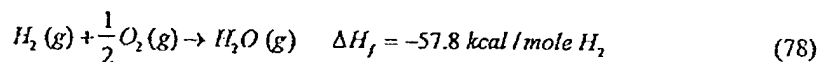
- 5 Without the combination of KNO_3 , $RbNO_3$, or $CsNO_3$ and hydrogen, only blackbody radiation from the tungsten heater was observed at lower wavelengths unless the low-voltage and temperature dependent plasma formed [7, 32-34]. Based on the VUV emission, the plasma was predominately a hydrogen plasma. The ionization of atomic hydrogen requires 13.6 eV. In the cases where plasma was observed, no possible chemical reaction of the
- 10 tungsten filament, the titanium screen, KNO_3 , $RbNO_3$, or $CsNO_3$, and low pressure hydrogen at a cell temperature of 750 °C could be found which accounted for the generation and sustaining of the plasma and observed spectra. In fact, no known chemical reaction releases enough energy to form an atomic hydrogen plasma of sufficient free electron and excitation temperature. Only the Lyman series of atomic hydrogen and molecular hydrogen emission and
- 15 alkali emission was observed in the VUV. Only alkali metal and ion lines and atomic and molecular hydrogen emission was observed in the visible. Thus, we considered energetic chemistry of the observed emitting species.

- The enthalpy of formation ΔH_f of potassium, rubidium, and cesium hydride is -14.13, -13.00, and -13.50 kcal/mole [35]. Thus, the formation of potassium, rubidium, and cesium
- 20 hydride releases 0.59, 0.54, and 0.56 eV per atom, respectively. In addition, these hydrides decompose in this temperature range (288 to 415 °C). Thus, hydride formation can not account for any emission of the hydrogen plasma.

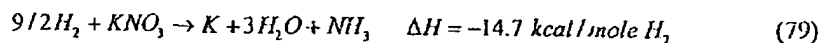
The enthalpy for the decomposition of KNO_3 [36] is



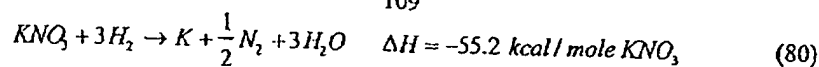
- 25 The enthalpy for combustion of the released oxygen to form $H_2O(g)$ is



or 1.25 eV per hydrogen atom. The reduction of KNO_3 to water, potassium metal, and NH_3 calculated from the heats of formation [37] only releases 0.3 eV per hydrogen atom.



- 30 Combining Eqs. (77-78) gives the enthalpy for the reduction of KNO_3 to water and nitrogen gas



or 0.399 eV per hydrogen atom. Whereas, the energy of Lyman emission is greater than 10.2 eV per atom.

The electrical input power required to maintain a glow discharge plasma in the one liter cell used to form the rt-plasmas was determined to be over 100 W. The complete combustion of the 5.5 sccm of hydrogen flow in the rt-plasmas would produce less than one watt based on the enthalpy of combustion of $-241.8 \text{ kJ/mole } H_2$. However, nitrate was the only source of oxygen gas. The titanium screen was coated with about 0.1 g of KNO_3 or $RbNO_3$. From Eq. (80), the reduction of 0.1 g of KNO_3 is $\Delta H = -55.17 \text{ kcal/mole } KNO_3$. Given, that the rt-plasma was continuous for over 6 hours, the corresponding power is less about 10 mW of heat which is negligible. The corresponding power density is $10 \text{ } \mu\text{W/cm}^3$; whereas, according to the Stefan-Boltzmann equation the thermal power required to maintain a hydrogen plasma (20,000 K) is about 4 MW/cm^3 .

The most energetic reaction is given by Eq. (79) with $\Delta H = -66.1 \text{ kcal/mole } KNO_3$. The corresponding power is also about 10 mW of heat. And, no rt-plasma formed with $Al(NO_3)_3$ and $Mg(NO_3)_2$.

Since K^+ was present initially as KNO_3 , we considered an electron transfer between K^+ and H . K^+ releases 4.34 eV when it is reduced to K , and H requires 13.6 eV to be ionized to H^+ . The combination of reactions K^+ to K and H to H^+ , then, has a net enthalpy of reaction of 9.26 eV—the opposite of the required release of energy of this magnitude or higher. The same conclusion is arrived at for Rb^+ and Cs^+ .

K^{2+} may ionize atomic hydrogen, but an energy significantly greater than 13.6 eV is required since this is not a known chemically stable state and at least 31.63 eV is required for its formation since the second ionization energy of potassium is 31.63 eV. In the case of Rb^{2+} and Cs^{2+} , sources of 27.28 eV and 23.16 eV, respectively, are required.

The dissociation of atomic hydrogen on the filament produces atomic hydrogen which may recombine to release 4.45 eV. Since atomic hydrogen is neutral, no contribution from the electric field of the filament was possible. Thus, excitation with energies of 4.45 eV or less was possible by the transport of thermal energy from the filament due to hydrogen dissociation followed by recombination. But, this reaction is not sufficiently energetic to support the observed VUV emission.

Chemical energy may have been transported from regions outside of the annular region

where most of the emission was observed. Dense and cold plasmas may have been created close to surfaces such as the titanium mesh due to chemical reactions. In such non ideal plasmas with electron densities close to solid density and temperatures below 0.5 eV, the potential energy of the electrons becomes comparable to their kinetic energy, and energy levels of bound electrons in atoms such as hydrogen are altered such that excitation and ionization energies are lowered [38]. This also applies to other elements of the plasma such as potassium. The electronic energy levels of the different species are further distorted when interacting with each other. The dissociation of molecules and ionization of both the molecules and atoms may become more probable with more species. However, the lowering of the ionization and excitation energies by the state of "non ideality" in dense plasmas is only about 1 eV even for potassium. Thus, the most energetic chemical source possible, dissociated atomic hydrogen, could not have provided more energy than the Frank-Condon energy of 4.45 eV during recombination. Thus, a state of "non ideality" of the plasma can not explain the energetic processes of at least 10 eV. Furthermore, the electron density measured using a Langmuir probe was $n_e = 2 \times 10^9 \text{ cm}^{-3}$ [39], 15 orders of magnitude less than solid density which eliminates any possibility of non ideality in these plasmas.

The measured electron temperature, $T_e < 1 \text{ eV}$, was over an order of magnitude too low to account for the hydrogen plasma. The filament electric field as the energy source of the excitation was also eliminated. It was reported previously that the emission occurred even when the electric field was set and measured to be zero [32-34]. The results could not be explained by electric field acceleration of charged species since the measured field of the incandescent heater was extremely weak, about 1 V/cm. The electron mean free path at the operating pressure range of 0.1 to 1 mbar was about 0.1 cm corresponding to a mean energy from the acceleration of electrons in the field of about 1 V/cm of under 1 eV. Thus, electron collisional excitation of Lyman emission or hydrogen ionization by a so called 'run-away-situation' of the velocities of free electrons is not probable. In addition, the correspond broadening of the Balmer line α would be much less than 1 eV compared that actually observed of over an order of a magnitude higher as shown in TABLE 4.

The field was negligible relative to that which causes an electrical discharge. At the same hydrogen pressure as that of the present studies, breakdown did not occur for an applied voltage of less than 3000 V or about 1000 V/cm across the leads with the filament disconnected. In this case, only an arc formed versus a plasma which filled the entire cell when incandescently heated KNO_3 , RbNO_3 , or CsNO_3 and hydrogen were present.

Temperature dependent electric fields also arise due to the greater mobility of electrons compared to ions. The generated voltage U for a plasma with a similar ion and electron temperature T is given by

$$U = \frac{kT}{2e} \ln \frac{m_i}{m_e} \quad (81)$$

5 where m_i is the mass of the ion such as the potassium ion or a proton, m_e is the electron mass, and e is the electron charge. From Eq. (81), the maximum voltage corresponding to the potassium ion was of the order of 1 V.

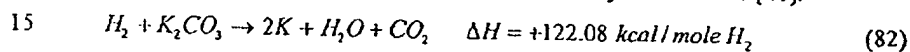
Excitation of hydrogen in one region of the cell with transport to produce excited state emission from the center of the cell was eliminated as a possibility. The emission was
10 observed from the gas in the annular space between the central filament and the outer titanium mesh. Since the lifetimes of $H(n=2)$ and $H(n=3)$ are each approximately 10^{-8} s and the average velocity of the fastest hydrogen atoms was $< 10^5$ m/s, the excitation must have been local [21].

Multi-collisional processes may be possible [40], but very dense, high-pressure plasmas
15 are required, and given an electron energy of $T_e < 1$ eV, about 30 concerted electron collisions would be required within 10^{-8} s—a definite impossibility.

Multiphoton absorption with excitation to intermediate virtual levels may be possible [41-43], but extraordinary power of the order of GW are required from pulsed lasers [44].

Resonant energy transfer from excited species to hydrogen atoms in the ground state is
20 possible to give predominantly Lyman α and Lyman β emission. Kurunczi, Shah, and Becker [40, 45-46] observed intense emission of Lyman α and Lyman β radiation at 121.6 nm and 102.5 nm, respectively, from microhollow cathode discharges in high-pressure Ne (740 Torr) with the addition of a small amount of hydrogen (up to 3 Torr). With essentially no molecular emission observed, Kurunczi et al. attributed the anomalous Lyman α emission to the near-
25 resonant energy transfer between the Ne_2^+ excimer and H_2 which leads to formation of $H(n=2)$ atoms, and attributed the Lyman β emission to the near-resonant energy transfer between excited Ne^+ atoms (or vibrationally excited neon excimer molecules) and H_2 which leads to formation of $H(n=3)$ atoms. However, the formation of this plasma resulting in Ne_2^+ excimers and excited Ne^+ atoms required a field of over 10^4 V/cm and a power density of
30 several hundred kilowatts per cm^3 . Whereas, the field in the heated cells was on the order of 1 V/cm, and power was only applied to the filament. Thus, this mechanism does not provide a source of energetic excited states that may resonantly transfer energy to atomic hydrogen.

The titanium-mesh hydrogen dissociator was present in all experiments. It was previously reported [32-33] that the emission was not observed with the cell alone, with hydrogen alone, or under identical conditions wherein Na_2CO_3 replaced K_2CO_3 . When the power was interrupted, the emission decayed in about two seconds. Decay was recorded over a time greater than 10,000 times the typical duration of a discharge plasma afterglow [47]. This experiment showed, that plasma emission was occurring even though the voltage between the heater wires was set to and measured to be zero for a time duration which was surprisingly extended. Since the thermal decay time of the filament for dissociation of molecular hydrogen to atomic hydrogen was similar to the plasma afterglow duration which required the presence of K_2CO_3 , the emission was determined to be due to a reaction of K_2CO_3 with atomic hydrogen. The minimum temperature requirement of the tungsten wire for emission also demonstrated the emission reaction's dependence on atomic hydrogen [32]. These results also could not be explained by a conventional chemical reaction since the reduction of K_2CO_3 by hydrogen calculated from the heats of formation is very endothermic [48].



The reaction absorbs 2.5 eV per hydrogen atom. A source of energy other than that provided by the electric field or known chemical reactions is required.

The observation, then, of population inversion also indicates the presence of free energy in the system. This is further evidence that a new chemical source of energy, greater than 12 eV/atom was present as is the observation of ions such as K^{3+} which requires an energy source of at least 81.7766 eV. The only possibility known to the authors is the proposed rt-plasma reaction [7]. We propose that the plasma formed chemically rather than electrically and that the product of the energetic chemical reaction of atomic hydrogen with potassium or rubidium ions which serve as catalysts as well as reactants are compounds having novel hydride ions reported previously [39]. Prior related studies that support the possibility of a novel reaction of atomic hydrogen which produces a chemically generated or assisted plasma (rt-plasma) and produces novel hydride compounds include VUV spectroscopy [7-8, 13-14, 22, 28, 32-34, 39, 49-55], characteristic emission from catalysts and the hydride ion products [28, 32, 39, 52-53], lower-energy hydrogen emission [13, 49-51, 54], chemically formed plasmas [7-8, 28, 32-34, 39, 52-53], Balmer α line broadening [8, 14, 22, 39, 49-50, 54-55], elevated electron temperature [14, 22, 49, 54], anomalous plasma afterglow duration [32-34], power generation [22, 49-50, 54], and analysis of novel chemical compounds [56-57].

The predicted catalyst ion emission was observed from rt-plasmas as presented in Sec.

3B. For example, characteristic emission was observed from K^{2+} as well as K^{3+} which confirmed the resonant energy transfer of 27.2 eV and 3·27.2 eV, respectively, from atomic hydrogen to the catalyst K^*/K^* and K , respectively. With a highly conductive plasma, the voltage of the cell was about 20 V, and the field strength was about 1-2 V/cm which was too low to ionize potassium to K^{3+} which requires at least 81.7766 eV. Similarly, the ionization of K^* to K^{2+} requires 31.63 eV which could not have been due to the weak electric field. Known chemical reactions are also of too low an energy by at least an order of magnitude to form K^{2+} and K^{3+} . The K^{3+} lines generated in the incandescently heated cell and due to the catalyst reaction of atomic hydrogen were confirmed by a high voltage discharge and NIST tables [16, 29].

Then the inverted population is explained by a resonant energy transfer between hydrogen and potassium or rubidium catalysts to yield fast $H(n=1)$ atoms. The emission of excited state H from fast $H(n=1)$ atoms excited by collisions with the background H_2 has been discussed by Radovanov et al. [20]. Collisions with oxygen may also play a role in the inversion since inverted hydrogen populations are observed in the case of alkali nitrates and water vapor plasmas [55]. Formation of H^* is also predicted which is far from thermal equilibrium in terms of the hydrogen atom temperature as discussed in Sec. 3A and modeled in Sec. 3D. Akatsuka et al. [6] show that it is characteristic of cold recombining plasmas to have the high lying levels in local thermodynamic equilibrium (LTE); whereas, population inversion is obtained when T_e suddenly decreases concomitant with rapid decay of the lower lying states.

D. Level Population Model and Lasing Ability

In order to estimate hydrogen excited state level populations and assess lasing ability, the collisional radiative model [6, 58] is applied to the plasma conditions obtained herein ($T_e \sim 0.8$ eV, $n_e \sim 10^9$ cm⁻³). The collisional radiative model explicitly includes all level population and de-population mechanisms for each excited level from every other excited level in the hydrogen atom. Excited level n is, then, populated by collisional excitation from all lower excited states, and collisional and radiative de-excitation from all higher excited states. De-population explicitly includes collisional and radiative de-excitation to all lower states, and collisional excitation to all higher levels. Independent ionization loss, radiative recombination, and dielectronic recombination are included for all levels as well. A separate balance equation is prescribed for each individual level and is coupled to all other level equations through the

population and de-population terms described above.

In order to close the set of equations, truncation was chosen at $n=5$. This is justified by both the experimental observation of very low measurable emission from higher lying states and *a posteriori* via the model results indicating a progression of negligibly smaller level

5 densities beyond $n=3$. The ground state ($n=1$) level population cannot be determined by this method since the important affects of dissociation, molecular recombination, and transport are not included. As discussed earlier (Sec. 3A), however, an estimate based on emission line profiles places the total H atom density $\sim 5 \times 10^{11} \text{ cm}^{-3}$. Since this is overwhelmingly dominated by the ground state, the assignment $N_1 = 5 \times 10^{11} \text{ cm}^{-3}$ will be made throughout.

10 Solution to the $n=2-5$ level equations under these conditions shows no inversion in any of the level populations. This is an expected result for a steady, thermal plasma. Also, as expected, the dominant mechanisms are found to be population by collisional excitation and de-population by radiative decay.

The results of this calculation ($N_{2-5} < 10^4 \text{ cm}^{-3}$) are inconsistent with the spectroscopic
15 observations. Absolutely calibrating the monochromator near H_α , however, yields $N_3 \sim 1.25 \times 10^8 \text{ cm}^{-3}$. There is, then, a heretofore undetermined mechanism providing direct excited state population, *i.e.* pumping. To help quantify the affects of this mechanism, the level equations are once again evaluated with N_3 fixed to $1.25 \times 10^8 \text{ cm}^{-3}$ and the inclusion of an independent pumping rate. Since spectroscopic results indicate $n=3-2$ inversion, pumping
20 is prescribed to the $n=3$ state from the ground state, $n=1$. The results from this calculation for $n=1-5$ are summarized in TABLE 8.

TABLE 8. Level densities N_n for excited states $n=1-5$ with an $n=3$ pumping mechanism.

n	$N_n (10^8 \text{ cm}^{-3})$
1	5000
2	0.18
3	1.25
4	0.000229
5	0.000138

25

Now collisional mechanisms from the $n=3$ state as well as ground state collisional

excitation and radiative decay significantly contribute to population and de-population rates. In addition, a demonstrated inversion in the population between the $n=3$ and 2 states is predicted. The reduced overpopulation density for this case is $\Delta(N/g) \sim 4.7 \times 10^6 \text{ cm}^{-3}$, slightly above the threshold of $4.4 \times 10^6 \text{ cm}^{-3}$. The pumping rate is also determined in this analysis yielding a rate of $\sim 6.44 \times 10^{16} \text{ cm}^{-3} \text{ s}^{-1}$. Since the $n=3$ state has a excitation energy of 12.08 eV, the pumping mechanism consumes energy at a rate of $\sim 0.124 \text{ W} \cdot \text{cm}^{-3}$, which is returned as H_α and H_β radiation.

4. Conclusion

The generation of the Lyman and Balmer series and the Lyman Werner bands of molecular hydrogen requires energies significantly greater than 10 eV. The formation of a hydrogen plasma by the cell loaded with KNO_3 , RbNO_3 , or CsNO_3 on titanium and operated in hydrogen required a minimum temperature. The heat from the filament and possibly the weak dipole field from the filament may sustain the hydrogen plasma; but, the latter is not be essential because hydrogen lines are emitted during times when this voltage is set to zero [32-34]. Furthermore, given the observations, free electrons could not excite these states. T_e was determined to be 0.84 eV and 0.76 eV for the K^+ and Rb^+ rt-plasma respectively. Similarly, $k_B T_e = (0.30 - 0.43) \text{ eV}$ was determined for a K^+ rt-plasma as reported by Conrads et al. [32] with the assumption of a Maxwell Boltzmann distribution of the level population, and a slightly higher temperature of $k_B T_e = (0.32 - 0.48) \text{ eV}$ was found when a corona model was applied. The data indicated that the electron temperature was not higher than $k_B T_e = 0.5 \text{ eV}$. On this basis, it was astonishing that a strong Lyman beta transition appeared in the spectra since an excitation energy of 12.1 eV is required. This energy is a factor of about 25 above the measured thermal energy. The amount of electrons in the Maxwell tail that had enough energy to enhance the Lyman transition was 11 orders of magnitude lower than the total number of electrons. Longer range fields (of the order of mm) were only about a 1 V/cm. In addition to electron collisional excitation, known chemical reactions, resonant photon transfer, and multiphoton absorption, and the lowering of the ionization and excitation energies by the state of "non ideality" in dense plasmas were also rejected as the source of ionization or excitation to form the hydrogen plasma.

$2\text{K}^+ \rightarrow \text{K} + \text{K}^{2+}$, $\text{Rb}^+ \rightarrow \text{Rb}^{2+}$, and $\text{Cs} \rightarrow \text{Cs}^{2+}$ each provide a reaction with a net

enthalpy equal to the potential energy of atomic hydrogen, 27.2 eV, and K to K^{3+} provides a reaction with a net enthalpy equal to 3·27.2 eV. The presence of these gaseous atoms and ions with thermally dissociated hydrogen formed a plasma having strong VUV emission. Emission was observed from Rb^+ , Rb^{2+} , K, K^+ , K^{2+} , K^{3+} , Cs, Cs^+ , and Cs^{2+} that

- 5 confirmed the resonant energy transfer with the formation of the corresponding rt-plasma. Emission was also observed from a continuum state of Cs^{2+} at 533 Å. The single emission feature with the absence of the other corresponding Rydberg series of lines from species confirmed the resonant energy transfer of 27.2 eV from atomic hydrogen to atomic cesium.

- A stationary inverted Lyman population was observed with potassium and rubidium
10 catalysts. The ionization and population of excited atomic hydrogen levels was attributed to energy provided by the rt-plasma reactions. The high hydrogen atom temperature with a relatively low electron temperature, $T_e < 1$ eV, were characteristic of cold recombining plasmas [6]. These conditions of the rt-plasmas favored an inverted population in the lower levels. Thus, the catalysis of atomic hydrogen may pump a cw HI laser. From our results, laser
15 oscillations are expected between $n = 3$ and $n = 2$.

References

1. C. Zimmernann, R. Kallenbach, T. W. Hansch, Phys. Rev. Lett., Vol. 65, (1990), p. 571.
2. T. Ibuki, Chem. Phys. Lett., Vol. 94, (1990), p. 169.
- 20 3. L. I. Gudzenko, L. A. Shelepin, Sov. Phys. JEPT, Vol. 18, (1963), p. 998.
4. S. Suckewer, H. Fishman, J. Appl. Phys., Vol. 51, (1980), p. 1922.
5. W. T. Silfvast, O. R. Wood, J. Opt. Soc. Am. B, Vol. 4, (1987), p. 609.
6. H. Akatsuka, M. Suzuki, "Stationary population inversion of hydrogen in arc-heated magnetically trapped expanding hydrogen-helium plasma jet", Phys. Rev. E, Vol. 49,
25 (1994), pp. 1534-1544.
7. R. Mills, J. Dong, Y. Lu, "Observation of Extreme Ultraviolet Hydrogen Emission from Incandescently Heated Hydrogen Gas with Certain Catalysts", Int. J. Hydrogen Energy, Vol. 25, (2000), pp. 919-943.
8. R. Mills and M. Nansteel, P. Ray, "Argon-Hydrogen-Strontium Discharge Light Source",
30 IEEE Transactions on Plasma Science, Vol. 30, No. 2, (2002), pp. 639-653.
9. R. Mills, *The Grand Unified Theory of Classical Quantum Mechanics*, September 2001 Edition, BlackLight Power, Inc., Cranbury, New Jersey, Distributed by Amazon.com; posted at www.blacklightpower.com.

10. R. Mills, "The Grand Unified Theory of Classical Quantum Mechanics", *Int. J. Hydrogen Energy*, Vol. 27, No. 5, (2002), pp. 565-590.
11. R. Mills, "The Nature of Free Electrons in Superfluid Helium--a Test of Quantum Mechanics and a Basis to Review its Foundations and Make a Comparison to Classical Theory", *Int. J. Hydrogen Energy*, Vol. 26, No. 10, (2001), pp. 1059-1096.
12. David R. Lide, *CRC Handbook of Chemistry and Physics*, 79 th Edition, CRC Press, Boca Raton, Florida, (1998-9), p. 10-175 to p. 10-177.
13. R. Mills, P. Ray, "Spectral Emission of Fractional Quantum Energy Levels of Atomic Hydrogen from a Helium-Hydrogen Plasma and the Implications for Dark Matter", *Int. J. Hydrogen Energy*, Vol. 27, No. 3, pp. 301-322.
14. R. L. Mills, P. Ray, B. Dhandapani, J. He, "Comparison of Excessive Balmer α Line Broadening of Glow Discharge and Microwave Hydrogen Plasmas with Certain Catalysts", *J. of Applied Physics*, in press.
15. H. R. Griem, *Principles of Plasma Spectroscopy*, Cambridge University Press, (1987).
16. NIST Atomic Spectra Database, www.physics.nist.gov/cgi-bin/AtData/display.ksh.
17. J. Tadic, I. Juranic, G. K. Moortgat, "Pressure dependence of the photooxidation of selected carbonyl compounds in air: n-butanal and n-pentanal", *J. Photochemistry and Photobiology A: Chemistry*, Vol. 143, (2000), 169-179.
18. I. R. Videnovic, N. Konjevic, M. M. Kuraica, "Spectroscopic investigations of a cathode fall region of the Grimm-type glow discharge", *Spectrochimica Acta, Part B*, Vol. 51, (1996), pp. 1707-1731.
19. M. Kuraica, N. Konjevic, "Line shapes of atomic hydrogen in a plane-cathode abnormal glow discharge", *Physical Review A*, Volume 46, No. 7, October (1992), pp. 4429-4432.
20. S. B. Radovanov, K. Dzierzega, J. R. Roberts, J. K. Olthoff, "Time-resolved Balmer-alpha emission from fast hydrogen atoms in low pressure, radio-frequency discharges in hydrogen", *Appl. Phys. Letts.*, Vol. 66, No. 20, (1995), pp. 2637-2639.
21. S. Djurovic, J. R. Roberts, "Hydrogen Balmer alpha line shapes for hydrogen-argon mixtures in a low-pressure rf discharge", *J. Appl. Phys.*, Vol. 74, No. 11, (1993), pp. 6558-6565.
22. R. L. Mills, P. Ray, "Substantial Changes in the Characteristics of a Microwave Plasma Due to Combining Argon and Hydrogen", *New Journal of Physics*, www.njp.org, Vol. 4, (2002), pp. 22.1-22.17.
23. J. Seidel, "Theory of two-photon polarization spectroscopy of plasma-broadened hydrogen

- L_{α} line", *Phys. Rev. Letts.*, Vol. 57, No. 17, (1986), p. 2154.
24. A. Czernikowski, J. Chapelle, *Acta Phys. Pol. A.*, Vol. 63, (1983), p. 67.
25. M. A. Gigos, V. Cardenoso, "New plasma diagnosis tables of hydrogen Stark broadening including ion dynamics", *J. Phys. B: At. Mol. Opt. Phys.*, Vol. 29, (1996), pp. 4795-4838.
- 5 26. H. Okabe, *Photochemistry of Small Molecules*, John Wiley & Sons, New York, (1978).
27. A. Corney, *Atomic and Laser Spectroscopy*, Clarendon Press, Oxford, (1977).
28. R. Mills, P. Ray, "Spectroscopic Identification of a Novel Catalytic Reaction of Potassium and Atomic Hydrogen and the Hydride Ion Product", *Int. J. Hydrogen Energy*, Vol. 27, No. 2, (2002), pp. 183-192.
- 10 29. R. Kelly, *Journal of Physical and Chemical Reference Data*, "Atomic and Ionic Spectrum Lines below 2000 Angstroms: Hydrogen through Krypton", Part I (H-Cr), Volume 16, (1987), Supplement No. 1, Published by the American Chemical Society and the American Institute of Physics for the National Bureau of Standards, pp. 418-422.
30. J. Reader, G. L. Epstein, "Resonance lines of Cs II, Ba III, and La IV", *Journal of the*
- 15 *Optical Society of America*, Vol. 65, No. 6, June, (1975), pp. 638-641.
31. I. S. Aleksakhin, G. G. Bogachev, A. I. Zapesochnyi, "Study of the emission of potassium, rubidium, and cesium in the 45-75 nm region during electron-atom collisions", *J. Applied Spectroscopy*, Vol. 23, No. 6, December, (1975), pp. 1666-1668. Translated from *Zh. Prikl. Spektrosk. (USSR)*, Vol. 23, No. 6, December (1975), pp. 1103-1105.
- 20 32. H. Conrads, R. Mills, Th. Wrubel, "Emission in the Deep Vacuum Ultraviolet from an Incandescently Driven Plasma in a Potassium Carbonate Cell", *Plasma Sources Science and Technology*, submitted.
33. R. Mills, "Temporal Behavior of Light-Emission in the Visible Spectral Range from a Ti-K₂CO₃-H-Cell", *Int. J. Hydrogen Energy*, Vol. 26, No. 4, (2001), pp. 327-332.
- 25 34. R. Mills, T. Onuma, and Y. Lu, "Formation of a Hydrogen Plasma from an Incandescently Heated Hydrogen-Catalyst Gas Mixture with an Anomalous Afterglow Duration", *Int. J. Hydrogen Energy*, Vol. 26, No. 7, July, (2001), pp. 749-762.
35. W. M. Muller, J. P. Blackledge, G. G. Libowitz, *Metal Hydrides*, Academic Press, New York, (1968), p. 201.
- 30 36. David R. Lide, *CRC Handbook of Chemistry and Physics*, 79th Edition, CRC Press, Boca Raton, Florida, (1998-9), p. 5-20.
37. David R. Lide, *CRC Handbook of Chemistry and Physics*, 79th Edition, CRC Press, Boca Raton, Florida, (1998-9), p. 5-18.

38. H. W. Darwin and P. Felenbok, "Data for Plasmas in Local Thermodynamic Equilibrium", Gauthier-Villars ed., Paris, (1965).
39. R. L. Mills, P. Ray, "A Comprehensive Study of Spectra of the Bound-Free Hyperfine Levels of Novel Hydride Ion H^- (1/2), Hydrogen, Nitrogen, and Air", Int. J. Hydrogen Energy, in press.
40. P. Kurunczi, H. Shah, and K. Becker, "Excimer formation in high-pressure microhollow cathode discharge plasmas in helium initiated by low-energy electron collisions", International Journal of Mass Spectroscopy, Vol. 205, (2001), pp. 277-283.
41. B. J. Thompson, *Handbook of Nonlinear Optics*, Marcel Dekker, Inc., New York, (1996), pp. 497-548.
42. Y. R. Shen, *The Principles of Nonlinear Optics*, John Wiley & Sons, New York, (1984), pp. 203-210.
43. B. de Beauvoir, F. Nez, L. Julien, B. Cagnac, F. Biraben, D. Touahri, L. Hilico, O. Accf, A. Clairon, and J. J. Zondy, Physical Review Letters, Vol. 78, No. 3, (1997), pp. 440-443.
44. E. Parra, I. Alexeev, J. Fan, K. Y. Kim, S. J. McNaught, and H. M. Milchberg, "X-ray and extreme ultraviolet emission induced by variable pulse-width irradiation of Ar and Kr clusters and droplets, Physical Review E, Vol. 62, No. 5, November (2000), pp. R5931-R5934.
45. P. F. Kurunczi, K. H. Becker, "Microhollow Cathode Discharge Plasma: Novel Source of Monochromatic Vacuum Ultraviolet Radiation", Proc. Hakone VII, Int. Symp. High Pressure, Low Temperature Plasma Chemistry, Greifswald, Germany, Sept. 10 - 13, (2000), Vol. 2, p. 491.
46. P. Kurunczi, H. Shah, and K. Becker, "Hydrogen Lyman- α and Lyman- β emissions from high-pressure microhollow cathode discharges in $Ne-H_2$ mixtures", J. Phys. B: At. Mol. Opt. Phys., Vol. 32, (1999), L651-L658.
47. A. Surmeian, C. Diplasu, C. B. Collins, G. Musa, I-Iovittz Popescu, J. Phys. D: Appl. Phys. Vol. 30, (1997), pp. 1755-1758.
48. R. C. Weast, CRC Handbook of Chemistry and Physics, 58 th Edition, CRC Press, West Palm Beach, Florida, (1977-78), pp. D-67-77.
49. R. L. Mills, P. Ray, B. Dhandapani, M. Nansteel, X. Chen, J. He, "Spectroscopic Identification of Transitions of Fractional Rydberg States of Atomic Hydrogen", J. of Quantitative Spectroscopy and Radiative Transfer, Vol. 76, No. 1, (2003), pp. 117-130.
50. R. L. Mills, P. Ray, B. Dhandapani, M. Nansteel, X. Chen, J. He, "New Power Source from

Fractional Quantum Energy Levels of Atomic Hydrogen that Surpasses Internal Combustion", J Mol. Struct., in press.

51. R. Mills, P. Ray, "Vibrational Spectral Emission of Fractional-Principal-Quantum-Energy-Level Hydrogen Molecular Ion", Int. J. Hydrogen Energy, Vol. 27, No. 5, (2002), pp. 533-564.
52. R. Mills, "Spectroscopic Identification of a Novel Catalytic Reaction of Atomic Hydrogen and the Hydride Ion Product", Int. J. Hydrogen Energy, Vol. 26, No. 10, (2001), pp. 1041-1058.
53. R. L. Mills, P. Ray, "Spectroscopic Identification of a Novel Catalytic Reaction of Rubidium Ion with Atomic Hydrogen and the Hydride Ion Product", Int. J. Hydrogen Energy, Vol. 27, No. 9, (2002), pp. 927-935.
54. R. L. Mills, X. Chen, P. Ray, J. He, B. Dhandapani, "Plasma Power Source Based on a Catalytic Reaction of Atomic Hydrogen Measured by Water Bath Calorimetry", Thermochemica Acta, submitted.
55. R. Mills, P. Ray, R. M. Mayo, "Stationary Inverted Balmer and Lyman Populations for a CW HI Water-Plasma Laser", IEEE Transactions on Plasma Science, submitted.
56. R. Mills, B. Dhandapani, M. Nansteel, J. He, T. Shannon, A. Echezuria, "Synthesis and Characterization of Novel Hydride Compounds", Int. J. of Hydrogen Energy, Vol. 26, No. 4, (2001), pp. 339-367.
57. R. Mills, B. Dhandapani, N. Greenig, J. He, "Synthesis and Characterization of Potassium Iodo Hydride", Int. J. of Hydrogen Energy, Vol. 25, Issue 12, December, (2000), pp. 1185-1203.
58. T. Fujimoto, J. Phys. Soc. Jpn., Vol. 47, (1979). p. 265.

7.2 Stationary Inverted Balmer and Lyman Populations for a CW HI Water-Plasma Laser

Abstract

Stationary inverted H Balmer and Lyman populations were observed from a low pressure water-vapor microwave discharge plasma. The ionization and population of excited atomic hydrogen levels was attributed to energy provided by a catalytic resonant energy transfer between hydrogen atoms and molecular oxygen formed in the water plasma. The catalysis mechanism was supported by the observation of O^{2+} and H Balmer line broadening of 55 eV compared to 1 eV for hydrogen alone. The high hydrogen atom temperature with a relatively low electron temperature, $T_e = 2$ eV, exhibited characteristics of cold recombining plasmas. These conditions of a water plasma favored an inverted population in the lower levels. Thus, the catalysis of atomic hydrogen may pump a cw HI laser. From our results, laser oscillations are may be possible from i) $n = 3, n = 4, n = 5, n = 6, n = 7$ and $n = 8$ to $n = 2$, ii) $n = 4, n = 5, n = 6$, and $n = 7$ to $n = 3$ and iii) $n = 5$ and $n = 6$ to $n = 4$. Lines of the Balmer series of $n = 5$, and $n = 6$ to $n = 2$ and the Paschen series of $n = 5$ to $n = 3$ were of particular importance because of the potential to design blue and 1.3 micron infrared lasers, respectively, which are ideal for many communications and microelectronics applications. At a microwave input power of $9 \text{ W} \cdot \text{cm}^{-3}$, a collisional radiative model showed that the hydrogen excited state population distribution was consistent with an $n = 1 \rightarrow 5, 6$ pumping power of an unprecedented $200 \text{ W} \cdot \text{cm}^{-3}$. High power hydrogen gas lasers are anticipated at wavelengths, over a broad spectral range from far infrared to violet which may be miniaturized to micron dimensions. Such a hydrogen laser represents the first new atomic gas laser in over a decade, and it may prove to be the most efficient, versatile, and useful of all. A further application is the direct generation of electrical power using photovoltaic conversion of the spontaneous or stimulated water vapor plasma emission.

1. Introduction

For the last fifteen years there has been an aggressive search for a blue laser. A blue laser would significantly improve the performance of many applications and open new venues. Blue lasers that are durable and bright have significant applications such as superior displays, optical sensors, laser printers and scanners, fiber optical and undersea optical communications, satellite and undersea detection and targeting of submarines, undersea mine detection, undersea salvage, medical devices, and higher density compact disk (CD) players. The shorter (blue)

wavelength could be more sharply focused such that the capacity of magnetic and optical storage may be increased. Digital versatile disks (DVDs) which rely on red aluminum indium gallium phosphide (AlInGaP) semiconductor lasers have a data capacity of about 4.7 gigabytes (Gbytes) compared to 0.65 for compact discs. The capacity could be increased to 15 Gbytes with a suitable violet laser. Despite the tremendous value of a blue laser, advancements have been limited due to a lack of materials which emit blue light or blue-emitting plasmas capable of lasing.

Recombination of injected electrons and holes in InGaN has been extensively pursued as a suitable blue laser [1, the numbers in brackets represent the reference number in the list disclosed herein below]. Unfortunately, after over a decade of effort with an estimated expenditure of \$1 B, blue diode lasers are still plagued by inadequate substrates, crystal layer dislocations, and defects that increase over time with the requisite high drive currents. Frustration over these and other impediments to commercialization of this important device has given rise to the view that commercial success may depend on the discovery of something completely new [2].

Inverted Lyman and Balmer populations may permit a continuous wave (cw) laser at blue wavelengths. For the last four decades, scientists from academia and industry have been searching for lasers using hydrogen plasma [3-6]. Developed sources that provide a usefully intense hydrogen plasma are high powered lasers, arcs and high voltage DC and RF discharges, synchrotron devices, inductively coupled plasma generators, and magnetically confined plasmas. However, the generation of population inversion is very difficult. Recombining expanding plasma jets formed by methods such as arcs or pulsed discharges is considered one of the most promising methods of realizing an H I laser.

Because the population of hydrogen states is overwhelmingly dominated by the ground state even in the most intense plasmas, the realization of an H I laser requires an overpopulation in a state with $n_i > 2$ which decays to a state with $1 < n < n_i$. Thus, an H I laser based on a Balmer transition is feasible for a mechanism which produces an overpopulation in a corresponding state. The Balmer α , β , γ , and δ lines of atomic hydrogen at 6562.8 Å, 4861.3 Å, 4340.5 Å, 4101.7 Å in the visible region are due to the transitions from $n = 3$, $n = 4$, $n = 5$, and $n = 6$ to $n = 2$, respectively. An H overpopulation of $n > 3$ that is above threshold could be the basis of a blue laser. But, lasing of a blue Balmer line has been difficult to achieve even with cold recombining plasmas. Akatsuka and Suzuki [6], for example, were able to achieve an overpopulation for level pairs 4-3 and 5-4 only for a recombining plasma

generated in a arc-heated magnetically trapped expanding plasma jet [6].

Rather than using recombining arcs or recombining electron-hole pairs in semiconductors to achieve lasing at blue wavelengths, a chemical approach was pursued. It was previously reported that a new chemically generated plasma source has been developed that operates by incandescently heating a hydrogen dissociator and a catalyst to provide atomic hydrogen and gaseous catalyst, respectively, which react to produce an energetic plasma called a resonant transfer (π)-plasma [7-8]. Intense VUV emission was observed at low temperatures (e.g. $\approx 10^3$ K) and an extraordinary low field strength of about 1-2 V/cm from atomic hydrogen and certain atomized elements or certain gaseous ions which singly or multiply ionize at integer multiples of the potential energy of atomic hydrogen, $E_h = 27.2$ eV where E_h is one hartree. The theory has been given previously [9-10].

The ionization of Rb^+ and an electron transfer between two K^+ ions (K^+ / K^+) provide a reaction with a net enthalpy of E_h . The presence of each of these gaseous reactants formed an π -plasma with atomic hydrogen having strong vacuum ultraviolet (VUV) emission. Remarkably, a stationary inverted Lyman population was also observed, and a collisional radiative model was used to determine that the observed overpopulation was above threshold for $n = 3$ demonstrating that these catalytic reactions may pump a red cw HI laser [11].

For oxygen, there are several chemical reactions that fulfill the catalyst criterion—a chemical or physical process with an enthalpy change equal to an integer multiple of E_h . The bond energy of the oxygen molecule is 5.165 eV, and the first, second, and third ionization energies of an oxygen atom are 13.61806 eV, 35.11730 eV, and 54.9355 eV, respectively [12]. The reactions $O_2 \rightarrow O + O^+$, $O_2 \rightarrow O + O^{2+}$, and $2O \rightarrow 2O^+$ provide a net enthalpy of about 2, 4, and 1 times E_h , respectively [12]. Lasing directly from oxygen is unknown, but lasing from inverted water vibration-rotational levels in water plasmas which may be from hydrogen-oxygen mixtures has been achieved several decades earlier [13]. In addition, helium-water plasmas as well as water plasma lasers were explored for a source of submillimeter wavelengths [14]. More recently, emission from OH^+ radicals in water and helium-hydrogen water plasmas has been investigated as an efficient source of radiation in the region $\lambda < 2000$ Å for the replacement of expensive working media based on krypton and xenon in microelectronics, photochemistry, and medical applications [15]. These prior water-plasma light sources were based on high-voltage glow discharges.

In our experiments, microwave water plasmas were used as sources of O_2 and atomic hydrogen. The energetic hydrogen atom densities and energies were calculated from the width

of the 6563 Å Balmer α line emitted from control hydrogen and water microwave plasmas. The characteristic emission from the oxygen catalyst was measured. The absolute hydrogen excited state level densities, reduced population densities, and overpopulation densities for lasing were determined from intensity-calibrated high resolution visible spectra in the region 4000 to 7000 Å and VUV spectra in the region 900-1300 Å. Remarkably, stationary inverted Balmer and Lyman populations were observed, and to our knowledge, this is the first report of population inversion in a water plasma. The parameters of a water-plasma laser of Balmer, Paschen, and Brackett series line emission were determined using the spectrally determined reduced population densities. The plasma was further characterized by measuring the electron temperature T_e and density using a Langmuir probe.

The oxygen catalytic reactions may pump a cw HI laser as predicted by a collisional radiative model used to determine that the observed overpopulation was above threshold. Characteristics of the pumping mechanism and laser power that were consistent with the measured electron temperature, electron density, and reduced population densities were determined from the model.

2. Experimental

The VUV spectrum (900 – 1300 Å), the width of the 6562.8 Å Balmer α line, and the high resolution visible spectra (4000-7000 Å) were recorded on light emitted from microwave, capacitively coupled RF, inductively coupled RF, and glow discharge water plasmas performed according to methods and setups reported previously [8-10, 16-18]. Hydrogen and hydrogen (10%) mixed with xenon, krypton, or nitrogen control plasmas were run under the same conditions. The microwave experimental set up shown in FIGURE 34 comprised a quartz tube cell, a source of water vapor or ultrapure hydrogen, a flow system, and a visible spectrometer or a VUV spectrometer that was differentially pumped. Water vapor was formed in a heated insulated reservoir and flowed through the half inch diameter quartz tube at a flow rate of 10 standard $\text{cm}^3 \cdot \text{min}^{-1}$ (sccm) at a corresponding pressure of 50-100 milli Torr. At this pressure, room temperature was sufficient for maintaining the water vapor. The tube was fitted with an Evenson coaxial microwave cavity (Ophos Model #B1) having an E-mode [19-20]. The input power to the plasma at 2.45 GHz by an Ophos model MPG-4M generator was set at 50 W and 90 W as described previously [9-10, 16-18]. The plasma volume was about 3 cm^3 . Hydrogen control plasma were run under the same conditions. Each gas flow was controlled by a 0-20 sccm range mass flow controller (MKS 1179A21CS1BB) with a readout (MKS type 246). The

cell pressure was monitored by a 0-10 Torr MKS Baratron absolute pressure gauge.

In addition, the effect of addition of oxygen or hydrogen to the intensities of the Balmer lines recorded on the water plasma was determined. Using the mass flow controller, 0, 2, 5, 10, and 20 volume % ultrapure gas was mixed with the water vapor while maintaining a constant flow rate and pressure, and each corresponding high resolution visible spectrum (4000-7000 Å) was recorded.

High resolution visible spectra (4000-7000 Å) were recorded on light emitted from hydrogen and water hollow cathode glow discharge plasmas performed according to methods reported previously [16, 18]. The glow discharge cell that comprised a five-way stainless steel cross that served as the anode with a hollow stainless steel cathode. The plasma was generated at the hollow cathode inside the discharge cell. The hollow cathode was constructed of a stainless steel rod inserted into a steel tube, and this assembly was inserted into an Alumina tube. A flange opposite the end of the hollow cathode connected the spectrometer with the cell. It had a small hole that permitted radiation to pass to the spectrometer. An DC power supply ($U = 0 - 1$ kV, $I = 0 - 100$ mA) was connected to the hollow cathode to generate a discharge. The DC voltage and current were 300 V and 300 mA, respectively, corresponding to an input power of 90 W. A Swagelok adapter at the very end of the steel cross provided a gas inlet and a connection with the pumping system, and the cell was pumped with a mechanical pump. Valves were between the cell and the mechanical pump, the cell and the monochromator, and the monochromator and its turbo pump. The five-way cross was pressurized with 50-100 milliTorr of gas which was maintained with a gas flow rate of 10 sccm.

High resolution visible spectra (4000-7000 Å) were recorded on light emitted from hydrogen and water capacitively coupled RF discharge plasmas performed according to methods reported previously [16]. The experimental set up comprised a Pyrex cell reactor (38 cm in length and 13 cm ID) with a diode configuration in which the plasma was confined between two parallel circular stainless steel electrodes (0.1 mm thick X 7.6 cm diameter with a 2 cm separation). For spectroscopic measurements on the plasma emission, a 1 cm diameter quartz window was located in the Pyrex cell wall at the center of the gap between the electrodes. At each end of the cell, a Pyrex cap was sealed to the cell with a Viton O ring and a C-clamp. One cap incorporated ports for gas inlet and cathode feedthrough. The other cap incorporated ports for gas outlet and anode feedthrough. The cathode was connected to an 13.56 MHz RF generator (RF VII, Inc., Model MN 500) with a matching network (RF Power

Products, Inc., Model RF 5S, 300 W). The forward RF power was 90 W, and the reflected power was less than 1 W. The gas flow rate and pressure were 10 sccm and 50-100 milliTorr, respectively.

High resolution visible spectra (4000-7000 Å) were recorded on light emitted from hydrogen and water inductively coupled RF discharge plasmas performed according to methods reported previously [16]. A quartz cell which was 500 mm in length and 50 mm in diameter served as the plasma reactor. A Pyrex cap was sealed to the quartz cell with a Viton O ring and a C-clamp incorporated ports for gas inlet, outlet, and photon detection. An unterminated, nine-turn, 17 cm long helical coil (18 gauge magnet wire) wrapped around the outside of the cell was connected to an 13.56 MHz RF generator (RF VII, Inc., Model MN 500) with a matching network (RF Power Products, Inc., Model RF 5S, 300 W). The coil inductance and resistance were 4.7 μH and 0.106 Ω, respectively. The coil impedance was 400 Ω at 13.56 MHz. The forward RF power was 90 W, and the reflected power was less than 1 W. The gas flow rate and pressure were 10 sccm and 50-100 milliTorr, respectively.

The plasma emission was fiber-optically coupled through a 220F matching fiber adapter positioned 2 cm from the cell wall to a high resolution visible spectrometer with a resolution of ±0.06 Å over the spectral range 1900-8600 Å. The spectrometer was a Jobin Yvon Horiba 1250 M with 2400 grooves/mm ion-etched holographic diffraction grating. The entrance and exit slits were set to 20 μm. The spectrometer was scanned between 6555-6570 Å and 4000-7000 Å using a 0.05 Å step size. The signal was recorded by a PMT with a stand alone high voltage power supply (950 V) and an acquisition controller. The data was obtained in a single accumulation with a 1 second integration time.

The method of Videnovic et al. [21] was used to calculate the energetic hydrogen atom densities and energies from the width of the 6562.8 Å Balmer α line emitted from hydrogen and water microwave plasmas. The full half-width Δλ_G of each Gaussian results from the Doppler (Δλ_D) and instrumental (Δλ_I) half-widths:

$$\Delta\lambda_G = \sqrt{\Delta\lambda_D^2 + \Delta\lambda_I^2} \quad (83)$$

Δλ_I for these experiments was 0.06 Å. The temperature was calculated from the Doppler half-width using the formula:

$$\Delta\lambda_D = 7.16 \times 10^{-6} \lambda_0 \left(\frac{T}{\mu} \right)^{1/2} \quad (\text{Å}) \quad (84)$$

where λ₀ is the line wavelength in Å, T is the temperature in K (1 eV = 11,605 K), and μ is the molecular weight (=1 for hydrogen). In each case, the average Doppler half-width that was

not appreciably changed with pressure varied by $\pm 5\%$ corresponding to an error in the energy of $\pm 10\%$. The corresponding number densities for noble gas-hydrogen mixtures varied by $\pm 20\%$.

To measure the absolute intensity, the high resolution visible spectrometer and
5 detection system were calibrated [22] with 5460.8 Å, 5799.6 Å, and 6965.4 Å light from a Hg-Ar lamp (Ocean Optics, model HG-1) that was calibrated with a NIST certified silicon photodiode. The population density of the $n = 3$ hydrogen excited state N_3 was determined from the absolute intensity of the Balmer α (6562.8 Å) line measured using the calibrated spectrometer. The spectrometer response was determined to be approximately flat in the 4000-
10 7000 Å region by ion etching and with a tungsten intensity calibrated lamp. The absolute intensities of $n = 4$ to 9 were determined from the absolute intensity of Balmer α ($n = 3$) and the relative intensity ratios.

The VUV spectrometer was a normal incidence 0.2 meter monochromator equipped with a 1200 lines/mm holographic grating with a platinum coating that covered the region
15 20 – 5600 Å. The VUV spectrum was recorded with a CEM. The wavelength resolution was about 0.2 Å (FWHM) with slit widths of 50 μm . The increment was 2 Å and the dwell time was 500 ms. The VUV spectra (900 – 1300 Å) of the water and control hydrogen plasmas were recorded at 90 W input power.

The spectrometer was calibrated between 400-2000 Å with a standard discharge light
20 source using He, Ne, Ar, Kr, and Xe lines: He I (584 Å), He II (304 Å), Ne I (735 Å), Ne II (460.7 Å), Ar I (1048 Å), Ar II (932 Å), Kr II (964 Å), Xe I (1295.6 Å), Xe II (1041.3 Å), Xe II (1100.43 Å). The wavelength and intensity ratios matched those given by NIST [23]. The spectrometer response was determined to be approximately flat in the 1000-1300 Å region. The calculation of the number density of the $n = 3$ to 9 states was corrected for the minor
25 variation of the sensitivity with wavelength in this region.

The electron density and temperature of the water plasma was determined using a compensated Langmuir probe according to the method given previously [24].

3. Results and discussion

30

A. Hydrogen Balmer and Lyman series emission

The high resolution visible spectra (4000-6700 Å) of the cell emission from a hydrogen microwave plasma with 90 W input power, a water microwave plasma with 50 W input power,

and a water microwave plasma with 90 W input power are shown in FIGURES 35-37, respectively. As shown by the absolute intensity measurements of the Balmer lines of the hydrogen microwave plasma, we observed the known ratios of the Balmer lines. In contrast, the population of the levels $n = 4$, $n = 5$, and $n = 6$ of hydrogen were continuously inverted with respect to $n = 3$ in the water plasma spectrum shown in FIGURE 36. The relative intensities of the Balmer lines of microwave plasmas of hydrogen (90-2%) mixed with xenon, krypton, or nitrogen at 50 W were equivalent to those of hydrogen alone; thus, the inversion is not inherent to a hydrogen plasma generated by microwaves. As shown in FIGURE 37, when the input power was increased to 90 W, the $n = 5$ and $n = 6$ levels were further continuously inverted with respect to $n = 4$. The levels $n = 7$, $n = 8$, and $n = 9$ of hydrogen were also continuously inverted with respect to $n = 3$. Thus, wavelength tuneability may be achieved by varying the microwave power with lasing between the corresponding power-dependent inverted levels. The requirement for a stoichiometric mixture was fairly exacting since it was observed that additions of increasing partial pressures of pure hydrogen or oxygen progressively reversed the inversion at a mole fraction over the stoichiometric ratio of greater than 2%.

The VUV spectra (900 – 1300 Å) of the cell emission from hydrogen microwave and the water microwave plasmas with 90 W input power are shown in FIGURE 38. An inverted Lyman population was also observed from the water plasma emission with the inversion observed in the visible as shown in FIGURE 35 extending to the $n = 2$ level. No inversion was observed for the hydrogen microwave plasma.

No inversion was observed with inductively or capacitively RF driven or high voltage glow discharge water plasmas as shown in FIGURES 39-41, respectively. However, intense emission of OH^* radicals in water plasmas was observed from glow discharge as well as microwave sources as shown in FIGURES 41 and 37, respectively. As discussed previously, the glow discharge plasma has been extensively studied as a light source based on the emission of OH^* radicals [15]. Shuaibov et al. [25] give the spectrum of a glow discharge of a He/H_2O mixture and assign the $OH(A-X)$ emission. As a comparison, the $OH(A-X)$ microwave water plasma emission spectrum in the region of 2800-3300 Å is given in FIGURE 42. The (1-0) R-branch and the (1-0) Q-branch are observed in the 2800-2950 Å region as shown in FIGURE 43. The (0-0) R-branch and the (0-0), (1-1), and (2-2) Q-branches are observed in the 3000-3300 Å region as shown in FIGURE 44.

We had shown previously that the conditions of the particular discharge may be a major

parameter in the observation of excessive Doppler Balmer line broadening with plasmas of hydrogen and a noble ion having an ionization potential of an integer multiple of E_h [8-11, 16-18]. We proposed that the corresponding energetic hydrogen formed with an Evenson microwave cavity may be a means to achieve population inversion.

- 5 Other explanations of the population inversion were ruled out. The spectrometer response was determined to be approximately flat in the 4000-7000 Å region by ion etching and with an intensity calibrated lamp. Furthermore, the Balmer and Lyman line intensity ratios of the control hydrogen plasmas closely matched those obtained using the NIST Einstein A coefficients [23]. Since these ratios did not change as the pressure was lowered, and the
10 hydrogen pressure was lower in the water plasma than the control, the NIST Einstein A coefficients were used to calculate the number density ratios from the water plasma emission.

To determine the optical thickness of the water plasmas of this study, $\tau_\omega(L)$, the effective path length at a given frequency ω , was calculated using

$$\tau_\omega(L) = \kappa_\omega L \quad (85)$$

- 15 where L is the path length and κ_ω is the absorption coefficient given by

$$\kappa_\omega = \sigma_\omega N_H \quad (86)$$

- where σ_ω is the absorption cross section and N_H is the number density of the absorber. For optically thin plasmas $\tau_\omega(L) < 1$, and for optically thick plasmas $\tau_\omega(L) > 1$. By orders of magnitude, self absorption of Lyman emission by $n = 1$ state hydrogen dominates since $n = 1$
20 H dominates the H population distribution. At 1215.67 Å, the effective path length $\tau_\omega(5 \text{ cm})$ was calculated from Eq. (85) using the absorption cross section for Lyman α emission, $\sigma = 4 \times 10^{-16} \text{ cm}^2$ [26], and $N_H = 6 \times 10^{13} \text{ cm}^{-3}$.

$$\tau_\omega(5 \text{ cm}) = \kappa_\omega L = (4 \times 10^{-16} \text{ cm}^2)(6 \times 10^{13} \text{ cm}^{-3})(5 \text{ cm}) = 1 \times 10^{-1} \quad (87)$$

- Since $\tau_\omega(5) \ll 1$, the water plasmas were optically thin. Furthermore, the water plasmas were
25 determined to be optically thin for hydrogen absorption of the Balmer and as well as the additional Lyman lines. Thus, absorption of 6562.8 Å and 4861.3 Å and 1215.67 Å emission by $n = 2$ and $n = 1$ state atomic hydrogen, respectively, may be neglected as the cause of the inverted ratios.

- The absorption cross section of Balmer emission by water is insignificant—nine orders
30 of magnitude less than in the Lyman region [27]. Thus, the Balmer lines were used to determine the over populations in TABLE 9, except for the $n = 2$ level which was determined from the intensities of the Lyman lines. The effective path length $\tau_\omega(5 \text{ cm})$ was calculated

from Eq. (85) using the absorption cross section of water for Lyman α emission, $\sigma = 1.6 \times 10^{-17} \text{ cm}^2$ [28], and the water number density, $N_{H_2O} = 2.5 \times 10^{15} \text{ cm}^{-3}$, calculated from the measured pressure. Thus, $\tau_\alpha(5 \text{ cm})$ is given by

$$\tau_\alpha(5 \text{ cm}) = \kappa_\alpha L = (1.6 \times 10^{-17} \text{ cm}^2)(2.5 \times 10^{15} \text{ cm}^{-3})(5 \text{ cm}) = 0.2 \quad (88)$$

- 5 Since $\tau_\alpha(5) < 1$, the water plasmas were optically thin for Lyman α emission.

TABLE 9. Level densities N_n , reduced population densities $\frac{N_n}{g_n}$ ^a, and overpopulation ratios

$\frac{N_n g_2}{N_2 g_n}$, $\frac{N_n g_3}{N_3 g_n}$, and $\frac{N_n g_4}{N_4 g_n}$ for excited states $n = 1$ to 9 with an $n > 2$ pumping mechanism

recorded on a water microwave plasma at 90 W input power.

10

Principal Quantum Number n	$N_n (10^9 \text{ cm}^{-3})$	$\frac{N_n}{g_n} (10^8 \text{ cm}^{-3})$	$\frac{N_n g_2}{N_2 g_n}$	$\frac{N_n g_3}{N_3 g_n}$	$\frac{N_n g_4}{N_4 g_n}$
1	60,000 ^b	30,000	—	—	—
2	1.39	1.74	—	—	—
3	6.20	3.44	1.98	—	—
4	28.9	9.02	5.18	2.62	—
5	1930	385	221	112	42.7
6	838	116	66.7	33.7	12.9
7	47.4	4.83	2.78	1.40	0.535
8	26.1	2.04	1.17	0.593	0.226
9	15.3	0.955	0.549	0.278	0.106

^a $g_n = 2n^2$ and n is the principal quantum number

^b calculated after ref. [21]

B. Measurement of hydrogen atom temperature and number density from Balmer line

15 broadening

To further characterize the water plasma, the width of the 6562.8 Å Balmer α line ($n = 3$ to $n = 2$) was measured on light emitted from the microwave discharges of pure

hydrogen alone and water vapor maintained under equivalent conditions using the high resolution visible spectrometer as shown in FIGURES 45 and 46, respectively. The method of Videnovic et al. [21] was used to calculate the hydrogen atom energies and densities from the line width. Significant line broadening of 55 eV and an atom density of $6 \times 10^{13} \text{ atoms/cm}^3$ was observed from the water plasma compared to an average hydrogen atom temperature of 1 eV and a density of $6 \times 10^{11} \text{ atoms/cm}^3$ for hydrogen alone. Similarly, using a Langmuir probe as described previously [24], the electron temperature T_e measured on the microwave water plasmas was higher, 2.0 eV, compared to the $T_e \leq 1 \text{ eV}$ measured on the hydrogen plasma at the same 50 W input power.

We have assumed that Doppler broadening due to thermal motion was the dominant source in the water plasmas to the extent that other sources may be neglected. To confirm this assumption, each source is now considered. In general, the experimental profile is a convolution of a Doppler profile, an instrumental profile, the natural (lifetime) profile, Stark profiles, van der Waal's profiles, a resonance profile, and fine structure. The instrumental half-width is measured to be $\pm 0.06 \text{ \AA}$. The natural half-width of the Balmer α line given by Djurovic and Roberts [29] is $1.4 \times 10^{-3} \text{ \AA}$ which is negligible. The fine structure splitting is also negligible.

Stark broadening of hydrogen lines in plasmas can not be measured at low electron densities using conventional emission or absorption spectroscopy because it is hidden by Doppler broadening. In the case of the Lyman α line, the Stark width exceeds the Doppler width only at $n_e > 10^{17} \text{ cm}^{-3}$ for temperatures of about 10^4 K [30].

The relationship between the Stark broadening $\Delta\lambda_s$ of the Balmer β line in nm, the electron density n_e in m^{-3} , and the electron temperature T_e in K is

$$\log n_e = C_0 + C_1 \log(\Delta\lambda_s) + C_2 [\log(\Delta\lambda_s)]^2 + C_3 \log(T_e) \quad (89)$$

where $C_0 = 22.578$, $C_1 = 1.478$, $C_2 = -0.144$, and $C_3 = 0.1265$ [31]. From Eq. (89), to get a Stark broadening of only 1 \AA with $T_e = 9000 \text{ K}$, an electron density of about $n_e \sim 3 \times 10^{15} \text{ cm}^{-3}$ is required compared to that of the water plasma of $n_e = 0.2 \times 10^8 \text{ cm}^{-3}$ determined using a Langmuir probe, over seven orders of magnitude less. Gigosos and Cardenoso [32] give the observed Balmer α Stark broadening for plasmas of hydrogen with helium or argon as a function of the electron temperature and density. For example, the Stark broadening of the Balmer α line recorded on a $H + He^+$ plasma is only 0.33 \AA with $T_e = 20,000 \text{ K}$ and $n_e = 1.4 \times 10^{14} \text{ cm}^{-3}$. Thus, the Stark broadening was also insignificant.

The statistical curve fit of the hydrogen and water microwave plasma emission are shown in FIGURES 45 and 46, respectively. In each case, the data matched a Gaussian profile having the X^2 and R^2 values given in FIGURES 45 and 46. The absence of Stark broadening in the water plasma is also evident by the good fit to a Gaussian profile rather than a Voigt profile as shown in FIGURE 46.

A linear Stark effect arises from an applied electric field that splits the energy level with principal quantum number n into $(2n - 1)$ equidistant sublevels. The magnitude of this effect given by Videnovic et al. [21] is about $2 \times 10^{-2} \text{ nm/kV} \cdot \text{cm}^{-1}$. No applied electric field was present in our study; thus, the linear Stark effect should be negligible.

The plasma was evaluated for optical thickness. The absorption cross section for Balmer α emission is $\sigma = 1 \times 10^{-16} \text{ cm}^2$ [26]. As discussed *infra.*, an estimate based on Lyman line intensity, the $n = 2$ H atom density is $\sim 1.39 \times 10^9 \text{ cm}^{-3}$. Thus, for a plasma length of 5 cm , the effective path length, $\tau_\alpha(5 \text{ cm})$, calculated from Eq. (85) for Balmer α is

$$\tau_\alpha(5 \text{ cm}) = \kappa_\alpha L = (1 \times 10^{-16} \text{ cm}^2)(1.39 \times 10^9 \text{ cm}^{-3})(5 \text{ cm}) = 6.95 \times 10^{-7} \quad (90)$$

Since $\tau_\alpha(5) \ll 1$, the water plasmas were optically thin; thus, the self absorption of 6562.8 \AA emission by $n = 2$ state atomic hydrogen may be neglected as a source of the observed broadening.

As discussed above, an estimate based on emission line profiles places the total H atom density of the water plasma at $\sim 6 \times 10^{13} \text{ cm}^{-3}$. Since this is overwhelmingly dominated by the ground state, $N_H = 6 \times 10^{13} \text{ cm}^{-3}$ will be used. Usually, the atomic hydrogen collisional cross section in plasmas is on the order of 10^{-18} cm^2 [33]. Thus, for $N_H = 6 \times 10^{13} \text{ cm}^{-3}$, collisional or pressure broadening is negligible.

Prior studies that reported fast H, attributed the observation to acceleration of ions in a high electric fields at the cathode fall region and an external field Stark effect [21, 34-35]. Observations with a microwave plasma having no high DC field present was reported previously [16-18]. Microwave helium-hydrogen and argon-hydrogen plasmas showed extraordinary broadening corresponding to an average hydrogen atom temperature of $180 - 210 \text{ eV}$ and $110 - 130 \text{ eV}$, respectively. Whereas, pure hydrogen and xenon-hydrogen microwave plasmas showed no excessive broadening corresponding to an average hydrogen atom temperature of $< 2 \text{ eV}$ [16-18]. The formation of fast H was explained by a resonant energy transfer between hydrogen atoms and Ar^* or He^* of an integer multiple of the potential energy of atomic hydrogen, 27.2 eV .

As in the case of the argon-hydrogen or helium-hydrogen plasmas, no hydrogen species, H^+ , H_2^+ , H_3^+ , H^- , H , or H_2 , of the water plasmas responds to the microwave field; rather, only the electrons respond. However, the measured electron temperature in these microwave plasmas was about 1-2 eV; whereas, the measured neutral hydrogen temperature was much higher, 55 eV. This requires that $T_i \gg T_e$ which can not be due to direct ion coupling to the microwave power or electron-collisional heating. Nor, can this result be explained by electric field acceleration of charged species as proposed for glow discharges [21, 34-35] since in microwave driven plasmas, there is no high electric field in a cathode fall region ($> 1 \text{ kV/cm}$) to accelerate positive ions. The observation of excessive Balmer line broadening in a microwave driven plasma requires a source of energy. In the case of the water plasma, we propose that the source is the energy is due to a resonant energy transfer between hydrogen atoms and oxygen. The catalysis mechanism was supported by the observation of O^{2+} at 3715.0 Å, 3754.8 Å, and 3791.28 Å as shown in FIGURE 47 as well as the extraordinary Balmer line broadening of 55 eV compared to 1 eV for hydrogen alone. This energy may further be the basis of the pumping source for the observed population inversions.

Then the inverted population is explained by a resonant energy transfer between hydrogen and oxygen to yield fast $H(n=1)$ atoms. The emission of excited state H from fast $H(n=1)$ atoms excited by collisions with the background H_2 has been discussed by Radovanov et al. [35]. Collisions with oxygen may also play a role in the inversion since inverted hydrogen populations are observed in the case of alkali nitrates [11] and water vapor plasmas. Formation of H^+ is also predicted by a collisional radiative model [11] which is far from thermal equilibrium in terms of the hydrogen atom temperature. Akatsuka et al. [6] show that it is characteristic of cold recombining plasmas to have the high lying levels in local thermodynamic equilibrium (LTE); whereas, population inversion is obtained when T_e suddenly decreases concomitant with rapid decay of the lower lying states.

C. Observed level population and lasing ability

To determine the potential of the water-plasma as a laser medium, the absolute reduced Balmer population density of the excited hydrogen atoms $\frac{N_n}{g_n}$ with principal quantum numbers $n = 1$ to 9 were obtained from N , their absolute intensity integrated over the visible spectral peaks shown in FIGURES 36 and 37 corrected by their Einstein coefficients, divided by g , the

statistical weight ($g = 2n^2$), as discussed by Akatsuka et al. [6]. As shown in TABLE 9, $\frac{N_n}{g_n}$ for quantum number $n = 3, 4, 5, 6$ recorded on a water microwave plasma at 90 W input was determined to be $3.44 \times 10^8 \text{ cm}^{-3}$, $3.44 \times 10^8 \text{ cm}^{-3}$, $9.02 \times 10^8 \text{ cm}^{-3}$, and $385 \times 10^8 \text{ cm}^{-3}$, respectively.

- 5 The population of the $n = 2$ level was determined from the VUV spectrum (900 – 1300 Å) of the microwave water plasma shown in FIGURE 38. From the number densities of the levels determined from the absolute Balmer line intensities given in TABLE 9 and the Lyman lines intensities shown in FIGURE 38, it was found that

$$\frac{N_4}{N_3} \text{ Balmer} = 4.66; \frac{N_4}{N_3} \text{ Lyman} = 4.46 \quad (91)$$

- 10 Since $\frac{N_4}{N_3}$ determined from the Lyman series and the Balmer series was about the same, and the Balmer α line was absolutely measured, the absolute number density for $n = 2$ given in TABLE 9 was determined from the absolute Balmer α line intensity.

$$(N_2)_{\text{Balmer}} = (N_3)_{\text{Balmer}} \times \left(\frac{(N_2)_{\text{Lyman}}}{(N_3)_{\text{Lyman}}} \right) \quad (92)$$

Using $N_3 = 6.20 \times 10^9 \text{ cm}^{-3}$ and $g_2 = 8$, $\frac{N_2}{g_2}$ was determined to be $1.74 \times 10^8 \text{ cm}^{-3}$.

15

TABLE 10. Potential laser transitions of atomic hydrogen in a microwave water-vapor plasma.

wavelength/Å	spectral region	electronic transition $n_{\text{initial}} - n_{\text{final}}$
74,578	IR	..
40,512	IR	..
26,252	IR	..
18,751	IR	..
12,818	IR	..
10,938	IR	..
10,049	IR	..
6,563	red	..

4,861	blue	..
4,340	violet	..
4,102	violet	..
3,970	violet	..
3,889	violet	..

With appropriate cavity length and mirror reflection coefficient, cw laser oscillations may be obtained between states having an overpopulation ratio determined by $\frac{N_i g_f}{N_f g_i} > 1$ as shown in TABLE 9 where i represents the quantum number of the initial state and f represents that of the final state [6]. On this basis, it was determined that lasing is possible over a wide range from far infrared to violet wavelengths. Representative transitions and wavelengths are shown in TABLE 10. The important parameter for lasing is that the reduced overpopulation density is above threshold. Using standard laser cavity equations [6], it was determined that the threshold condition is achievable with micron to submillimeter laser cavities for several commercially important wavelengths emitted from these plasmas. For plasma properties of this experiment determined using a Langmuir probe ($T_e = 2.0$ eV, electron density $n_e = 0.2 \times 10^8 \text{ cm}^{-3}$), conditions for lasing at 12,818.1 Å, 4340.5 Å, and 4101.7 Å corresponding to the transitions $5 \rightarrow 3$, $5 \rightarrow 2$, and $6 \rightarrow 2$, respectively, were determined assuming a cavity length of 100 cm and a combined mirror reflection coefficient of 0.99, as given in TABLE 11. The overpopulation ratios $\frac{N_5 g_3}{N_3 g_5}$, $\frac{N_5 g_2}{N_2 g_5}$, and $\frac{N_6 g_2}{N_2 g_6}$ given in TABLE 9 were 112, 221, and 67, respectively. Threshold reduced $n = 5$ overpopulation densities of about $0.49 \times 10^7 \text{ cm}^{-3}$ and $4.6 \times 10^7 \text{ cm}^{-3}$ are required for lasing to $n = 3$ and $n = 2$, respectively, and, a corresponding threshold reduced $n = 6$ overpopulation density of $6.9 \times 10^7 \text{ cm}^{-3}$ is required for lasing to $n = 2$. The actual reduced overpopulation densities were much greater, $3.8 \times 10^{10} \text{ cm}^{-3}$, $3.8 \times 10^{10} \text{ cm}^{-3}$, and $1.2 \times 10^{10} \text{ cm}^{-3}$, respectively. Thus, lasing may be possible with cavity lengths as small as 0.01 cm, 0.2 cm, and 0.6 cm, respectively.

TABLE 11. Observed reduced overpopulation densities recorded on a water microwave plasma at 90 W input power, threshold overpopulation densities for lasing with a 100 cm length cavity, and the minimum laser cavity length to achieve lasing for the observed reduced

overpopulation densities for the transitions 5-2, 5-3, and 6-2.

Laser Transition n	ΔE (eV)	Wavelength (Å)	A_{ki} ^a $10^4 s^{-1}$	Reduced Overpopulation Density ($10^{10} cm^{-3}$)	Threshold Reduced Overpopulation Density ^b ($10^7 cm^{-3}$)	Minimum Length (cm)
5-2	2.86	4340.5	0.094	3.83	4.61	0.212
			3			
5-3	0.966	12,818.1	0.033	3.82	0.494	0.013
			9			
6-2	3.02	4101.7	0.051	1.15	6.92	0.605
			5			

^a Einstein A coefficient for the transition from level k to level i

^b for a laser cavity length of 100 cm and R=0.99

5

D. Level population model and inversion pumping

In order to estimate hydrogen excited state level populations and inversion pumping, the collisional radiative model [6, 36] is applied to the plasma conditions obtained herein ($T_e \sim 0.8 eV$, $n_e \sim 10^9 cm^{-3}$). The collisional radiative model explicitly includes all level population and de-population mechanisms for each excited level from every other excited level in the hydrogen atom. Excited level n is, then, populated by collisional excitation from all lower excited states, and collisional and radiative de-excitation from all higher excited states. De-population explicitly includes collisional and radiative de-excitation to all lower states, and collisional excitation to all higher levels. Independent ionization loss, radiative recombination, and dielectronic recombination are included for all levels as well. A separate balance equation is prescribed for each individual level and is coupled to all other level equations through the population and de-population terms described above.

In order to close the set of equations, truncation was chosen at $n = 9$. This is justified by both the experimental observation of no measurable emission from higher lying states and *a posteriori* via the model results indicating a progression of negligibly small level densities beyond $n = 6$. The ground state ($n = 1$) level population cannot be determined by this method since the important affects of dissociation, molecular recombination, and transport are not included. As discussed earlier (Sec. 3A), however, an estimate based on emission line profiles places the total H atom density $\sim 6 \times 10^{13} \text{ cm}^{-3}$. Since this is overwhelmingly dominated by the ground state, the assignment $N_1 = 6 \times 10^{13} \text{ cm}^{-3}$ will be made throughout.

Solution to the $n = 2$ to 9 level equations under these conditions shows no inversion in any of the level populations. This is an expected result for a steady, thermal plasma. Also, as expected, the dominant mechanisms are found to be population by collisional excitation and de-population by radiative decay.

The results of this calculation are inconsistent with the spectroscopic observations. Absolutely calibrating the monochromator for the Balmer lines however yields, $N_{3-6} > 10^9 \text{ cm}^{-3}$ as shown in TABLE 9. There is, then, a heretofore undetermined mechanism providing direct excited state population, *i.e.* pumping. To help quantify the affects of this mechanism, the level equations are once again evaluated with N_{3-6} fixed to the values given in TABLE 9 and the inclusion of independent pumping rates for $n = 5$ and 6. Since spectroscopic results indicate $n = 3$ to 8 inversion, pumping is prescribed to the $n = 5$ and 6 states from the ground state, $n = 1$. The results from this calculation for $n = 1$ to 9 are summarized in TABLE 12.

TABLE 12. Model calculated level densities N_n for excited states $n = 1$ to 9 with an $n = 3$ to 8 pumping mechanisms.

Principal Quantum Number n	$N_n (10^9 \text{ cm}^{-3})$
1a	60,000
2	24.4
3	11.7
4	78.4

138	
5a	1930
6a	838
7	2.3
8	2.5
9	2.6

^a held fixed at the measured values

Now collisional mechanisms from the $n = 5$ and 6 states as well as ground state collisional excitation and radiative decay significantly contribute to population and de-
 5 population rates. In addition, demonstrated inversion in the populations with the possibility of laser transitions from i) $n = 3$, $n = 4$, $n = 5$, $n = 6$, and $n = 7$ to $n = 2$, ii) $n = 4$, $n = 5$, and $n = 6$ to $n = 3$ and iii) $n = 5$ and $n = 6$ to $n = 4$ are predicted.

The pumping rates and corresponding powers were also determined in this analysis yielding the rates given in TABLE 13. For example, in order for the $n = 5$ state to be pumped
 10 to the desired level, the pumping mechanism must represent a transition rate density of $8.4 \times 10^{19} \text{ cm}^{-3} \cdot \text{s}^{-1}$ from $n = 1$ to $n = 5$. Since the $n = 5$ state has a excitation energy of 13.05 eV, this pumping mechanism consumes energy at a rate of $\sim 175.3 \text{ W} \cdot \text{cm}^{-3}$. Since this plasma is in the steady state, energy consumption at this rate implies an equivalent production at the same rate which is returned as H radiation corresponding to transitions to $n < 5$. No
 15 other source of power was evident except the that proposed due to the catalytic reaction of oxygen with hydrogen.

TABLE 13. The pumping rate and pumping power calculated from the collisional-radiative model for laser transitions 5-2, 5-3, and 6-2.

20

Laser Transition	Calculated Pumping Rate of Upper Level	Calculated Pumping Power
	$(10^{19} \text{ cm}^{-3} \cdot \text{s}^{-1})$	$(\text{W} \cdot \text{cm}^{-3})$

139

5-2		
	8.4 ^a	175.3 ^a
5-3		
6-2	2.12	44.8

^a for 5-2 and 5-3 transitionsE. Blue and infrared laser and power applications

A micro-water laser may possible using proven approaches. As an advancement to the liquid based predecessor, micro-organic dye lasers have been developed by suspending each dye molecule in a cavity of a zeolite rather than in solution [37]. If they can be electrically pumped, such devices may eventually be competitive with semiconductor diode lasers; however, currently they require optical pumping. Microwaves are transparent to materials comprised of silicon or aluminium oxides. Thus, microcavities containing water vapor could potentially provide more competitive alternative microlasers for microelectronics applications that do not suffer from lattice constant and thermal expansion coefficient incompatibilities or require sophisticated materials or structures such as multiple quantum wells [1, 38].

Lasing is possible at blue wavelengths which are ideal for many communications and microelectronics applications as well as at a wavelength of 1.3 μm which is ideal for transmission through glass optical fibers. The emission wavelength of the potential water laser is about 400 nm which is suitable for the next generation 15-Gbyte DVDs [1]. Currently, the ideal laser diode for telecommunications applications is the $In_xGa_{1-x}As_yP_{1-y}$ diode laser wherein a lattice constant mismatch requires that the laser be separate from the silicon circuits. An integrated laser would revolutionize telecommunications, electronics, and computing [39]. Conceptually, we see no obvious impediment to integration of a water-plasma laser. In addition, many more laser wavelengths corresponding to Balmer, Paschen, and Brackett lines are possible.

The observed 175 $W \cdot cm^{-3}$ pumping power of the $n = 5$ state is unprecedented given the microwave input power of $\sim 9 W \cdot cm^{-3}$. Using the model, the corresponding lasing power and efficiency of the 5-2 transition are high, 5 $W \cdot cm^{-3}$ and 56%, respectively, compared to the highest power commercially available for a He/Ne laser of about 50 mW at 0.01%

efficiency. Our results indicate that with a microwave input power of 9 kW, 1000 cm^3 of water vapor plasma medium is capable of 5 kW cw laser power, comparable to the most powerful industrial cutting and welding lasers at about 50 times the efficiency. This obviously changes the prospects for many laser applications that have been limited by size or power requirements such as space-based lasers [40] and the National Ignition Facility (NIF) [41].

An even more significant opportunity exists for electric power generation. Compact magnetron-tube microwave power sources that are ubiquitous in applications such as microwave ovens are about 70-85% efficient and are extremely inexpensive and light-weight (unit cost for heating applications is about \$10/kW with mass <1 kg/kW [42-44]). In addition, conversion of monochromatic spontaneous and/or stimulated emission from the water plasma cell to electricity using a photovoltaic (PV) with a band gap that is matched to the wavelength can be achieved with greater than 80% efficiency at a photovoltaic cell irradiation up to 1000 $\text{W} \cdot \text{cm}^{-2}$ (7300 suns equivalent) requiring less than 1/7300 the PV active area of solar conversion [45-48]. Given that ultra-light, thin film photovoltaics are mass-produced at about $\sim 2\text{¢} \cdot \text{cm}^{-2}$ [49], we propose a competitive direct electric power generation system comprising an open cavity microwave driven water plasma surrounded by a photovoltaic converter where the cavity and converter reside inside the plasma vacuum vessel. This design eliminates the need for a window since the results of the model indicate that over 90% of the 200 $\text{W} \cdot \text{cm}^{-3}$ of optical power (total $n = 1 \rightarrow 5, 6$ pumping power given in TABLE 13) due to catalysis involves Lyman emission. For short wavelength radiation, the quantum efficiency may be significantly greater than one which compensates for the photon-band-gap energy mismatch [50]. Using current technology, plasma cell power densities comparable to those of an internal combustion engine (ICE) and the efficient direct conversion of the power into electricity may be realizable with a system having reduced weight, capital cost, infrastructure requirements, and environmental impact than the ICE. Furthermore, this technology is sustainable; whereas, the ICE is not.

4. Conclusion

The reactions O_2 to O and O^{2+} , O_2 to O and O^{3+} , and 2O to 2O^+ provide a net enthalpy of an integer multiple of the potential energy of atomic hydrogen of 2, 4, and 1 times 27.2 eV, respectively. Stationary inverted H Balmer and Lyman populations were observed from a low pressure water-vapor microwave discharge plasmas. The ionization and population of excited atomic hydrogen levels was attributed to energy provided by the catalytic resonant

energy transfer between hydrogen atoms and molecular oxygen formed in the water plasma. The catalysis mechanism was supported by the observation of O^{2+} and H Balmer line broadening of 55 eV compared to 1 eV for hydrogen alone. The catalysis reaction, and consequently the inversion, depended on specific plasma conditions provided by the Evenson
 5 microwave cavity. In contrast, no inversion was observed using RF or glow discharge cells. In addition, the requirement for the natural hydrogen-oxygen stoichiometry of the water plasma was stringent in that a deviation by over 2% excess of either gas caused a reversal of the inversion.

The high hydrogen atom temperature with a relatively low electron temperature,
 10 $T_e = 2 \text{ eV}$, due to the catalysis reaction were characteristic of cold recombining plasmas. These conditions of a water plasma favored an inverted population in the lower levels. Thus, the catalysis of atomic hydrogen may pump a cw HI laser with expected laser oscillations from i) $n = 3, n = 4, n = 5, n = 6, n = 7$ and $n = 8$ to $n = 2$, ii) $n = 4, n = 5, n = 6$, and $n = 7$ to $n = 3$ and iii) $n = 5$ and $n = 6$ to $n = 4$. A micro-water laser capable of integration may
 15 possible using proven approaches. Many more laser wavelengths corresponding to Balmer, Paschen, and Brackett lines are possible. With the capability of lasing over the widest range of atomic wavelengths of any known atomic laser, far infrared to violet, the hydrogen laser based on water-plasma may prove to be the most versatile laser yet discovered.

With the development of a pumping power of over $200 \text{ W} \cdot \text{cm}^{-3}$ for a microwave input
 20 power of $\sim 9 \text{ W} \cdot \text{cm}^{-3}$, new opportunities are possible for laser applications that are limited by power and/or size considerations. In addition, a potential revolutionary application is the direct generation of electrical power using photovoltaic conversion of the spontaneous or stimulated water vapor plasma emission. Energy balances of 100 times that of hydrogen combustion have been reported previously [51] which has implications for a sustainable energy technology that
 25 surpasses internal combustion.

References

1. S. Nakamura, "The roles of structural imperfections in InGaN-based blue light-emitting diodes and laser diodes, *Science*, Vol. 281, (1998), pp. 956-962.
- 30 2. R. W. Hardin, "Challenges remain for blue diode lasers", *OE Reports*, SPIE, No. 192, Dec. (1999), <http://www.spie.org/web/ocr/december/dec99/cover1.html>.
3. L. I. Gudzenko, L. A. Shelepin, *Sov. Phys. JETP*, Vol. 18, (1963), p. 998.
4. S. Suckewer, H. Fishman, *J. Appl. Phys.*, Vol. 51, (1980), p. 1922.

5. W. T. Silfvast, O. R. Wood, *J. Opt. Soc. Am. B*, Vol. 4, (1987), p. 609.
6. H. Akatsuka, M. Suzuki, "Stationary population inversion of hydrogen in arc-heated magnetically trapped expanding hydrogen-helium plasma jet", *Phys. Rev. E*, Vol. 49, (1994), pp. 1534-1544.
- 5 7. R. Mills, J. Dong, Y. Lu, "Observation of Extreme Ultraviolet Hydrogen Emission from Incandescently Heated Hydrogen Gas with Certain Catalysts", *Int. J. Hydrogen Energy*, Vol. 25, (2000), pp. 919-943.
8. R. Mills and M. Nansteel, P. Ray, "Argon-Hydrogen-Strontium Discharge Light Source", *IEEE Transactions on Plasma Science*, Vol. 30, No. 2, (2002), pp. 639-653.
- 10 9. R. L. Mills, P. Ray, B. Dhandapani, M. Nansteel, X. Chen, J. He, "Spectroscopic Identification of Transitions of Fractional Rydberg States of Atomic Hydrogen", *J. of Quantitative Spectroscopy and Radiative Transfer*, Vol. 76, No. 1, (2003), pp. 117-130.
10. R. L. Mills, P. Ray, B. Dhandapani, M. Nansteel, X. Chen, J. He, "New Power Source from Fractional Quantum Energy Levels of Atomic Hydrogen that Surpasses Internal
15 Combustion", *J Mol. Struct.*, in press.
11. R. Mills, P. Ray, R. M. Mayo, "Chemically-Generated Stationary Inverted Lyman Population for a CW HI Laser", *J Vac. Sci. and Tech. A*, submitted.
12. D. R. Lide, *CRC Handbook of Chemistry and Physics*, 79 th Edition, CRC Press, Boca Raton, Florida, (1998-1999), p. 9-55 and p. 10-175.
- 20 13. A., Crocker, H. A. Gebbie, M. F. Kimmitt, L. E. S. Mathias, "Stimulated emission in the far infra-red", *Nature*, Vol. 201, (1964), pp. 250-251.
14. W. J. Sarjeant, Z. Kucеровsky, E. Brannen, "Excitation processes and relaxation rates in the pulsed water vapor laser", *Applied Optics*, Vol. 11, No. 4, (1972), pp. 735-741.
15. A. K. Shuaibov, A. I. Dashchenko, I. V. Shevera, "Stationary radiator in the 130-190 nm
25 range based on water vapour plasma", *Quantum Electronics*, Vol. 31, No. 6, (2001), pp. 547-548.
16. R. L. Mills, P. Ray, E. Dayalan, B. Dhandapani, J. He, "Comparison of Excessive Balmer α Line Broadening of Inductively and Capacitively Coupled RF, Microwave, and Glow Discharge Hydrogen Plasmas with Certain Catalysts", *IEEE Transactions on Plasma
30 Science*, submitted.
17. R. L. Mills, P. Ray, "Substantial Changes in the Characteristics of a Microwave Plasma Due to Combining Argon and Hydrogen", *New Journal of Physics*, www.njp.org, Vol. 4, (2002), pp. 22.1-22.17.

18. R. L. Mills, P. Ray, B. Dhandapani, J. He, "Comparison of Excessive Balmer α Line Broadening of Glow Discharge and Microwave Hydrogen Plasmas with Certain Catalysts", J. of Applied Physics, submitted.
19. F. C. Fehsenfeld, K. M. Evenson, H. P. Broida, "Microwave discharges operating at 2450 MHz", Review of Scientific Instruments, Vol. 35, No. 3, (1965), pp. 294-298.
20. B. McCarroll, "An improved microwave discharge cavity for 2450 MHz", Review of Scientific Instruments, Vol. 41, (1970), p. 279.
21. I. R. Vidcovic, N. Konjevic, M. M. Kuraica, "Spectroscopic investigations of a cathode fall region of the Grimm-type glow discharge", Spectrochimica Acta, Part B, Vol. 51, (1996), pp. 1707-1731.
22. J. Tadic, I. Juranic, G. K. Moortgat, "Pressure dependence of the photooxidation of selected carbonyl compounds in air: n-butanal and n-pentanal", J. Photochemistry and Photobiology A: Chemistry, Vol. 143, (2000), 169-179.
23. NIST Atomic Spectra Database, www.physics.nist.gov/cgi-bin/AtData/display.ksh.
24. D. Barton, J. W. Bradley, D. A. Steele, and R. D. Short, "Investigating radio frequency plasmas used for the modification of polymer surfaces," J. Phys. Chem. B, Vol. 103, (1999), pp. 4423-4430.
25. A. K. Shuaibov, L. L. Shimon, A. I. Dashchenko, I. V. Shevera, "Optical characteristics of a glow discharge in a He/H_2O mixture", Plasma Physics Reports, Vol. 27, No. 10, (2001), pp. 897-900.
26. H. Okabe, *Photochemistry of Small Molecules*, John Wiley & Sons, New York, (1978).
27. J. G. Calvert, J. N. Pitts, *Photochemistry*, John Wiley & Sons, New York, (1966), pp. 200-202.
28. R. K. Vatsa, H. R. Volpp, "Absorption cross-section for atmospheric important molecules at the H atom Lyman α wavelength (121.567 nm)", Chemical Physics Letters, Vol. 340, (2001), pp. 289-295.
29. S. Djurovic, J. R. Roberts, "Hydrogen Balmer alpha line shapes for hydrogen-argon mixtures in a low-pressure rf discharge", J. Appl. Phys., Vol. 74, No. 11, (1993), pp. 6558-6565.
30. J. Seidel, "Theory of two-photon polarization spectroscopy of plasma-broadened hydrogen L_α line", Phys. Rev. Letts., Vol. 57, No. 17, (1986), p. 2154.
31. A. Czernikowski, J. Chapelle, Acta Phys. Pol. A., Vol. 63, (1983), p. 67.
32. M. A. Gigosos, V. Cardenoso, "New plasma diagnosis tables of hydrogen Stark broadening

- including ion dynamics", *J. Phys. B: At. Mol. Opt. Phys.*, Vol. 29, (1996), pp. 4795-4838.
33. A. Comey, *Atomic and Laser Spectroscopy*, Clarendon Press, Oxford, (1977).
34. M. Kuraica, N. Konjevic, "Line shapes of atomic hydrogen in a plane-cathode abnormal glow discharge", *Physical Review A*, Volume 46, No. 7, October (1992), pp. 4429-4432.
- 5 35. S. B. Radovanov, K. Dzierzega, J. R. Roberts, J. K. Olthoff, "Time-resolved Balmer-alpha emission from fast hydrogen atoms in low pressure, radio-frequency discharges in hydrogen", *Appl. Phys. Letts.*, Vol. 66, No. 20, (1995), pp. 2637-2639.
36. T. Fujimoto, *J. Phys. Soc. Jpn.*, Vol. 47, (1979). p. 265.
37. S. R. Forrest, "Solid-state lasers: Lasing from a molecular sieve", *Nature* Vol. 397, (1999), pp. 294-295.
- 10 38. T. Someya, R. Werner, A. Forchel, M. Catalano, R. Cingolani, Y. Arakawa, "Room temperature lasing at blue wavelengths in gallium nitride microcavities", *Science*, Vol. 285, (1999), pp. 1905-1906.
39. P. Ball, "Let there be light", *Nature*, Vol. 409, (2001), pp. 974-976.
- 15 40. <http://www.airbornelaser.com>; <http://home.achilles.net/~jtalbot/history/starwars.html>;
<http://www.peacevision.org.uk/papers/webb.html>.
41. R. L. McCrory, et al., "OMEGA ICF experiments and preparation for direct drive ignition on NIF", *Nuclear Fusion*, Vol. 41, No. 10, (2001), pp. 1414-1422.
42. Panasonic specifications sheet on model #2M167B-M10G, Two Panasonic Way, 7E-2, Secaucus, NJ 07094, February, 25, 2000.
- 20 43. R. M. Dickinson, Chairman NASA SSP Wireless Power Transmission Working Group, presentation at http://ssp.jpl.nasa.gov/ssp_wireless_pres/wireless.ppt.
44. V. L. Granastein, R. K. Parker, C. M. Armstrong, "Scanning the technology vacuum electronics at the dawn of the twenty-first century", *Proceedings of the IEEE*, May, (1999), Vol. 87, No. 5, <http://www.spectrum.ieee.org/pubs/trans/9905/87proc05-granastein.html>,
25 (accessed January 2001).
45. L. C. Olsen, D. A. Huber, G. Dunham, F. W. Addis, "High efficiency monochromatic GaAs solar cells", in *Conf. Rec. 22nd IEEE Photovoltaic Specialists Conf.*, Las Vegas, NV, Vol. I, Oct. (1991), pp. 419-424.
- 30 46. R. A. Lowe, G. A. Landis, P. Jenkins, "Response of photovoltaic cells to pulsed laser illumination", *IEEE Transactions on Electron Devices*, Vol. 42, No. 4, (1995), pp. 744-751.
47. R. K. Jain, G. A. Landis, "Transient response of gallium arsenide and silicon solar cells under laser pulse", *Solid-State Electronics*, Vol. 4, No. 11, (1998), pp. 1981-1983.

48. P. A. Iles, "Non-solar photovoltaic cells", in *Conf. Rec. 21st IEEE Photovoltaic Specialists Conf.*, Kissimmee, FL, Vol. I, May, (1990), pp. 420-423.
49. <http://www.nrel.gov/docs/fy01osti/28928.pdf>.
50. R. Hartmann, K. -H. Stephan, L. Struder, "The quantum efficiency of pn-detectors from the near infrared to the soft X-ray region", *Nuclear Instruments and Methods in Physics Research A*, Vol. 439, (2000), pp. 216-220.
51. R. L. Mills, X. Chen, P. Ray, J. He, B. Dhandapani, "Plasma Power Source Based on a Catalytic Reaction of Atomic Hydrogen Measured by Water Bath Calorimetry", *Thermochimica Acta*, submitted.

10

In the lasers described herein above, the inverted hydrogen population can easily be formed in situ, which means that the inverted hydrogen population can be formed within a chemically generated plasma contained in a cell, without requiring rapid expansion of a plasma in a vacuum.

15

CLAIMS

1. A plasma comprising an in situ inverted hydrogen population.
- 5 2. A stationary inverted hydrogen population not formed by rapid expansion of a plasma into a vacuum.
3. A stationary inverted hydrogen population formed by the catalytic reaction of hydrogen atoms to lower-energy hydrogen atoms.
- 10 4. A stationary inverted hydrogen population according to any of the preceding claims, wherein the inverted hydrogen population is not powered by a high voltage electrical or radio discharge or arc, a high powered laser, synchrotron device, inductively coupled plasma generator, or expanding plasma jet.
- 15 5. A hydrogen reactor for forming a stationary inverted hydrogen population according to any of the preceding claims, the reactor comprising:
 - a cell constructed and arranged for forming a catalysis of atomic hydrogen under conditions that produce lower-energy hydrogen and form a continuous stationary
 - 20 inverted hydrogen population,
 - a source of catalyst for catalyzing the reaction of hydrogen atoms to lower-energy hydrogen atoms, and
 - a source of atomic hydrogen.
- 25 6. A hydrogen reactor according to any of the preceding claims, further comprising means to convert the plasma power to electrical power.
7. A hydrogen reactor according to any of the preceding claims, wherein the cell is constructed and arranged to produce chemical compounds containing lower-energy
- 30 hydrogen.
8. A hydrogen reactor according to any of the preceding claims, further comprising a converter for converting plasma energy to electrical energy.
- 35 9. A compound comprising:
 - (a) at least one neutral, positive, or negative increased binding energy hydrogen species having a binding energy
 - (i) greater than the binding energy of the corresponding ordinary
 - hydrogen species, or

(ii) greater than the binding energy of any hydrogen species for which the corresponding ordinary hydrogen species is unstable or is not observed because the ordinary hydrogen species' binding energy is less than thermal energies at ambient conditions, or is negative; and

(b) at least one other element, formed during the formation of the inverted hydrogen population according to any of the preceding claims.

10. A compound according to claim 9, wherein the increased binding energy hydrogen species is selected from the group consisting of H_n , H_n^- , and H_n^+ where n is a positive integer, with the proviso that n is greater than 1 when H has a positive charge.

11. A compound of claim 9, wherein the increased binding energy hydrogen species is selected from the group consisting of (a) hydride ion having a binding energy that is greater than the binding of ordinary hydride ion (about 0.8 eV) for $p = 2$ up to 23 in which the binding energy is represented by

$$\text{Binding Energy} = \frac{\hbar^2 \sqrt{s(s+1)}}{8\mu_e a_0^2 \left[\frac{1 + \sqrt{s(s+1)}}{p} \right]^2} - \frac{\pi\mu_0 e^2 \hbar^2}{m_e^2} \left(\frac{1}{a_H^3} + \frac{2^2}{a_0^3 \left[\frac{1 + \sqrt{s(s+1)}}{p} \right]^3} \right)$$

where p is an integer greater than one, $s = 1/2$, π is pi, \hbar is Planck's constant bar, μ_0 is the permeability of vacuum, m_e is the mass of the electron, μ_e is the reduced

electron mass given by $\mu_e = \frac{m_e m_p}{\frac{m_e}{\sqrt{\frac{3}{4}}} + m_p}$ where m_p is the mass of the proton, a_H is the

radius of the hydrogen atom, a_0 is the Bohr radius, and e is the elementary charge; (b) hydrogen atom having a binding energy greater than about 13.6 eV; (c) hydrogen molecule having a first binding energy greater than about 15.3 eV; and (d) molecular hydrogen ion having a binding energy greater than about 16.3 eV.

12. A compound of claim 11, wherein the increased binding energy hydrogen species is a hydride ion having a binding energy of about 3, 6.6, 11.2, 16.7, 22.8, 29.3, 36.1, 42.8, 49.4, 55.5, 61.0, 65.6, 69.2, 71.6, 72.4, 71.6, 68.8, 64.0, 56.8, 47.1, 34.7, 19.3, and 0.69 eV.

13. A compound of claim 9, wherein the increased binding energy hydrogen species is a hydride ion having the binding energy:

$$\text{Binding Energy} = \frac{\hbar^2 \sqrt{s(s+1)}}{8\mu_e a_0^2 \left[\frac{1 + \sqrt{s(s+1)}}{p} \right]^2} - \frac{\pi\mu_0 e^2 \hbar^2}{m_e^2} \left(\frac{1}{a_H^3} + \frac{2^2}{a_0^3 \left[\frac{1 + \sqrt{s(s+1)}}{p} \right]^3} \right)$$

where p is an integer greater than one, $s = 1/2$, π is pi, \hbar is Planck's constant bar, μ_0 is the permeability of vacuum, m_e is the mass of the electron, μ_e is the reduced

electron mass given by $\mu_e = \frac{m_e m_p}{\frac{m_e}{\sqrt{3}} + m_p}$ where m_p is the mass of the proton, a_H is the

radius of the hydrogen atom, a_0 is the Bohr radius, and e is the elementary charge.

14. A compound of claim 9, wherein the increased binding energy hydrogen species is selected from the group consisting of:

(a) a hydrogen atom having a binding energy of about $\frac{13.6 \text{ eV}}{\left(\frac{1}{p}\right)^2}$ where p is an

integer,

(b) an increased binding energy hydride ion (H^-) having a binding energy of about

$$\text{Binding Energy} = \frac{\hbar^2 \sqrt{s(s+1)}}{8\mu_e a_0^2 \left[\frac{1 + \sqrt{s(s+1)}}{p} \right]^2} - \frac{\pi\mu_0 e^2 \hbar^2}{m_e^2} \left(\frac{1}{a_H^3} + \frac{2^2}{a_0^3 \left[\frac{1 + \sqrt{s(s+1)}}{p} \right]^3} \right)$$

where p is an integer greater than one, $s = 1/2$, π is pi, \hbar is Planck's constant bar, μ_0 is the permeability of vacuum, m_e is the mass of the electron, μ_e is the reduced

electron mass given by $\mu_e = \frac{m_e m_p}{\frac{m_e}{\sqrt{3}} + m_p}$ where m_p is the mass of the proton, a_H is the

radius of the hydrogen atom, a_0 is the Bohr radius, and e is the elementary charge;

(c) an increased binding energy hydrogen species $H_4^+(1/p)$;

(d) an increased binding energy hydrogen species trihydrino molecular ion, $H_3^+(1/p)$, having a binding energy of about $\frac{22.6}{\left(\frac{1}{p}\right)^2} \text{ eV}$ where p is an integer,

(e) an increased binding energy hydrogen molecule having a binding energy of

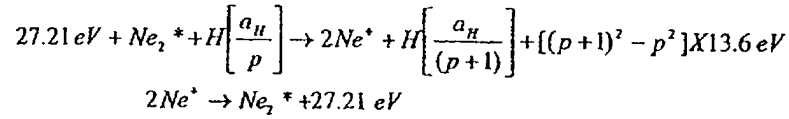
about $\frac{15.3}{\left(\frac{1}{p}\right)^2} eV$; and

(f) an increased binding energy hydrogen molecular ion with a binding energy of about $\frac{16.3}{\left(\frac{1}{p}\right)^2} eV$.

- 5 15. A reactor according to any of the preceding claims, wherein the catalyst comprises a chemical or physical process that provides a net enthalpy of $m \cdot 27.2 \pm 0.5 eV$ where m is an integer or $m/2 \cdot 27.2 \pm 0.5 eV$ where m is an integer greater than one.
- 10 16. A reactor according to any of the preceding claims, wherein the catalyst provides a net enthalpy of $m \cdot 27.2 \pm 0.5 eV$ where m is an integer or $m/2 \cdot 27.2 \pm 0.5 eV$ where m is an integer greater than one corresponding to a resonant state energy level of the catalyst that is excited to provide the enthalpy.
- 15 17. A reactor according to any of the preceding claims, wherein a catalytic system is provided by the ionization of t electrons from a participating species such as an atom, an ion, a molecule, and an ionic or molecular compound to a continuum energy level such that the sum of the ionization energies of the t electrons is approximately $m \cdot 27.2 \pm 0.5 eV$ where m is an integer or $m/2 \cdot 27.2 \pm 0.5 eV$ where m is an integer greater than one and t is an integer.
- 20 18. A reactor according to any of the preceding claims, wherein the catalyst is provided by the transfer of t electrons between participating ions; the transfer of t electrons from one ion to another ion provides a net enthalpy of reaction whereby the sum of the ionization energy of the electron donating ion minus the ionization energy of the electron accepting ion equals approximately $m \cdot 27.2 \pm 0.5 eV$ where m is an integer or $m/2 \cdot 27.2 \pm 0.5 eV$ where m is an integer greater than one and t is an integer.
- 25 19. A reactor according to any of the preceding claims, wherein m is an integer less than 400.
- 30 20. A reactor according to any of the preceding claims, wherein the catalysts comprises He^+ which absorbs $40.8 eV$ during the transition from the $n = 1$ energy level to the $n = 2$ energy level which corresponds to $3/2 \cdot 27.2 eV$ ($m = 3$) that serves as a catalyst for the transition of atomic hydrogen from the $n = 1$ ($p = 1$) state to the $n = 1/2$ ($p = 2$) state.
- 35

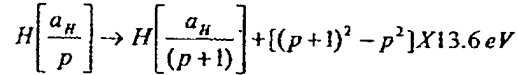
21. A reactor according to any of the preceding claims, wherein the catalyst comprises Ar^{2+} which absorbs 40.8 eV and is ionized to Ar^{3+} which corresponds to $3/2 \cdot 27.2 \text{ eV}$ ($m = 3$) during the transition of atomic hydrogen from the $n = 1$ ($p = 1$) energy level to the $n = 1/2$ ($p = 2$) energy level .
22. A reactor according to any of the preceding claims, wherein the catalyst comprises at least one selected from the group of Li, Be, K, Ca, Ti, V, Cr, Mn, Fe, Co, Ni, Cu, Zn, As, Se, Kr, Rb, Sr, Nb, Mo, Pd, Sn, Te, Cs, Ce, Pr, Sm, Gd, Dy, Pb, Pt, He^+ , Na^+ , Rb^+ , Sr^+ , Fe^{3+} , Mo^{2+} , Mo^{4+} , and In^{3+} .
23. A reactor according to any of the preceding claims, wherein the catalyst of atomic hydrogen is capable of providing a net enthalpy of $m \cdot 27.2 \pm 0.5 \text{ eV}$ where m is an integer or $m/2 \cdot 27.2 \pm 0.5 \text{ eV}$ where m is an integer greater than one and capable of forming a hydrogen atom having a binding energy of about $\frac{13.6 \text{ eV}}{\left(\frac{1}{p}\right)^2}$ where p is an integer wherein the net enthalpy is provided by the breaking of a molecular bond of the catalyst and the ionization of t electrons from an atom of the broken molecule each to a continuum energy level such that the sum of the bond energy and the ionization energies of the t electrons is approximately $m \cdot 27.2 \pm 0.5 \text{ eV}$ where m is an integer or $m/2 \cdot 27.2 \pm 0.5 \text{ eV}$ where m is an integer greater than one.
24. A reactor according to any of the preceding claims, wherein the catalyst comprises at least one of C_2 , N_2 , O_2 , CO_2 , NO_2 , and NO_3 .
25. A reactor according to any of the preceding claims, wherein the catalyst comprises a molecule in combination with an ion or atom catalyst.
26. A reactor according to any of the preceding claims, wherein the catalyst comprises at least one molecule selected from the group of C_2 , N_2 , O_2 , CO_2 , NO_2 , and NO_3 in combination with at least one atom or ion selected from the group of Li, Be, K, Ca, Ti, V, Cr, Mn, Fe, Co, Ni, Cu, Zn, As, Se, Kr, Rb, Sr, Nb, Mo, Pd, Sn, Te, Cs, Ce, Pr, Sm, Gd, Dy, Pb, Pt, Kr, He^+ , Na^+ , Rb^+ , Sr^+ , Fe^{3+} , Mo^{2+} , Mo^{4+} , In^{3+} , He^+ , Ar^+ , Xe^+ , Ar^{2+} and H^+ , and Ne^+ and H^+ .
27. A reactor according to any of the preceding claims, wherein the catalyst comprises helium excimer, Ne_2^+ , which absorbs 27.21 eV and is ionized to $2Ne^+$, to catalyze the transition of atomic hydrogen from the (p) energy level to the $(p + 1)$ energy level

given by



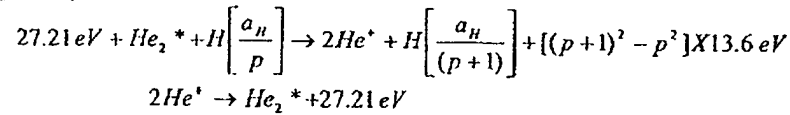
5

And, the overall reaction is



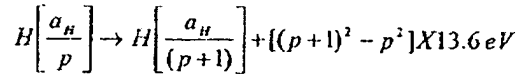
10

28. A reactor according to any of the preceding claims, wherein the catalyst comprises helium excimer, He_2^* , which absorbs 27.21 eV and is ionized to 2He^+ , to catalyze the transition of atomic hydrogen from the (p) energy level to the (p+1) energy level given by



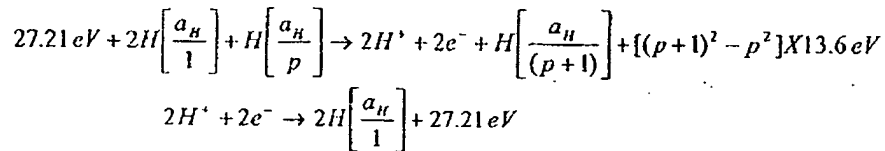
And, the overall reaction is

15



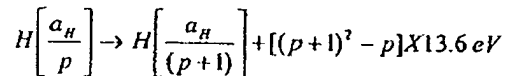
20

29. A reactor according to any of the preceding claims, wherein the catalyst comprises two hydrogen atoms which absorbs 27.21 eV and is ionized to 2H^+ , to catalyze the transition of atomic hydrogen from the (p) energy level to the (p+1) energy level given by



And, the overall reaction is

25



30

30. A reactor according to any of the preceding claims, wherein the catalyst comprises a catalytic disproportionation reaction of atomic hydrogen wherein lower-energy hydrogen atoms, hydrinos, can act as catalysts because each of the metastable excitation, resonance excitation, and ionization energy of a hydrino atom is $m \times 27.2 \text{ eV}$.

31. A reactor according to claim 30, wherein catalytic reaction of a first hydrino atom to a

lower energy state affected by a second hydrino atom involves the resonant coupling between the atoms of m degenerate multipoles each having 27.21 eV of potential energy.

- 5 32. A reactor according to claim 30, wherein the energy transfer of $m \times 27.2 \text{ eV}$ from the first hydrino atom to the second hydrino atom causes the central field of the first atom to increase by m and its electron to drop m levels lower from a radius of $\frac{a_H}{p}$ to a radius of $\frac{a_H}{p+m}$.
- 10 33. A reactor according to claim 30, wherein the second interacting lower-energy hydrogen is either excited to a metastable state, excited to a resonance state, or ionized by the resonant energy transfer.
- 15 34. A reactor according to claim 30, wherein the resonant transfer may occur in multiple stages.
35. A reactor according to claim 34, wherein a nonradiative transfer by multipole coupling may occur wherein the central field of the first increases by m , then the electron of the first drops m levels lower from a radius of $\frac{a_H}{p}$ to a radius of $\frac{a_H}{p+m}$ with further resonant energy transfer.
- 20 36. A reactor according to claim 30, wherein the energy transferred by multipole coupling may occur by a mechanism that is analogous to photon absorption involving an excitation to a virtual level.
- 25 37. A reactor according to claim 30, wherein the energy transferred by multipole coupling during the electron transition of the first hydrino atom may occur by a mechanism that is analogous to two photon absorption involving a first excitation to a virtual level and a second excitation to a resonant or continuum level.
- 30 38. A reactor according to any of the preceding claims, wherein a catalytic reaction with hydrino catalysts for the transition of $H\left[\frac{a_H}{p}\right]$ to $H\left[\frac{a_H}{p+m}\right]$ induced by a multipole resonance transfer of $m \cdot 27.21 \text{ eV}$ and a transfer of $[(p')^2 - (p' - m')^2] \times 13.6 \text{ eV} - m \cdot 27.2 \text{ eV}$ with a resonance state of $H\left[\frac{a_H}{p' - m'}\right]$ excited

in $H\left[\frac{a_H}{p'}\right]$ is represented by

$$H\left[\frac{a_H}{p'}\right] + H\left[\frac{a_H}{p}\right] \rightarrow H\left[\frac{a_H}{p'-m'}\right] + H\left[\frac{a_H}{p+m}\right] + [(p+m)^2 - p^2 - (p'^2 - (p'-m')^2)] \times 13.6 \text{ eV}$$

where p , p' , m , and m' are integers.

5

39. A reactor according to any of the preceding claims, wherein a hydrino atom with the initial lower-energy state quantum number p and radius $\frac{a_H}{p}$ may undergo a transition to the state with lower-energy state quantum number $(p+m)$ and radius $\frac{a_H}{(p+m)}$ by reaction with a hydrino atom with the initial lower-energy state quantum number m' , initial radius $\frac{a_H}{m'}$, and final radius a_H that provides a net enthalpy of $m \cdot 27.2 \pm 0.5 \text{ eV}$ where m is an integer or $m/2 \cdot 27.2 \pm 0.5 \text{ eV}$ where m is an integer greater than one.

10

40. A reactor according to claim 36 of hydrogen-type atom, $H\left[\frac{a_H}{p}\right]$, with the hydrogen-type atom, $H\left[\frac{a_H}{m'}\right]$, that is ionized by the resonant energy transfer to cause a transition reaction is represented by

15

$$m \times 27.21 \text{ eV} + H\left[\frac{a_H}{m'}\right] + H\left[\frac{a_H}{p}\right] \rightarrow H^+ + e^- + H\left[\frac{a_H}{(p+m)}\right] + [(p+m)^2 - p^2 - (m'^2 - 2m)] \times 13.6 \text{ eV}$$

$$H^+ + e^- \rightarrow H\left[\frac{a_H}{1}\right] + 13.6 \text{ eV}$$

And, the overall reaction is

20

$$H\left[\frac{a_H}{m'}\right] + H\left[\frac{a_H}{p}\right] \rightarrow H\left[\frac{a_H}{1}\right] + H\left[\frac{a_H}{(p+m)}\right] + [2pm + m^2 - m'^2] \times 13.6 \text{ eV} + 13.6 \text{ eV}$$

41. A reactor according to any of the preceding claims, wherein the catalyst comprises a mixture of a first catalyst and a source of a second catalyst.

42. A reactor according to claim 41, wherein the first catalyst produces the second catalyst from the source of the second catalyst.
- 5 43. A reactor according to claim 41, wherein the energy released by the catalysis of hydrogen by the first catalyst produces a plasma in the energy cell.
- 10 44. A reactor according to claim 41, wherein the energy released by the catalysis of hydrogen by the first catalyst ionizes the source of the second catalyst to produce the second catalyst.
- 15 45. A reactor according to claim 41, wherein the source of the second catalyst comprises at least one selected from the group consisting of helium, neon, argon, water vapor, or ammonia and the second catalyst is selected from the group of He^+ , Ne^+ , Ar^+ , O_1 , and N_2 wherein the catalyst ion is generated from the corresponding atom by a plasma created by catalysis of hydrogen by the first catalyst.
- 20 46. A reactor according to any of the preceding claims, wherein the reactor comprises at least one selected from the group consisting of an rf-plasma cell, a plasma electrolysis reactor, a barrier electrode reactor, an RF plasma reactor, a pressurized gas energy reactor, a gas discharge energy reactor, a microwave cell energy reactor, and a combination of a glow discharge cell and a microwave and or RF plasma reactor.
- 25 47. A reactor according to any of the preceding claims, wherein the reactor is a gas plasma forming type gas cell comprising a vessel having a chamber capable of containing a vacuum or pressures greater than atmospheric, a source of atomic hydrogen comprising a means to dissociate molecular hydrogen to atomic hydrogen, and a means to heat the source of catalyst capable of providing a net enthalpy of $m \cdot 27.2 \pm 0.5 \text{ eV}$ where m is an integer or $m/2 \cdot 27.2 \pm 0.5 \text{ eV}$ where m is an integer greater than one.
- 30 48. A reactor according to claim 47, wherein the hydrogen dissociator comprises a filament.
- 35 49. A reactor according to claim 47, wherein the filament comprises a tungsten filament.
50. A reactor according to any of claims 47-49, further comprising a heater to heat the catalyst to form a gaseous catalyst.
51. A reactor according to any of claims 47-50, wherein the catalyst comprises at least one

of potassium, rubidium, cesium and strontium metal, nitrate, or carbonate.

52. A reactor according to any of claims 47-51, further comprising a hydrogen supply tube and a hydrogen supply passage to supply hydrogen gas to the vessel.
53. A reactor according to any of claims 47-52, further comprising a hydrogen flow of hydrogen flow controller and valve to control the flow of hydrogen to the chamber.
54. A reactor according to any of claims 47-53, further comprising a plasma gas, a plasma gas supply, and a plasma gas passage.
55. A reactor according to any of claims 47-54, further comprising lines, valves, and flow regulators such that the plasma gas flows from the plasma gas supply via the plasma gas passage into the vessel.
56. A reactor according to any of claims 47-55, further comprising a plasma gas flow controller and control valve control the flow of plasma gas into the vessel.
57. A reactor according to any of claims 47-56, further comprising a hydrogen-plasma-gas mixer and mixture flow regulator.
58. A reactor according to any of claims 47-57, further comprising a hydrogen-plasma-gas mixture, a hydrogen-plasma-gas mixer, and a mixture flow regulator which control the composition of the mixture and the its flow into the vessel.
59. A reactor according to any of claims 47-58, further comprising a passage for the flow of the hydrogen-plasma-gas mixture into the vessel.
60. A reactor according to claim 54, wherein the plasma gas comprises at least one of the group of helium, neon, argon, water vapor, or ammonia.
61. A reactor according to claim 54, wherein the plasma gas comprises a source of the catalyst selected from the group of He^+ , Ne^+ , Ar^+ , O_2 , and N_2 .
62. A reactor according to claim 54, wherein the plasma gas is a source of catalyst and the hydrogen-plasma-gas mixture flows into the plasma and becomes catalyst and atomic hydrogen in the vessel.
63. A reactor according to any of claims 47-62, further comprising a vacuum pump and

vacuum lines.

- 5 64. A reactor according to any of claims 47-63, further comprising a gas flow means to provide that the reactor is operated under flow conditions with the hydrogen and the catalyst supplied continuously from the catalyst source and the hydrogen source.
- 10 65. A reactor according to any of claims 47-64, further comprising a catalyst reservoir and a catalyst supply passage for the passage of the gaseous catalyst from the reservoir to the vessel.
- 15 66. A reactor according to any of claims 47-65, further comprising a catalyst reservoir heater and a power supply to heat the catalyst in the catalyst reservoir to provide the gaseous catalyst.
- 20 67. A reactor according to claim 66, wherein the heater comprises a temperature control means wherein the vapor pressure of the catalyst is controlled by controlling the temperature of the catalyst reservoir.
- 25 68. A reactor according to any of the preceding claims, wherein the catalyst comprises at least one selected from the group consisting of Li, Be, K, Ca, Ti, V, Cr, Mn, Fe, Co, Ni, Cu, Zn, As, Se, Kr, Rb, Sr, Nb, Mo, Pd, Sn, Te, Cs, Ce, Pr, Sm, Gd, Dy, Pb, Pt, He^+ , Na^+ , Rb^+ , Sr^+ , Fe^{3+} , Mo^{2+} , Mo^{4+} , and In^3 .
- 30 69. A reactor according to any of claims 47-68, further comprising a chemically resistant open container such as a ceramic boat located inside the vessel which contains the catalyst.
- 35 70. A reactor according to claim 69, further comprising a heater to maintain an elevated cell temperature such that the catalyst in the boat is sublimed, boiled, or volatilized into the gas phase.
71. A reactor according to claim 69, further comprising a boat heater, and a power supply that heats the catalyst in the catalyst boat to provide the gaseous catalyst to the vessel.
72. A reactor according to claim 71, wherein the catalyst boat heater comprises a temperature control means wherein the vapor pressure of the catalyst is controlled by controlling the temperature of the catalyst boat.
73. A reactor according to any of claims 47-72, further comprising a lower-energy

hydrogen species and lower-energy hydrogen compound trap.

- 5 74. A reactor according to claim 73, further comprising a vacuum pump in communication with the trap to cause a pressure gradient from the vessel to the trap to cause gas flow and transport of the lower-energy hydrogen species or lower-energy hydrogen compound.
- 10 75. A reactor according to claim 74 further comprising a passage from the vessel to the trap and a vacuum line from the trap to the pump, and further comprising valves to and from the trap.
76. A reactor according to any of claims 47-75, wherein the vessel comprises a stainless steel alloy cell, a molybdenum cell, a tungsten cell, a glass, quartz, or ceramic cell.
- 15 77. A reactor according to any of claims 47-76, further comprising at least one of the group of an aspirator, atomizer, or nebulizer to form an aerosol of the source of catalyst.
- 20 78. A reactor according to claim 77, wherein the aspirator, atomizer, or nebulizer injects the source of catalyst or catalyst directly into the plasma.
79. A reactor according to any of claims 47-78, further comprising a plasma gas and a catalyst that is agitated from a source and supplied to the vessel through a flowing gas stream.
- 25 80. A reactor according to claim 80, wherein the flowing gas stream comprises hydrogen gas or plasma gas which may be an additional source of catalyst.
81. A reactor according to claim 80, wherein the source of catalyst comprises helium, neon, argon, water vapor, or ammonia.
- 30 82. A reactor according to any of claims 47-81, wherein the catalyst is dissolved or suspended in a liquid medium such as water and solution or suspension is aerosolized.
- 35 83. A reactor according to claim 82, wherein the medium is contained in the catalyst reservoir.
84. A reactor according to claim 82, wherein the solution or suspension containing catalyst is transported to the vessel by a carrier gas.

85. A reactor according to claim 84, wherein the carrier gas comprises at least one selected from the group consisting of hydrogen, helium, neon, argon, water vapor, or ammonia.
- 5 86. A reactor according to claim 84, wherein the carrier gas comprises at least one selected from the group consisting of helium, neon, argon, water vapor, or ammonia which serves as a source of catalyst and is ionized by the plasma to form at least one of the catalysts He^+ , Ne^+ , and Ar^+ or decomposed to form at least one of the catalysts O_2 and N_2 .
- 10 87. A reactor according to any of claims 47-86, wherein the nonthermal plasma temperature is maintained in the range of 5,000-5,000,000 °C.
88. A reactor according to any of claims 47-87, wherein the cell temperature is maintained above that of the catalyst reservoir which serves as a controllable source of catalyst.
- 15 89. A reactor according to any of claims 47-88, wherein the cell temperature is maintained above that of the catalyst boat which serves as a controllable source of catalyst.
90. A reactor according to any of claims 47-89, wherein a stainless steel alloy cell is maintained in the temperature range of 0-1200°C.
- 20 91. A reactor according to any of claims 47-90, wherein a molybdenum cell is maintained in the temperature range of 0-1800 °C.
- 25 92. A reactor according to any of claims 47-91, wherein a tungsten cell is maintained in the temperature range of 0-3000 °C.
93. A reactor according to any of claims 47-92, wherein a glass, quartz, or ceramic cell is maintained in the temperature range of 0-1800 °C.
- 30 94. A reactor according to any of claims 47-93, wherein molecular and atomic hydrogen partial pressures in the vessel is maintained in the range of 1 mtorr to 100 atm.
95. A reactor according to any of claims 47-94, wherein molecular and atomic hydrogen partial pressures in the vessel is maintained in the range of 100 mtorr to 20 torr.
- 35 96. A reactor according to any of claims 47-95, wherein catalyst partial pressure in the vessel is maintained in the range of 1 mtorr to 100 atm.

97. A reactor according to any of claims 47-96, wherein the catalyst partial pressure in the vessel is maintained in the range of 100 mtorr to 20 torr.
98. A reactor according to any of claims 47-97, wherein the flow rate of the plasma gas is
5 0-1 standard liters per minute per cm^3 of vessel volume.
99. A reactor according to any of claims 47-98, wherein the flow rate of the plasma gas is 0.001-10 sccm per cm^3 of vessel volume.
100. A reactor according to any of claims 47-99, wherein the flow rate of the hydrogen
10 gas is 0-1 standard liters per minute per cm^3 of vessel volume.
101. A reactor according to any of claims 47-100, wherein the flow rate of the hydrogen
15 gas is 0.001-10 sccm per cm^3 of vessel volume.
102. A reactor according to any of claims 47-101, wherein a hydrogen-plasma-gas
mixture in the vessel comprises at least one selected from the group consisting of
helium, neon, and argon comprising a composition of the plasma gas in the range of 99
20 to 1%.
103. A reactor according to any of claims 47-102, wherein a hydrogen-plasma-gas
mixture in the vessel comprises at least one selected from the group consisting of
helium, neon, and argon comprising a composition of the plasma gas in the range of 99
25 to 95%.
104. A reactor according to claim 102, wherein the flow rate of the hydrogen-plasma-
gas mixture is 0-1 standard liters per minute per cm^3 of vessel volume.
105. A reactor according to claim 102, wherein the flow rate of the hydrogen-plasma-
30 gas mixture is 0.001-10 sccm per cm^3 of vessel volume.
106. A reactor according to any of claims 47-105, further comprising a selective valve
for removal of lower-energy hydrogen products.
107. A reactor according to claim 106, wherein selectively removed lower-energy
35 hydrogen products comprise dihydrido molecules.
108. A reactor according to any of claims 47-107, further comprising a cold wall or
cryotrap to which at least one of increased binding energy hydrogen compounds and

dihydrido gas are cryopumped.

109. A reactor according to any of claims 1-46, wherein the reactor comprises a glow discharge cell comprising a vessel having a chamber capable of containing a vacuum or pressures greater than atmospheric, a source of atomic hydrogen, a cathode, an anode, a discharge power source to produce a glow discharge plasma, a source of atomic hydrogen, a source of catalyst, and a vacuum pump.
110. A reactor according to claim 109, wherein an offset voltage is between 0.5 and 500 V or the offset voltage is set to provide a field between 1 V/cm to 10 V/cm.
111. A reactor according to any of claims 109-110, wherein the discharge current is intermittent or pulsed.
112. A reactor according to claim 111, wherein the pulse frequency is between 0.1 Hz and 100 MHz and a duty cycle is between 0.1% and 95%.
113. A reactor according to any of claims 109-112, further comprising a hollow cathode comprising a compound electrode comprising multiple electrodes in series or parallel that may occupy a substantial portion of the volume of the reactor.
114. A reactor according to any of claims 109-113, comprising multiple hollow cathodes in parallel so that a desired electric field is produced in a large volume to generate a substantial power level.
115. A reactor according to claim 114, wherein the compound electrode comprises an anode and at least one of the group of multiple concentric hollow cathodes each electrically isolated from the common anode and multiple parallel plate electrodes connected in series.
116. A reactor according to any of claims 1-46, wherein the reactor comprises a microwave plasma forming gas cell comprising a vessel having a chamber capable of containing a vacuum or pressures greater than atmospheric, a source of atomic hydrogen comprising plasma dissociation of molecular hydrogen, a source of microwave power, and a source of catalyst capable of providing a net enthalpy of $m \cdot 27.2 \pm 0.5 \text{ eV}$ where m is an integer or $m/2 \cdot 27.2 \pm 0.5 \text{ eV}$ where m is an integer greater than one.
117. A reactor according to claim 116, wherein the source of microwave power is a

microwave generator, a tunable microwave cavity, waveguide, and a RF transparent window.

- 5 118. A reactor according to claim 116, wherein the source of microwave power is a microwave generator, a tunable microwave cavity, waveguide, and an antenna.
- 10 119. A reactor according to claim 118, wherein the microwaves are tuned by a tunable microwave cavity, carried by waveguide, and are delivered to the vessel through the RF transparent window.
120. A reactor according to claim 117, wherein the microwaves are tuned by a tunable microwave cavity, carried by waveguide, and are delivered to the vessel through the antenna.
- 15 121. A reactor according to claim 120, wherein the waveguide is either inside or outside of the cell.
122. A reactor according to claim 118, wherein the antenna is either inside or outside of the cell.
- 20 123. A reactor according to any of claims 116-122, further comprising a microwave generator comprising at least one selected from the group consisting of traveling wave tubes, klystrons, magnetrons, cyclotron resonance masers, gyrotrons, and free electron lasers.
- 25 124. A reactor according to claim 116, further comprising a microwave window comprising an Alumina or quartz window.
- 30 125. A reactor according to any of claims 116-124, wherein the vessel comprises a microwave resonator cavity.
126. A reactor according to claim 125, wherein the cavity comprises at least one selected from the group consisting of Evenson, Beenakker, McCarrol, and cylindrical cavity.
- 35 127. A reactor according to any of claims 116-126, wherein the vessel comprising a cavity that is a reentrant microwave cavity and the source of microwave power that excites a plasma in the reentrant cavity.

128. A reactor according to claim 127, wherein the recirculant cavity comprises an Evenson microwave cavity.
- 5 129. A reactor according to any of claims 116-128, wherein the microwave frequency of the source of microwave power is selected to efficiently form atomic hydrogen from molecular hydrogen.
- 10 130. A reactor according to any of claims 116-128, wherein the microwave frequency of the source of microwave power is selected to efficiently form ions that serve as catalysts from a source of catalyst.
- 15 131. A reactor according to claim 130, wherein the source of catalyst and catalyst comprise helium, neon, argon, water vapor, and ammonia, and He^+ , Ne^+ , Ar^+ , O_2 and N_2 , respectively.
132. A reactor according to any of claims 116-132, wherein the microwave frequency of the source of microwave power is in the range of 1 MHz to 100 GHz.
- 20 133. A reactor according to any of claims 116-132, wherein the microwave frequency of the source of microwave power is in the range of 50 MHz to 10 GHz.
134. A reactor according to any of claims 116-132, wherein the microwave frequency of the source of microwave power is in the range of 75 MHz \pm 50 MHz.
- 25 135. A reactor according to any of claims 116-132, wherein the microwave frequency of the source of microwave power is in the range of 2.4 GHz \pm 1 GHz.
136. A reactor according to any of any of the previous claims, wherein the catalyst is atomic hydrogen wherein;
- 30 the hydrogen pressure of the hydrogen microwave plasma is in the range of about 1 mtorr to about 100 atm, preferably the pressure is in the range of about 100 mtorr to about 1 atm, more preferably the pressure is about 100 mtorr to about 10 torr, the microwave power density is in the range of about 0.01 W to about 100 W/cm³ vessel volume, and
- 35 the hydrogen flow rate is in the range of about 0-1 standard liters per minute per cm³ of vessel volume and more preferably about 0.001-10 sccm per cm³ of vessel volume.

137. A reactor according to any of claims 116-136, wherein the power density of the source of plasma power is 0.01 W to 100 W/cm³ vessel volume.
- 5 138. A reactor according to any of claims 116-137, wherein the cell is a microwave resonator cavity.
139. A reactor according to any of claims 116-138, wherein the source of microwave supplies sufficient microwave power density to the cell to ionize a source of catalyst to form the catalyst.
- 10 140. A reactor according to claim 139, wherein the source of catalyst comprises at least one selected from the group consisting of helium, neon, argon, water vapor, or ammonia to form a catalyst such as He⁺, Ne⁺, Ar⁺, O₂, and N₂, respectively.
- 15 141. A reactor according to any of claims 116-140, wherein the microwave power source forms a nonthermal plasma.
142. A reactor according to any of claims 116-141, wherein the microwave power source or applicator is an antenna, waveguide, or cavity.
- 20 143. A reactor according to any of claims 116-128, wherein the species corresponding to the source of catalyst have a higher temperature than that at thermal equilibrium.
- 25 144. A reactor according to claim 143, wherein the source of catalyst comprises at least one selected from the group consisting of helium, neon, and argon atoms.
- 30 145. A reactor according to any of claims 116-144, wherein higher energy states such as ionized states of the source of catalyst are predominant over that of hydrogen compared to a corresponding thermal plasma wherein excited states of hydrogen are predominant.

164

146. A reactor according to any of claims 116-145, comprising a plurality of sources of microwave power.
147. A reactor according to claim 146, wherein the plurality of microwave sources are used simultaneously.
148. A reactor according to claim 146, wherein the plurality of microwave sources comprise Evenson cavities.
149. A reactor according to claim 148, wherein a nonthermal plasma is maintained by multiple Evenson cavities operated in parallel.
150. A reactor according to any of claims 116-149, wherein the vessel is cylindrical and comprises a quartz cell with Evenson cavities spaced along the longitudinal axis.
151. A reactor according to any of claims 1-46, wherein the reactor comprises an RF plasma forming gas cell comprising a vessel, a source of atomic hydrogen from RF plasma dissociation of molecular hydrogen, a source of RF power, and a catalyst capable of providing a net enthalpy of $m \cdot 27.2 \pm 0.5 \text{ eV}$ where m is an integer or $m/2 \cdot 27.2 \pm 0.5 \text{ eV}$ where m is an integer greater than one.
152. A reactor according to claim 151, wherein the RF power is capacitively or inductively coupled to the cell.
153. A reactor according to any of claims 151-152, further comprising two electrodes.
154. A reactor according to any of claims 151-153, further comprising a coaxial cable connected to a powered electrode by a coaxial center conductor.
155. A reactor according to any of claims 151-154, further comprising a coaxial center conductor connected to an external source coil which is wrapped around the cell.

165

156. A reactor according to claim 155, wherein the coaxial center conductor connected to an external source coil which is wrapped around the cell terminates without a connection to ground.
- 5 157. A reactor according to claim 155, wherein the coaxial center conductor connected to an external source coil which is wrapped around the cell is connect to ground.
- 10 158. A reactor according to any of claims 151-157, further comprising two electrodes wherein the electrodes are parallel plates.
159. A reactor according to claim 158, wherein the one of the parallel plate electrodes is powered and the other is connected to ground.
- 15 160. A reactor according to any of claims 151-159, wherein the cell comprises a Gaseous Electronics Conference (GEC) Reference Cell or modification.
161. A reactor according to any of claims 151-160, wherein the RF power is at 13.56 MHz.
- 20 162. A reactor according to any of claims 151-161, wherein at least one wall of the cell wrapped with the external coil is at least partially transparent to the RF excitation.
- 25 163. A reactor according to any of claims 151-162, wherein the RF frequency is in the range of about 100 Hz to about 100 GHz.
164. A reactor according to any of claims 151-162, wherein the RF frequency is preferably in the range of about 1 kHz to about 100 MHz.
- 30 165. A reactor according to any of claims 151-162, wherein the RF frequency is in the range of about 13.56 MHz \pm 50 MHz.
166. A reactor according to any of claims 151-162, wherein the RF frequency is in

166

the range of about 2.4 GHz \pm 1 GHz.

167. A reactor according to any of claims 1-46, wherein the reactor comprises an inductively coupled toroidal plasma cell comprising a vessel, a source of atomic hydrogen comprising RF plasma dissociation of molecular hydrogen, a source of RF power, and a catalyst capable of providing a net enthalpy of $m \cdot 27.2 \pm 0.5 \text{ eV}$ where m is an integer or $m/2 \cdot 27.2 \pm 0.5 \text{ eV}$ where m is an integer greater than one.
168. A reactor according to claim 167, comprising the Astron system of Astex Corporation described in US Patent No. 6,150,628.
169. A reactor according to any of claims 167-168, further comprising a primary of a transformer circuit.
170. A reactor according to any of claims 167-169, further comprising a primary of a transformer circuit driven by a radio frequency power supply.
171. A reactor according to any of claims 167-170, further comprising a primary of a transformer circuit wherein the plasma is a closed loop which acts as a secondary of the transformer circuit.
172. A reactor according to any of claims 167-171, wherein the RF frequency is in the range of about 100 Hz to about 100 GHz.
173. A reactor according to any of claims 167-171, wherein the RF frequency is in the range of about 1 kHz to about 100 MHz.
174. A reactor according to any of claims 167-171, wherein the RF frequency is in the range of about 13.56 MHz \pm 50 MHz.
175. A reactor according to any of claims 167-171, wherein the RF frequency is in the range of about 2.4 GHz \pm 1 GHz.

176. A reactor according to any of claims 1-46, wherein the reactor comprises a plasma forming electrolytic cell comprising a vessel, a cathode, an anode, an electrolyte, a high voltage electrolysis power supply, and a catalyst capable of providing a net enthalpy of $m \cdot 27.2 \pm 0.5 \text{ eV}$ where m is an integer or $m/2 \cdot 27.2 \pm 0.5 \text{ eV}$ where m is an integer greater than one.
177. A reactor according to claim 176, wherein the voltage is in the range 10-50 kV and the current density in the range of 1 to 100 A/cm².
178. A reactor according to any of claims 176-177, wherein the cathode comprises tungsten.
179. A reactor according to any of claims 176-177, wherein the anode comprises platinum.
180. A reactor according to any of claims 176-179, wherein the catalyst comprises at least one selected from the group consisting of Li, Be, K, Ca, Ti, V, Cr, Mn, Fe, Co, Ni, Cu, Zn, As, Se, Kr, Rb, Sr, Nb, Mo, Pd, Sn, Te, Cs, Ce, Pr, Sm, Gd, Dy, Pb, Pt, He^+ , Na^+ , Rb^+ , Sr^+ , Fe^{3+} , Mo^{2+} , Mo^{4+} , and In^{3+} .
181. A reactor according to any of claims 176-180, wherein the catalyst is formed from a source of catalyst.
182. A reactor according to claim 181, wherein the source of catalyst which forms the catalyst comprising at least one selected from the group consisting of Li, Be, K, Ca, Ti, V, Cr, Mn, Fe, Co, Ni, Cu, Zn, As, Se, Kr, Rb, Sr, Nb, Mo, Pd, Sn, Te, Cs, Ce, Pr, Sm, Gd, Dy, Pb, Pt, He^+ , Na^+ , Rb^+ , Sr^+ , Fe^{3+} , Mo^{2+} , Mo^{4+} , In^{3+} and K^+/K^+ .
183. A reactor according to any of claims 1-46, wherein the reactor comprises a radio frequency (RF) barrier electrode discharge cell comprising a vessel, a source of atomic hydrogen from the RF plasma dissociation of molecular hydrogen, a source of RF power, a cathode, an anode, and a catalyst capable of providing a net enthalpy of $m \cdot 27.2 \pm 0.5 \text{ eV}$ where m is an integer or $m/2 \cdot 27.2 \pm 0.5 \text{ eV}$ where m is an integer

greater than one.

184. A reactor according to claim 183, wherein at least one of the cathode and the anode is shielded by a dielectric barrier.

5

185. A reactor according to claim 184, wherein the dielectric barrier comprises at least one selected from the group consisting of glass, quartz, Alumina, and ceramic.

186. A reactor according to any of claims 183-185, wherein the RF power may be capacitively coupled to the cell.

10

187. A reactor according to any of claims 183-186, wherein the electrodes are external to the cell.

188. A reactor according to claim 187, wherein a dielectric layer separates the electrodes from the cell wall.

15

189. A reactor according to any of claims 183-188, wherein a high driving voltage may be AC and may be high frequency.

20

190. A reactor according to any of claims 183-189, wherein the RF source of power comprises a driving circuit comprising a high voltage power source which is capable of providing RF and an impedance matching circuit.

191. A reactor according to any of claims 183-190, wherein the frequency is in the range 100 Hz to 10 GHz.

25

192. A reactor according to any of claims 183-190, wherein the frequency is in the range 1 kHz to 1 MHz.

30

193. A reactor according to any of claims 183-190, wherein the frequency is in the range 5-10 kHz.

194. A reactor according to any of claims 183-193, wherein the voltage is in the range 100 V to 1 MV.
195. A reactor according to any of claims 183-193, wherein the voltage is in the range 1 kV to 100 kV.
196. A reactor according to any of claims 183-193, wherein the voltage is in the range 5 to 10 kV.
197. A reactor according to any of the preceding claims, further comprising a water vapor generator wherein the source of atomic hydrogen, and source of oxygen as the catalysts is water vapor from the water vapor generator.
198. A reactor according to claim 197, wherein the water vapor pressure is maintained in the range of about 0.1 mTorr to 10,000 Torr.
199. A reactor according to claim 197, wherein the water vapor pressure is maintained in the range of about 10 mTorr to 100 Torr.
200. A reactor according to claim 197, wherein the water vapor pressure is maintained in the range of about 10 mTorr to 10 Torr.
201. A reactor according to claim 197, wherein the water vapor pressure is maintained in the range of about 10 mTorr to 1 Torr.
202. A reactor according to any of claims claim 197-201, wherein the water vapor flow rate is about 0-1 standard liters per minute per cm^3 of vessel volume.
203. A reactor according to any of claims claim 197-201, wherein the water vapor flow rate is about 0.001-10 sccm per cm^3 of vessel volume.
204. A reactor according to any of claims 197-203, wherein the power density of the source of plasma power is in the range of about 0.01 W to about 100 W/cm^3 vessel

volume.

- 5
205. A reactor according to any of claims 197-203, wherein the power density of the source of plasma power is in the range of about 1 to 10 W/cm³ vessel volume.
206. A reactor according to any of claims 197-205, wherein water vapor may also be supplied by flowing hydrogen and oxygen into the cell which forms water vapor.
- 10
207. A reactor according to any of claims 197-206, wherein the mole fraction of hydrogen and oxygen may be stoichiometric for water.
208. A reactor according to any of claims 197-206, wherein an excess of hydrogen or oxygen is maintained.
- 15
209. A reactor according to any of claims 197-206, wherein the mole fraction of H₂ or O₂ does not vary from that which is stoichiometric for water by more than ± 99%.
- 20
210. A reactor according to any of claims 197-206, wherein the mole fraction of H₂ or O₂ does not vary from that which is stoichiometric for water by more than ± 50%.
211. A reactor according to any of claims 197-206, wherein the mole fraction of H₂ or O₂ does not vary from that which is stoichiometric for water by more than ± 10%.
- 25
212. A reactor according to any of claims 197-206, wherein the mole fraction of H₂ or O₂ does not vary from that which is stoichiometric for water by more than ± 2%.
- 30
213. A reactor according to any of claims 197-212, further comprising a source of ammonia wherein a source of atomic hydrogen and source of nitrogen as the catalysts comprises ammonia from the ammonia source.
214. A reactor according to claim 213, wherein the ammonia pressure is maintained in the range of about of 0.1 mTorr to 10,000 Torr.

215. A reactor according to claim 213, wherein the ammonia pressure is maintained in the range of about 10 mTorr to 100 Torr.
- 5 216. A reactor according to claim 213, wherein the ammonia pressure is maintained in the range of about 10 mTorr to 10 Torr.
217. A reactor according to claim 213, wherein the ammonia pressure is maintained in the range of about 10 mTorr to 1 Torr.
- 10 218. A reactor according to any of claims 213-217, wherein the ammonia flow rate is about 0-1 standard liters per minute per cm^3 of vessel volume.
219. A reactor according to any of claims 213-217, wherein the ammonia flow rate is about 0.001-10 sccm per cm^3 of vessel volume.
- 15 220. A reactor according to any of claims 197-219 wherein the power density of the source of plasma power is in the range of about 0.01 W to about 100 W/ cm^3 vessel volume.
- 20 221. A reactor according to any of claims 197-219 wherein the power density of the source of plasma power is in the range of about 1 to 10 W/ cm^3 vessel volume.
222. A reactor according to any of claims 213-221, wherein ammonia is supplied by flowing hydrogen and nitrogen into the cell which forms ammonia.
- 25 223. A reactor according to any of claims 213-222, wherein the mole fraction of hydrogen and nitrogen may be stoichiometric for ammonia.
- 30 224. A reactor according to any of claims 213-222, wherein an excess of hydrogen or nitrogen is maintained.
225. A reactor according to any of claims 213-220, wherein the mole fraction of H_2

or N_2 does not vary from that which is stoichiometric for ammonia by more than about $\pm 99\%$.

5 226. A reactor according to any of claims 213-220, wherein the mole fraction of H_2 or N_2 does not vary from that which is stoichiometric for ammonia by more than about $\pm 50\%$.

10 227. A reactor according to any of claims 213-220, wherein the mole fraction of H_2 or N_2 does not vary from that which is stoichiometric for ammonia by more $\pm 10\%$.

228. A reactor according to any of claims 213-220, wherein the mole fraction of H_2 or N_2 does not vary from that which is stoichiometric for ammonia by more $\pm 2\%$.

15 229. A reactor according to any of the preceding claims, further comprising a photon-to-electric power converter.

20 230. A reactor according to claim 229, further comprising a microwave cell wherein the microwave cavity is an open mesh cavity that transmits the plasma photons to a photon-to-electric power converter.

231. A reactor according to any of claims 229-231, wherein the photon-to-electric power converter comprises a photovoltaic.

25 232. A reactor according to any of claims 229-232, wherein the converter lines the plasma cell comprising a vacuum chamber.

30 233. A reactor according to any of claims 229-232, wherein the converter is radiation hardened and converts ultraviolet and extreme ultraviolet radiation to electricity.

234. A reactor according to any of claims 229-232, further comprising a light propagation structure comprising at least part of the cell wall that is transparent to a desired wavelength and/or wavelength range.

235. A reactor according to any of claims 229-232, further comprising a light propagation structure that is coated with a phosphor that converts one or more short wavelengths to desired longer wavelengths.
- 5 236. A reactor according to any of claims 229-232, wherein the converter converts at least one of ultraviolet and extreme ultraviolet light to light to which the converter is responsive such as visible light.
- 10 237. A reactor according to any of the preceding claims, further comprising a laser cavity.
238. A reactor according to claim 237, wherein hydrogen atoms and hydrino atoms that undergo transitions to lower-energy states with energy levels of about $\frac{13.6 \text{ eV}}{\left(\frac{1}{p}\right)^2}$
- 15 where p is an integer are the inverted population which lases.
239. A reactor according to any of claims 237-238, wherein the laser cavity further comprises a high reflectivity mirror.
- 20 240. A reactor according to claims 239, wherein the mirror reflects 95 to 99.9999% of the light and comprises a reflective spherical cavity mirror.
241. A reactor according to claims 239, further comprising an output coupler having transmission in the range 0.1 to 50%.
- 25 242. A reactor according to claims 239, further comprising an output coupler having transmission in the range 1 to 10%.
- 30 243. A reactor according to any of claims 237-242, further comprising windows, such as Brewster angle windows, that direct the laser beam and an optical rail which allows for adjustments of the cavity length to achieve lasing at a desired wavelength.

244. A reactor according to any of claims 237-243, wherein fast hydrogen atoms are formed by the catalysis of atomic hydrogen to lower-energy states with energy levels of about $\frac{13.6 \text{ eV}}{\left(\frac{1}{p}\right)^2}$ where p is an integer, excited state H is formed from fast $H(n=1)$
- 5 atoms by collisions with the background gas such as H_2 , and inversion is achieved by collisions with heavier gases or gases which provide a resonant excitation by the collision with fast H such as at least one molecule from the list of O_2 , H_2O , CO_2 , N_2 , NO_2 , NO , CO , and a halogen gas.
- 10 245. A reactor according to claim 244, wherein the lasing species is at least one of OH^* , CO_2 , and H_2O .
246. A reactor according to any of claims 237-246, further comprising a plasma gas of a noble gas and at least one halogen gas such that excimers form, and the power is
- 15 extracted by the excimer laser emission.
247. A reactor according to any of claims 237-246, further comprising a plasma gas that is excited by at least one of the pumping mechanism and an energy transfer from the excited state species such as excited atomic hydrogen.
- 20 248. A reactor according to any of the preceding claims, further comprising a means to propagate the light corresponding to the plasma.
249. A reactor according to claim 248, wherein at least one of extreme ultraviolet,
- 25 ultraviolet, visible, infrared, microwave, or radio wave radiation is produced and propagated using the propagation means.
250. A reactor according to any of claims 248-249, wherein the means to propagate the light corresponding to the plasma that is selective for a desired wavelength and/or
- 30 wavelength range.

251. A reactor according to any of claims 248-250, wherein the means to propagate the light comprises quartz that transmits extreme ultraviolet and ultraviolet light.
252. A reactor according to any of claims 248-251, wherein the reactor produces short wavelength light directly for photolithography.
253. comprises glass that transmits visible light.
254. A reactor according to any of claims 248-253, wherein the means to propagate the light comprises at least part of the cell wall that is transparent to a desired wavelength and/or wavelength range.
255. A reactor according to any of claims 248-254, wherein the means to propagate the light is coated with a phosphor that converts one or more short wavelengths to desired longer wavelengths.
256. A reactor according to claim 255, wherein the phosphor converts at least one of ultraviolet and extreme ultraviolet light to visible light.
257. A reactor according to any of claims 248-256, wherein at least a portion of the cell wall is insulated such that an elevated temperature may be maintained in the cell.
258. A reactor according to claim 257, wherein the cell wall comprises a double wall with a separating vacuum space.
259. A reactor according to any of claims 248-258, wherein the source of atomic hydrogen comprising a hydrogen dissociator.
260. A reactor according to claim 259, wherein the hydrogen dissociator comprises a filament.
261. A reactor according to claim 260, wherein the filament comprises a tungsten filament.

262. A reactor according to any of claims 248-260, further comprising a heater to heat the catalyst to form a gaseous catalyst.
- 5 263. A reactor according to any of claims 248-261, wherein the catalyst comprises at least one selected from the group consisting of potassium, rubidium, cesium and strontium metal, nitrate or carbonate.
- 10 264. A reactor according to claim 263, wherein a second catalyst from a source of second catalyst may be generated by a first catalyst.
265. A reactor according to claim 264, wherein the source of second catalyst comprises at least one selected from the group consisting of helium, neon, argon, water vapor, or ammonia.
- 15 266. A reactor according to claim 264, wherein the second catalyst comprises at least one selected from the group consisting of He^+ , Ne^+ , Ar^+ , O_2 , and N_2 .
- 20 267. A reactor according to any of claims 264-266, wherein the second catalyst is formed by ionization of the source of second catalyst by the plasma formed by the first catalyst.
268. A reactor according to any of claims 248-267, further comprising a hydride that decomposes over time to maintain a desired hydrogen partial pressure.
- 25 269. A reactor according to claim 268, further comprising a means to control the temperature of the cell to maintain a desired decomposition rate of the hydride to provide a desired hydrogen partial pressure.
- 30 270. A reactor according to claim 269, wherein the control means comprises a heater and a heater power controller.
271. A reactor according to claim 270, wherein the heater and controller comprise a

filament and a filament power controller.

272. A reactor according to any of claims 248-271, further comprising a source of microwave power to at least partially maintain the plasma.

273. A reactor according to any of claims 248-272, wherein the source of catalyst comprises at least one selected from the group consisting of helium, neon, argon, water vapor, or ammonia.

274. A reactor according to claim 273, wherein the catalyst comprises at least one selected from the group consisting of He^+ , Ne^+ , Ar^+ , O_2 , and N_2 .

275. A reactor according to any of claims 248-274, wherein a source of atomic hydrogen and the source of catalyst comprises a mixture of about 10% hydrogen with at least one selected from the group consisting of helium, neon, and argon.

276. A reactor according to any of claims 248-275, wherein a lower-energy hydrogen product comprising a dihydrido molecular ion is produced wherein emission from vibrational energy level transitions are a source of tunable laser light.

277. A reactor according to claim 276, wherein the lower-energy hydrogen product comprising $H_2(1/4)^+$ having energies of $\nu^* \cdot 1.18 \text{ eV}$, $\nu^* = \text{integer}$ that are a source of tunable laser light.

278. A reactor according to any of claims 248-277, further comprising a laser cavity.

279. A reactor according to any of claims 248-261, further comprising at least two electrodes and a power source to at least partially maintain the plasma by a glow discharge.

280. A method for producing power and lower-energy-hydrogen species and compounds comprising the steps of reacting the catalyst with the atomic hydrogen to form lower-energy-hydrogen species and compounds in any of the reactors of claims 1-

280.

281. A method for producing power and lower-energy-hydrogen species and compounds of claim 280 further comprising the steps of flowing a plasma gas that is a source of catalyst into the vessel.

282. A method according to any of claims 280-281, further comprising controlling the power by controlling an amount of gaseous catalyst.

283. A method according to claim 282, wherein the amount of gaseous catalyst is controlled by controlling the plasma gas flow rate.

284. A method according to any of claims 280-284, further comprising controlling the power by controlling the amount of hydrogen.

285. A method according to any of claims 280-284, further comprising controlling the power by controlling the flow of hydrogen from the source of hydrogen.

286. A method according to any of claims 280-284, further comprising controlling the power by controlling the flow of hydrogen and plasma gas and the ratio of hydrogen to plasma gas in a mixture.

287. A method according to claim 282, wherein the source of catalyst is at least one selected from the group of helium, neon, argon, water vapor, or ammonia which provides catalysts He^+ , Ne^+ , Ar^+ , O_2 , and N_2 , respectively.

288. A method according to any of claims 280-284, further comprising controlling the power by controlling the hydrogen flow rate, plasma gas flow rate, and hydrogen-plasma-gas flow rate with at least one of the group of a flow regulator, a hydrogen-plasma-gas mixer, flow rate controllers, and valves.

289. A method according to any of claims 280-284, further comprising controlling the power by controlling the temperature of the plasma with the power supplied by the

source of microwave power.

290. A method according to any of claims 280-289, further comprising the steps of providing a source of catalyst from a catalyst reservoir.

5

291. A method according to claim 290, further comprising the steps of controlling the temperature of the catalyst from a catalyst reservoir to control its vapor pressure.

10

292. A method according to any of claims 280-289, further comprising the steps of providing a source of catalyst from a catalyst boat.

293. A method according to claim 292, comprising the steps of controlling the temperature of the catalyst from a catalyst boat to control its vapor pressure.

15

294. A laser produced by the inverted hydrogen population according to any of the preceding claims.

295. Use of the laser according to claim 294.

20

296. Electricity converted from photons produced the inverted hydrogen population according to any of the preceding claims.

297. Use of the electricity according to claim 296.

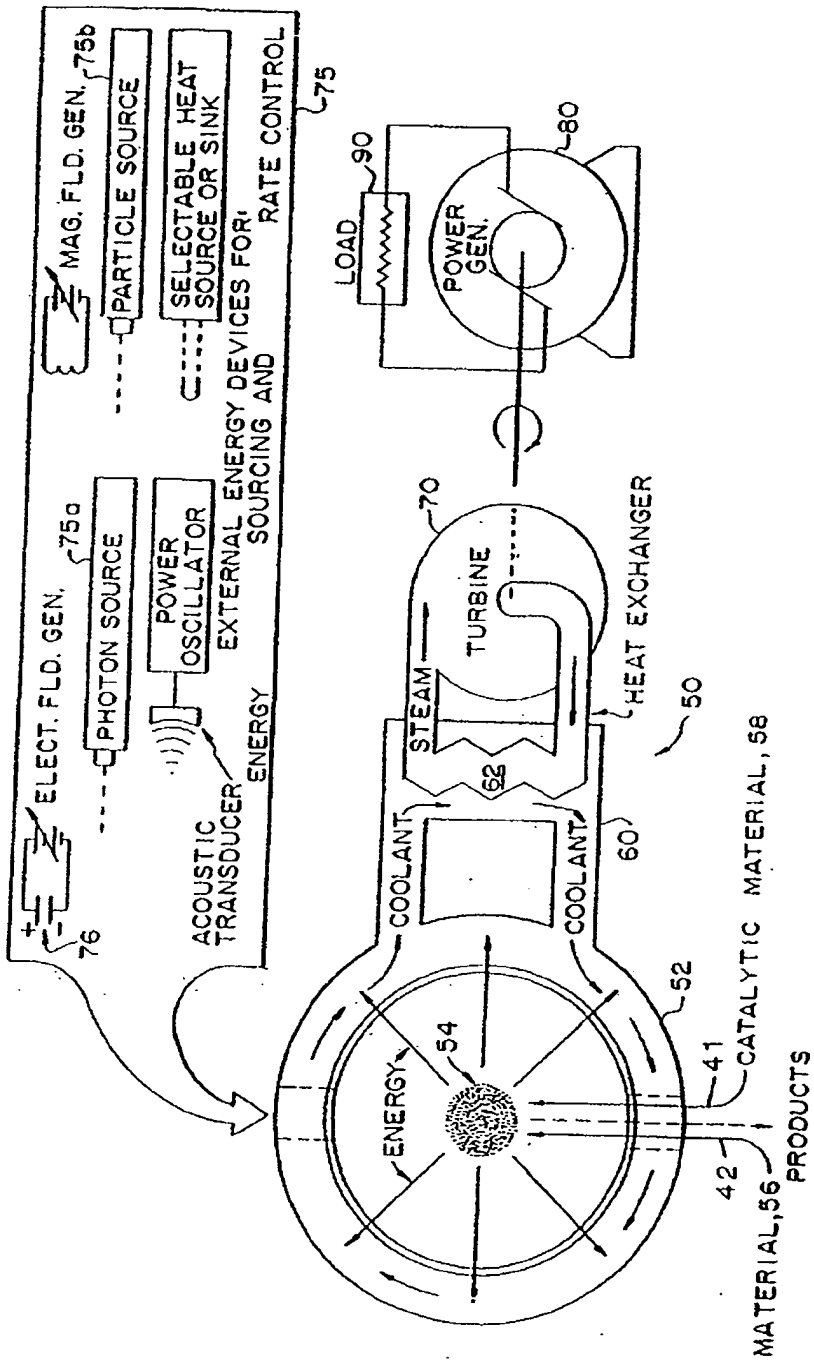


Fig. 1

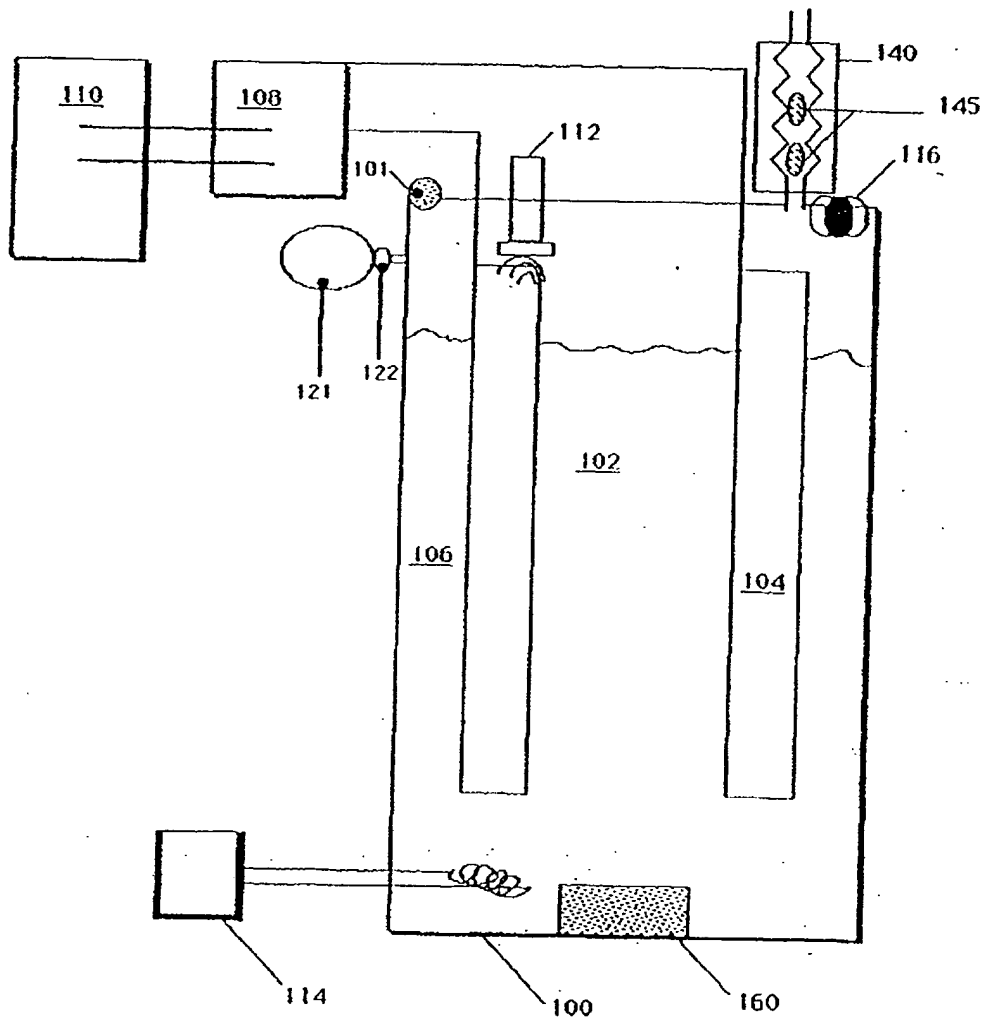


Fig. 2

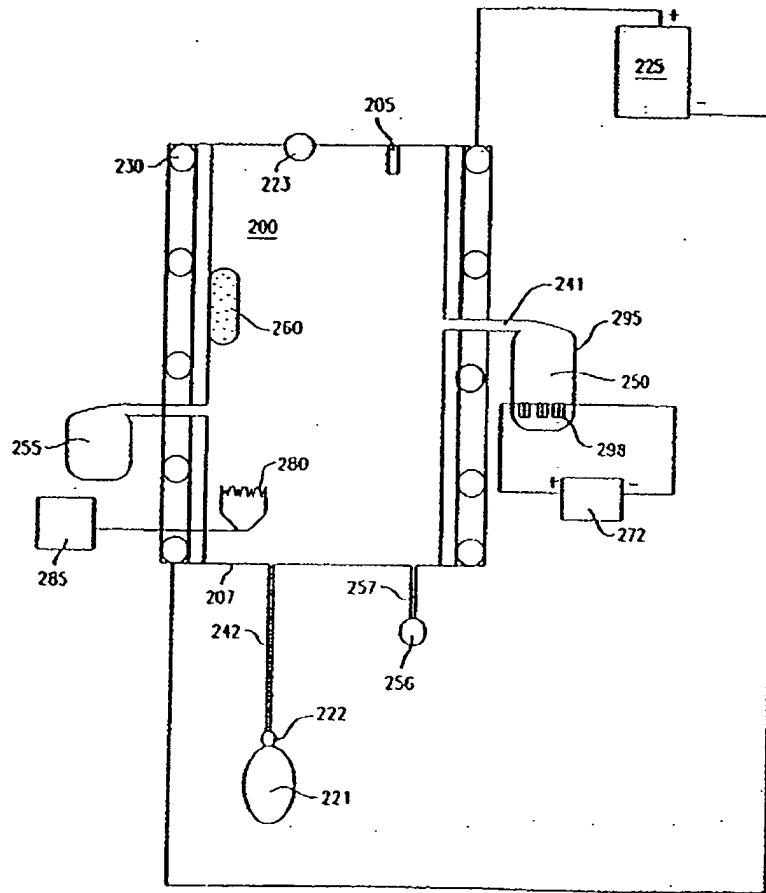


Fig. 3

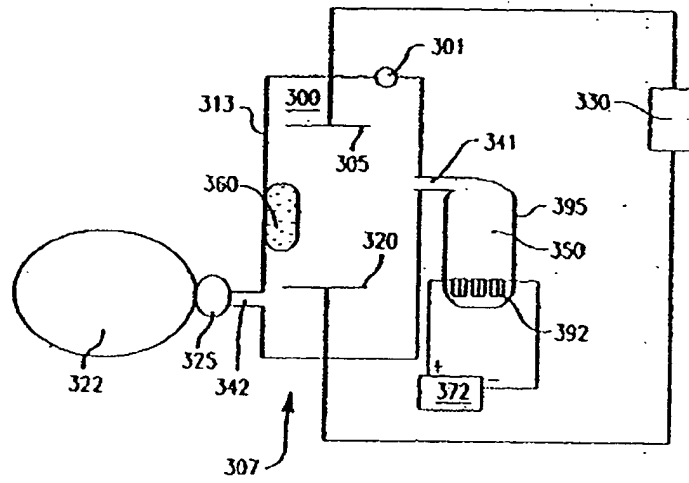


Fig. 4

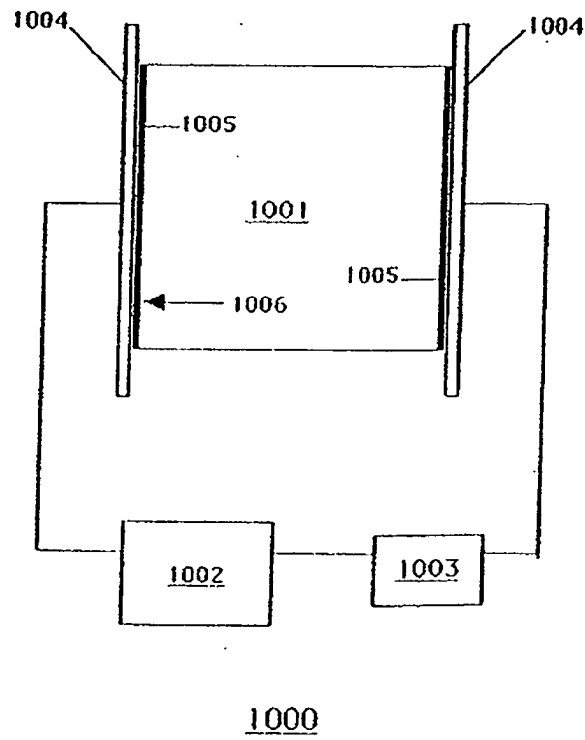


Fig. 5

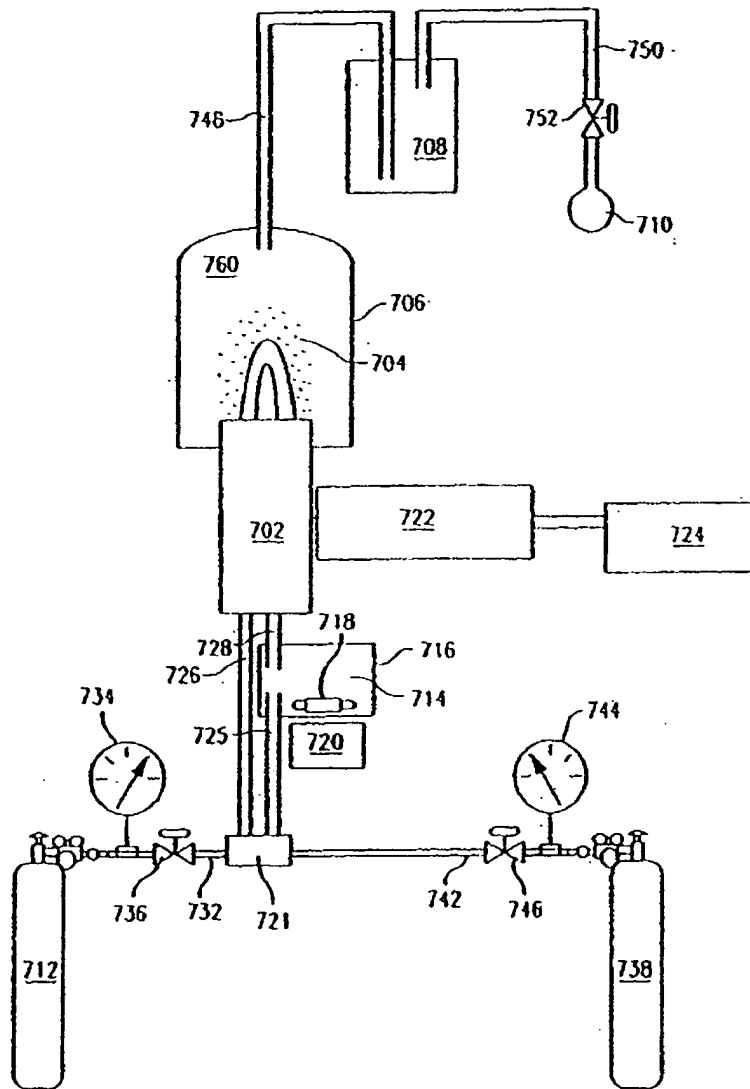


Fig. 6

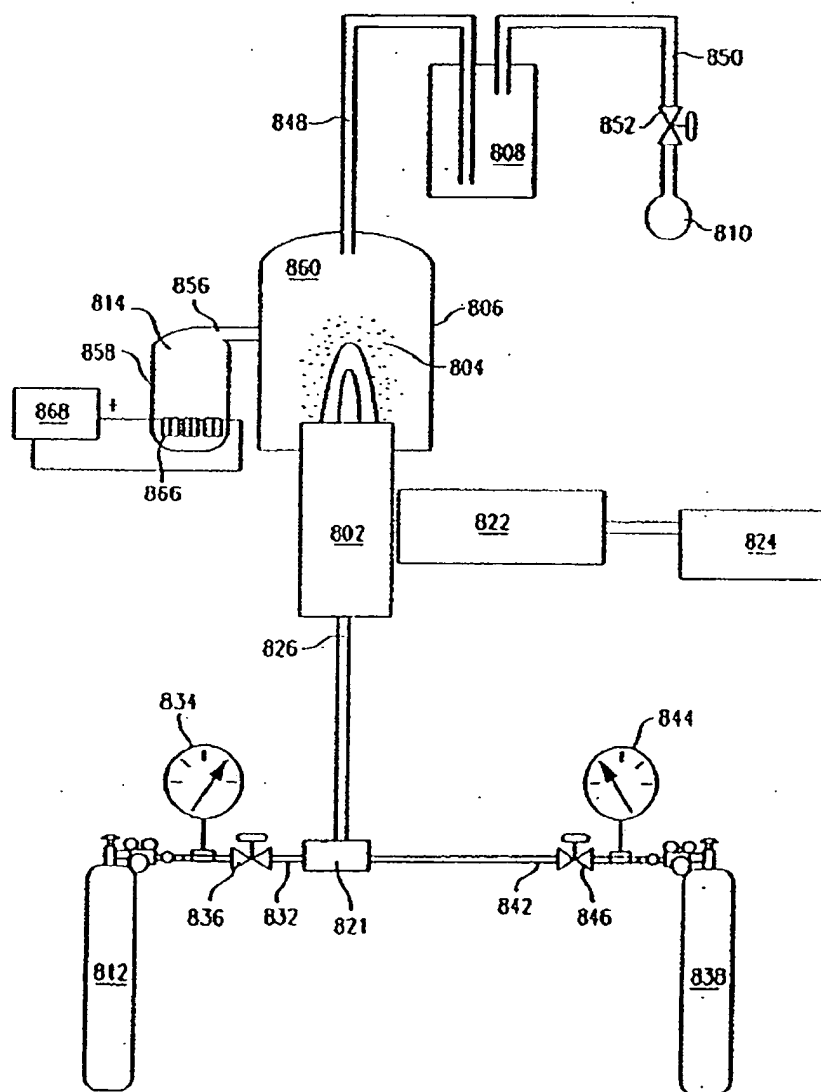


Fig. 7

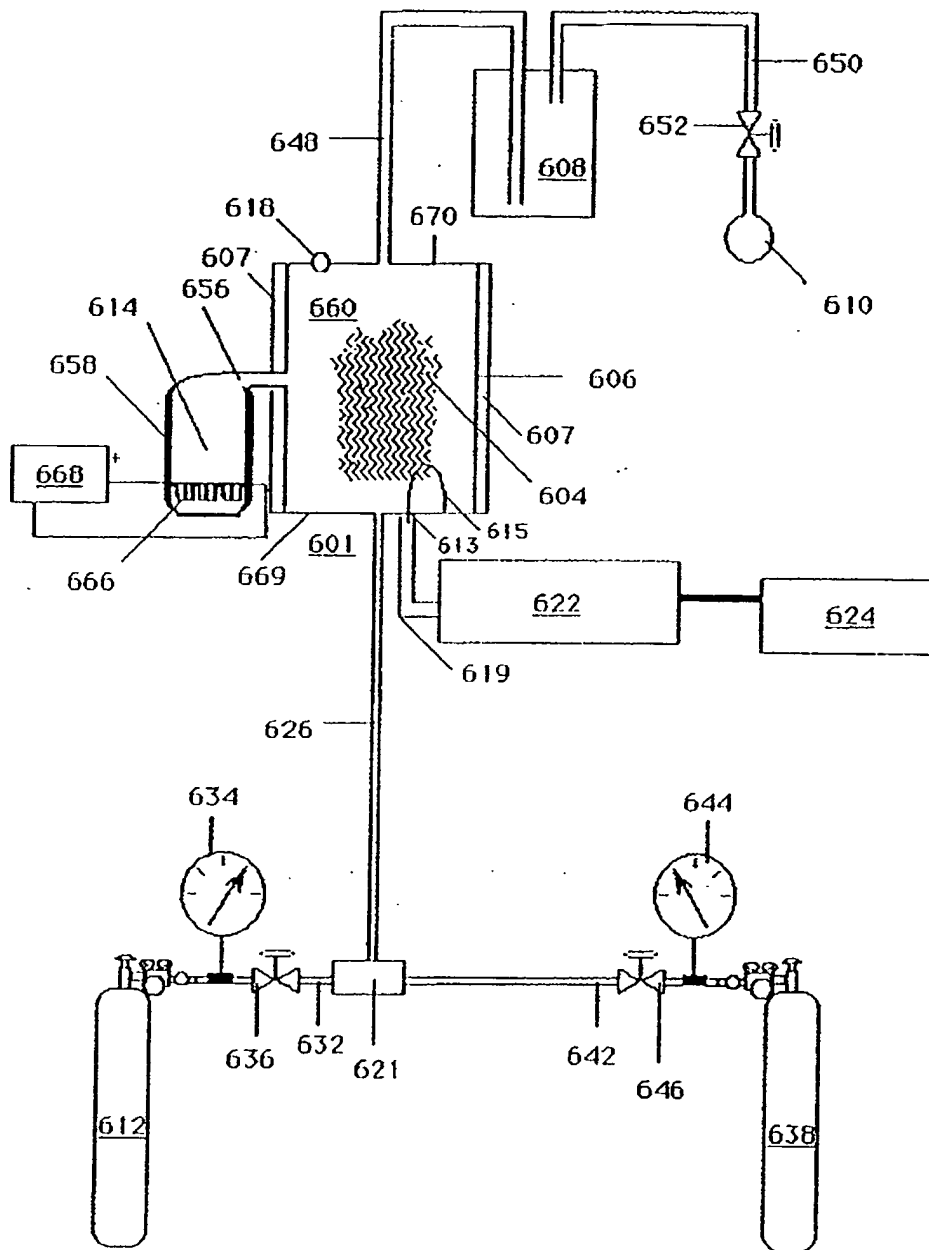
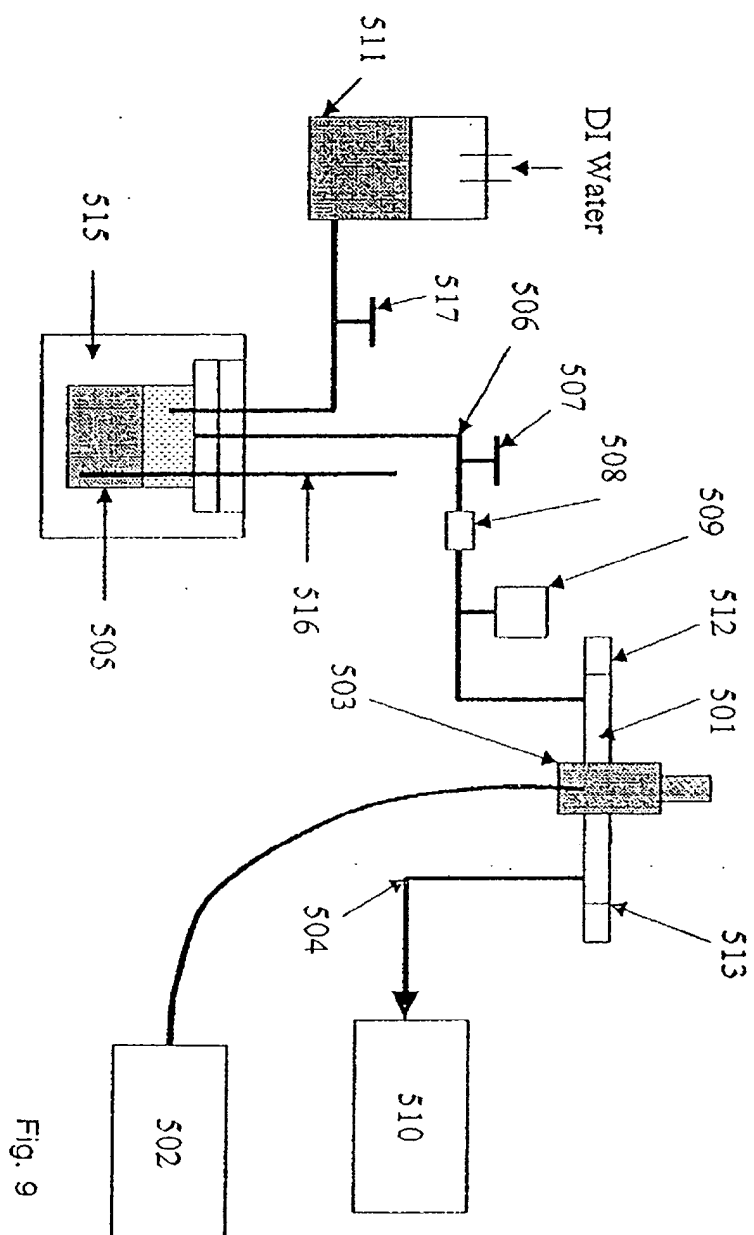


Fig. 8



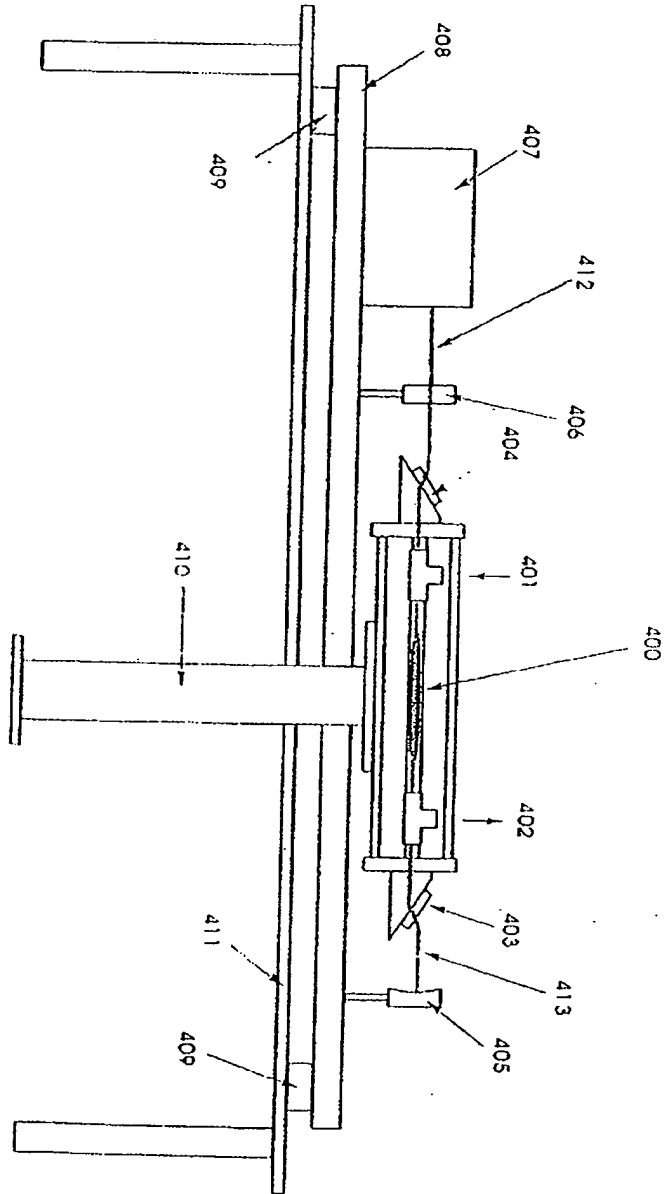


Fig. 10

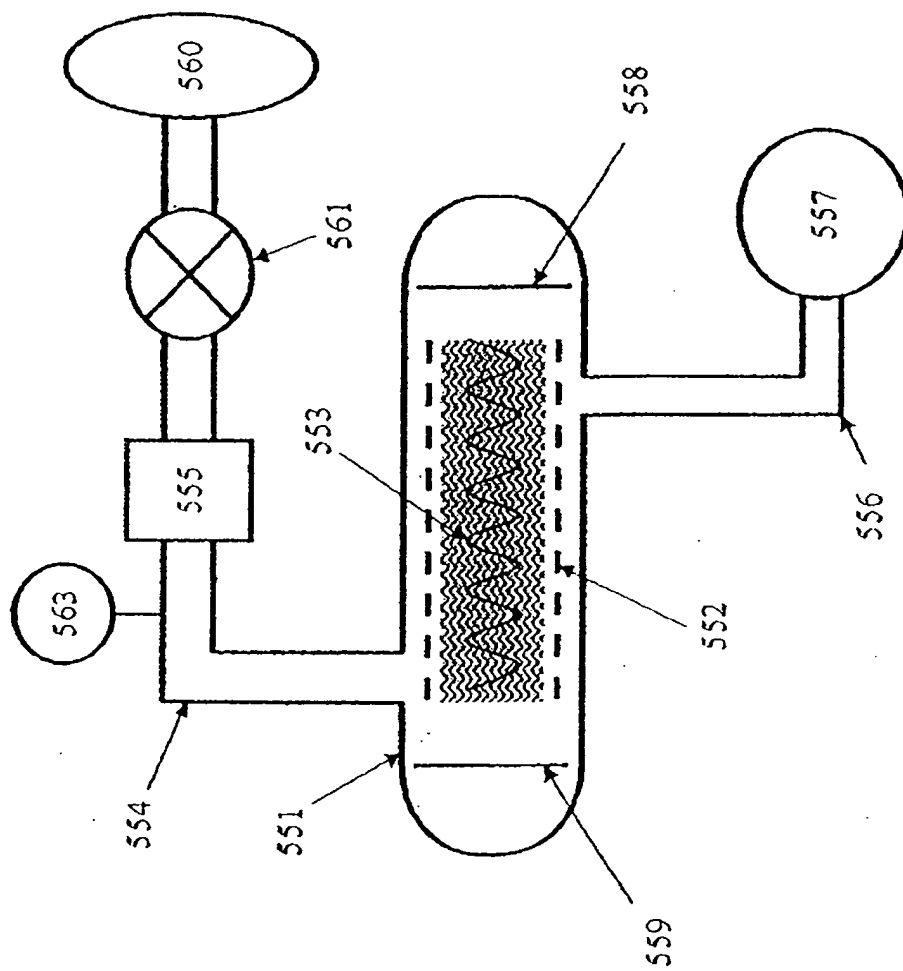


Fig. 11

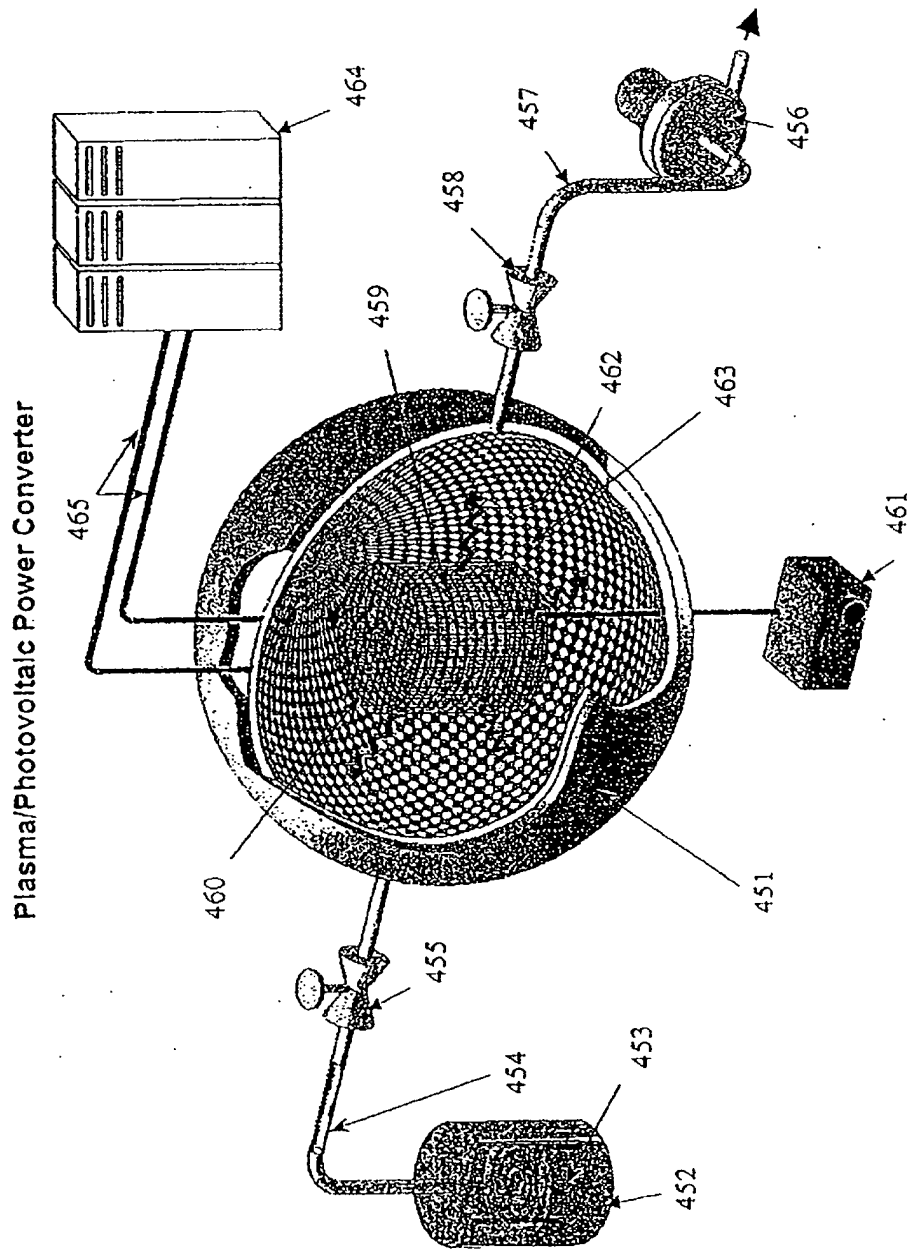


Fig. 12

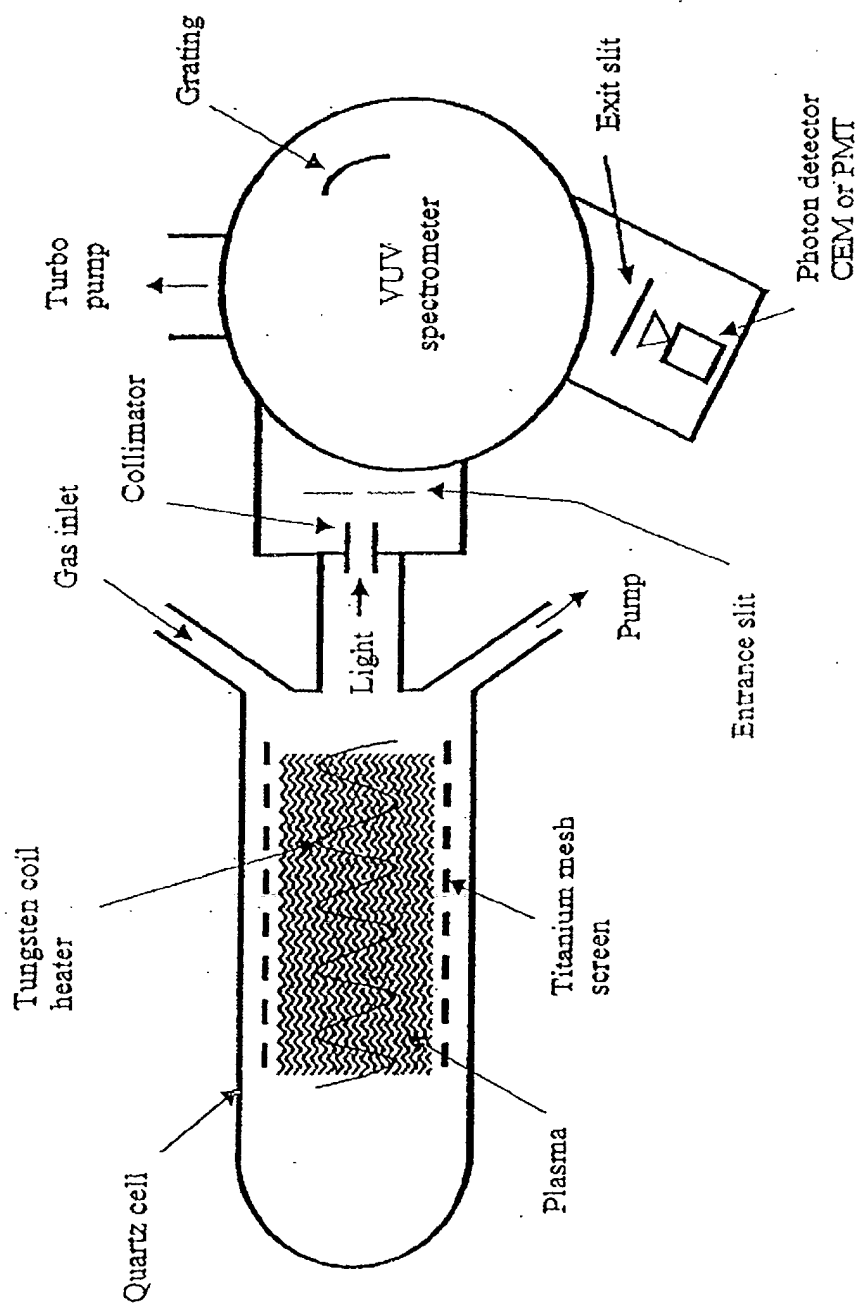


Fig. 13

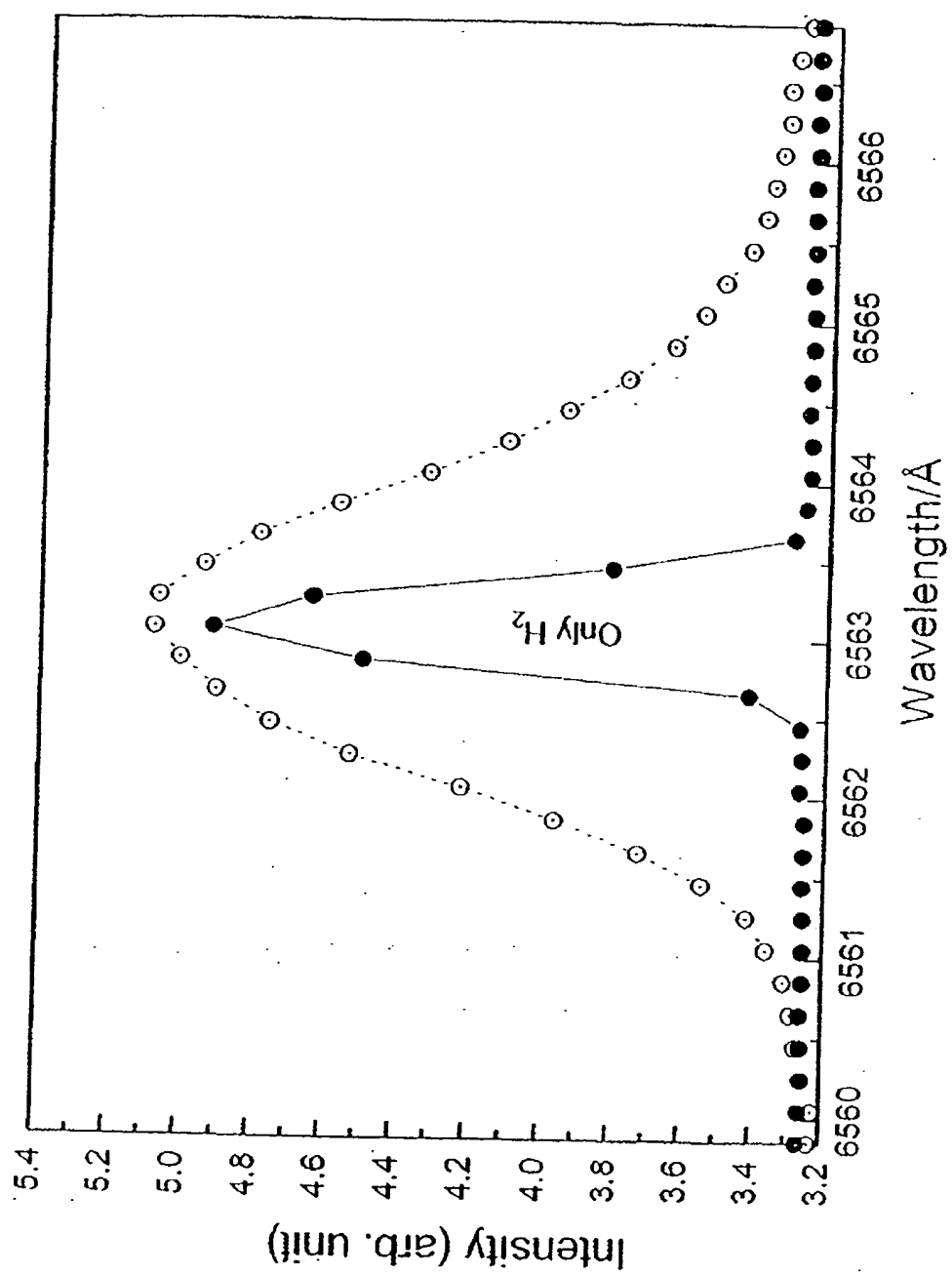


Fig. 14

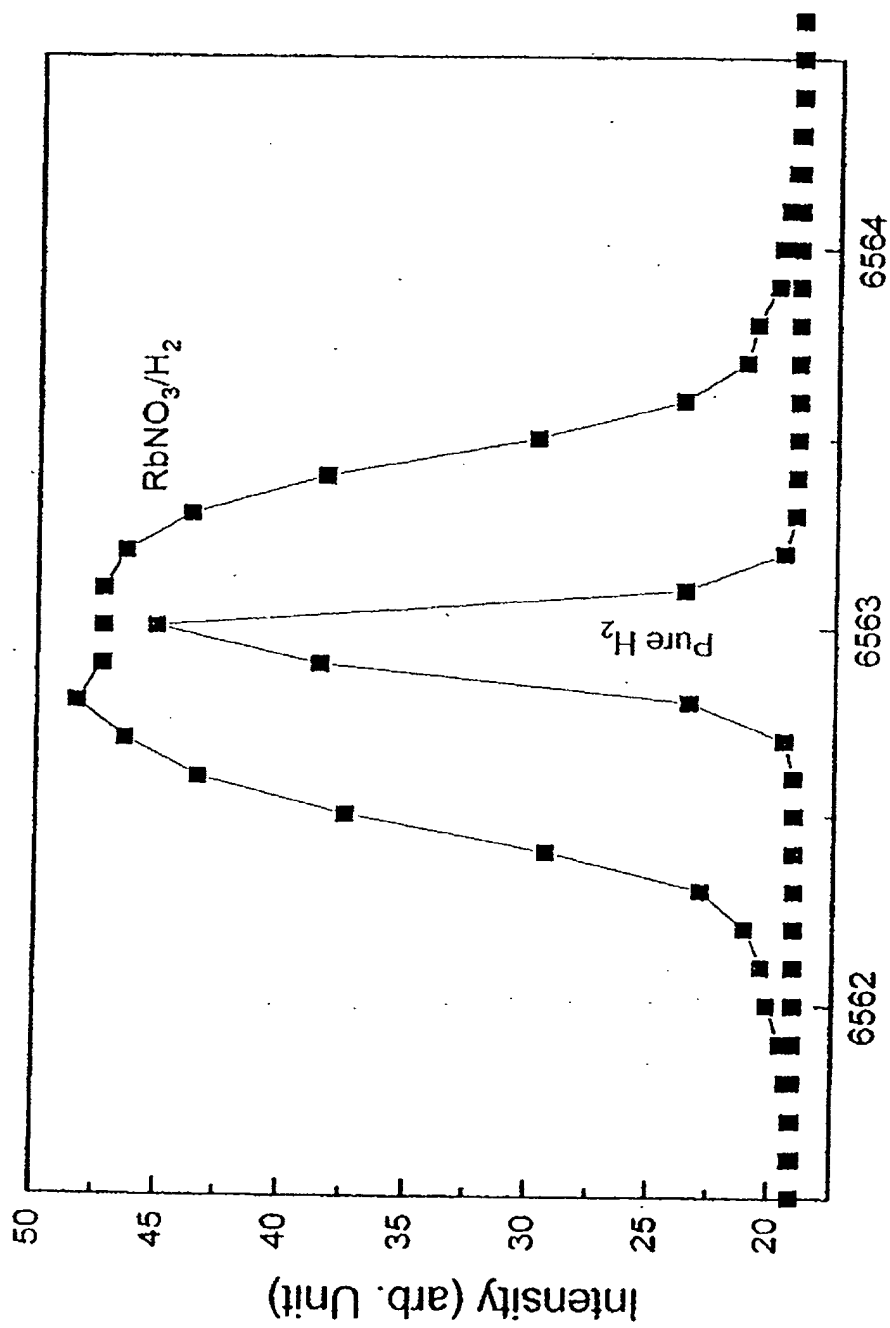


Fig. 15

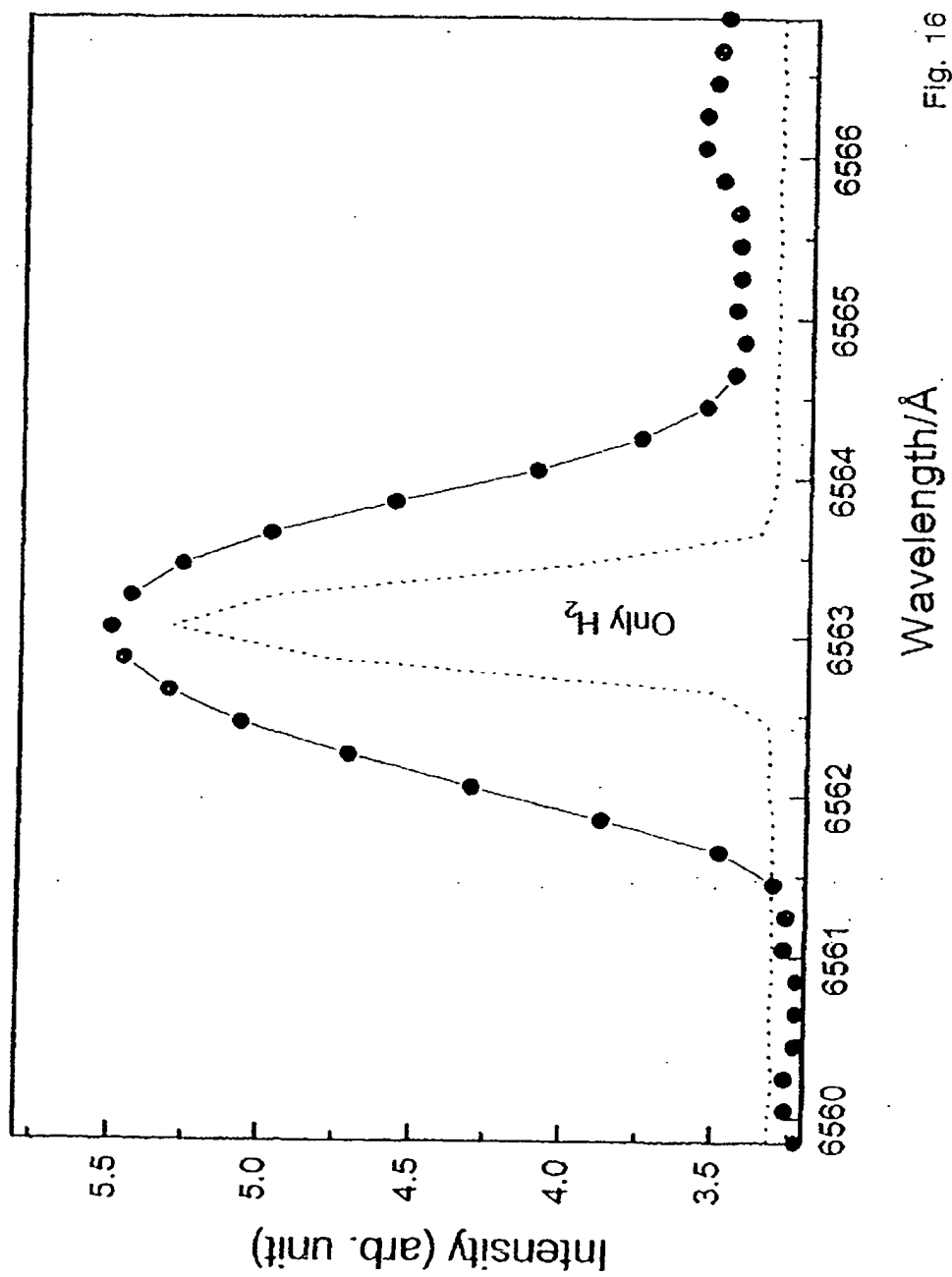


Fig. 16

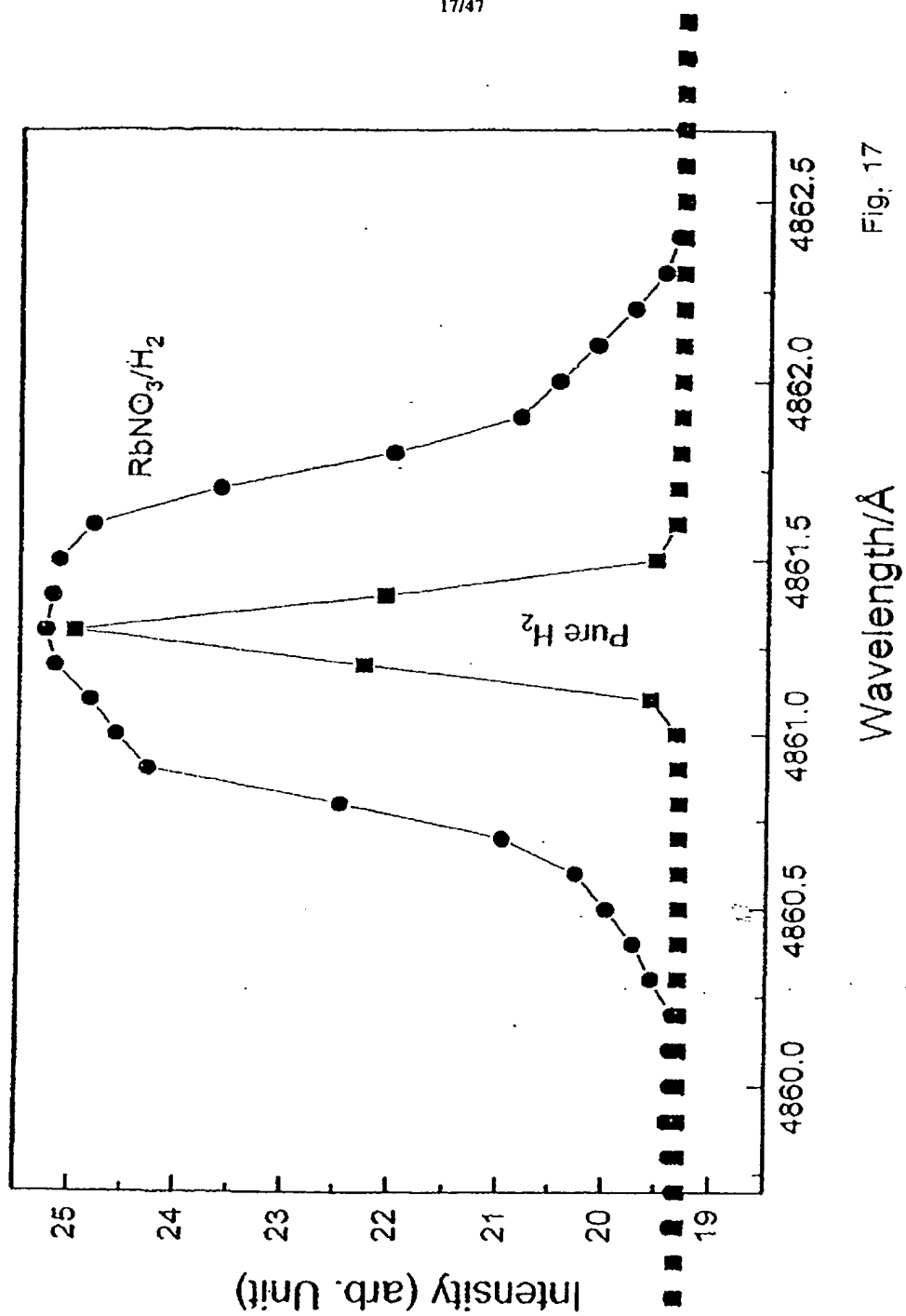


Fig. 17

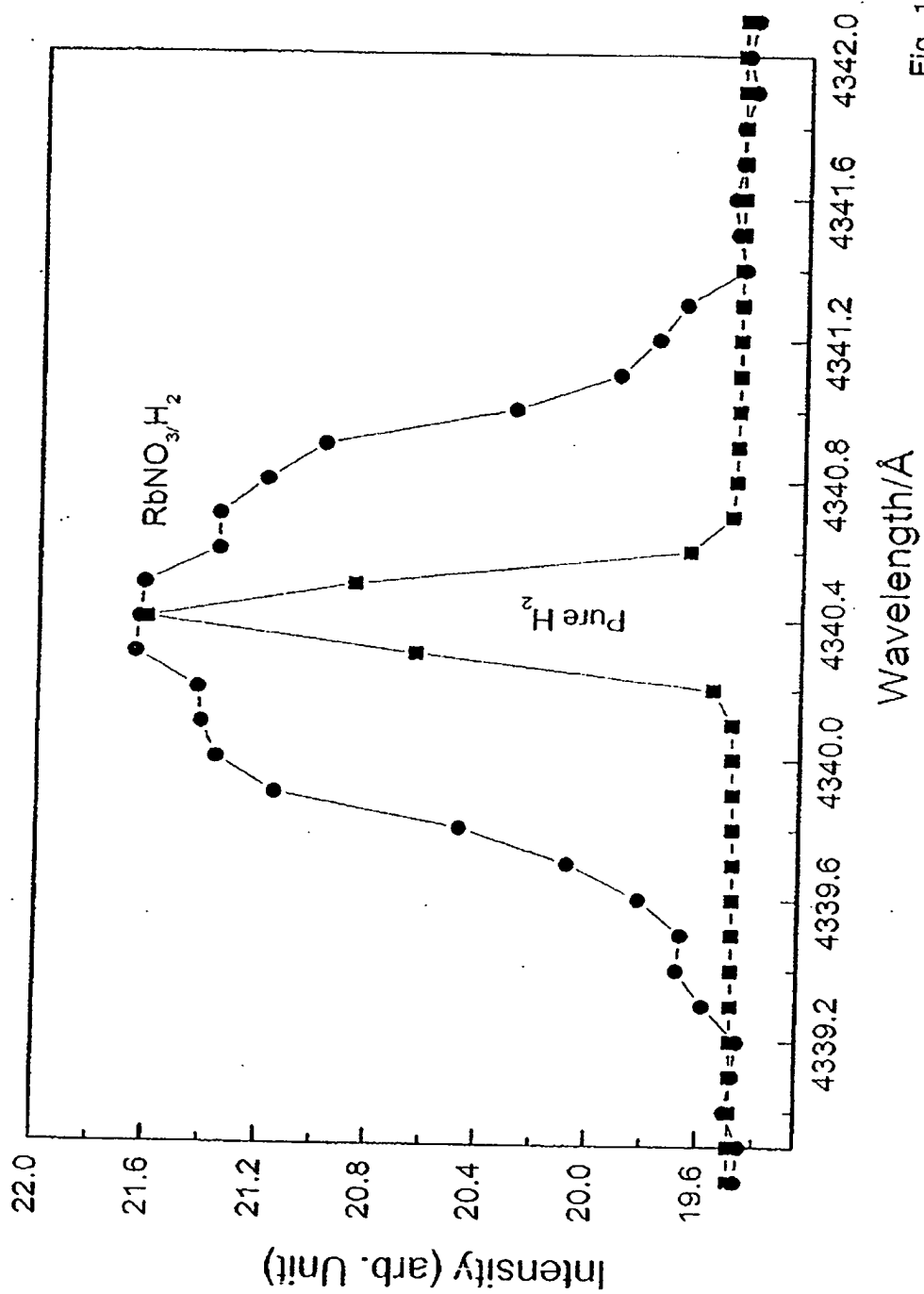


Fig. 18

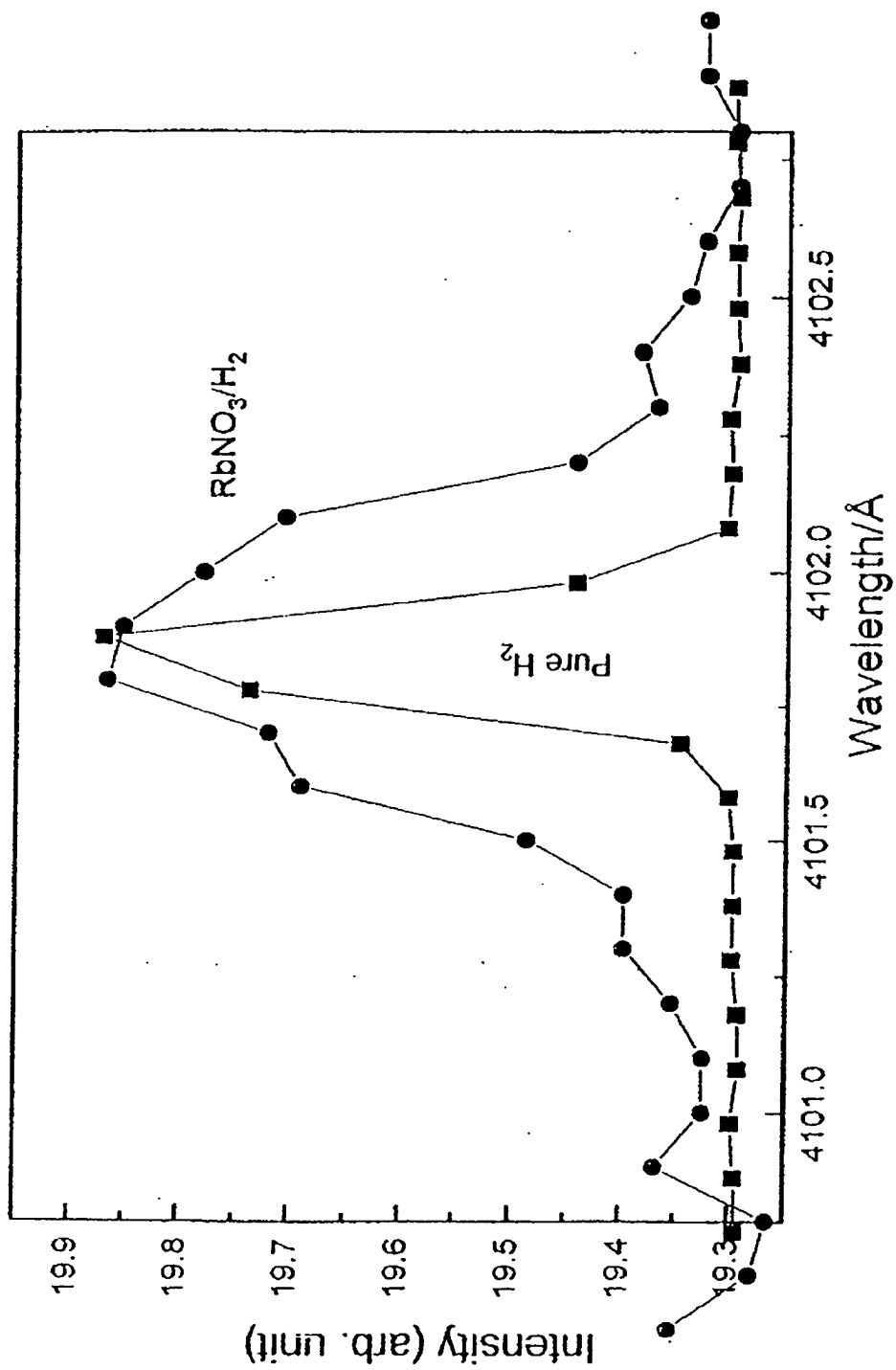


Fig. 19

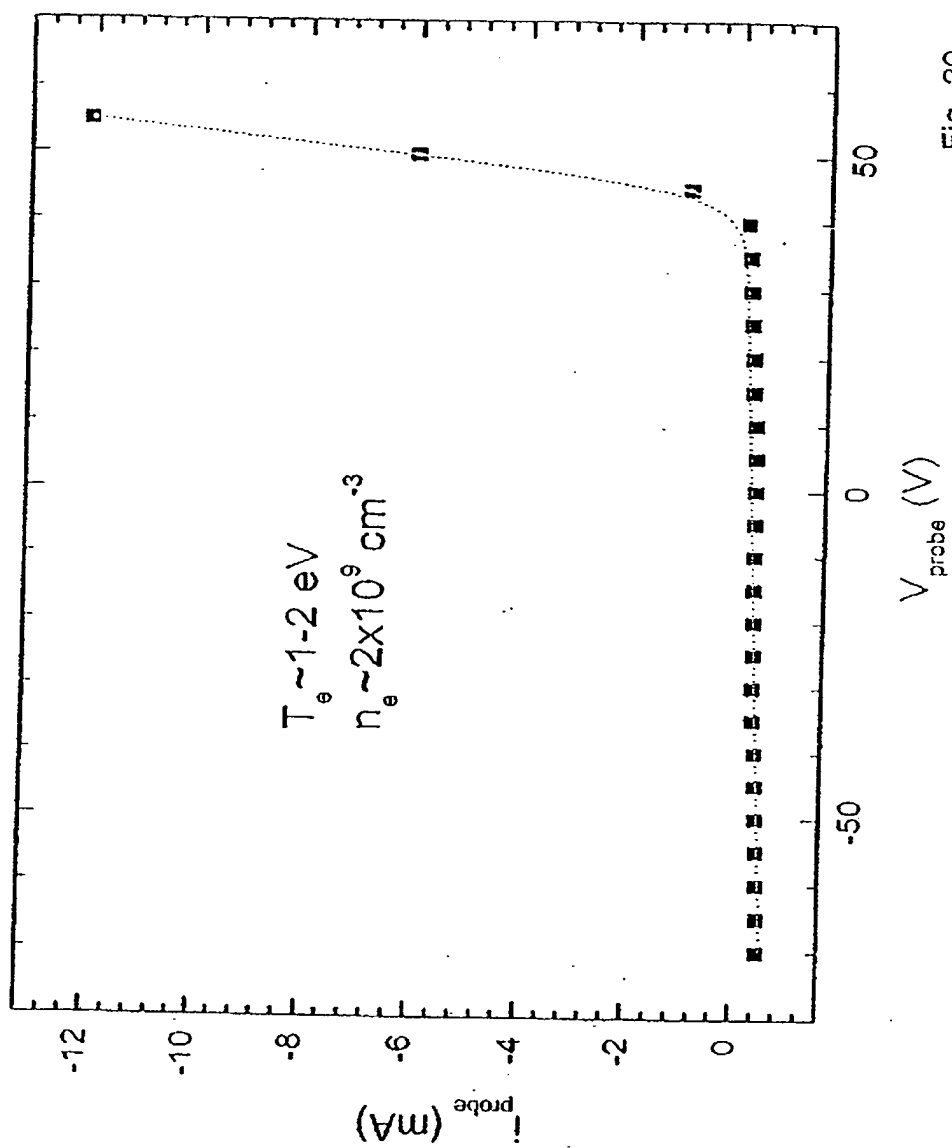


Fig. 20

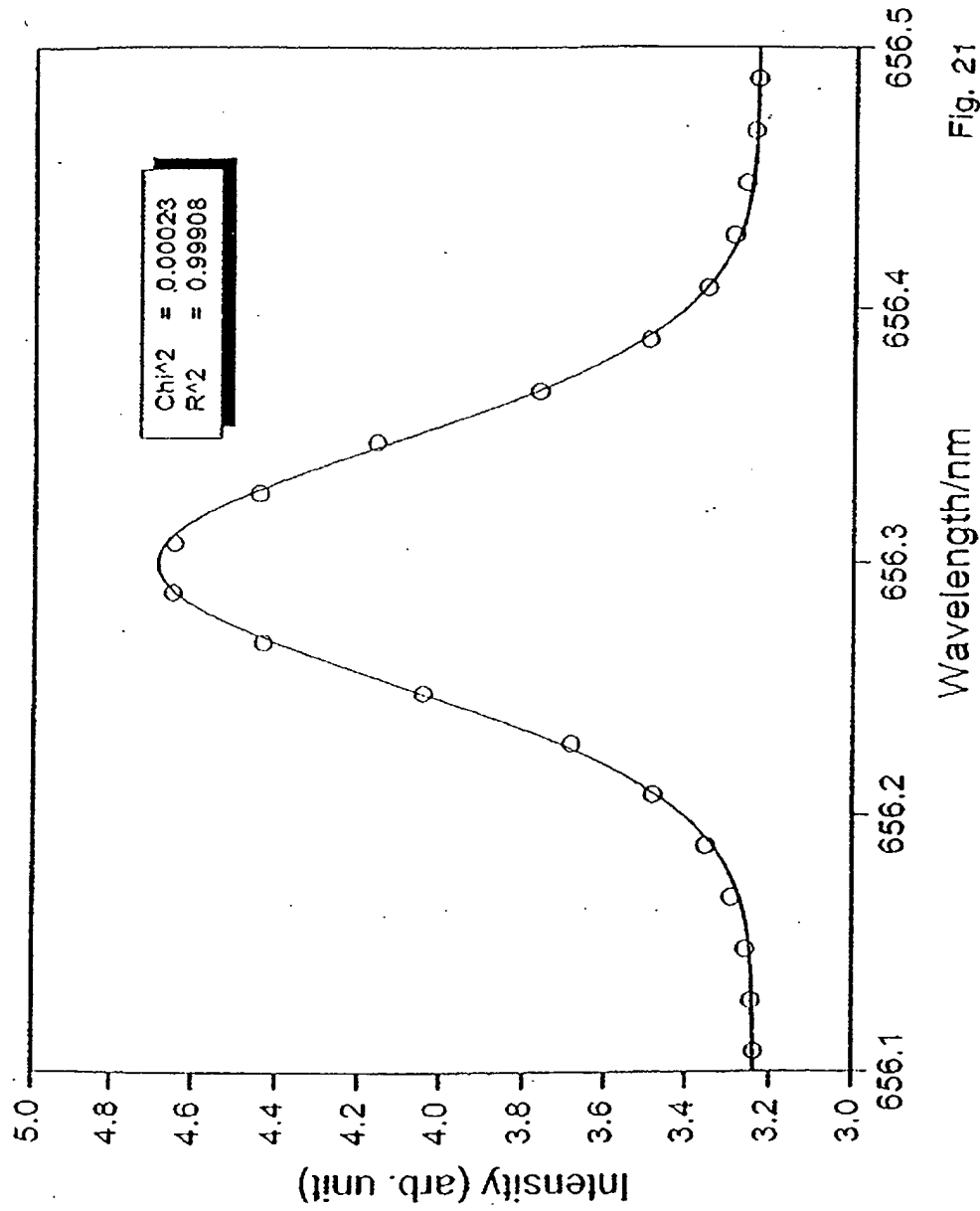


Fig. 21

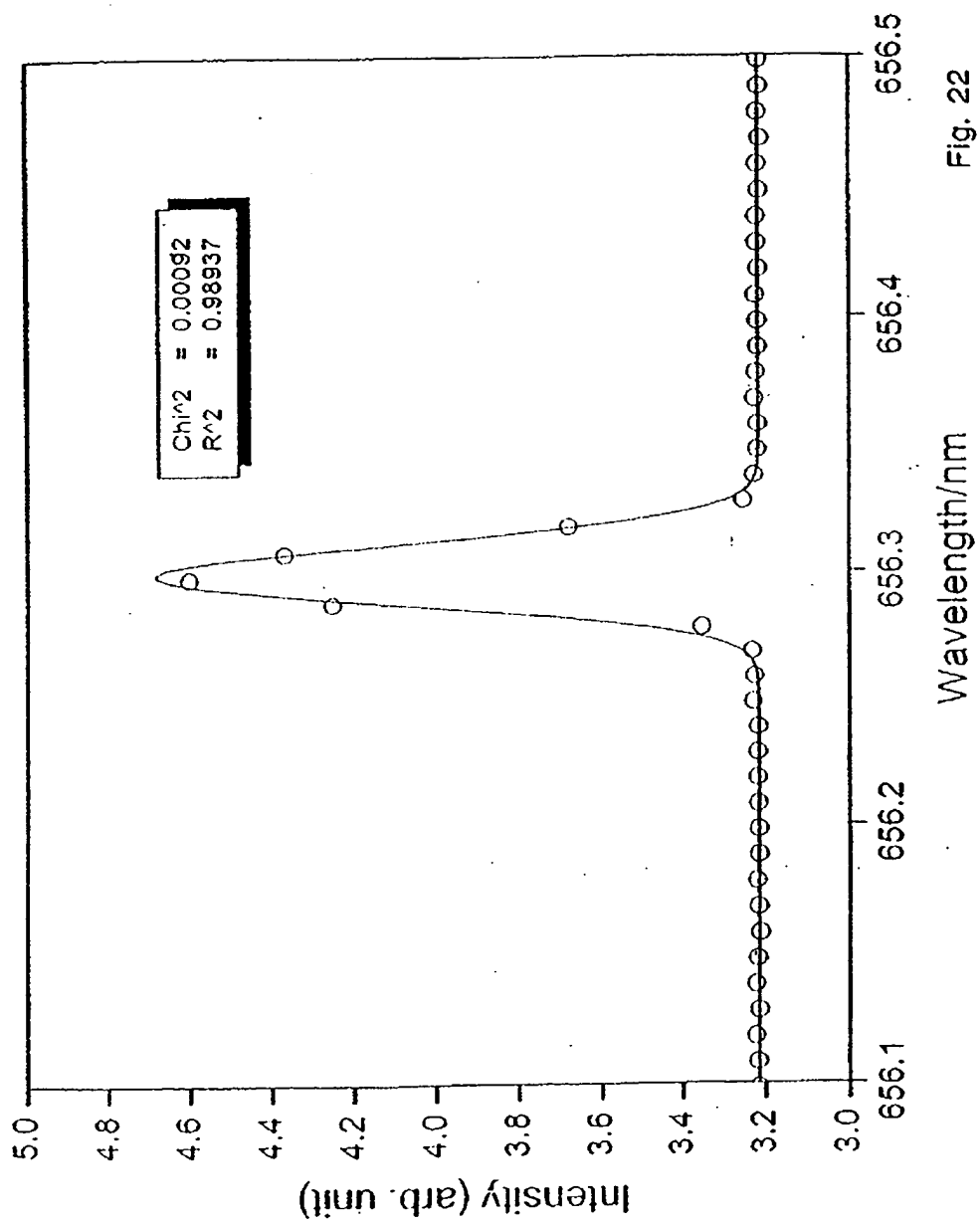
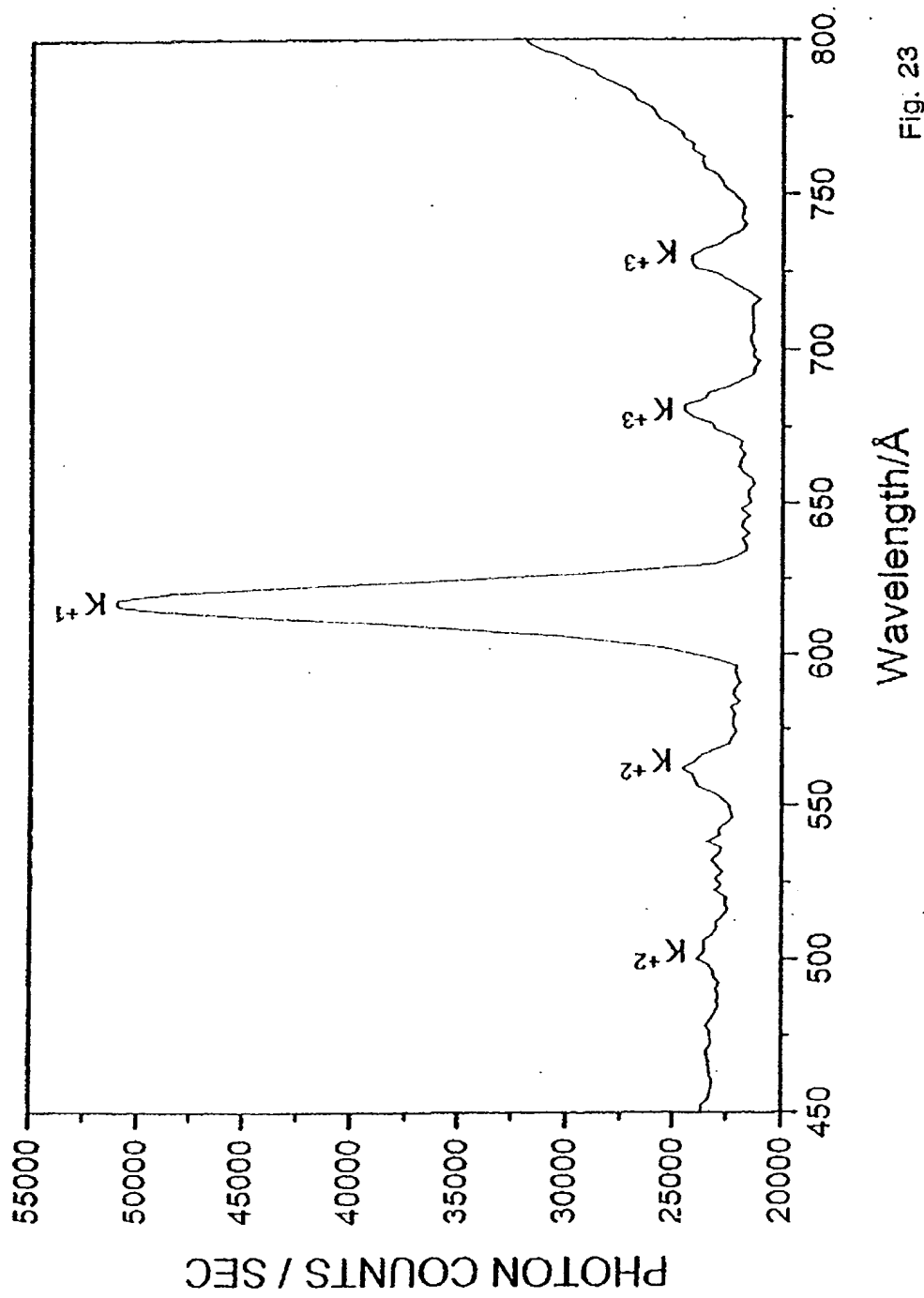


Fig. 22



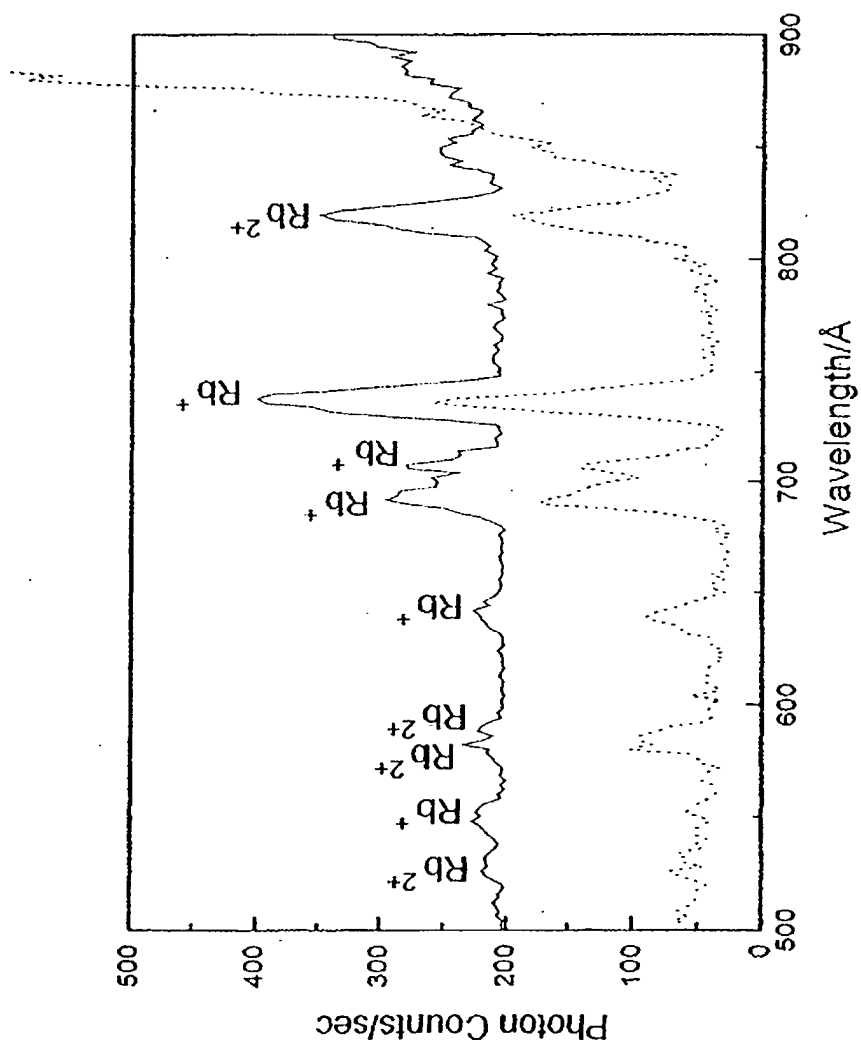
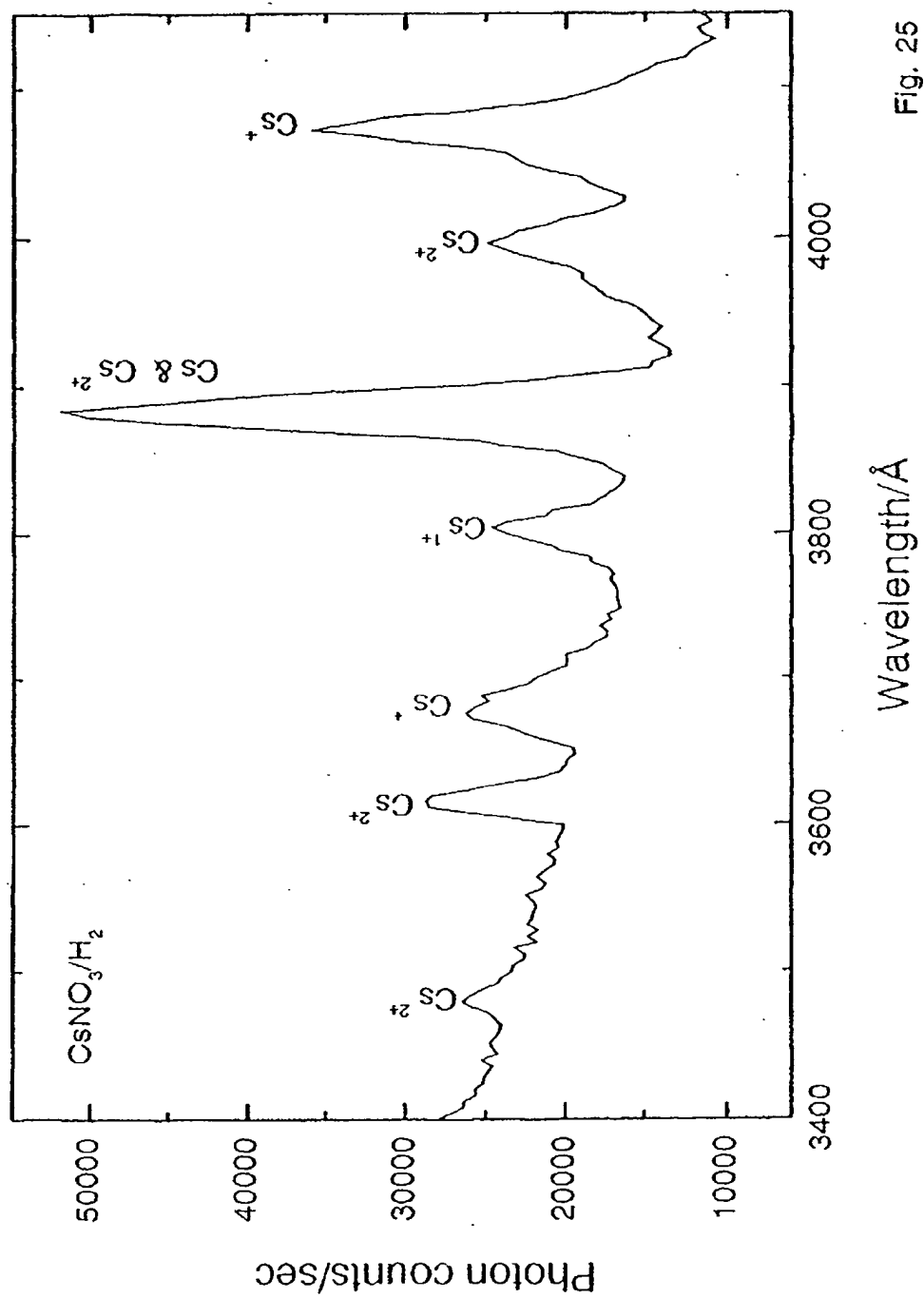


Fig. 24



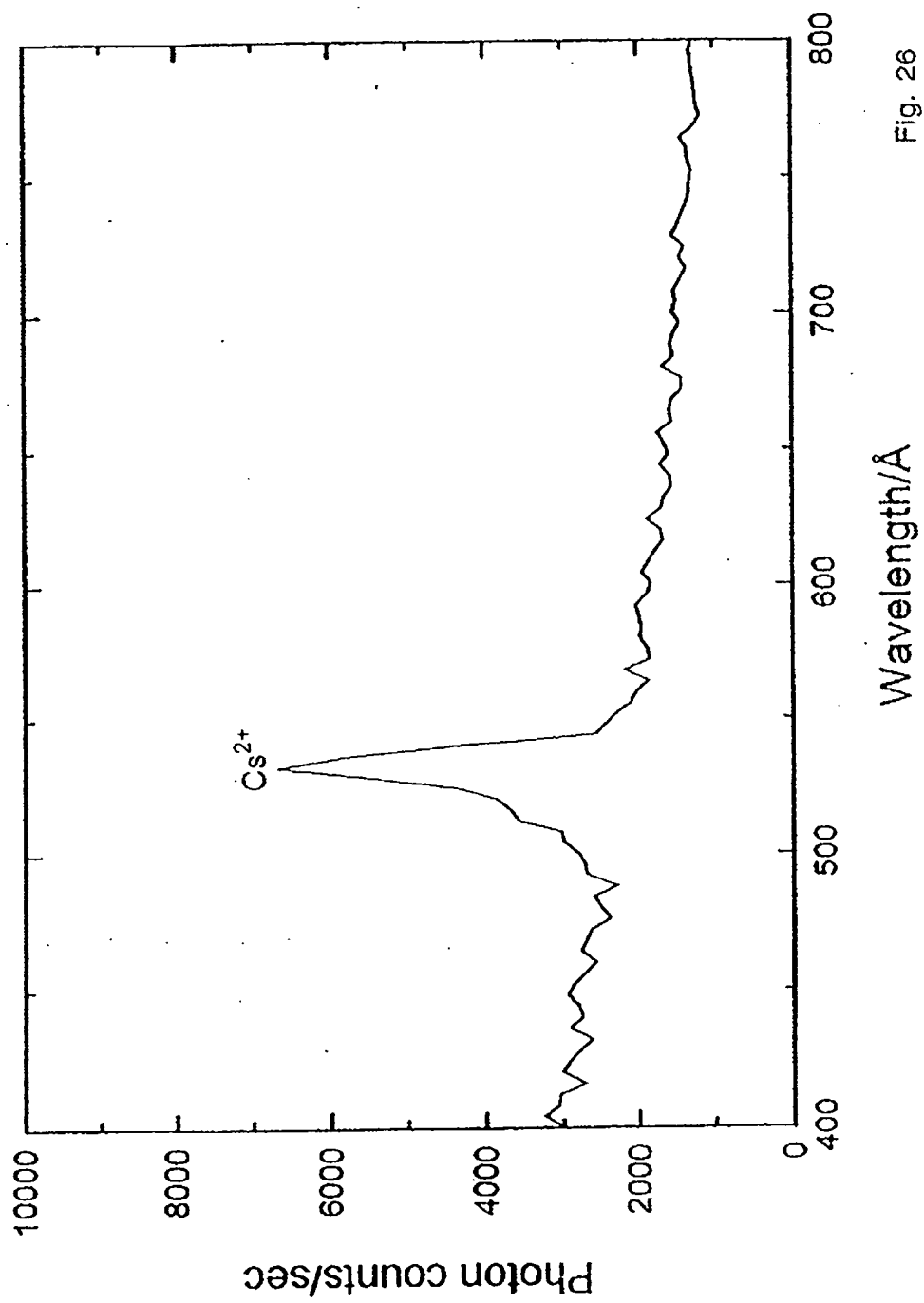


Fig. 26

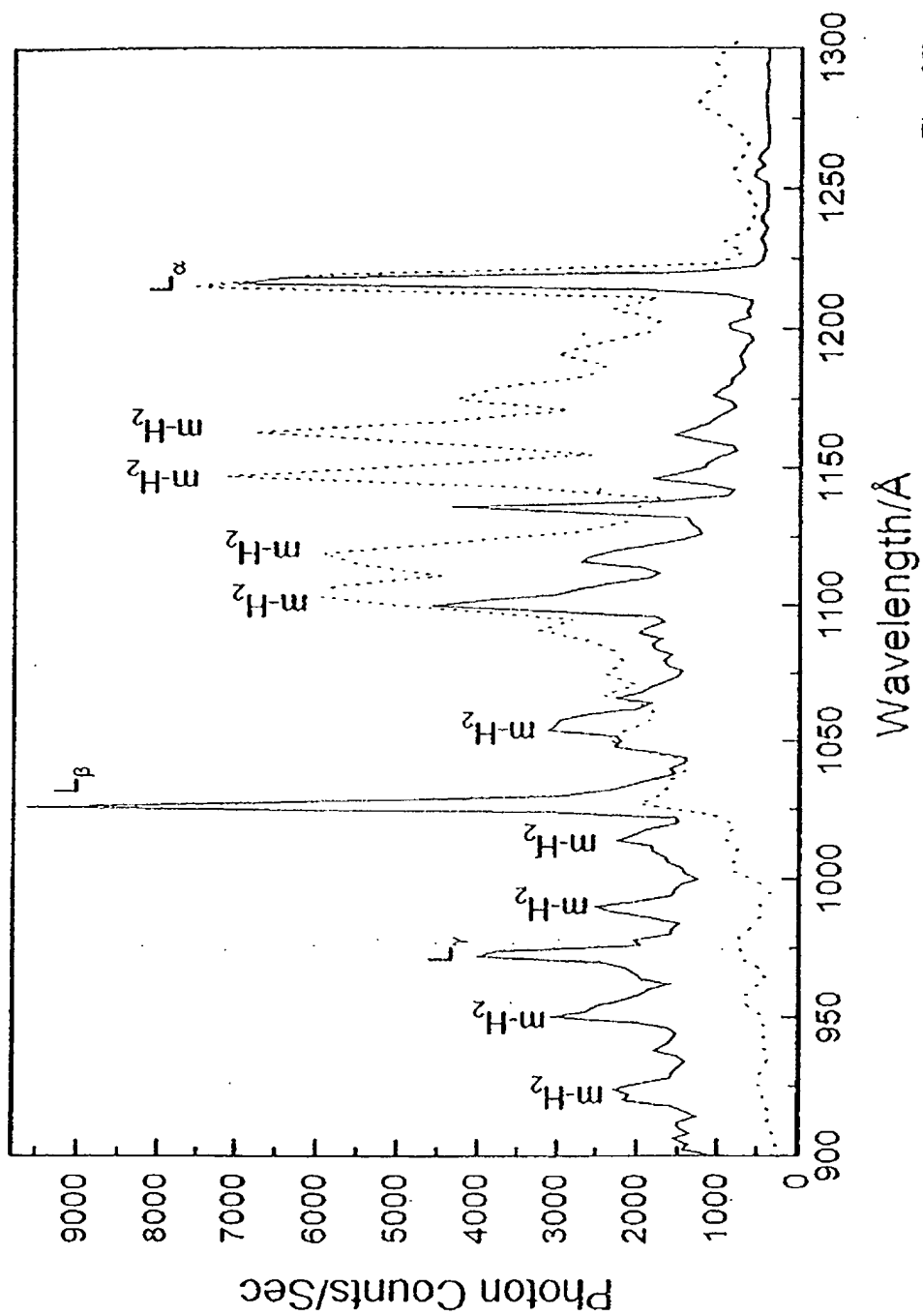
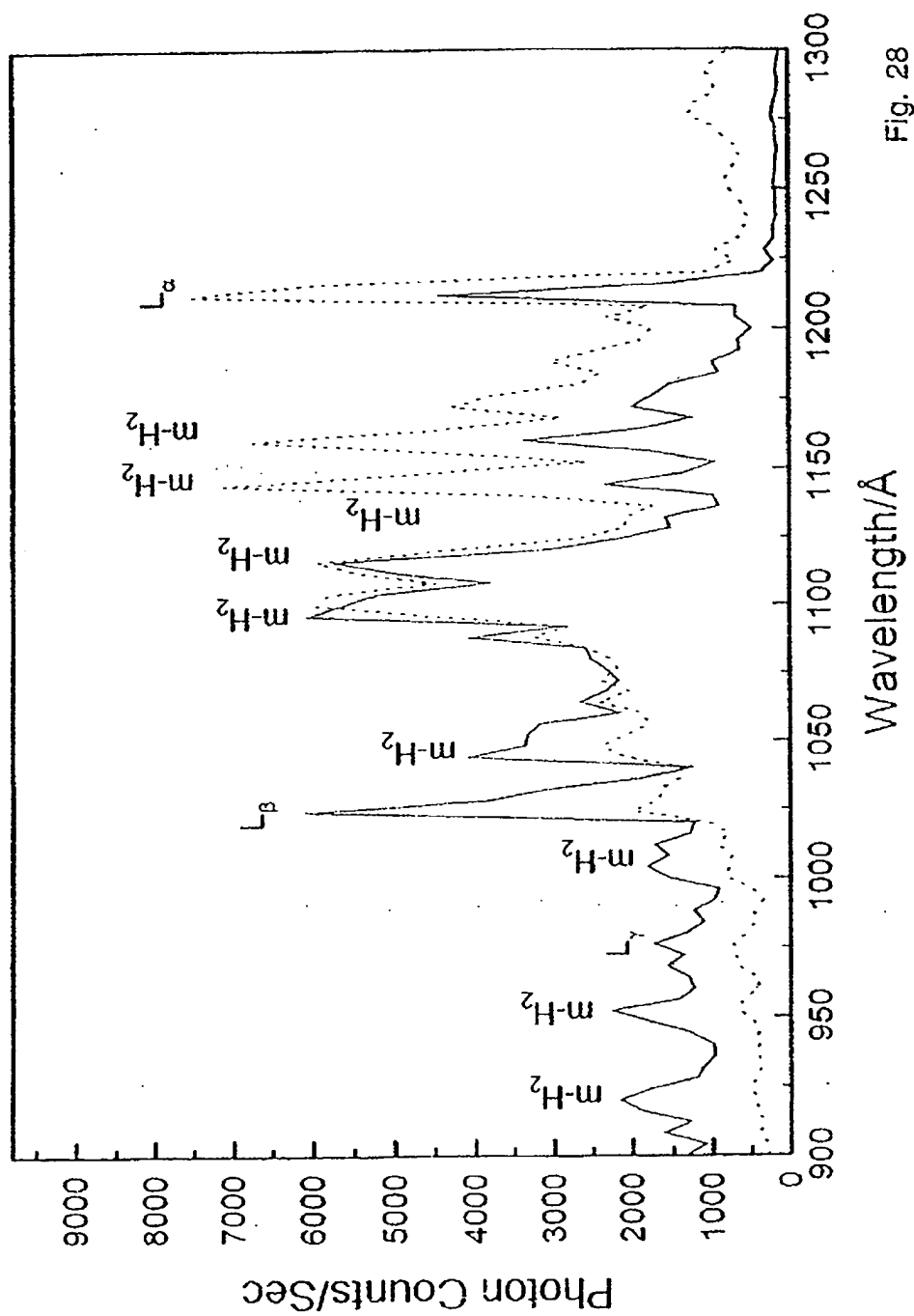


Fig. 27



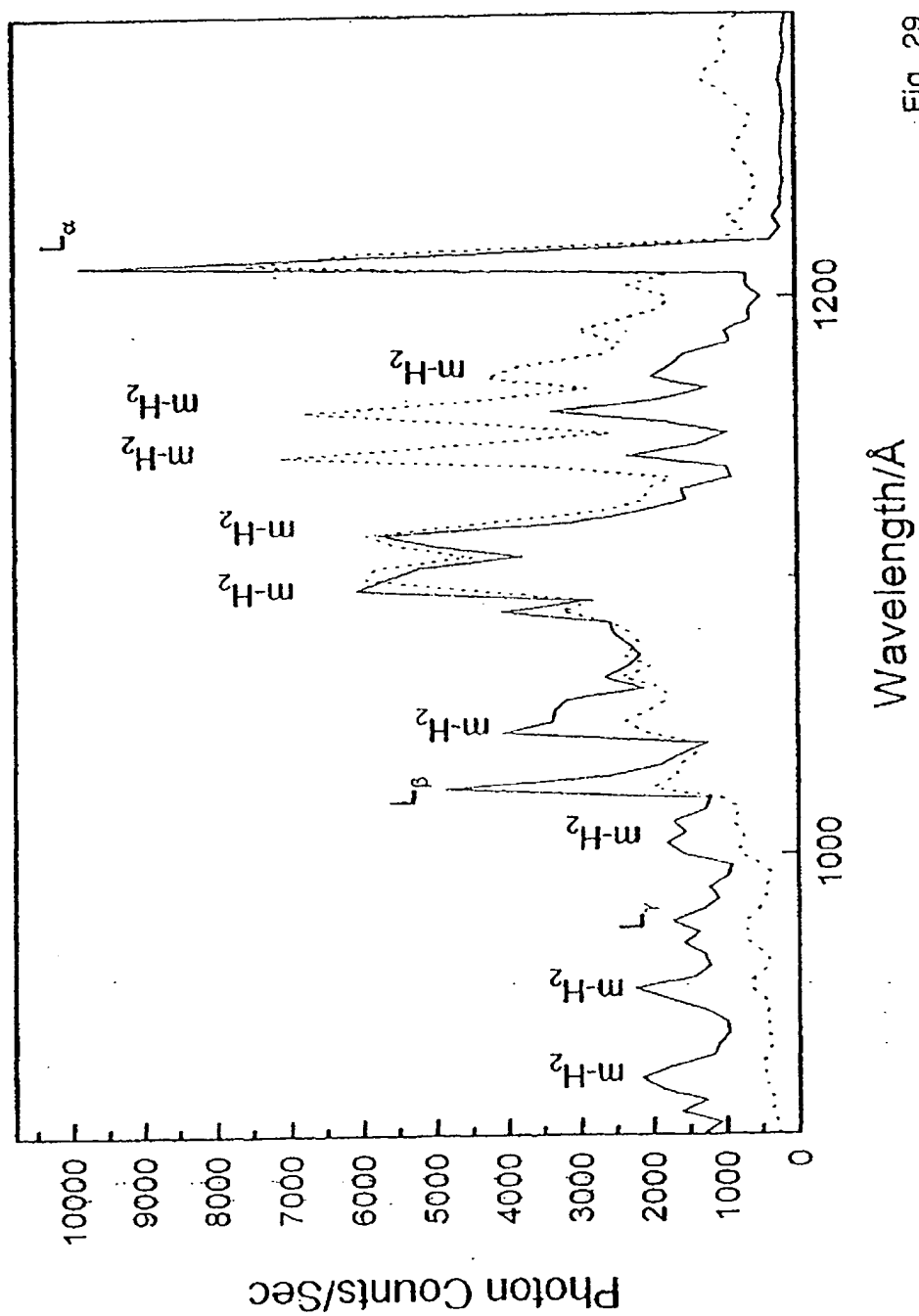
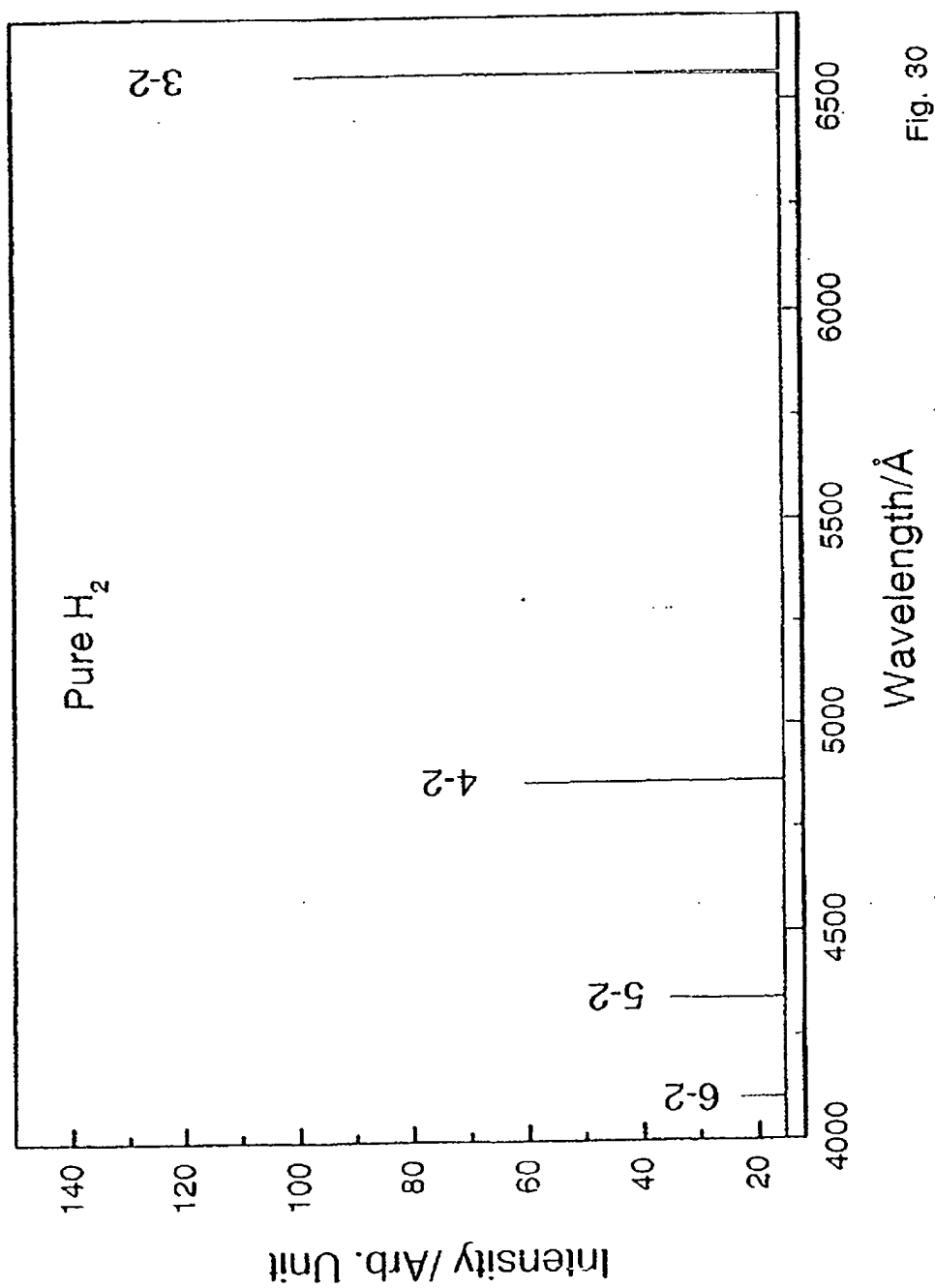


Fig. 29



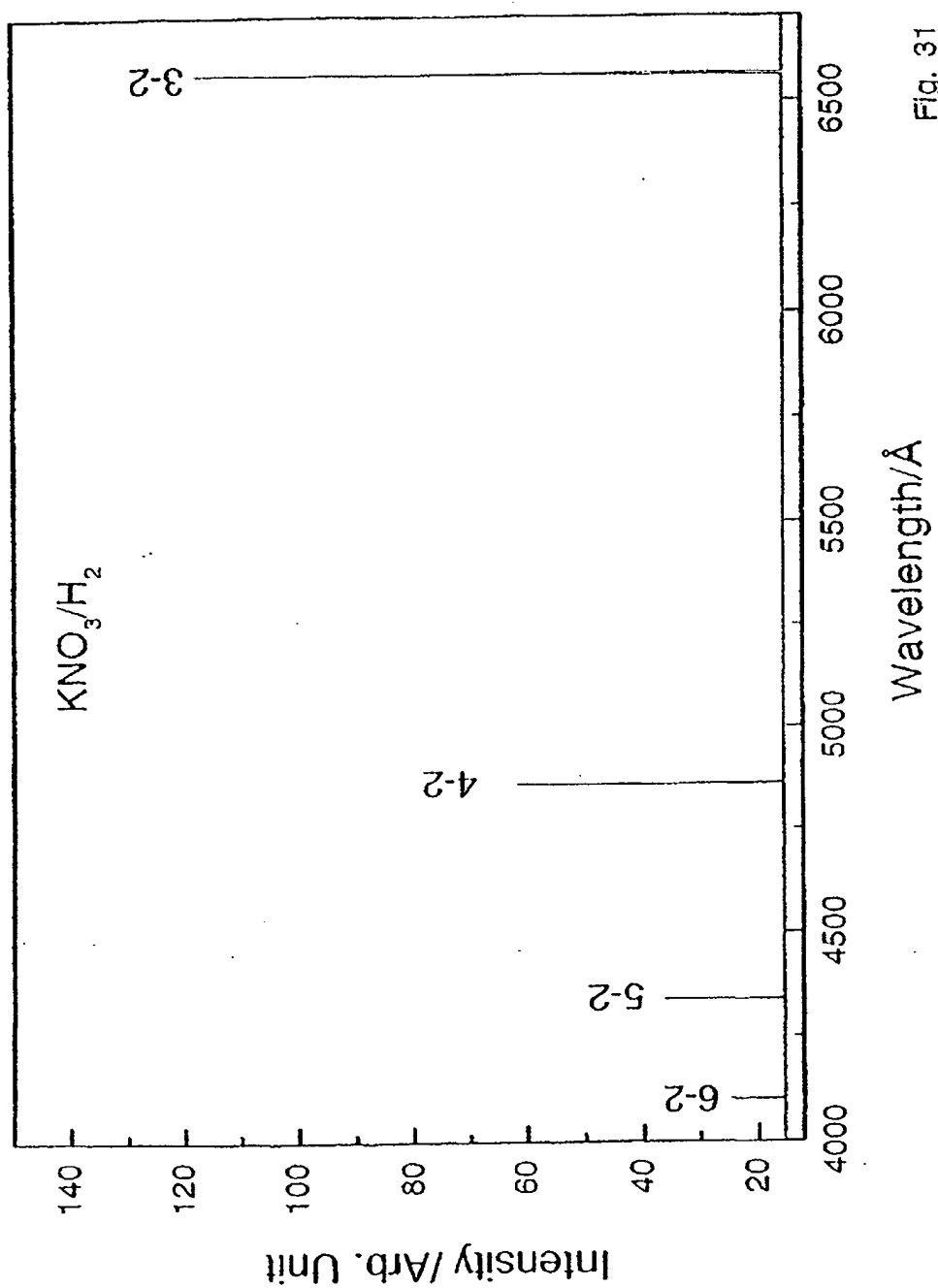


Fig. 31

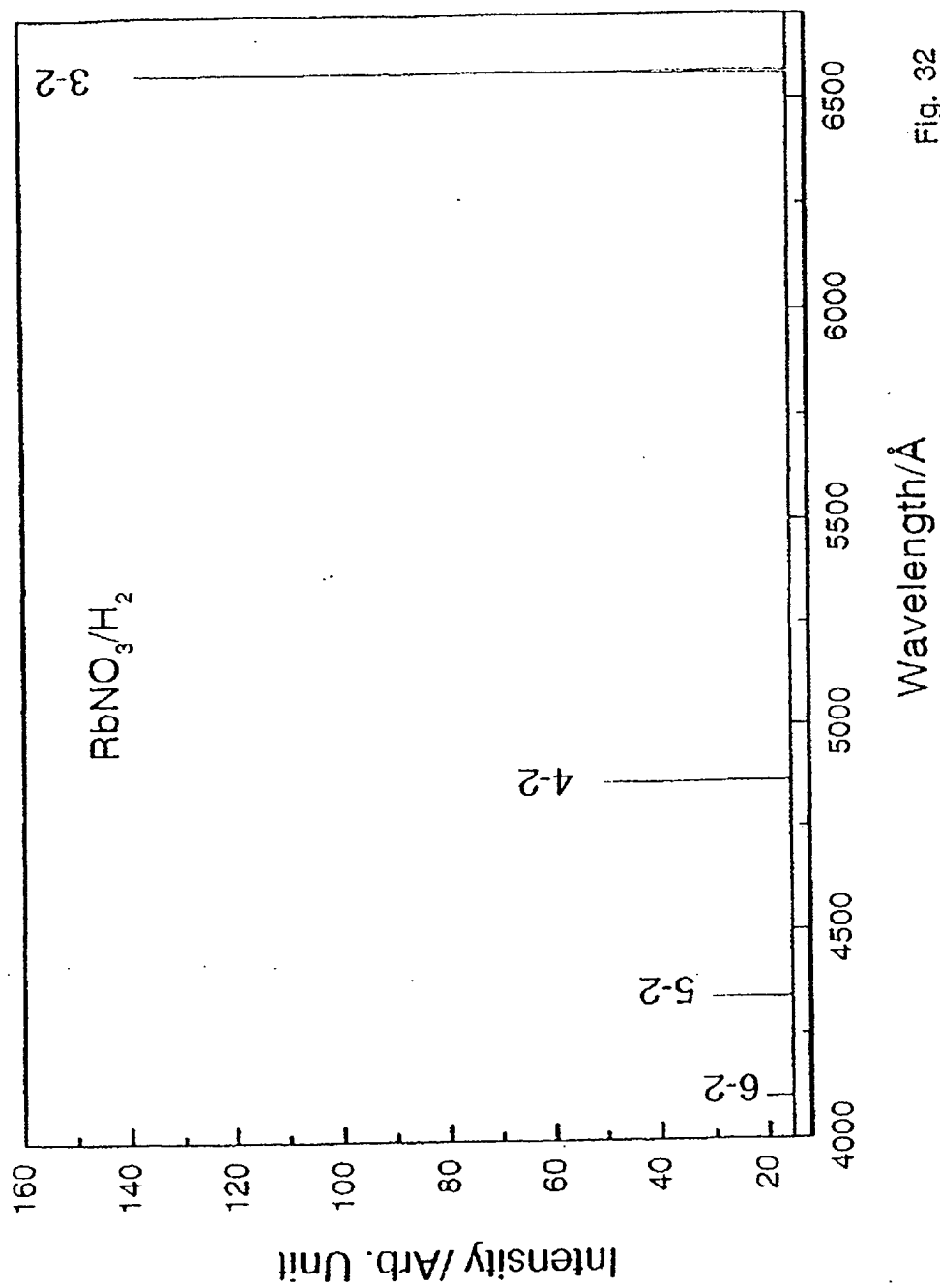


Fig. 32

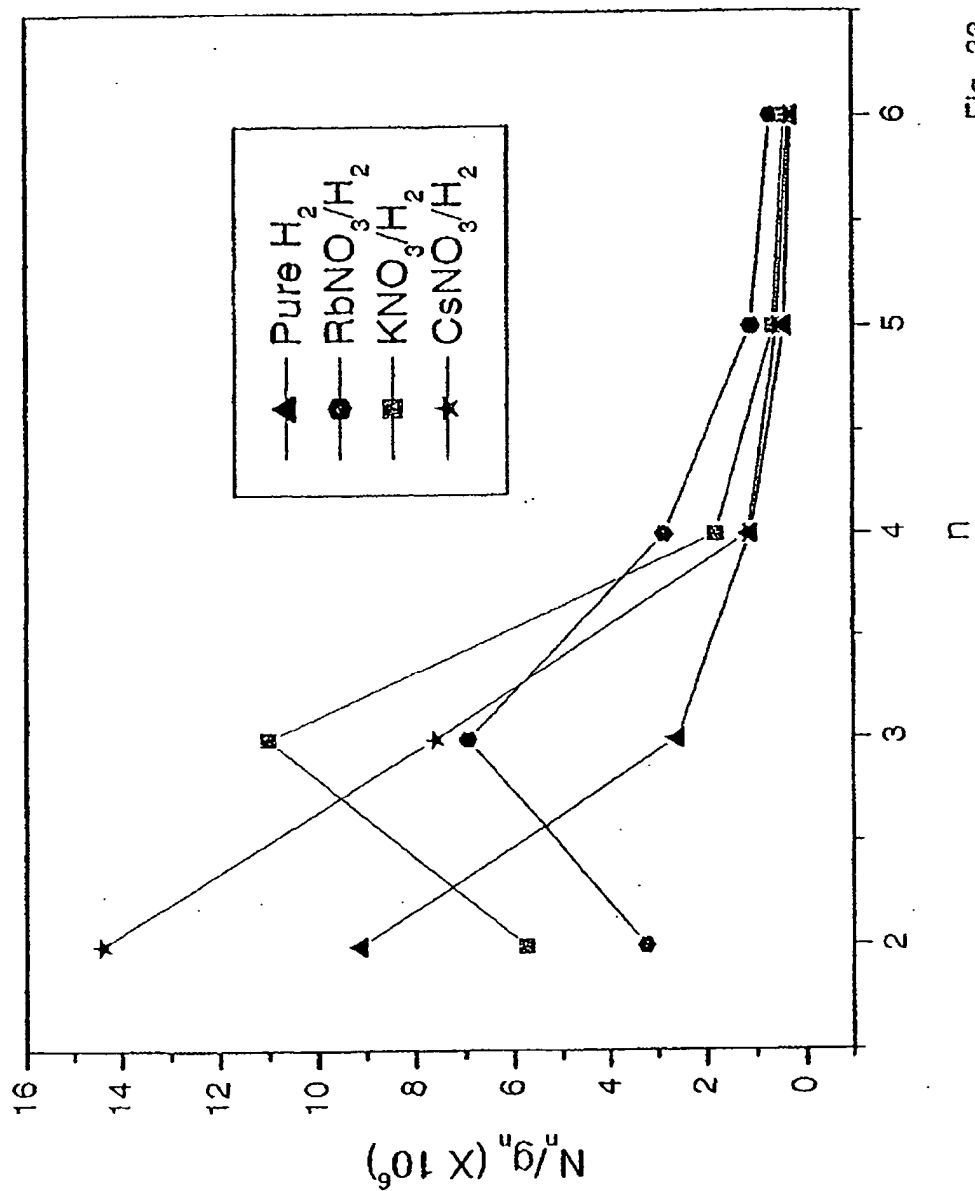


Fig. 33

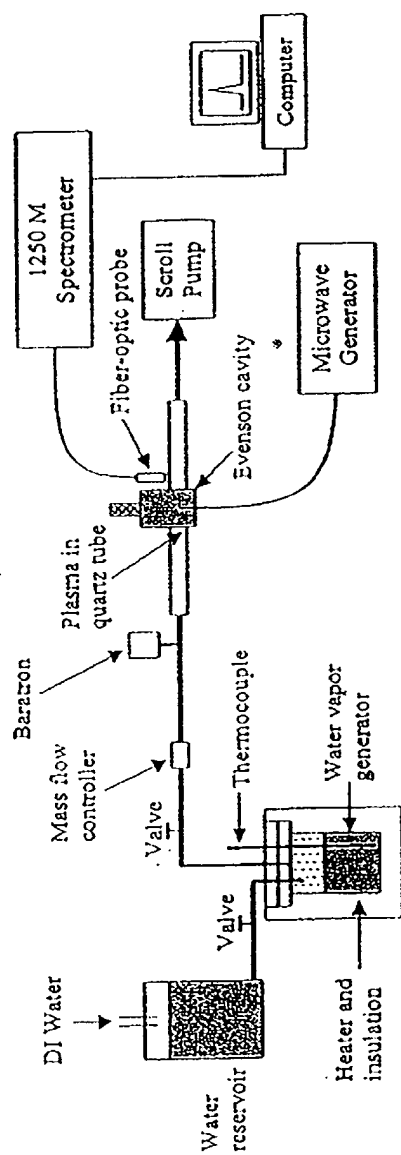


Fig. 34

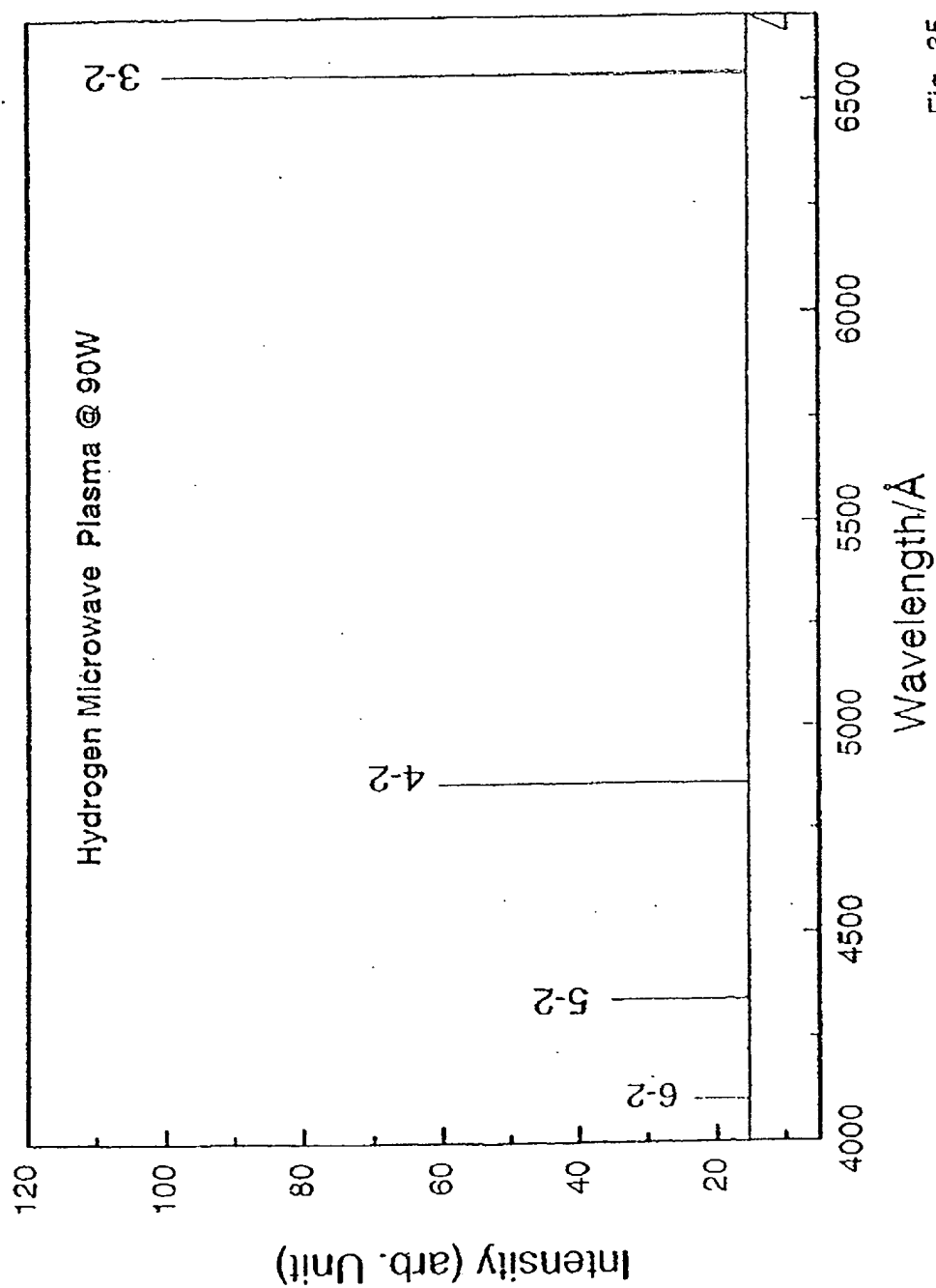


Fig. 35

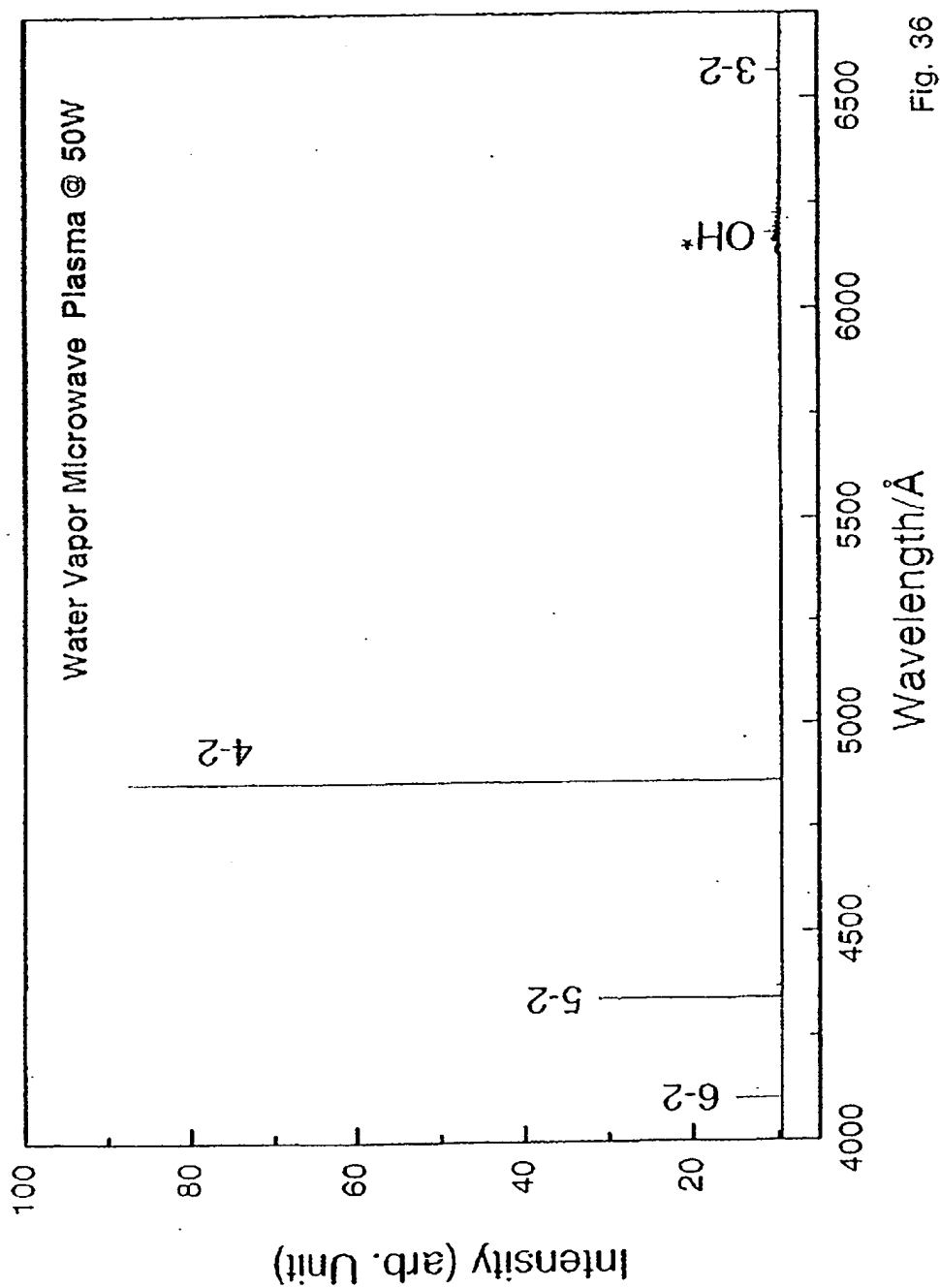


Fig. 36

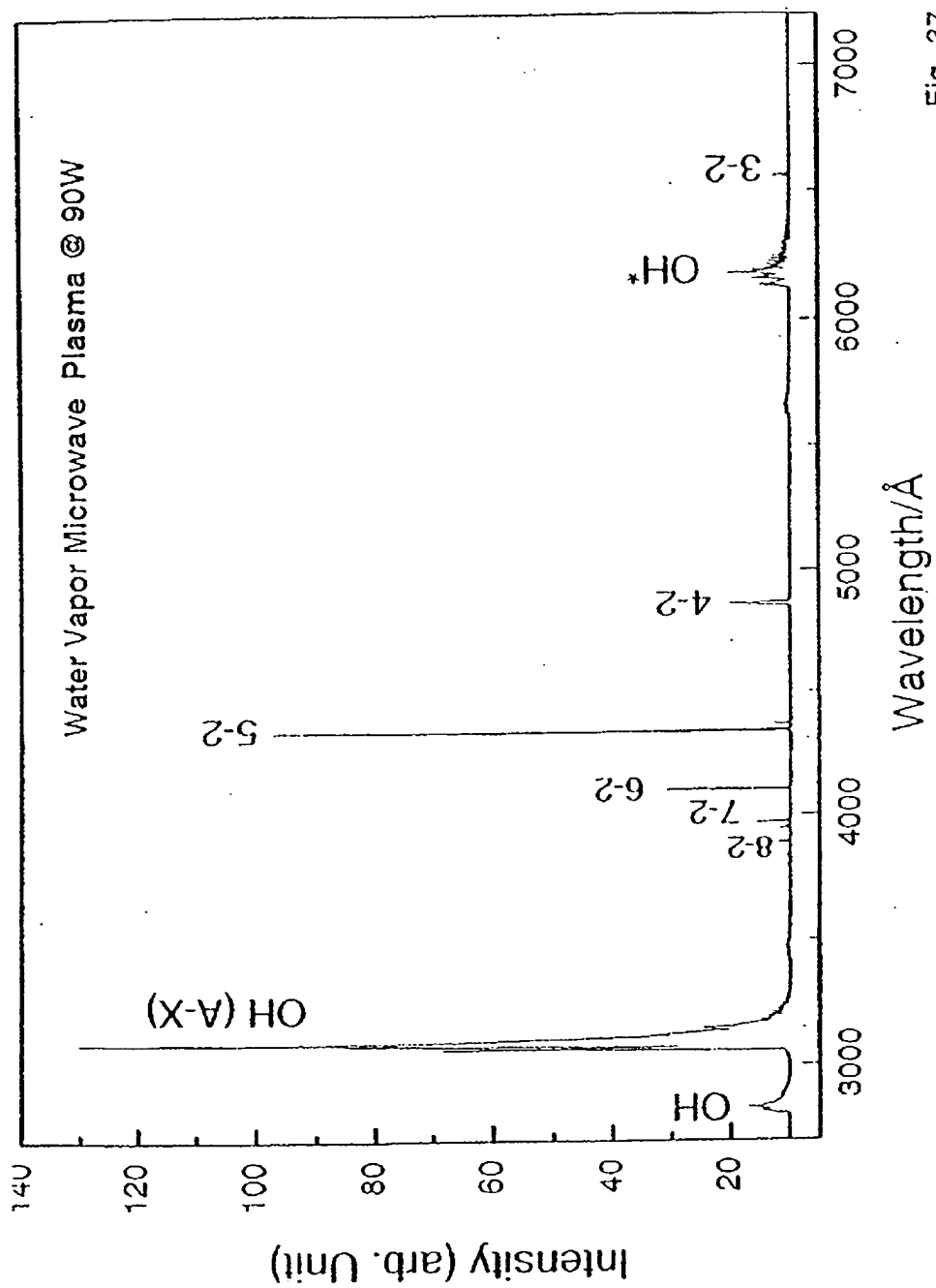


Fig. 37

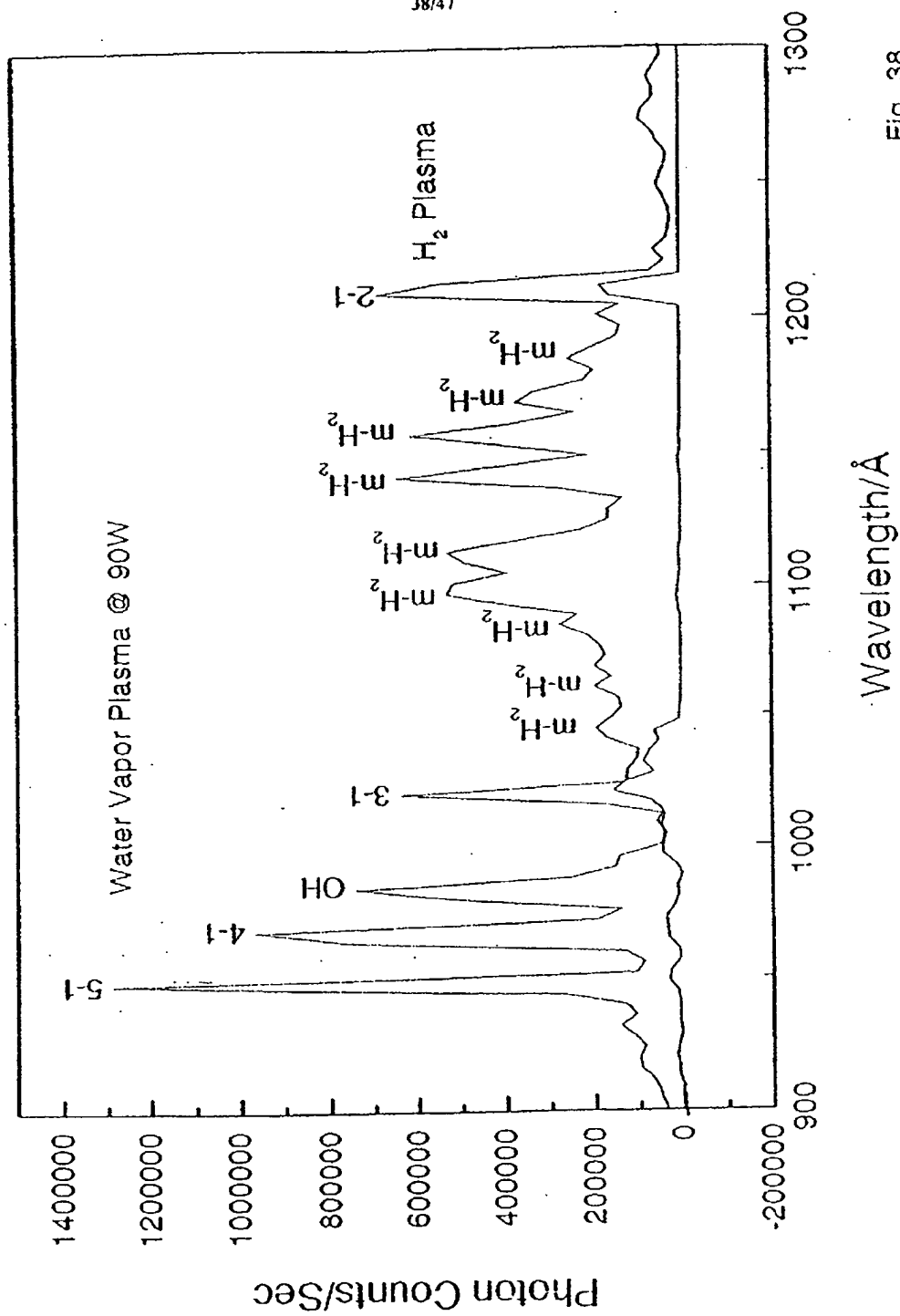
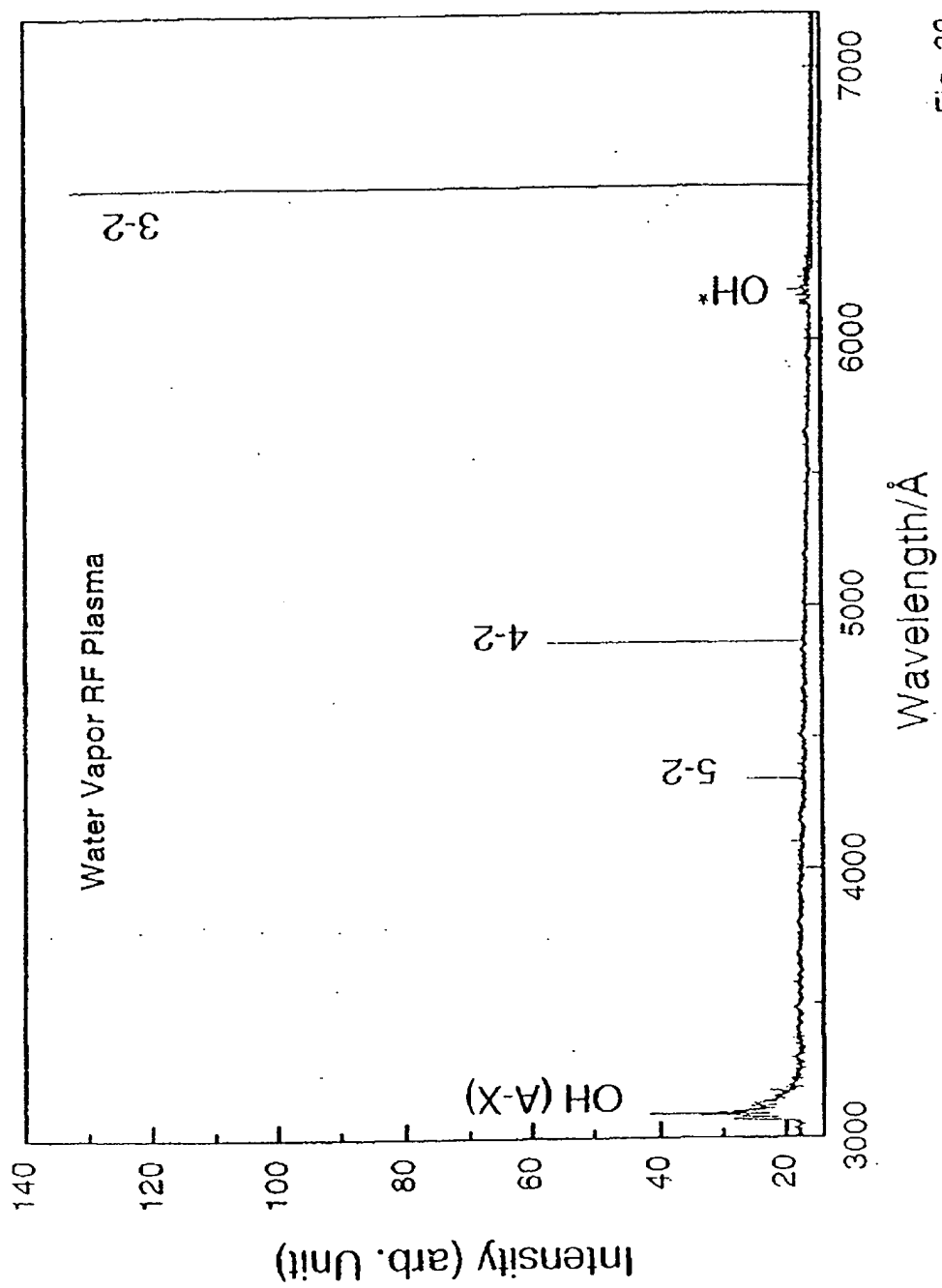
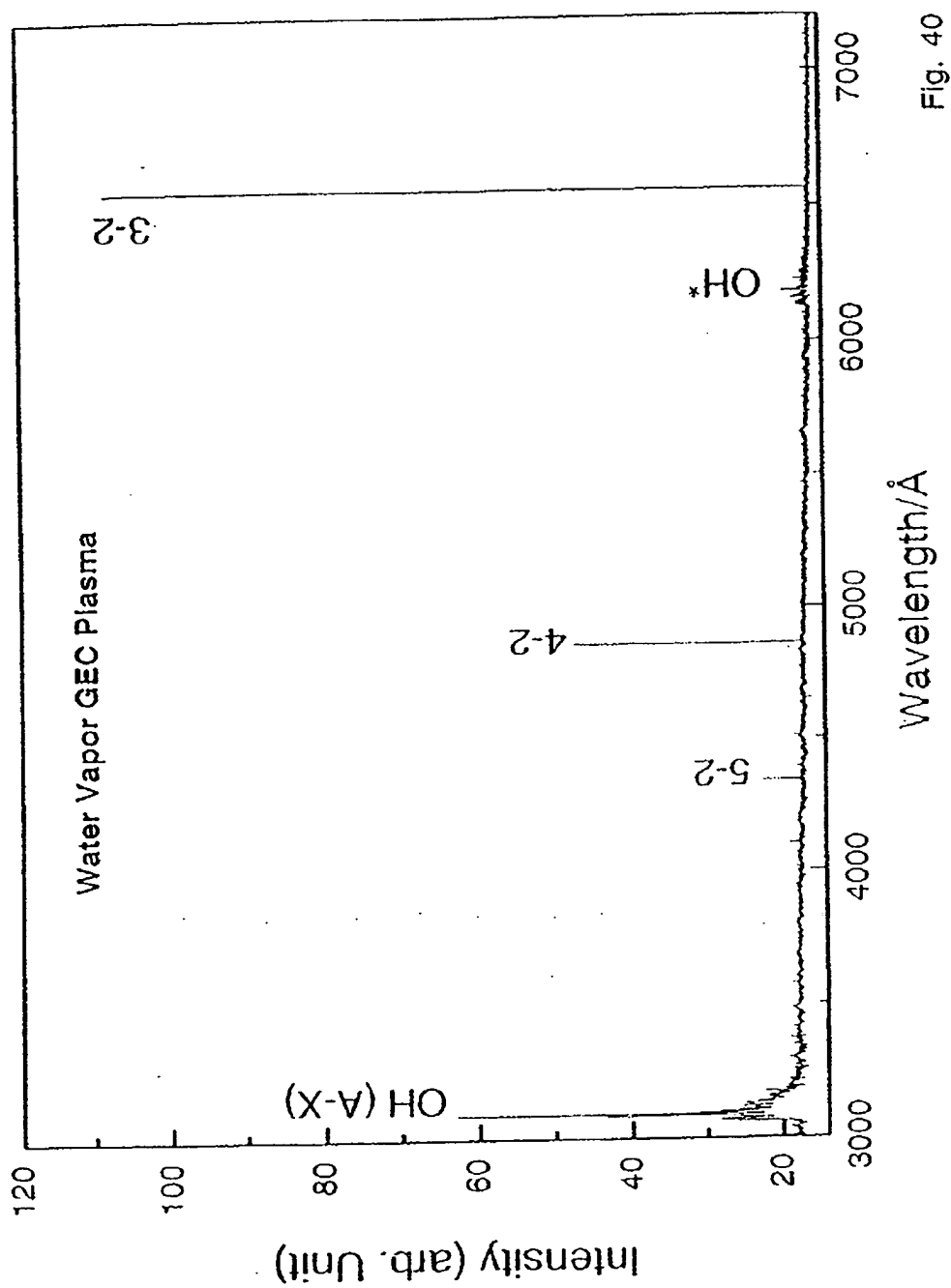


Fig. 38





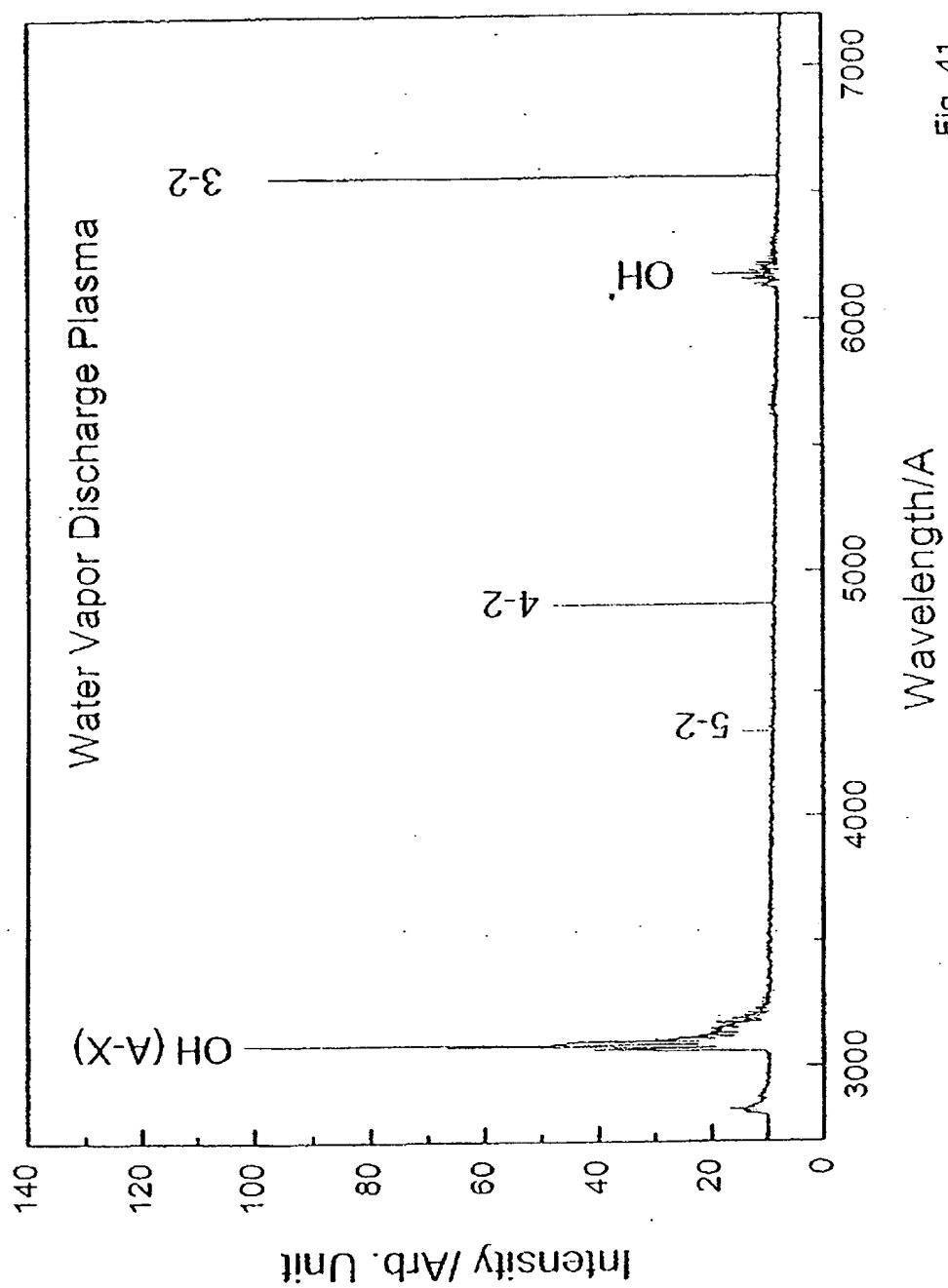


Fig. 41

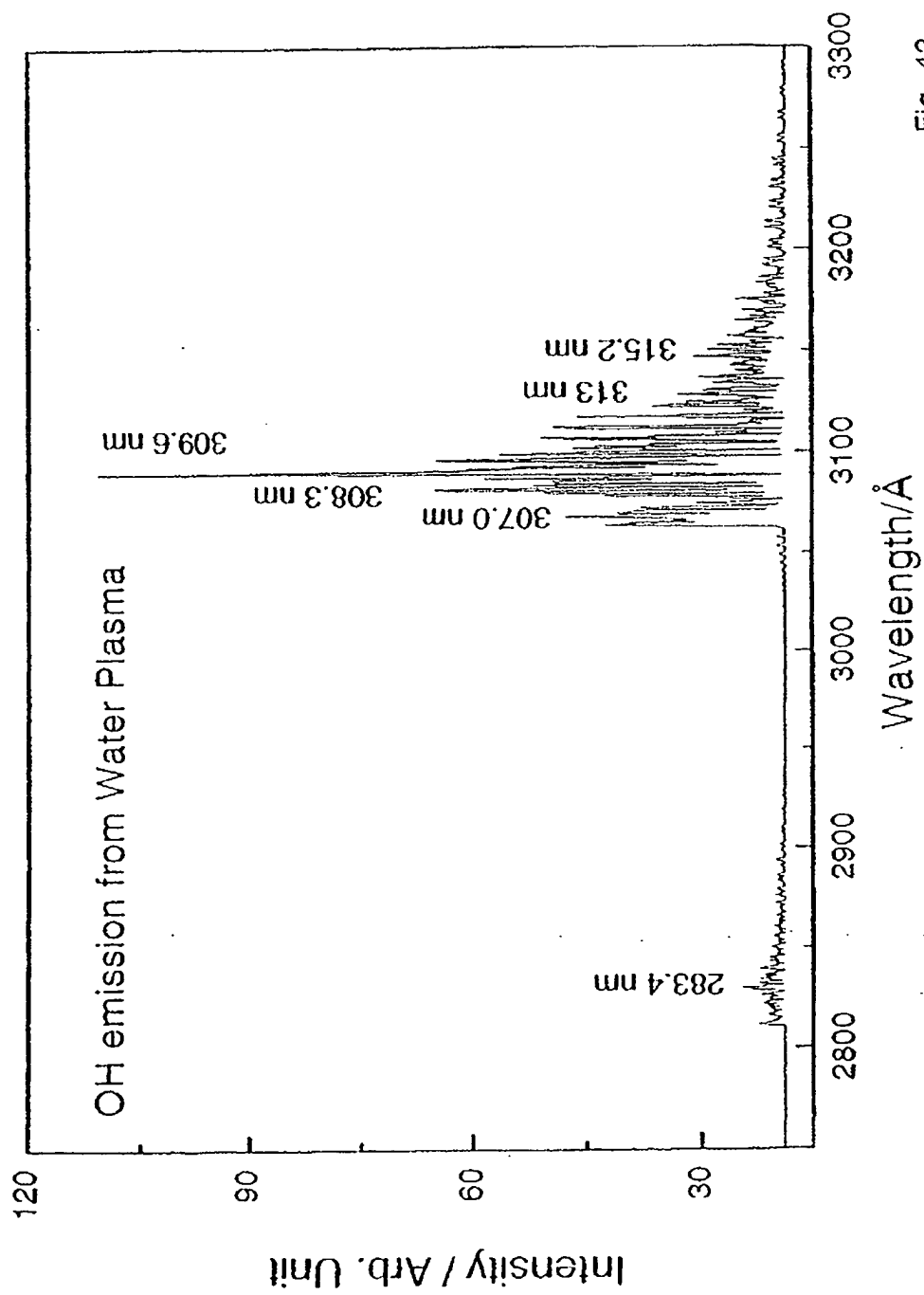
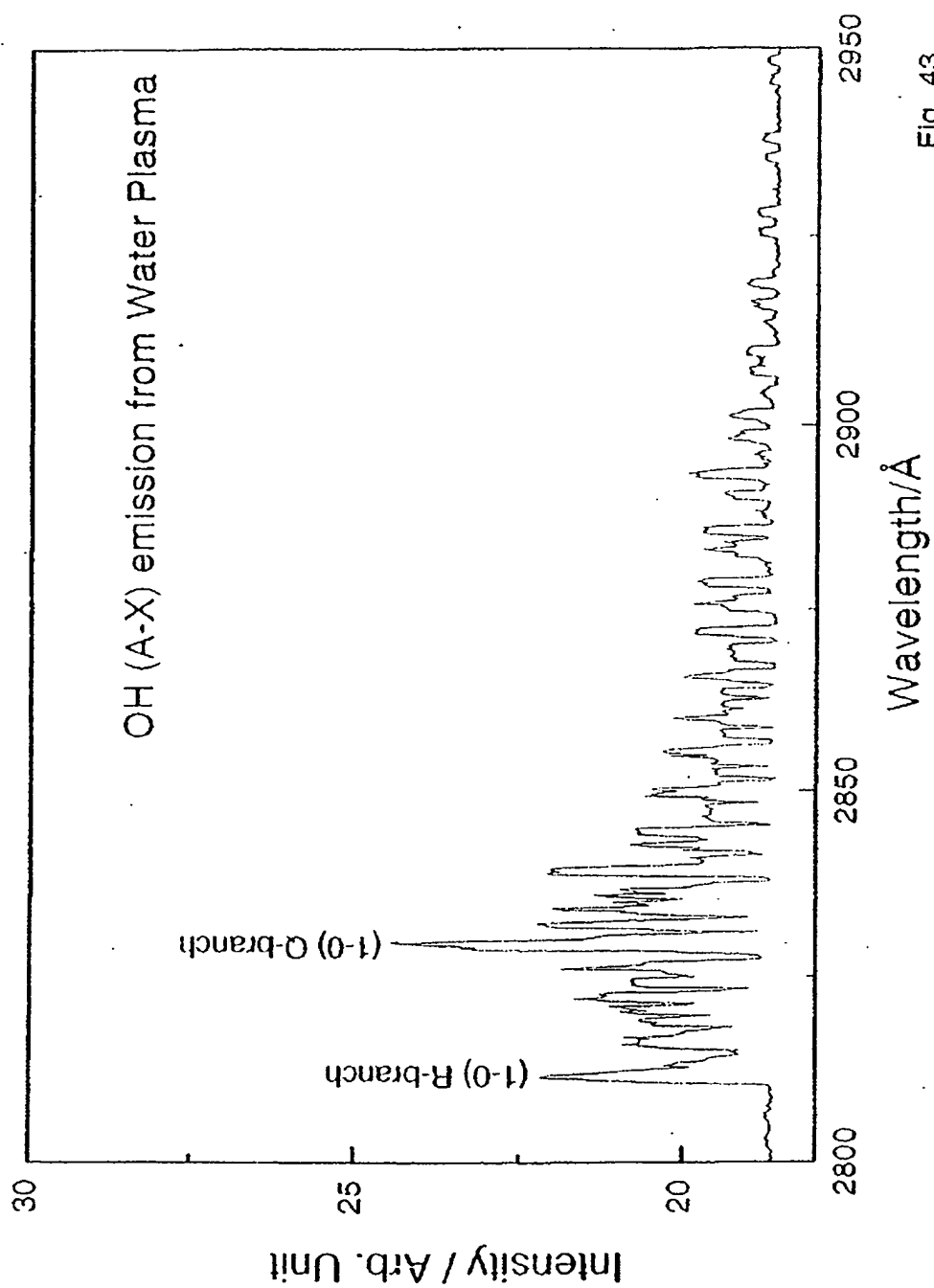
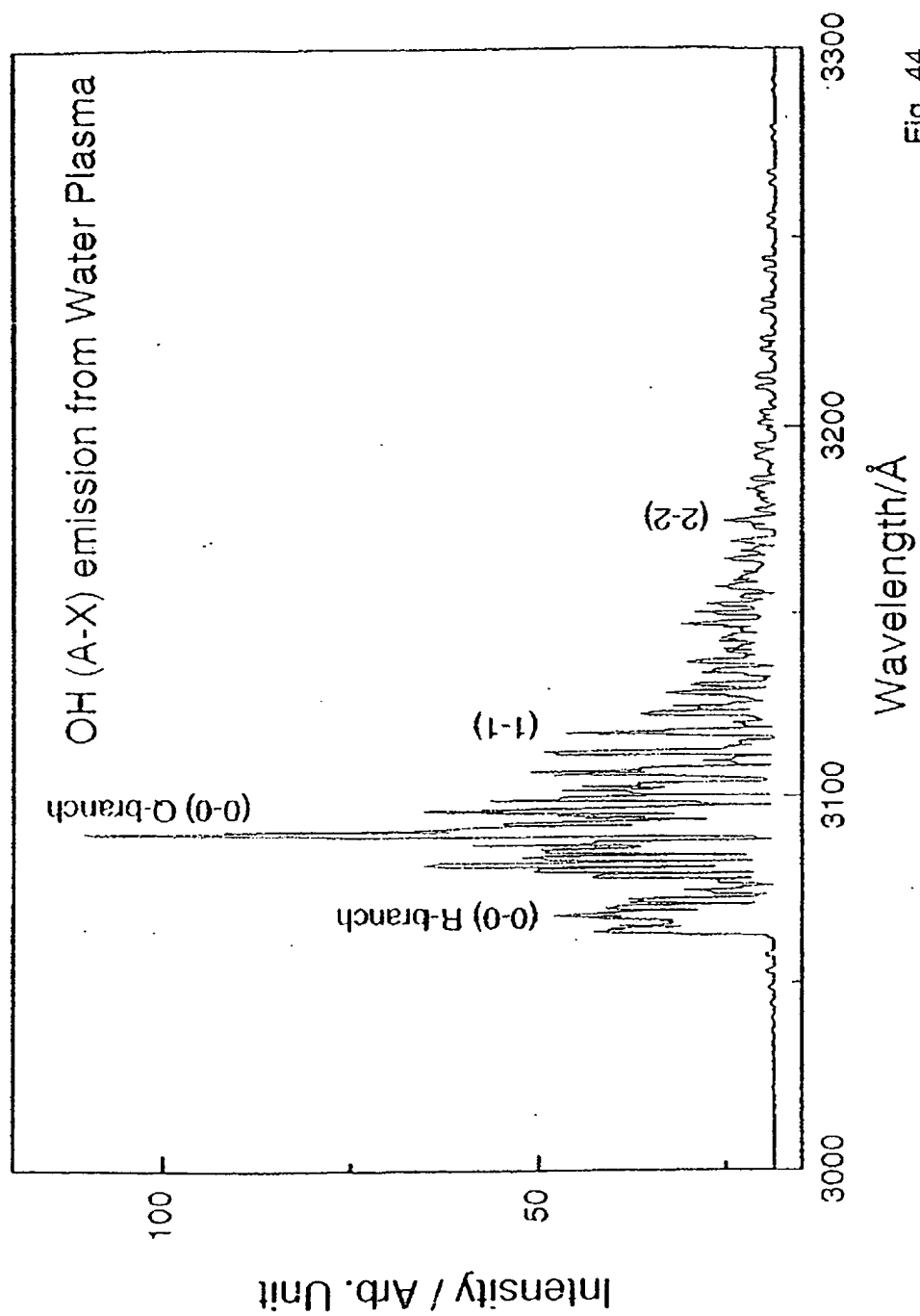


Fig. 42





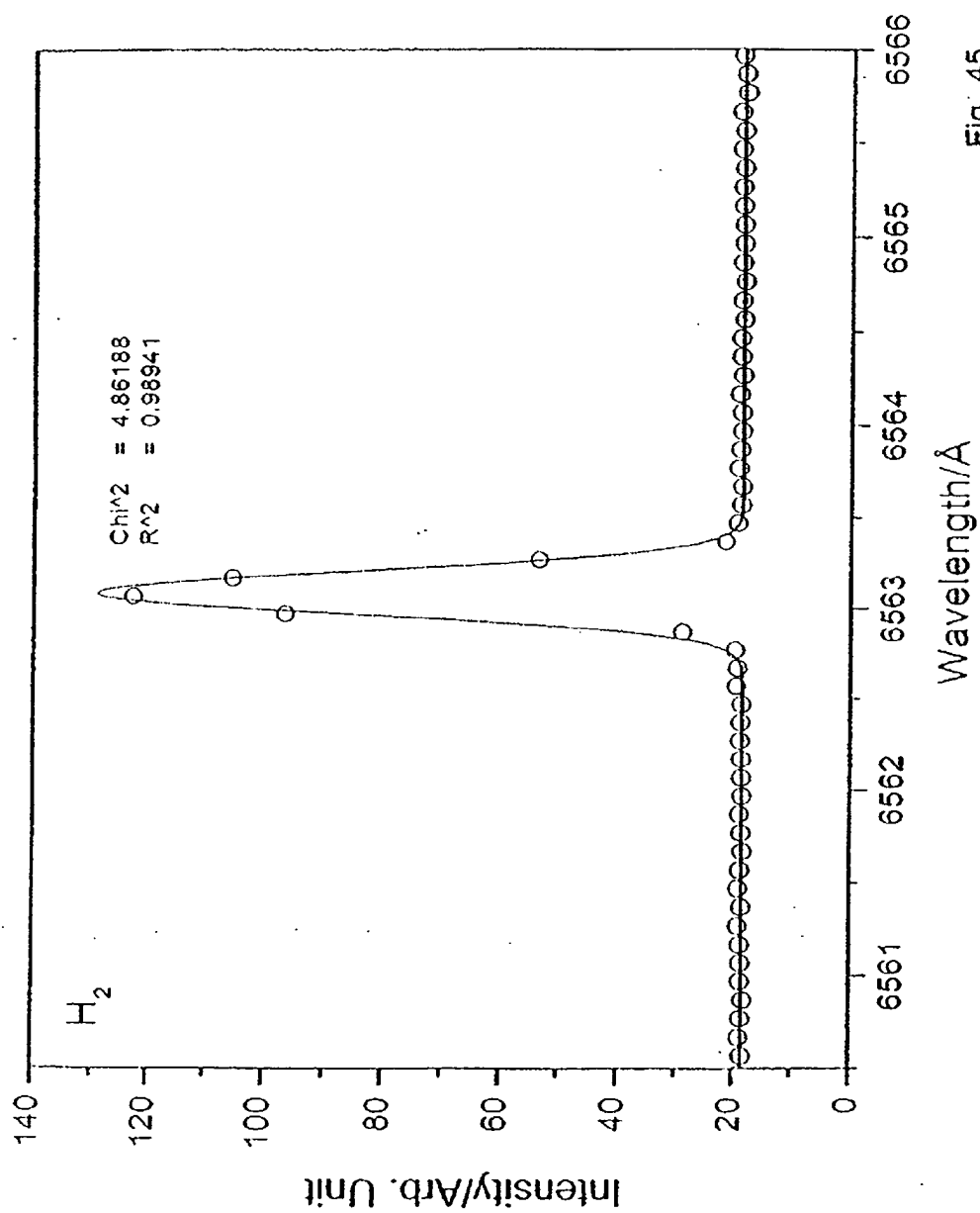


Fig. 45

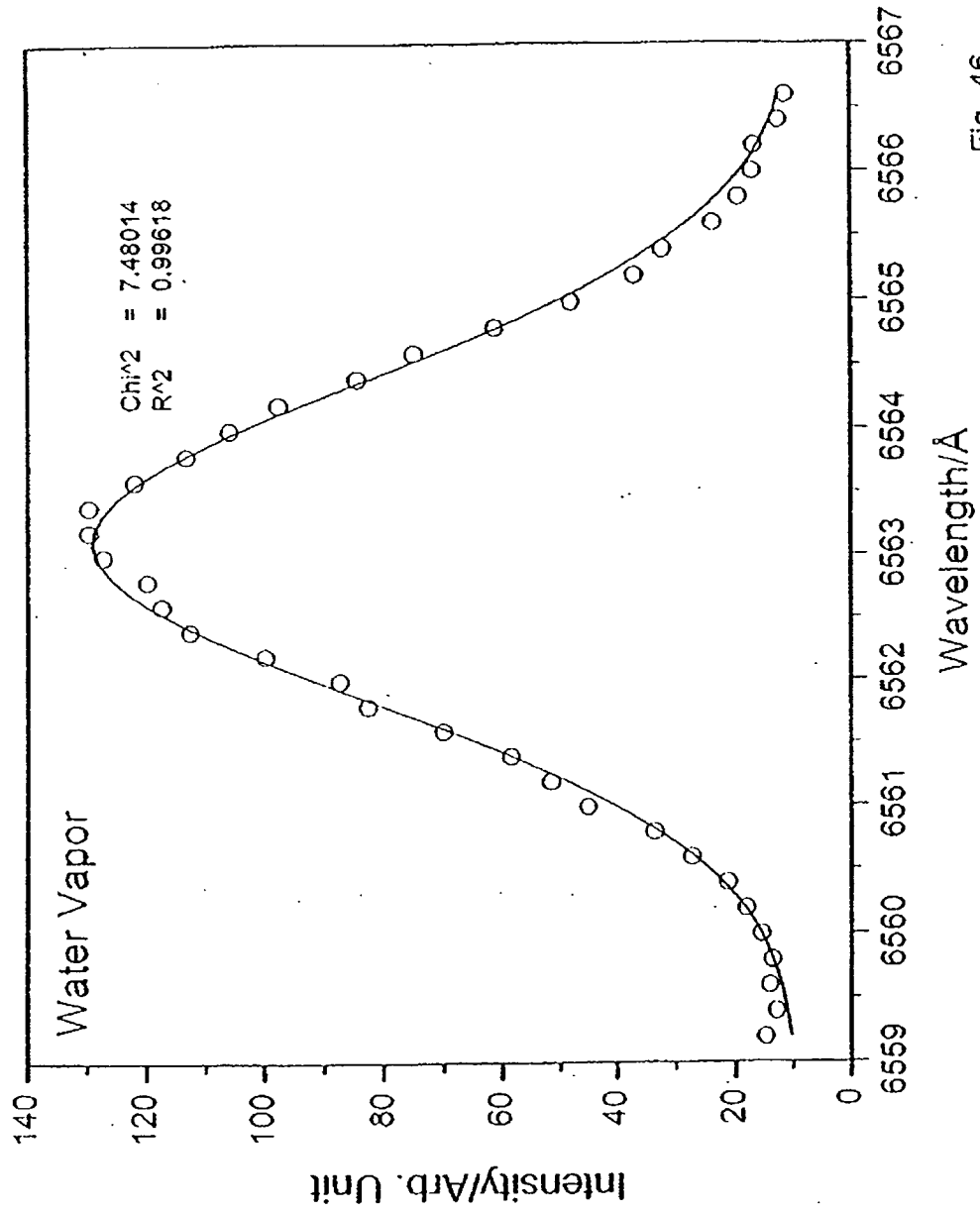


Fig. 46

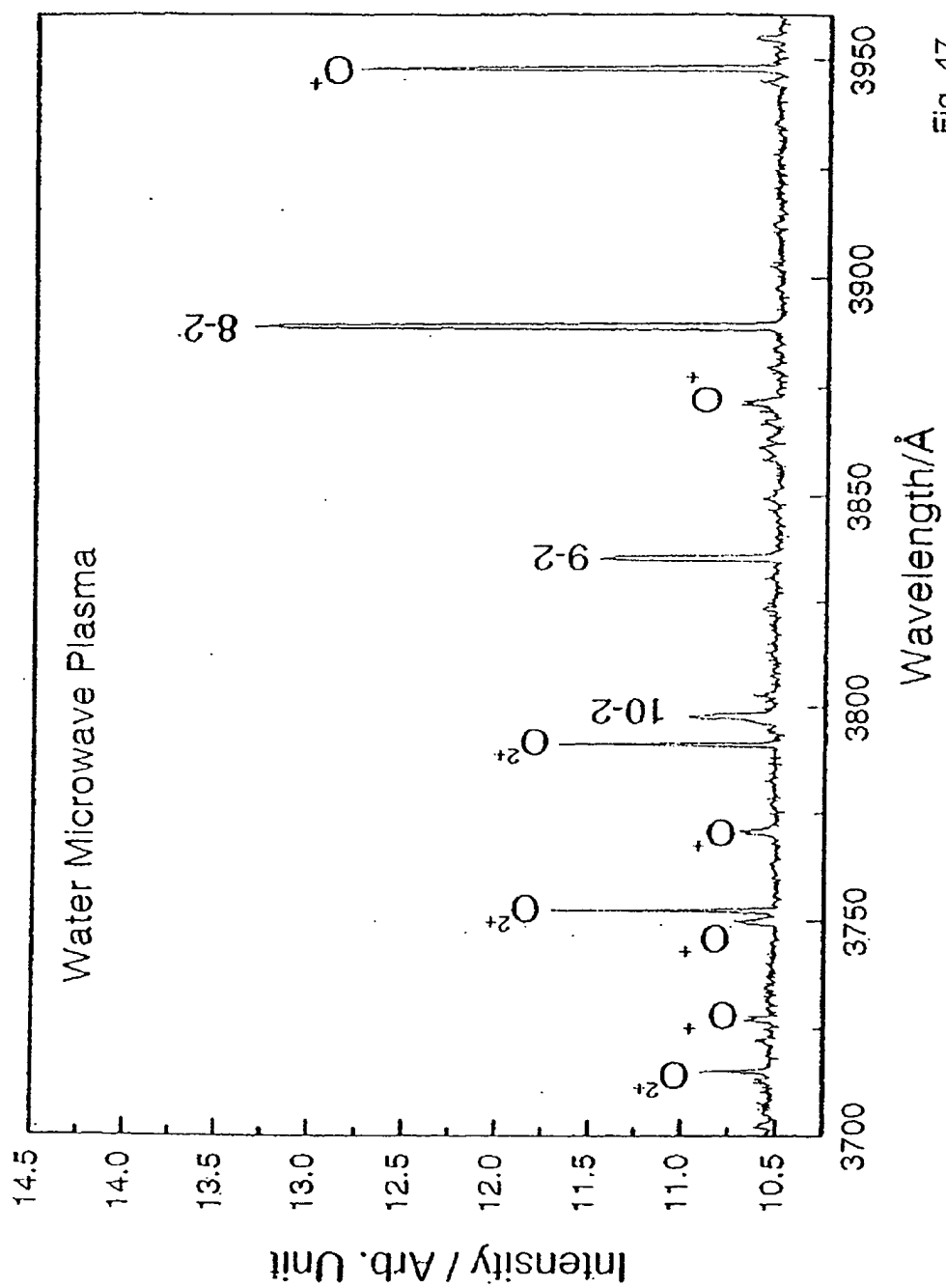


Fig. 47

REVISED VERSION

(19) World Intellectual Property
Organization
International Bureau



(43) International Publication Date
14 August 2003 (14.08.2003)

PCT

(10) International Publication Number
WO 2003/066516 A2

(51) International Patent Classification⁷: C01B 3/00

(21) International Application Number:
PCT/US2002/035872

(22) International Filing Date:
8 November 2002 (08.11.2002)

(25) Filing Language: English

(26) Publication Language: English

(30) Priority Data:
60/331,308 14 November 2001 (14.11.2001) US
60/342,114 26 December 2001 (26.12.2001) US
60/380,846 17 May 2002 (17.05.2002) US
60/385,892 6 June 2002 (06.06.2002) US
60/398,135 25 July 2002 (25.07.2002) US
60/399,739 1 August 2002 (01.08.2002) US

(71) Applicant (for all designated States except US): BLACK-LIGHT POWER, INC. [US/AUS]; 493 Old Trenton Road, Cranbury, NJ 08512 (US).

(72) Inventor: MILLS, Randall, L. [US/US]; 7 Weatherfield Drive, Newtown, PA 18940 (US).

(74) Agent: MELCHER, Jeffrey, S.; Manelli Denison & Selter, PLLC, 2000 M Street, N.W., 7th Floor, Washington, DC 20036-3307 (US).

(81) Designated States (national): AE, AG, AL, AM, AT, AU, AZ, BA, BB, BG, BR, BY, BZ, CA, CH, CN, CO, CR, CU, CZ, DE, DK, DM, DZ, EC, EE, ES, FI, GB, GD, GE, GH, GM, HR, HU, ID, IL, IN, IS, JP, KE, KG, KP, KR, KZ, LC, LK, LR, LS, LT, LU, LV, MA, MD, MG, MK, MN, MW, MX, MZ, NO, NZ, OM, PH, PL, PT, RO, RU, SD, SE, SG, SI, SK, SL, TJ, TM, TN, TR, TT, TZ, UA, UG, US, UZ, VN, YU, ZA, ZM, ZW.

(84) Designated States (regional): ARIPO patent (GH, GM, KE, LS, MW, MZ, SD, SL, SZ, TZ, UG, ZM, ZW), Eurasian patent (AM, AZ, BY, KG, KZ, MD, RU, TJ, TM), European patent (AT, BE, BG, CH, CY, CZ, DE, DK, EE, ES, FI, FR, GB, GR, IE, IT, LU, MC, NL, PT, SE, SK, TR), OAPI patent (BF, BJ, CF, CG, CI, CM, GA, GN, GQ, GW, ML, MR, NE, SN, TD, TG).

Published:
— with declaration under Article 17(2)(a); without abstract;
title not checked by the International Searching Authority

(48) Date of publication of this revised version:
6 January 2005

(15) Information about Correction:
see PCT Gazette No. 01/2005 of 6 January 2005, Section II

For two-letter codes and other abbreviations, refer to the "Guidance Notes on Codes and Abbreviations" appearing at the beginning of each regular issue of the PCT Gazette.

WO 2003/066516 A2

(54) Title: HYDROGEN POWER, PLASMA, AND REACTOR FOR LASING, AND POWER CONVERSION

(57) Abstract:

PATENT COOPERATION TREATY

PCT

DECLARATION OF NON-ESTABLISHMENT OF INTERNATIONAL SEARCH REPORT

(PCT Article 17(2)(a), Rules 13ter.1(c) and Rule 39)


Applicant's or agent's file reference 62226-LAS	IMPORTANT DECLARATION	Date of filing (day/month/year) 25/08/2003
International application No. PCT/US 02/ 35872	International filing date(day/month/year) 08/11/2002	(Earliest) Priority date(day/month/year) 14/11/2001
International Patent Classification (IPC) or both national classification and IPC B01J19/00		
Applicant BLACKLIGHT POWER, INC.		

This International Searching Authority hereby declares, according to Article 17(2)(a), that no international search report will be established on the international application for the reasons indicated below

1. ☐ The subject matter of the international application relates to:
 - a. ☐ scientific theories.
 - b. ☐ mathematical theories
 - c. ☐ plant varieties.
 - d. ☐ animal varieties.
 - e. ☐ essentially biological processes for the production of plants and animals, other than microbiological processes and the products of such processes.
 - f. ☐ schemes, rules or methods of doing business.
 - g. ☐ schemes, rules or methods of performing purely mental acts.
 - h. ☐ schemes, rules or methods of playing games.
 - i. ☐ methods for treatment of the human body by surgery or therapy.
 - j. ☐ methods for treatment of the animal body by surgery or therapy.
 - k. ☐ diagnostic methods practiced on the human or animal body.
 - l. ☐ mere presentations of information.
 - m. ☐ computer programs for which this International Searching Authority is not equipped to search prior art.
2. ☒ The failure of the following parts of the international application to comply with prescribed requirements prevents a meaningful search from being carried out:

☐ the description
☒ the claims
☐ the drawings
3. ☐ The failure of the nucleotide and/or amino acid sequence listing to comply with the standard provided for in Annex C of the Administrative Instructions prevents a meaningful search from being carried out:

☐ the written form has not been furnished or does not comply with the standard.
☐ the computer readable form has not been furnished or does not comply with the standard.
4. Further comments: See extra sheet

Name and mailing address of the International Searching Authority  European Patent Office, P.B. 5818 Patentlaan 2 NL-2280 HV Rijswijk Tel. (+31-70) 340-2040, Tx. 31 651 epo nl, Fax (+31-70) 340-3016	Authorized officer Toñi Muñoz-Manneken
---	--

FURTHER INFORMATION CONTINUED FROM PCT/ISA/

Certain claims lack of essential features and the present application fails to comply with the clarity and conciseness requirements of Article 6 PCT (see also Rule 6.1(a) PCT) to such an extent that a meaningful search on the basis of the claims is impossible. In view of the large number and also the wording of the claims presently on file, which render it difficult, if not impossible, to determine the matter for which protection is sought, a meaningful search on the basis of the claims is impossible. Consequently, no search report can be established for the present application.

According to PCT Article 17 (3) (a) and Rule 13.1, an application shall relate to one invention only or to a group of inventions so linked to form a single general inventive concept. Further, according to PCT Rule 13.2 the requirement of unity of invention is fulfilled only when there is a technical relationship among the claimed inventions involving one or more of the same or corresponding technical features. The special technical feature shall also define a contribution, which each of the claimed inventions, considered as a whole, makes over the general state of the art.

The applicant's attention is drawn to the fact that claims relating to inventions in respect of which no international search report has been established will not be the subject of an international preliminary examination (Rule 66.1(e) PCT). This is the case irrespective of whether or not the claims are amended following receipt of the search report or during any Chapter II procedure.